Effects of biodegradation on crude oil compositions and reservoir profiles in the Liaohe basin, NE China

by

Haiping Huang

A thesis submitted to the University of Newcastle upon Tyne in partial fulfilment of the requirements for the degree of Doctor of Philosophy in the Faculty of Science

UNIVERSITY OF
NEWCASTLE

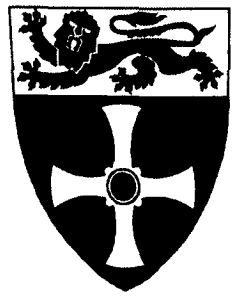

School of Civil Engineering and Geosciences
University of Newcastle upon Tyne, UK.

January 2004

DECLARATION

I hereby certify that the work described in this thesis is my own, except where otherwise acknowledged, and has not been submitted previously for a degree at this or any other university.

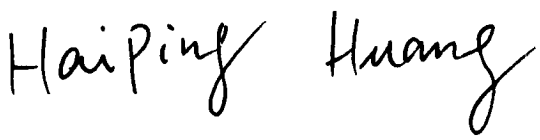

Haiping Huang

Acknowledgements

I would like to thank my supervisor Professor Steve Larter for all of his help and encouragement throughout this project. Thanks also go to Professor Andy Aplin and Dr Gordon Love for their continued advice and suggestions during the course of this research. I would especially like to thank Mr Berni Bolwer for both laboratory assistance and language correction. Dr Barry Bennett, Dr Thomas Oldenburg, Dr Paul Farrimond, Dr Martin Jones, Dr Geoff Abbott and Dr Yunlai Yang are thanked for scientific help and inspiration over the last four years. The technical assistance of Paul Donohoe and Kimberly Noke with GC-MS analyses was greatly appreciated. Ian Harrison, Trevor Whitfield and Robert Hunter all made the laboratory work run relatively smoothly and this fact is gratefully acknowledged. Mrs. Yvonne Hall is thanked for all her patience and assistance. Also, to all other staff and students within the department who assisted or encouraged me in any way throughout the production of this dissertation, I owe a huge thank-you.

Liaohe Oil Company is acknowledged provision the majority of the samples for this project, and its staff, Mr Mingzhi Piao, Mr Jinyou Li are thanked for their support. I would also thank Mr Kanchuang Ma and Mr Yabin Zheng from China University of Geosciences for their assistance in sample collection and variety of helps.

I thank the Overseas Research Scholarship (ORS) and University of Newcastle upon Tyne and Bacchus Consortia Project for providing partially funding of my Ph.D project.

Finally thanks to my wife Zhili Zhao and my daughter Danning Huang for their love and support.

ABSTRACT

Biodegradation of crude oil in reservoirs has major economic consequences. While the effects of biodegradation are empirically well known, the processes involved, the fraction of oil destroyed and the critical factors controlling degradation remain obscure. A suite of oils and reservoir extracts from the Liaohe basin, NE China, was analyzed to investigate the effects and controls of biodegradation on petroleum composition. The aims of this project were to further our understanding of the factors which influence the biodegradation of crude oils, and the processes by which these factors interact and to assess the role played by biodegradation in controlling the composition of a wide range of crude oils.

The geological settings of the study area have been addressed in detail, including structural and stratigraphic characteristics, source rock and reservoir characteristics, tectonic evolution and hydrocarbon generation history, formation water composition. A single source and similar maturity make the study area an ideal site to investigate the constraint of biodegradation.

Systematic changes seen as marked gradients in petroleum bulk composition, component concentrations and molecular indicators have been observed in biodegraded oil columns. The susceptibilities of several aromatic hydrocarbon, alkylcarbazole and alkylphenol isomers to biodegradation have been discussed for the first time in this thesis. The author also addressed the biodegradation effects on many classical geochemical evaluation procedures such as those involving facies and maturity assessment and on the physical and chemical properties of petroleum.

The variation in the degree of biodegradation at different sites of the column is controlled by water leg size, with a higher level of degradation being associated with a thicker water leg. The supply of nutrients from the water leg is thought to have a significant impact upon the degree of biodegradation. In addition to water leg size/nutrient supply, the compositional gradients are also controlled by the relative rate of mixing of fresh and degraded oils. The conceptual biodegradation model proposed couples geochemical and geological factors to provide a coherent approach to ascertain the impact of degradation on petroleums and to help to reliably predict biodegradation risk for an exploration target. Our data suggest that biodegradation occurs within a narrow region near the base of the oil column, probably at the oil water contact (OWC), and that in this reservoir there has been a late charge of oil to the top of the column. The mixing of oils through continuous charging and the diffusion of hydrocarbons towards the OWC, and the diffusion of metabolites of degraded oil away from the reaction site may be considered as the most important factor controlling the biodegradation process.

Based on an oil charging-biodegradation model (Larter *et al.*, 2003) mass balance calculation has been carried out and the results indicate at level 5 biodegradation up to 50% of petroleum mass has been depleted, beyond this level of biodegradation loss of oil mass is less significant but structural rearrangements are important.

List of Contents

1 INTRODUCTION

The composition of reservoired oil integrates all the processes occurring during petroleum generation, migration, accumulation and secondary alteration. Although source origin and maturity take certain controls in present oil composition, in most cases secondary alterations are more important. The chemical characteristics of oil often provide clues for deciphering the evolution of an oil with regard to all of these processes (England *et al.*, 1987; Lafargue and Barker, 1988; Leythaeuser and Rückheim, 1989; Horstad *et al.*, 1992; Larter and Aplin, 1995; Holba *et al.*, 1996; Hunt, 1996).

1.1 Petroleum alteration processes

Once expelled from source rocks, crude oils are subject to a complex series of subsequent compositional modifications that may occur during migration and within the reservoir (Tissot and Welte, 1984; Lafargue and Barker, 1988; Hunt, 1996). Two most important alteration processes are thermal maturation after expulsion and biodegradation. Thermal maturation, a consequence of increasing burial depth and higher temperature, will form increasingly lighter gravity oils until extreme temperatures result in cracking of the parent kerogen and/or oil to gas (Horsfield *et al.*, 1992; Schenk *et al.*, 1997; Vandenbroucke *et al.*, 1999; Dahl *et al.*, 1999). By contrast, biodegradation by subsurface microbial communities at shallow depths leads to higher gravity heavy oils (Seifert and Moldowan, 1979; Connan, 1984; Volkman *et al.*, 1984; Peters and Moldowan, 1993). In addition, more complex phenomena involving evaporative fractionation, water washing, gas washing, deasphalting, thermochemical sulfate reduction, gravity segregation, and dewaxing may all contribute, to varying extents, to alteration of crude oils either in the reservoir or along migration pathways (England *et al.*, 1987; Thompson, 1987; 1988; Goldstein and Aizenshtat, 1994; Larter and Aplin, 1995; Curiale and Bromley, 1996; di Primio, 2002). Most of these alteration processes in petroleum reservoir usually reduce the commercial value of the oil and complicate the development procedures.

1.1.1 Thermal maturation

Thermal maturation or cracking affects liquid oils trapped in reservoirs at temperature over about 160 °C. Heavier fractions of the petroleum are broken down to form light oil, condensate, and finally gas, where liquid petroleum (C_{6+}) no longer exists (Hunt, 1996). Although most models of oil-to-gas cracking assume multiple first-order parallel reactions, the kinetic parameters determined by different workers

vary widely (Waples, 2000 and references therein). Therefore, predictive temperatures for the oil deadline remain uncertain. For example, the thermal stability of hydrocarbons (Mango, 1991) and the occurrence of oils at high reservoir temperatures (Horsfield *et al.*, 1992; Price and Schoell, 1995; Pepper and Corvi, 1995) suggest that liquid components may be preserved at higher temperatures than previously thought. Using the kinetic parameters of Waples (2000), the maximum temperature where oil is preserved varies from 170 °C at geologically slow heating rates to over 200 °C at geologically fast heating rates. At temperatures over 200 °C, gases such as propane or butane may be broken down to methane. Meanwhile, a carbon rich deposit called pyrobitumen may form in the reservoir as a by-product of the thermal cracking process. Pyrobitumen formation is especially common if biodegraded oils are thermally cracked (Horsfield *et al.*, 1992; Stasiuk, 1997). Pyrobitumen will block the reservoir pores and prevent oil production (Lomando, 1992). The degree of oil cracking is hard to determine since no proper tool available. Recently Dahl *et al.* (1999) reported diamondoids contents in oil or condensate can be used directly to determine the extent of oil-to-gas cracking in reservoirs. Their method may also offer a means to recognize mixtures of high- and low-maturity oils even though depositional environmental effects can not be ruled out (Schulz *et al.*, 2001).

1.1.2 Biodegradation

Under certain conditions, living microorganisms (primarily bacteria, but also archea, yeasts, molds, and filamentous fungi) can alter and/or metabolize various classes of compounds present in oil, a set of processes collectively called oil biodegradation. Biodegradation not only affects oil spills and surface seeps, but also alters subsurface oil accumulations (Bailey *et al.*, 1973; Connan; 1984; Peters and Moldowan, 1993; Wenger and Isaksen, 2002). As a matter of fact, the vast majority of the world's petroleum is severely biodegraded oil. There are sixteen very large tarsand deposits estimated to contain 2,100 billion barrels of oil. The seven largest tarsand deposits contain 98% of the world's heavy oil, as much oil in place as the world's 264 giant oil fields (Demaison, 1977).

Shallow oil accumulations (< 80 °C reservoir temperature) are commonly found to be biodegraded to some degree. Oils from shallower, cooler reservoirs tend to be progressively more biodegraded than those in deeper, hotter reservoirs. Bacteria utilize nutrients such as phosphate ion and an oxidant present in the reservoir to oxidize hydrocarbons and non-hydrocarbons to provide energy for themselves and produce altered petroleums. Increasing levels of biodegradation generally cause a decline in oil quality and serious problems for oil production, transportation and

refining. In some cases biodegraded oil is too viscous to be produced from the reservoir, while in some slightly less viscous biodegraded oil steam is required to recover the oil from reservoir. Biodegraded oils are often rich in sulfur and asphaltene which not only cause problems with pipelines but also can damage production and refinery equipment (Wenger *et al.*, 2002). Biodegradation reduces the economical values of the oil. On the other hand, with the depletion of conventional crude oils, these biodegraded heavy oils may become the most appropriate energy resource in the next half century. Since most heavy oil reserves in the world are formed by biodegradation (Connan, 1984; Hunt, 1996), to understand biodegradation processes and mechanisms will provide great benefit to utilize these potential resources in future. That is one of the most important reasons why this thesis chose biodegradation as the main topic.

It was generally accepted in western literature that most surface and subsurface biodegradation are caused by aerobic bacteria (e.g. Palmer, 1993). Sufficient oxygen and nutrient supply for the action of aerobic bacteria in undeveloped reservoirs was assumed to be provided by meteoric waters. Nonetheless, it is difficult to explain how biodegraded accumulations the size of the Alberta tar sands (~269.8 billion m^3) could be degraded solely by aerobic microbes, when small plumes of organic contaminants are sufficient to remove oxygen from near surface groundwater (Baedecker *et al.*, 1993). More recently, it has been recognized that anaerobic sulfate-reducing and fermenting bacteria also can degrade petroleum where oxygen is not available but anoxic conditions prevail (Coates *et al.*, 1996; Connan *et al.*, 1996; Caldwell *et al.*, 1998; Zengler *et al.*, 1999). A variety of metabolites which solely occur under anaerobic conditions were found in reservoired oils provide convincing evidence that oil biodegradation is mainly an anaerobic process (Aitken, 2004).

Petroleum biodegradation can be demonstrated by compositional alterations in the reservoir profiles, isotopic fractionations and specific metabolic product identification. Biodegradation modelling in particular is a useful tool to imitate biodegradation processes. Microcosm studies are also a useful tool to identify degradation mechanisms and to understand the role of specific electron acceptors and redox conditions.

1.1.3 Water Washing

Crude oils may be substantially altered during migration, or in the reservoir, by water washing concomitant with biodegradation (Seifert and Moldowan, 1979; Lafargue and Barker, 1988). Aerobic biodegradation requires moving water to provide nutrients and dissolved oxygen (Connan, 1984), and so, to some extent, water

washing is essential for aerobic biodegradation to proceed (Volkman *et al.*, 1984). However, water washing can occur in reservoirs unsuitable for bacterial growth and along migration routes, so it is an important alteration process to consider in order understanding variations in oil composition. Conditions favorable for water washing are known to exist during oil migration, especially when oil is migrating through a hydrologically active water-wet carrier bed and reservoir system close to mountain ranges or other elevated terrain where ground water at height can drive water flow in the subsurface.

Oil geochemistry analyses can be used to decipher water washing effects. My recent case study in the Erlian basin, Northern China indicated water washing can form unusual heavy oil. In such a process biodegradation is insignificant due to no obvious loss of *n*-alkanes. The aromatic data for the water washed oil showed a dramatic depletion of naphthalene, methylnaphthalenes, phenanthrene, dibenzothiophene (DBT) and C_1–DBTs; an enrichment of the C_3–alkylhomologues within the naphthalene, phenanthrene and DBT series; and an increase in the concentrations of the aromatic steroid hydrocarbons (Huang *et al.*, 2003b). In general, water washing results from the removal of water soluble contents in the petroleum by slowly moving groundwater in the reservoir. Low molecular weight aromatic compounds are several orders of magnitude more soluble than saturated hydrocarbons with a similar carbon number, and the solubility of both saturated and aromatic hydrocarbons decreases with increased carbon number (Lafargue and Barker, 1988; Kuo, 1994;). Water washing is particularly effective within the low-boiling range of hydrocarbons followed by sequestering of low molecular weight aromatic hydrocarbons (i.e., benzene, and toluene) before light alkanes and naphthenes are removed (Connan 1984; Palmer, 1984, 1993; Lafargue and Thiez, 1996). The water-washing phenomenon can be simulated in model laboratory conditions (de Hemptinne *et al.*, 2001). Water washing without concomitant biodegradation is indicated by: (1) a decrease in the amount of aromatic hydrocarbons and low molecular weight *n*-alkanes while naphthenes are unaltered, (2) partial removal of C_{15+} aromatic hydrocarbons while C_{15+} alkanes are unaffected, and (3) a decrease in sulfur-bearing aromatic hydrocarbons (especially dibenzothiophene) (Palmer, 1993; Lafargue and Barker, 1988).

1.1.4 Phase fractionation

Phase fractionation is another process that could have affected oil compositions. Phase fractionation, also termed evaporative fractionation (Thompson, 1987; 1988) or migration fractionation (Dzou and Hughes, 1993; Curiale and Bromley, 1996;

Napitupulu *et al.*, 2000), is suggested for the complex phenomena involved in the separation of gas from oil in the subsurface. This process is characterized by several phenomena. Since the oil is frequently partially vaporized in the reservoir, the vaporized fraction, bearing substantial portions of the oil in solution, is migrated to form an independent gas condensate, and residual oil formed in this fashion bears internal evidence of fractionation. There are several ways that result in reservoired oil over-saturated with gas. One typical situation is upward migration and pressure depletion. The other case is extra gas charged in (Dzou and Hughes, 1993; Curiale and Bromley, 1996; Napitupulu *et al.*, 2000). The result is the single phase fluid separates into an oil-saturated gas phase and a gas-saturated oil phase (Thompson, 1987, 1988). The frequency of phase fractionation and occurrence of derived gas condensates depends on geological conditions such as the frequency of fault movement (Dzou and Hughes, 1993; Losh *et al.*, 2002) since fault activities take vital role to connect source kitchen and reservoirs in most geological situations. The availability of extra gas to supply the reservoir is also essential for the occurrence of phase fractionation (Curiale and Bromley, 1996; Napitupulu *et al.*, 2000).

Thompson (1987) postulated that many of the gas condensates in the Gulf of Mexico basin resulted from phase fractionation. Thompson's concepts were supported by Larter and Mills (1991), who performed experiments to determine the compositional changes that a migrating fluid undergoes. There is evidence in the literature that phase fractionation occurs in many areas around the world (Dzou and Hughes, 1993; Meulbroek *et al.*, 1998; Huang, 2000; Masterson *et al.*, 2001).

On the basis of aromaticity and paraffinicity relationships, evaporative gas condensates are distinguishable from those generated by thermal cracking. Thompson (1987; 1988) proposed some molecular parameters to recognize phase fraction process. In the phase fractionation process, low molecular weight saturated hydrocarbons are preferentially incorporated into the vapour phase, relative to aromatic components, and tend to remigrate from the original reservoir. Remigrated oils and derived condensates are generally reservoired at shallower depths and enriched in light *n*-alkanes relative to the parent oil. By comparison, residual oils are generally found in deeper reservoirs and deplete the light components and increase in aromatic hydrocarbons relative to *n*-alkanes.

The effect of phase fractionation on saturated and aromatic biomarker and carbon isotope indicators commonly measured in crude oils and condensates have been documented in variety of studies (Thompson, 1987, 1988; Larter and Mills, 1991; Dzou and Hughes, 1993; Curiale and Bromley, 1996; Hunt, 1996; van Graas *et al.*,

2000). Recognition of the process of phase fractionation and understanding its effect on petroleum composition are critical because molecular and isotopic geochemical parameters are widely used in oil-to-oil and oil-to-source correlations as well as indicators of alteration, source type and thermal maturity.

1.1.5 Deasphalting

The asphaltenes are the largest molecules dissolved in oil, with about 70 carbon atoms per molecule and they become insoluble when the oil becomes charged with much gas and they precipitate to form a feature known as a solid bitumen or tar mat (Wilhelms and Larter., 1994). This process is called deasphalting, leaving oil with a higher API gravity. Laboratory or refinery deasphalting is used to remove complex components from oil by adding light hydrocarbons, such as pentane or hexane. Deasphalting of petroleum can occur with increasing thermal maturation or when methane and other gases that escape from deep reservoirs enter a shallower oil reservoir (Mossman and Nagy, 1996). Some solid bitumen, characterized by a high abundance of asphaltenes, polar compounds and sulfur, may be formed by deasphalting of an original oil (George *et al.*, 1994). Several large oilfields in the world have thick tarmats, the Prudhoe bay field in Alaska and the Oseberg oilfield in the North Sea both having tar mats greater than 10 meters in thickness at the base of the oil column in the trap (Wilhelms and Larter, 1994). Tarmats complicate the production of the oil and often in oil fields with tarmats present asphaltene deposits also form in the production piping causing production problems and blockages.

1.1.6 Sulfate reduction

When oil is in contact with dissolved sulfate, it is thermodynamically unstable and some redox-reactions may occur (Peters and Fowler, 2002). Sulfate reduced by hydrocarbons bacterially is called bacterial sulfate reduction (BSR) while the abiological reduction of sulfate is referred to thermochemical sulfate reduction (TSR). BSR is common in diagenetic settings up to about 60-80 °C. Above this temperature range, almost all sulfate-reducing microbes cease to metabolize. TSR begins in the range 127-140 °C, depending on the hydrocarbons in the reservoir, and higher temperatures are required to initiate TSR for methane than for heavier hydrocarbons (Worden and Smalley, 1996; Machel, 2001).

Their geologically and economically significant products are similar. BSR is geologically instantaneous in most geologic settings. Rates of TSR are much lower, but still geologically significant. The main organic reactants for BSR are organic acids and other products of aerobic or fermentative biodegradation. The main organic

reactants for TSR are branched and *n*-alkanes, followed by cyclic and mono-aromatic species, in the gasoline range. Sulfate is derived almost invariably from the dissolution of gypsum and/or anhydrite (Machel, 2001).

TSR is a less common alteration process whereby methane, and sometimes other hydrocarbons in the petroleum react with sulfate ion in the formation waters to produce hydrogen sulfide and remove the hydrocarbon lowering the value of the deposit. Hydrogen sulfide rich gases associated with TSR are common features of petroleums found in deep reservoirs in the Gulf of Mexico area USA (Claypool and Mancini, 1989) and Alberta, Canada (Krouse *et al.*, 1989).

With increasing thermal maturation of crude oil, saturated hydrocarbons increase relative to aromatic hydrocarbons (Tissot and Welte, 1984). The opposite trend occurs during TSR due to the greater reactivity of saturated compared to aromatic hydrocarbons. The concentration of aromatic sulfur compounds increases with H_2S content during TSR because these compounds are formed as by-products. Changes in the composition of gasoline-range hydrocarbons caused by TSR can complicate correlation of condensates (Peters and Fowler, 2002 and references therein).

1.1.7 Mixing

Mixing, a very common process in geological situations, has significant influence on oil composition and property. One case is mixing of crude oils with different maturities when they were expelled from the source rocks. Petroleum generation is a dynamic process that occurs over a long (geologic) time scale, with late charged oils being more mature. When two oils mix in the reservoir, their physical property and chemical composition are unlike either end members and their maturity indicators conflict in different components (England *et al.*, 1987). A more complicated filling/charge situation is when the first oil charge is subjected to biodegradation and the later charges mix in the reservoir, resulting in non-biodegraded and biodegraded oils within the same reservoir interval. The other case is two separated charges (not necessary from the same source) mix biodegraded oils with non-biodegraded oils. In some scenarios that biodegradation of previous charge oil is severe enough to remove the *n*-alkanes and isoprenoids, affect the steranes, and convert a significant fraction of the hopanes to their demethylated hopane homologs, while late charge oil is not altered. The mixed oil contains both 25-norhopanes and *n*-alkanes (Rooney *et al.*, 1998; Koopmans *et al.*, 2002). In many other cases, biodegradation is not severe enough to form large quantity of 25-norhopanes, but gas chromatographic (GC) analysis of the composite oil can clearly indicate such mixing process since a large unresolved mixture (UCM) is generally a common signature for this process.

In-reservoir mixing between biodegraded and fresh oils has dominant control on bulk and molecular composition of present crude oils (Cassani and Eglinton, 1986; Barnard and Bastow, 1991; Horstad and Larter, 1997; Masterson *et al.*, 2001; Koopmans *et al.*, 2002; Larter *et al.*, 2003). This explains why, so frequently, geochemical biodegradation level schemes fail to work even when only one oil charge appears to be present based on the proportions of resolved to unresolved GC components. Oil mixing is the primary control on present oil properties such as viscosity/API gravity. Larter *et al.* (2003) proposed that fresh charge mixing concurrent with biodegradation is the key to understanding oil composition and properties in degraded oilfields.

1.2 Biodegradation conditions

There are a number of conditions necessary for biodegradation of petroleum: a) low reservoir temperature, < 100 °C usually 20-60 °C; b) the presence of water or other type of electron acceptor (Fe, SO_4^{2-}, N, Mn); c) an oil-water contact; d) the presence of microorganisms; e) nutrients (e.g. nitrate, phosphate) (Connan, 1984; Palmer, 1993; Wenger *et al.*, 2002; Larter *et al.*, 2003).

1.2.1 Temperature

Reservoir temperature is the primary control on the degree of biodegradation. The reservoir temperature must be less than about 80 °C, which corresponds to depths shallower than about 2000-2500 m under typical geothermal gradients. Connan (1984) proposed that the upper limit for bacteria surviving appears to be 100 °C, as no bacteria were found, in several basins, at temperatures above 88 °C. This is close to the maximum biodegradation temperature of 80 °C given by Palmer (1993). Oils from shallower, cooler reservoirs tend to be progressively more biodegraded than those in deeper, hotter reservoirs. At 80 °C the probability of finding oils in reservoirs degraded to PM level 5 is close to 0 while at 50 °C it is near 0.7 (Pepper and Santiago, 2001). Bernard and Connan (1992) concluded reservoirs are sterile above 80 °C and Wilhelms *et al.* (2001) further suggested a 80 °C 'cut-off' temperature and inferred this temperature as the deadline for deep subsurface biosphere.

However, not all oils discovered in shallow reservoirs are biodegraded. Wilhelms *et al.* (2001) proposed an explanation for this observation. They suggested that if an oil reservoir has been heated to more than 80 °C, the reservoir is paleopasteurized and not recolonized even after the basin was uplifted. Therefore, oil reservoirs that have experienced significant uplift may contain non-degraded oil, despite the currently shallow depth and low temperature of the reservoir. The other possibility for the

occurrence of non-biodegraded oils in shallower reservoir is purely recent charge, where bacterial have no enough time to degrade oils. An oil-charged reservoir at < 50 °C, charged over a long period of time, has a greater biodegradation risk than a reservoir that was rapidly charged recently, but still under 50 °C (Yu *et al.*, 2002). Therefore, reservoir temperature history, rather than present temperature and the residence time of oil in the reservoir are two primary control factors for petroleum biodegradation risk.

Biodegraded oils can be found in hotter reservoirs but this is usually put down to subsidence and reburial of once shallow reservoirs (Palmer, 1993; Peters and Fowler, 2002).

1.2.2 Salinity

Salinity is also important as biodegradation limits are controlled by an interdependent relationship of temperature and water salinity (Grassia *et al.*, 1996). Mille *et al.* (1991) used a mixed bacterial community (EH1) isolated from a marine sediment to investigate varying concentration of sodium chloride (0 to 2 mol/l) effect on the biodegradation of the Ashtart crude oil. They found that the amount of oil degraded increased initially with increasing salt concentrations to a maximum level for 0.4 mol/l NaCl concentration. Thereafter the amount of oil degraded decreased with increasing salt concentrations. Diaz *et al.* (2000) isolated two bacterial consortia from a North Sea crude oil and from sediment associated with mangrove roots, which were able to degrade both aliphatic and aromatic hydrocarbons very effectively in seawater (35 g/L NaCl) and synthetic media containing 0 to 100 g/L NaCl (1.7 M). They noticed that salinities over twice that of normal seawater decreased the biodegradation rates. However, even at the highest salinity biodegradation was still significant. Results obtained during a bioremediation test indicated that microbial degradation of all the dispersants decreased with increasing salt concentration (Okpokwasili and Odokuma, 1990). Although it is difficult to assign a salinity value at which hydrocarbon biodegradation becomes severely limited, highly saline formation waters may inhibit bacterial degradation and effectively shield oils from oil-quality deterioration (Wenger *et al.*, 2002). This consideration is very important when reservoirs are related with abundant diapiric salt.

1.2.3 Nutrients and electron acceptors

Biodegradation in oil reservoirs requires that water, nutrients and hydrocarbons are available to sustain bacterial communities. The rates and mechanisms of degradation remain poorly understood, and therefore our ability to predict the

occurrence of biodegraded oils remains poor. However, oil fields at moderate subsurface depth harbor a complex microbial community that is being characterized in increasing detail (Voordouw *et al.*, 1992). The metabolic potential of these communities is characterized by an abundance of electron donors (e.g. aliphatic and aromatic hydrocarbons, and organic acids), but a shortage of electron acceptors (in increasing order of redox potential; CO_2, sulfur and sulfate, ferric iron, nitrate and oxygen) (Telang *et al.*, 1997).

Transport of oxygen to fuel hydrocarbon degradation in petroleum reservoirs through deep aquifers seems unlikely (Horstad *et al.*, 1992); however, water movement may enhance mineral dissolution and release nutrients such as phosphate, promoting microbial activity. Phosphorus and nitrogen are essential for the survival of virtually all living organisms. Ideally, nutrient concentration in contact with oil should be sufficient to support the maximal growth rate of oil-degrading microorganisms. However, in petroleum reservoirs, these nutrients can be quite scarce and can represent limiting elements for growth of subsurface microorganisms. Numerous studies from ground water samples suggested that mineral weathering by bacteria is driven by the nutrient requirements of the microbial consortium. The progression of mineral weathering may be influenced by a mineral's nutritional potential, with microorganisms destroying only beneficial minerals (Bennett *et al.*, 1993; 2000; 2001; Rogers *et al.*, 1998; Ehrenberg and Jakobsen, 2001). It can be inferred that the subsurface distribution of microorganisms in reservoir biodegradation may, in part, be controlled by the mineralogy and by the ability of an organism to take advantage of mineral-bound nutrients. In petroleum reservoirs the key nutrients are probably supplied diffusively from mineral dissolution reactions for hydrocarbon degradation in aquifers. This situation is most likely to occur at the oil-water contact (OWC) although it is also possible for bacterial communities to grow at interfaces between mineral grains, bound water and hydrocarbons in pore spaces throughout the oil column.

It is obvious that oil biodegradation rate is not limited by electron donor supply (i.e. hydrocarbons) but by supply of nutrients or oxidants. This implies supply of nutrients or electron acceptor to the site of degradation is a major factor controlling rate and extent of subsurface oil biodegradation, with diffusion of nutrients in the water leg probably being adequate to supply the degrading biosphere with nutrients (Larter *et al.*, 2003; Head *et al.*, 2003). Since the obvious scarcity of nutrient supply from mineral dissolution by formation water, the organisms in petroleum reservoirs were probably starved (Röling *et al.*, 2003).

1.2.4 Aerobic vs. anaerobic biodegradation

Aerobic biodegradation of hydrocarbons dominated thinking in western literature about the mechanisms of subsurface oil biodegradation for many years (Winters and Williams, 1969; Evans *et al.*, 1971; Hunt, 1996). In the past it has been thought that fresh, oxygenated waters contain large quantity of aerobic bacteria to drive oil biodegradation (Plamer, 1993). Sufficient oxygen and nutrient supply for the action of aerobic bacteria in undeveloped reservoirs was assumed to be provided by meteoric waters. Although oxygen is a viable oxidant in shallow diagenetic conditions, dissolved oxygen is limited in ground water. Aerobic biodegradation requires large amounts of water to transport the necessary oxygen, even if the ground water is oxygen saturated. Horstad's *et al.* (1992) conservative mass balances indicated that the volumes of water needed to transport sufficient oxygen are impossible in most geological cases. Even where meteoric water has flushed basins, oxygen was hardly carried to the deep reservoirs since oxygen is readily consumed with reactive organic matter and pyrite in shallow strata (Larter *et al.*, 2003). It is therefore almost certain that oil biodegradation in deep subsurface petroleum reservoirs proceeds via anaerobic microbial metabolism rather than by aerobic mechanisms.

Where oxygen is limited biodegradation continues under anaerobic conditions, although for most hydrocarbons degradation will continue at a slower rate (Baedecker *et al.*, 1993). As result alternative electron acceptors such as NO, SO_4^{2-}, Mn^{4+}, Fe (III) and CO_2 are reduced as organic compounds are oxidized. There have been many papers published on anaerobic processes in recent years. While no convincing data on anaerobic hydrocarbon degraders from petroleum reservoirs exist, they have been isolated frequently from hydrocarbon-polluted environments. These strains are able to metabolize mono- and polycyclic aromatic hydrocarbons or alkanes under denitrifying, iron-, sulfate-reducing, and methanogenic conditions (Baedecker *et al.*, 1993; Hunkler *et al.*, 1998; Holliger and Zehnder, 1996; Widdel and Rabus, 2001). Some metabolites such as two classes of aromatic acids: (i) benzylsuccinate, *E*-phenylitaconate, and their methyl homologs, and (ii) benzoate, and methyl-, dimethyl-, and trimethylbenzoates are proposed as potential indicators of *in situ* anaerobic alkylbenzene (Beller, 2000). Metabolites isolated from oil samples including 5,6,7,8-tetrahydro-2-naphthoic acid and two isomers of decahydro-2-naphthoic acid are indicative of anaerobic hydrocarbon degradation in sub-surface oil reservoirs (Aitken, 2004).

Iron is potentially a major electron acceptor in the subsurface. Depending on the environment of deposition various forms of ferric iron can be incorporated into the

sediment in significant concentrations, providing an additional source of oxidation potential. Lovley and Phillips (1986) studied the potential for ferric iron reduction with complex organic matter amongst other components as electron donors with sediments from freshwater and brackish water sites. Their results indicated that Fe (III) reduction is of major importance in the anaerobic degradation of organic matter in sediments. Microorganisms have been observed reducing Fe (III) in clay minerals and have been recognised as an important mechanism in the oxidation of pollutants in soils and sediments (Ernstsen *et al.*, 1998). This could possibly imply that the microbial reduction of Fe (III) might also provide a mechanism for the oxidation of hydrocarbons in reservoirs (Ernstsen *et al.*, 1998; Vargas *et al.*, 1998).

Anaerobic bacteria that might contribute to oil alteration during biodegradation are frequently encountered in oil and gas fields (Bernard and Connan, 1992). Of particular interest in this study is the widespread occurrence of sulfate-reducing bacteria in oil reservoirs (Mueller and Nilsen, 1996). Sulfate reduction in oil reservoirs is often observed when sulfate-rich sea waters are injected into the reservoir during secondary oil recovery. Pure cultures of sulfate-reducing bacteria were isolated from sediments and formation water. *n*-Alkanes, alkylbenzenes, polycyclic aromatic hydrocarbons like naphthalene, methylnaphthalene, phenanthrene, fluorene and fluoranthene were found to be degradable under sulfate-reducing conditions (Coates *et al.*, 1996; Caldwell *et al.*, 1998; Wilkes *et al.*, 2000).

The capacity of denitrifying bacteria for anaerobic utilization of hydrocarbons was reported in various studies. Ehrenreich *et al.*, (2000) investigated variations of different chain length *n*-alkanes during enrichment cultures containing nitrate as electron acceptor. Quantification of substrate consumption and cell growth revealed the capacity for complete oxidation of alkanes under strictly anoxic conditions, with nitrate being reduced to dinitrogen. Wilkes *et al.* (2003) recently reported the formation of metabolites during anaerobic biodegradation of saturated hydrocarbons directly from crude oil under denitrifying condition. Azoarcus-like strain HxN1 can utilise C_6-C_8 *n*-alkanes anaerobically as growth substrates.

Methanogenic biodegradation of aromatic and aliphatic hydrocarbons has also been demonstrated to be a significant process for in-reservoir biodegradation (Larter *et al.*, 1999; Pallasser, 2000). Methanogenesis requires no exogenously supplied oxidant, as inorganic carbon produced from organic material can be used or methanogenesis can proceed through disproportionation reactions (Mueller and Nielsen, 1996; Nazina *et al.*, 1995). Since there is no direct biochemical pathway available to derive methane from petroleum, many geochemists have difficulty

accepting the concept that methane can be generated from the biodegradation of petroleum. Nonetheless, there have been numerous environmental studies that have observed high methane concentrations in soil and groundwater contaminated by refined petroleum products (Scott *et al.*, 1994; Hunkeler *et al.*, 1998; Zengler *et al.*, 1999). Methanogenesis is a likely fate for most carbon dioxide produced during biodegradation and microbial methane production from carbon dioxide reduction may be a major process in subsurface petroleum degradation.

Correlation between biodegraded oils and biodegraded dry gas lead Pallasser (2000) to propose the "secondary biogenic gas" concept that refers to the gas formed from the bacterial destruction of oil. He linked the processes of methanogenesis and oil biodegradation by the prominence of methanogenic CO_2 in these types of accumulations along with some isotopically-depleted methane. Röling *et al.* (2003) speculated that methanogenesis through carbon dioxide reduction may be a dominant terminal process in petroleum biodegradation in the subsurface as biodegraded petroleum reservoirs are often associated with abundant methane, rarely contain anomalous carbonate mineralization and usually show carbon dioxide contents comparable to equivalent non-degraded petroleums.

1.3 Biodegradation effect on petroleum compositions

1.3.1 Physical properties, bulk composition and isotopic composition

Biodegradation of crude oil in reservoirs has major economic consequences. Increasing levels of biodegradation generally cause a decline in oil quality, diminishing the producibility and value of the oil (Hunt, 1996; Wenger *et al.*, 2002). The effects of biodegradation on the physical properties and bulk composition of petroleum have been summarized by numerous studies. With increasing biodegradation, oils become more viscous, richer in sulfur, resins, asphaltenes, and metals (e.g. Ni and V), increase in total acid numbers and have lower API gravities (Volkman *et al.*, 1984; Connan, 1984; Miiller *et al.*, 1987; Palmer, 1993; Peters and Moldowan, 1993; Meredith *et al.*, 2000). For example, in a set of genetically related oils from Oklahoma, Miiller *et al.* (1987) found the following changes in oil properties and bulk compositions with increasing levels of biodegradation (Table 1-1).

Table 1-1 Changes in oil properties with increasing levels of biodegradation (after Miiller *et al.*, 1987)

	API (°)	Sulfur (wt%)	Vanadium (ppm)	Nickel (ppm)	Saturate (%)	Aromatic (%)	Polar (%)	Asphaltene (%)
Non-degraded Oil	32	0.6	30.6	16.4	55	23	21	2
Moderately Biodegraded Oil	12	1.6	224	75.1	25	21	39	14
Heavy Biodegradation(Tar Sand)	4	15	137.5	68.5	20	21	41	21

In general, biodegraded oils are less desirable because they are difficult to produce and they pose problems for refineries due to high sulfur and asphaltene content. The sulfur in biodegraded oil can be utilized by bacteria in the production waters to form H_2S which is toxic and will damage production and refinery equipment. High amounts of asphaltene in the biodegraded oils will slow down their flow ability and cause serious production problems. More risk is associated with exploration and development opportunities where biodegradation might adversely affect the quality of petroleum and make the investment fail (Evans *et al.*, 1971; Connan, 1984; Volkman *et al.*, 1984; Rowland *et al.*, 1986; Palmer, 1993; Hunt, 1996; Wenger *et al.*, 2002).

The effects of biodegradation on isotopic compositions consistently lead to enrichment in ^{13}C for each remaining hydrocarbons, due to preferential removal of ^{12}C since the bond energy between ^{12}C–^{12}C is lower than ^{13}C–^{12}C bonds. The level of enrichment in ^{13}C can reflect either the differences in the susceptibilities to biodegradation of different components or degree of biodegradation one component has experienced. Biodegradation effects on bulk oil isotopic compositions are generally minimal, i.e. 1-2‰, while different fractions show different behaviour. The carbon isotopic effects of biodegradation show a decreasing level of isotopic enrichments in ^{13}C with increasing molecular weight. In some lighter components such as C_{6-7}-alkanes, benzene and toluene, isotopic fractionation caused by biodegradation is quite distinct, while C_{15+} components undergo less significant isotopic fractionation as a result of biodegradation (Masterson *et al.*, 2001; George *et al.*, 2002). This suggests that the kinetic isotope effect associated with biodegradation is site-specific and often related to a terminal carbon, where its impact on the isotopic composition becomes progressively `diluted' with increasing carbon number.

One distinct feature for oil biodegradation is associated with isotopically light methane and methanogenic CO_2. The methane in some shallow reservoired gas accumulations is marked by bacterial genetic isotopic characteristics, while the carbon isotopic values in associated CO_2 show great variations (Sweeney and Taylor, 1999; Pallasser, 2000; Masterson *et al.*, 2001).

1.3.2 Aliphatic hydrocarbons

There is an extensive literature on the effects of biodegradation on aliphatic hydrocarbon compositions (Goodwin *et al.*, 1983; Connan, 1984; Palmer, 1993; Peters and Moldowan, 1993; Hunt, 1996). Different classes of compounds in petroleum have different susceptibilities to biodegradation. Biodegradation proceeds along a path of stepwise depletion of compound classes. Among the aliphatic hydrocarbons, the normal alkanes are removed first followed by loss of acyclic

isoprenoids (e.g., norpristane, pristine, phytane, etc.). As *n*-alkanes and acyclic isoprenoids are removed by microbial action, the elevated chromatographic baseline consisting of complex unresolved compounds becomes more prominent. Discrete peaks protruding above the elevated baseline are the more resistant compounds, such as hopanes. Compounds derived from natural products by molecular rearrangement are usually biodegraded less rapidly than the non-rearranged hydrocarbons. For example, diasteranes are less readily biodegraded than steranes (Seifert and Moldowan, 1979; Mackenzie, 1984).

Although slight differences existed among different studies, a rough removal order for aliphatic hydrocarbons can be established as follows (From most susceptible to least susceptible): *n*-alkanes > alkylcyclohexanes > cyclohexanes > acyclic isoprenoids > bicyclic alkanes > C_{27}-C_{29} steranes > C_{30}-C_{35} hopanes > diasteranes > C_{27} -C_{29} hopanes > C_{21}-C_{22} steranes > tricyclic terpanes (Goodwin *et al.*, 1983; Volkman *et al.*, 1984; Connan, 1984). However, even the tricyclic terpanes can be degraded as biodegradation proceeds (Peters, 2000; Alberdi *et al.*, 2001).

1.3.3 Aromatic hydrocarbons

The effects of biodegradation on aromatic hydrocarbon distributions have been investigated in oil reservoirs, surface spills and in laboratory experiments by numerous studies (Volkman *et al.*, 1984; Rowland *et al.*, 1986; Fisher *et al.*, 1996; Thierry *et al.*, 1996; Budzinski *et al.*, 1998; Trolio *et al.*, 1999). The biodegradation of PAHs is highly dependent on the number of aromatic rings they consist of and the rate of biodegradation decreases with increasing number of aromatic rings (Volkman *et al.*, 1984; George *et al.*, 2002). The lower molecular weight and more water-soluble compounds usually degrade in preference to higher molecular weight and less water-soluble compounds (Tissot and Welte, 1984; Lafargue and Thiez, 1996). Similarly for aromatic hydrocarbons alkylbenzenes are removed before diaromatic and triaromatic hydrocarbons (Volkman *et al.*, 1984) with aromatic steroid hydrocarbons being resistant until very severe levels of biodegradation (Peters and Moldowan, 1993). The alkylation is another critical factor that controls the rate of biodegradation and level of biodegradation decreases with increasing number of alkyl substituents (Volkman *et al.*, 1984; Palmer, 1993; Fisher *et al.*, 1996; George *et al.*, 2002). Within compound classes, however, some isomers are more susceptible to biodegradation than others, which are controlled by the position of the alkyl substituents. Field studies of oil and ground water revealed that 1,2,3-trimethylbenzene and 1,2,3,4-tetramethylbenzene are more resistant to biodegradation than other C_3- and C_4-alkylbenzenes (George *et al.*, 2002 and reference therein). Under reservoir conditions dimethylnaphthalenes with β

substituents are readily biodegradable (Volkman *et al.*, 1984), an observation also made by Fisher *et al.* (1996) in oil contaminated sediments. The most resistant trimethylnaphthalenes and tetramethylnaphthalenes (Rowland *et al.*, 1986; Fisher *et al.*, 1996) also have been identified. Alkylnaphthalenes with methyl substituents at the 1and 6 positions have been reported to be less resistant to biodegradation (Fisher *et al.*, 1996). Alkylphenanthrenes with substituents at the 9 or 10 positions have been reported to be more resistant to biodegradation than alkylphenanthrenes with substituents at other positions (Rowland *et al.*, 1986; Budzinski *et al.*, 1995).

Aromatic steroid hydrocarbons are highly resistant to biodegradation and they are degraded only in some extreme conditions. Monoaromatic steroid hydrocarbons appear to be more resistant to biodegradation than the triaromatic steroid hydrocarbons (Lin *et al.*, 1989). In severely biodegraded oils Volkman *et al.* (1984) found the absence of C_{20} and C_{21} triaromatic hydrocarbons. There is a preferential depletion of the 20R isomers in the mono- and triaromatic steroids and the C_{26} homologues compared with the higher homologues (Wardroper *et al.*, 1984; Lin *et al.*, 1989; Cassani and Eglinton, 1991).

There are at least two major pathways known for the aerobic degradation of alkyl aromatic hydrocarbons; oxidative attack on aromatic ring carbons and oxidation of the alkyl carbons (Sabate *et al.*, 1999; Vila *et al.*, 2001; Dean-Ross *et al.*, 2002). PAHs are typically thought to be recalcitrant to biodegradation without oxygen as a reactant (Genthner *et al.*, 1997). However, recent results demonstrate that both monoaromatic compounds and PAHs can be degraded anaerobically. Laboratory experiments have shown that $C_{1\text{-}5}$-alkylbenzenes can be removed selectively from crude oil by sulfate-reducing bacteria (Wilkes *et al.*, 2000). Bicyclics and PAHs biodegradation were observed under nitrate- and sulfate-reducing conditions in PAH-contaminated sediments (Rockne and Strand, 1998). It is now generally agreed that multiple redox environments involving, among others, iron reduction and methanogenesis, do play an important role in anaerobic microbial oil degradation and that water may also be directly involved (Bennett *et al.*, 1993; Harwood *et al.*, 1998; Zengler *et al.*, 1999; Heider *et al.*, 1999; Rockne and Strand, 2001).

1.3.4 Carbazoles

Carbazole is a tricyclic aromatic nitrogen compound which may be alkylated and annelated to form two main series of derivatives, namely alkylated carbazoles and alkylated benzo- and dibenzocarbazoles. These compounds are common constituents of crude oils and source rocks and are readily analyzable (Li *et al.*, 1995; Larter *et al.*, 1996a; Harrison *et al.*, 1997; Clegg *et al.*, 1998a; Horsfield *et al.*, 1998). Atlas (1981)

provided some early general observations about the ability of microbes to metabolize petroleum compounds, indicating that heteroaromatic NSO compounds with a small number of rings might be biodegradable. Fedorak and Westlake (1984) reported the degradation of a wide range of alkylcarbazoles (C_1 to C_5) contained in a Norman Wells crude oil by an oil-degrading mixed bacterial culture enriched by growth on carbazole. Their results showed that most of the C_1-, C_2-, and C_3-alkylcarbazoles and one of the C_4-alkylisomers were degraded aerobically within 8 days. Zhang *et al.* (1999) noticed a reduction in alkylcarbazole concentrations and variation in isomer ratios with increasing degree of biodegradation in some Chinese lacustrine oils. Mueller *et al.* (1989) provided an overview of biodegradation for a similar range of compounds, with reference to environmental contamination by creosote. They cited several laboratory studies where the biodegradation of polycyclic aromatic hydrocarbons (PAHs), heteroaromatic compounds and phenolic compounds had been demonstrated and where specific strains of microbes able to utilize these compounds have been isolated from environmental samples. Dyreborg *et al.* (1997) investigated the potential of groundwater microorganisms to degrade selected NSO-compounds under four redox conditions over a period of 846 days. Carbazole was fast degraded in aerobic microcosms, and pyrrole and 1-methylpyrrole were more slowly degraded. The anaerobic degradation rate was significantly slower than the aerobic degradation rate.

Ouchiyama *et al.* (1993) proposed an aerobic carbazole degradation pathway by *Pseudomonas spp.* CA06 and CA10, and they identified anthranilic acid and catechol as the main metabolites. The *meta*-cleavage enzymes of the two strains for biphenyl-2,3-diol were induced during growth on carbazole. Shotbolt-Brown *et al.* (1996) isolated three different bacteria which were capable of mineralizing carbazole. Schneider *et al.* (2000) isolated *Ralstonia sp.* RJGII.123 and suggested that it used carbazole as a sole source of carbon and nitrogen. At least 10 ring-cleavage products of carbazole degradation were identified, including anthranilic acid, indole-2-carboxylic acid, indole-3-carboxylic acid, and (1H)-4-quinolinone. Kirimura *et al.* (1999) noted that *Sphingomonas sp.* CDH-7 can use carbazole as a sole source of carbon and nitrogen, and metabolized carbazole to ammonia via anthranilic acid as an intermediate product.

1.3.5 Alkylphenols

Biodegradation has a strong impact on the production and destruction of the alkylphenols. Most work on phenol biodegradation has been in contaminated aquifers and laboratory scale (see Broholm and Arvin, 2000 for summary). Phenol and

alkylphenols can be biodegraded under both aerobic and anaerobic conditions. The enzymic mechanism for the catabolism of phenols is inducible in many bacteria, fungi and yeasts, and involves hydroxylation of the aromatic nucleus by either a monooxygenase or phenol oxidized enzyme to form an *ortho*-dihydroxybenzene (Hinteregger *et al.* 1992; Semple and Cain, 1997). It is also possible that alkylphenols may be formed as by-products during the microbial alteration of aromatic hydrocarbons in crude oil because alkylphenols are intermediates in a number of aromatic hydrocarbon degradation pathways (Broholm and Arvin, 2000).

There are relatively few reported field studies of phenol biodegradation under petroleum reservoir condition. Biodegradation may result in diminished alkylphenol concentrations in oil. Taylor *et al.* (2001) noticed that biodegradation of crude oils reduced the total abundance of alkylphenols and highly alkylated C_2- and C_3-alkylphenols are depleted more significantly, while water washing preferentially removed the phenol and cresols leaving relatively enhanced C_2- and C_3-alkylphenol distributions. Lucach *et al.* (2002) made similar observations while they studied the migration effects on the Dhahaban petroleum system in Oman. However, previous studies of phenol biodegradation have focused on the concentrations of total phenol compounds and the different homologue groups. There is little information on the potential for biodegradation of individual phenolic isomers within a group.

1.3.6 Carboxylic acids

Biodegradation has been suggested as a cause of highly acidic oils (Jaffé and Gallardo, 1993), and Mackenzie *et al.* (1983) argued that the high acidity of an oil generally implied that biodegradation was ongoing, or had occurred in the recent past. The occurrence of phytanic acid has been reported to be an indicator of the early stages of biodegradation (Mackenzie *et al.*, 1983). The reduction in acid molecular weight with the extent of biodegradation, observed by Mackenzie *et al.* (1983) is consistent with the mechanisms of alkane degradation. The alkanes are bioxidised through a series of intermediaries to form *n*-alkanoic acids. These acids then undergo further degradation by oxidative decarboxylation to yield successively smaller acids, ultimately converting the alkanes to CO_2 and water. High molecular weight carboxylic acids have been shown to be biodegraded by microbial populations indigenous to oil sand tailings (Herman *et al.*, 1994). Laboratory microcosm experiments with aquifer material support the hypothesis that organic acids observed in the groundwater originate from the microbial degradation of aromatic hydrocarbons under anoxic conditions (Cozzarelli *et al.*, 1994). Although there have been no detailed studies on the biodegradation of carboxylic acids in petroleum reservoirs, the work by Herman *et*

al. (1994) suggests that such degradation may be possible. Meredith *et al.* (2000) found that both the TAN and yield of acids increased with increasing biodegradation. It is these heterocyclic acids with multiple different heteroatoms that are the main cause of corrosion problems during processing of degraded oils.

As a matter of fact, the principal metabolites of hydrocarbon degradation either aerobically or anaerobically might be carboxylic acids. It has been found that many aromatic compounds such as benzene, toluene and xylenes can be degraded with anaerobic bacteria following similar processes to aerobic bacteria (Phelps and Young, 2001). Generally, the activation step consists of a radical reaction of the hydrocarbon with fumarate, yielding a substituted succinate that is further metabolized (Widdel and Rabus, 2001). Typical intermediates in the anaerobic degradation of aromatic hydrocarbons are (alkyl-)benzoates. 2-Naphthoic acid, and a range of ring reduction products, also indicate anaerobic degradation of aromatic hydrocarbons (Phelps *et al.*, 2002), while 2-methyl fatty acids and fatty acids with even carbon methyl substitutions are other potential markers of anaerobic alkane degradation (So and Young, 1999).

Benzoic acids also occur in fossil fuel contaminated anoxic aquifers where they are assumed to be anaerobic oxidation products of alkylbenzenes (Cozzarelli *et al.*, 1990; Schmitt *et al.*, 1996), however, they have not yet been described to occur in oils and formation waters. Wilkes *et al.* (2000) described a detailed investigation of alkylbenzene degradation in crude oils by the enrichment culture and by two pure strains of sulphate-reducing bacteria isolated from this enrichment culture. Alkylated benzoic acids were the main metabolic products during growth of the enrichment culture and the pure strains on crude oil. They inferred that the same process may occur in oil reservoirs under sulfate-reducing conditions and alkylated benzoic acids may be the dead-end metabolites of partial oxidation of alkylbenzenes.

1.3.7 Biodegradation degree assessment

The effect of biodegradation on the composition of oil has been most comprehensively studied for the saturated petroleum hydrocarbon fraction. Therefore, it is this class of compound which is most widely used in assessing the degree of biodegradation which an oil has undergone. The early stages of oil biodegradation (loss of *n*-alkanes followed by loss of acyclic isoprenoids) can be readily detected by gas chromatography (GC) analysis of the oil. However, in heavily biodegraded oils, GC analysis alone cannot distinguish differences in degree of biodegradation due to interference of the unresolved complex mixture (UCM or "hump") that dominates the GC traces of heavily degraded oils. Among such oils, differences in the extent of

biodegradation can be assessed using gas chromatography-mass spectrometry (GC-MS) to quantify the concentrations of biomarkers with differing resistances to biodegradation. The UCM present on the GC trace of a heavily degraded oil does not affect this GC-MS analysis.

The sequential removal of certain compound classes of the oil during biodegradation forms the base to rank biodegradation scales. Volkman *et al.* (1984) proposed a 9 point scale to classify the degree of biodegradation of a given oil (Table 1-2). Peters and Moldowan (1993) proposed a 1-10 scale (Fig. 1-1) on which the extent of biodegradation of an oil can be ranked based on the analysis of the oil geochemistry (e.g., using the presence or absence of various biomarkers that have different susceptibilities to biodegradation, with "1" indicating very early degradation (partial loss of *n*-paraffins) and "10" indicating severely degraded oil. In this thesis all biodegradation level refers to Peters and Moldowan (1993) scales and abbreviated as PM level.

Table 1-2. The biodegradation scale (after Volkman *et al.*, 1984).

Level	Chemical Composition	Extent of Biodegradation
1	Abundant *n*-alkanes	Not degraded Minor
2	Light-end *n*-alkanes removed	
3	>90% *n*-alkanes; >50% biphenyl and methylbiphenyls removed	
4	Alkylcyclohexanes and alkylbenzenes removed;acyclic isoprenoid alkanes and naphthalene reduced	Moderate
5	Isoprenoid alkanes and methylnaphthalenes removed; selective removal of C_2-naphthalenes	
6	$C_{14} - C_{16}$ bicyclic alkanes removed	Extensive
7	>50% (20R)-5a(H), 14a(H), 17a(H) steranes removed	Very extensive
8	Distribution of steranes and triaromatic steroids altered; demethylated hopanes abundant	Severe
9	No steranes; demethylated hopanes predominate	Extreme

The biodegradation scales have limited applicability for oil quality assessments in some cases because they are focused on heavy and severe biodegradation when complete removal of certain compound series (e.g. *n*-alkanes, isoprenoids) and the alteration of biomarker components occurs. However, the greatest impact on oil quality parameters for conventional production occurs at much lower levels of biodegradation (under PM level 3). In some deepwater offshore plays, oil quality reduction due to biodegradation may render a discovery uneconomic without

proceeding to levels where any of the more resistant biomarker constituents have been altered. More sensitive assessments for lower biodegradation stages are required to relate with oil quality in unpenetrated compartments.

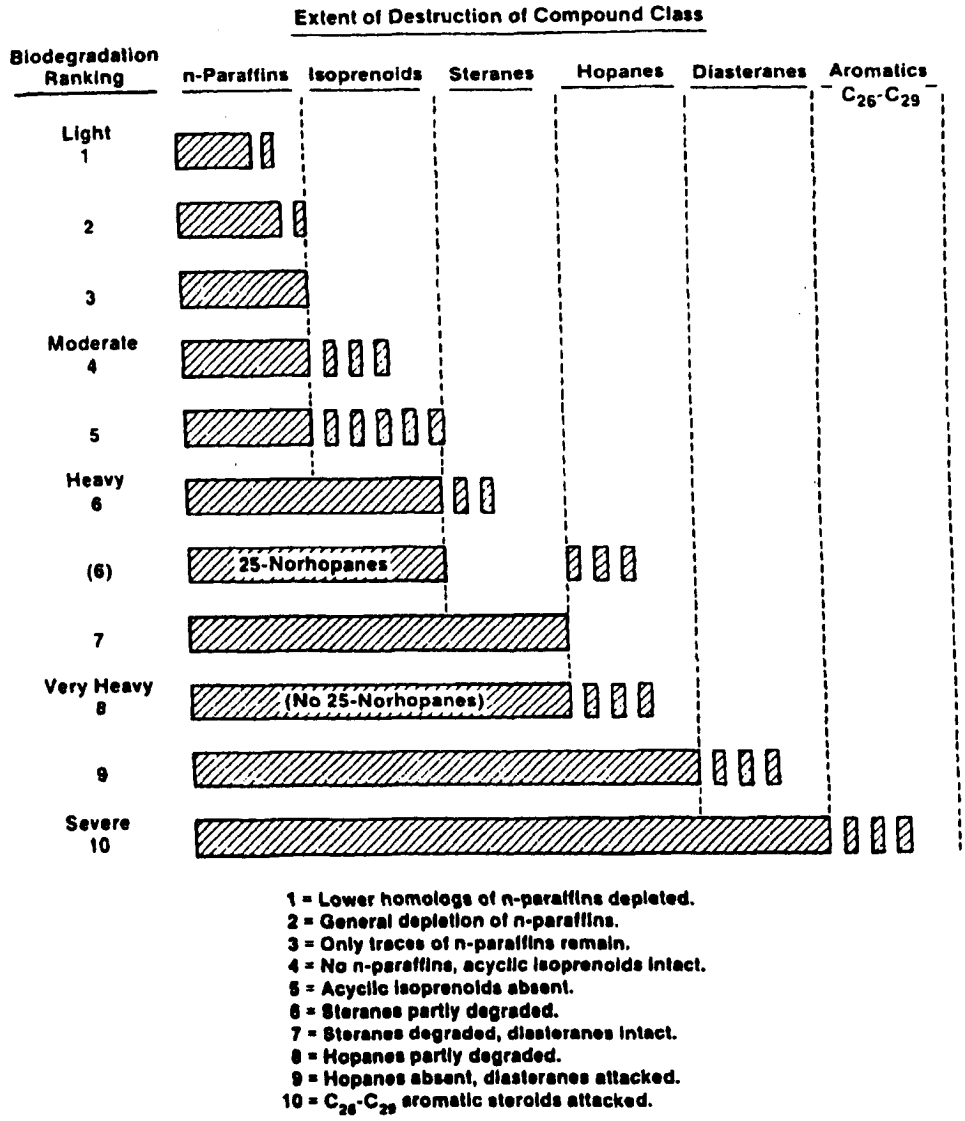

Fig. 1-1 Biodegradation scale produced by Peters and Moldowan (1993) with a 10 point quasi-stepwise biodegradation sequence for the compound groups.

1.4 Quantification and prediction of biodegradation

Although the phenomena of biodegradation have been observed for over half century and numerous empirical descriptions are available in the literature, the quantification of oil loss and biodegradation rate remains a big challenge. Most quantitative laboratory studies are difficult to simulate reservoir conditions since many laboratory simulations use lower temperatures than those in biodegraded reservoirs, or grow the bacteria under low pressures and without any rock matrix (Goodwin *et al.*, 1983; Watson *et al.*, 2002). Also, studies of biodegradation in the natural environment, such as oil spills on beaches, are not directly comparable with

reservoir biodegradation (Fisher *et al.*, 1996). The bacteria at the surface are unlikely to be the same as those that are found in reservoirs, and temperature, pressure, and oxygen availability are very different. The most obvious biodegradation-resistant tracers of original oil mass, such as oil vanadium or nickel content vary in concentration by orders of magnitude as the oils are generated through the oil window (Head *et al.*, 2003). The metal content in the biodegraded oils is hardly to reflect oil mass loss caused by biodegradation if oil maturity varies during charge process.

In an attempt to link qualitative descriptors of oil biodegradation (Volkman *et al.*, 1984; Connan, 1984; Peters and Moldowan, 1993) with quantitative estimates of the mass of oil destroyed, various estimation methods are applied to calculate bacterial consumption (Prince, 1994; Ahsan *et al.*, 1997; Larter *et al.*, 2003).

1.4.1 Internal standards

Chemical techniques for quantifying biodegradation *in situ* are being developed by a number of researchers. One approach involves comparing concentrations of susceptible components relative to conserved compounds. These conserved compounds are usually resistant to bacterial attack. A ratio of the susceptible to the conserved compound(s) concentrations can be used as a biodegradation 'index' (Prince, 1994; Whittaker and Pollard, 1997). For example, hopanes are common constituents of crude oils, and they are very resistant to biodegradation. They can therefore serve as 'conserved' internal standards for assessing the biodegradation of the more degradable compounds in the oil. The depletion of *n*-alkanes can be monitored through evaluation of an [*n*-alkanes/17α(H),21β(H)-hopane] index, where a decrease in the value of the index is presented as evidence of oil biodegradation. Ratios of other components such as isoprenoids, steranes, alkylnaphthalenes and alkylphenanthrenes compared to hopane standard also reflect biodegradation effects. Comparing the initial ratio with end point measures the variation of these components during biodegradation and can estimate the mass loss. These compound groups represent however only the fraction of the oil which appears as resolved peaks on the chromatograms. This approach does not include the unresolved complex mixture and can be referred to as "peaks only".

With the application of 'conserved' internal standards, a number of issues regarding their use are emerging. The assumed microbial recalcitrance of some selected conserved internal markers, such as hopanes, is questionable. There are two important questions that attend such use. The first is whether the 'internal standard' is being created during the biodegradation process itself, for this could result in an overestimate of the extent of biodegradation. The second is whether the 'internal

standard' is indeed resistant to biodegradation; for if it was not, this could result in an underestimate of the extent of biodegradation. In petroleum reservoir such kind of internal standards seem to hardly exist since hopane biodegradation is in no doubt (Volkman *et al.*, 1983; Peters *et al.*, 1996). The use of 'internal standards' in oil has also been challenged because individual compounds have been affected by facies and maturity variation (Moldowan *et al.*, 1985; Peters and Moldowan, 1993).

1.4.2 Volumetric calculation of biodegradation loss

Relating the molecular effect of biodegradation to the amount of oil that has been removed is important in predicting the likely effects upon bulk geochemical and physical properties of degraded oils. Considering the mass balance approach, the saturated hydrocarbons are the clearly most susceptible compound class to biodegradation and two assumptions are made: a) only the saturated fraction is affected by biodegradation; b) no significant formation of non-hydrocarbons (Bacchus unpublished data). Obviously, these two assumptions are not accurate since the aromatic hydrocarbons and even light polar components also biodegraded at varying degree (Volkman *et al.*, 1983; van Aarssen *et al.*, 1999; Huang *et al.*, 2003b). The percentage of oil lost is underestimated. On the other hand, some metabolites such as carboxylic acids are formed during this process (Meredith *et al.*, 2000; Wilkes *et al.*, 2000; 2003). The percentage of oil lost may be overestimated under this consideration. However, our provisional study (Bacchus unpublished result) suggested the amount of metabolites generated during biodegradation is 1-2 orders of magnitude less than the loss of potential precursors. However, this estimate will be only approximate and seems the minim values.

The calculation method is illustrated in Figure 1-2. In a hypothetical case that saturated hydrocarbon fraction was reduced from 50 to 30 wt.%. This means the less susceptible non-saturated compound classes had increased (50 to 70 wt.%). Therefore, the ratio of saturated to non-saturated compound classes (aromatic HCs + polars + asphaltenes) decreased from 1.0 to 0.428. This represents a 57 wt.% loss in the saturated hydrocarbon fraction. Since the saturated hydrocarbons comprised 50 wt.% of the original oil, the total weight loss was 29% mass of the assumed original oil (i.e. 57% of 50%). A similar method was applied by Ahsan *et al.* (1997) to calculate biodegradation effect on the North Sea oil.

Larter *et al.* (2003) used oil charging-biodegradation models to produce broad estimates that oils exhibiting heavy levels of biodegradation (PM 5) have typically lost up to 50% of their mass. Beyond this level of degradation loss of oil mass from marine oils is less significant (ca. only a further 10-20% of original oil mass is lost)

and it seems likely that structural rearrangements predominate subsequent changes in oil composition.

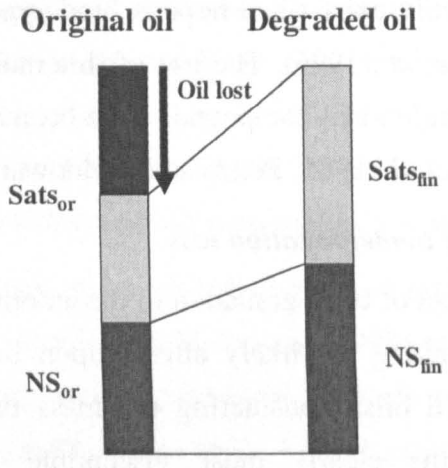

$$\% \text{ original oil lost} = \frac{\%NS_{or} \times \%Sats_{fin}}{\%NS_{fin}} - \%Sats_{or}$$

Fig. 1-2. Method to estimate the amount of oil degraded based on the change in bulk composition of oil (Modified from Ahsan *et al.*, 1997).

1.4.3 Biodegraded oil property prediction

Biodegradation has a deep influence on oil physical properties, which are critical during development of an oilfield since these properties can impact the choice of which reservoir intervals to complete in which wells. Prediction of oil gravity and viscosity variations within an oilfield is important when evaluating the economics of undrilled targets. A variety of studies demonstrated how oil properties in biodegraded oil accumulations can be predicted from core and cutting extracts prior to well testing using geochemical parameters sensitive to biodegradation (Baskin and Jones, 1993; McCaffrey *et al.*, 1996; Smalley *et al.*, 1997; Guthrie *et al.*, 1998; Koopmans *et al.*, 2002). For example, Smalley *et al.* (1997) noted that lateral and vertical variations in oil quality (viscosity, gravity) in a North Slope field were controlled by two phenomena: (1) lateral and vertical variations in the degree of biodegradation; and (2) lateral and vertical variations in fresh oil mixing. The authors identified geochemical parameters that are sensitive to the degree of oil biodegradation and to the quantity of the secondary charge and then developed transforms that related those geochemical parameters to oil quality (viscosity or gravity). Those transforms were used to predict oil quality from geochemical analysis of sidewall cores. Oil property variations caused by different degrees of biodegradation can be mapped throughout a field using a variety of geochemical tools. Such techniques allow the targeting of "sweet-spots" (areas of less degraded oil) within an accumulation that has been affected by

biodegradation.

McCaffrey *et al.* (1996), Guthrie *et al.* (1998) and Koopmans *et al.*, 2002 used a similar approach to predict oil viscosity in a biodegraded heavy oil accumulation. In their studies, chemical properties were calibrated with a set of produced oils of known physical properties and related to (sidewall) core samples. Guthrie *et al.* (1998) developed a predictive model of oil quality based on a sample set of produced oils from Venezuela for predicting viscosity, API gravity, and sulfur content in oil-stained sidewall cores where these properties cannot be measured directly. Koopmans *et al.* (2002) analyzed reservoir core extracts from a single Eocene sandstone reservoir section in the Liaohe basin, NE China. They found the large variation in viscosity can be explained by mixing, to various extents, of heavy biodegraded oils with less degraded oils. They established a simple mixing model, which may assist in predicting the viscosity of reservoired oils before production. Their models can be used to optimize the placement of new wells and completion intervals, and to monitor relative amounts of production from discrete intervals in the well.

1.4.4 Biodegradation rate

A quantitative methodology for the field-scale biodegradation rates has not been fully established. Larter *et al.*, (2003) used whole oil-column minimum rate estimates, diffusion-controlled oil column compositional gradient modeling and mixed oil kinetic models to assess biodegradation rates in oilfields. Biodegradation rate constants (first order) are around 10^{-6}-10^{-7} yr^{-1} for hydrocarbons in the degradation zones these corresponding well with zero order field-wide minimum rate estimates of about 10^{-8} kg hydrocarbons/kg oil/year for the whole oil column. The rate of petroleum biodegradation in the subsurface appears to be limited by available nutrients and not by the carbon source (Larter *et al.*, 2003). Hence, the size of the water leg (which impacts nutrient delivery) impacts degradation rates.

1.5 Aims of the project

The topic of petroleum biodegradation lay largely dormant for around a decade from the early 1980's, not least perhaps because the process was thought to be well understood. The historical view of biodegradation in the reservoir was that it takes place under oxic conditions in western literature, which requires a flow of meteoric water to replenish the molecular oxygen needed by the aerobic bacteria involved. Aerobic oxidation was believed to be dominant since it had not been demonstrated that anaerobic bacteria could degrade saturated hydrocarbons in the laboratory. Petroleum biodegradation became a 'hot topic' again in the 1990's partly due to the

recognition anaerobic biodegradation process. But will an improved basic understanding of this and other mechanisms of biodegradation allow prospect-level prediction of petroleum biodegradation? This suggests the need for a method to reliably and conveniently ascertain a semi-quantitative judgment as to the biodegradation risk for the exploration target. To this end, models are needed to understand the mechanisms of biodegradation and to develop reliable biodegradation rate estimation methods.

A statistical approach on a regional scale normally can present a good trend that degree of biodegradation decreases with increasing burial depth (or temperature), but it is also very common that adjacent reservoirs with similar depths could show very different levels of degradation. This means that uncertainties over a certain temperature range suggests that biodegradation prediction is almost impossible in a specific target. Thus I focused on the local case study in a restricted geographical area with reservoirs of the same age at similar burial depths, but containing petroleum which is variably biodegraded. It is important to notice that the biomarkers and aromatic compounds in the suite of the Lengdong oils clearly indicated the same source rock and similar maturity. The differences in oil properties and chemical compositions are, therefore, attributed to different degrees of biodegradation. An unambiguous compositional gradient is shown from the Es1 and Es3 columns because of different stages of biodegradation and low mixing rate across the fields. This unique case study will provide a basis to perform an investigation of the compositional variations in the various fields as a function of biodegradation and/or mixing and use them to understand the potential biodegradation.

The aims of this project were to further our understanding of the factors which influence the biodegradation of crude oils, and the processes by which these factors interact. In addition, there appears to have been relatively little previous work published on biodegradation effects on polar compounds such alkylphenols and alkylcarbazoles. Quantification methodology of biodegradation is still not fully established. Therefore, a major aim of this study was to assess the role played by biodegradation in controlling the composition of a wide range of crude oils.

Although some efforts have been made to use biodegraded oil signals to optimize field development and predict reservoir fluid quality (McCaffrey *et al.*, 1996; Smalley *et al.*, 1997; Mathur *et al.*, 2001; Koopmans *et al.*, 2002), application of systematic biodegradation studies to production and exploration for conventional crude oil has not been reported. Our current knowledge levels do not allow effective pre-drilling prediction of whether a petroleum accumulation would be degraded or not, nor do

they allow effective evaluation of the extent to which degradation perturbs our ability to make conventional geological interpretations from molecular geochemistry. I have coupled a reservoir geochemical study of a very heavy oil reservoir from NE China with geological constraints in order to investigate intrinsic biodegradation characteristics. The outcome of this study will be used to discuss whether or not a greater understanding of fundamental mechanisms could actually lead to improved prediction of presence of biodegraded petroleum at the prospect level.

2 METHODS

2.1 Iatroscan

The Iatroscan thin layer chromatography and flame ionization detection (TLC-FID) technique can screen petroleum reservoir solvent extracts and provide data appropriate for selection of samples for high-resolution analysis (Karlsen and Larter, 1991). This technique can often be used to obtain preliminary discrimination of petroleum populations by using a SARA type analysis (SARA refers to saturated hydrocarbons, aromatic hydrocarbons, resin, asphaltene) and to provide indicators of polar compound enrichments.

A very fast extraction procedure called 'microextraction' was used for extracting a large suite of samples. In this procedure, finely crushed reservoir sample (ca. 1 g) was mixed with a known amount of solvent (e.g., 5 ml DCM+methanol 93:7 vol%) in a vial, then sealed and agitated. The samples were placed in the dark for 1-2 days and were shaken three times during that period. The solvent extracted bitumen from the samples. The extract was then taken directly out of the vials by syringe, avoiding the need for a concentration step. A 3µl aliquot of the extract was spotted on to a silica gel powder coated rods. Samples were analyzed in duplicate. The rods were sequentially developed in solvents of increasing polarity as follows: Step 1: elution in *n*-hexane up to 100% of silica rod length then air dried for 3 minutes; Step 2: elution in toluene up to 60% of silica rod length then air dried for 6 minutes; Step 3: elution in DCM: methanol 93:7 v/v up to 30% of silica rod length and dried at 60 °C for 90 seconds to remove the residual solvents and for standardizing samples with a large volatile C_{14}-fraction. The rods were scanned through a flame ionisation detector (FID) using an Iatroscan MK IV analyzer interfaced to an electronic scanner (30 scans/min). Pure grade hydrogen (190 ml/min) and air (2.1 l/min) supplied by a pump were used for the detector. The relative percentages of aliphatic hydrocarbons, aromatic hydrocarbons, resins and asphaltenes were calculated using peak area and response factor integration for each compound fraction referenced against standards.

This technique is a fast and cost-effective way to obtain quantitative data on the composition of crude oils and solvent extracts of rocks. The authentic reference compounds squalane, anthracene and undecanol typically used in analysis are not representative of many oil characteristics especially the polar compound responses. Therefore, the Iatroscan technique depends on correct calibration of the instrument using standards based on separated crude oil fraction, since the use of synthetic

standards had resulted in erroneous response factors. I adapted the calibrated method described by Bharati *et al.* (1997). An oil from the Lengdong field was fingerprinted and separated into saturated hydrocarbons, aromatic hydrocarbons and polars (resins + asphaltenes) on a large scale, using preparative TLC. These fractions were later quantitatively remixed to provide a standard, which was used to calibrate Iatroscan and monitor the responses of the individual fractions. The response factors obtained with these compounds are slightly different to those for the reference compounds. Values for the duplicates were averaged after being blank corrected, and the quantification of the SARA fractions were corrected for relative response factors using the mixed standard. The results were recorded and processed using a LabSystems XChrom data system.

2.2 Bulk fraction isolation

2.2.1 Asphaltene precipitation

An aliquot of the extract or crude oil (ca. 50 mg) was dissolved in 8 ml cold hexane and sonicated for a few seconds until the oil and hexane were mixed. The sample was then left in a fridge at 4°C overnight to allow precipitation of asphaltenes. The asphaltenes were pelleted by centrifugation at 3000 rpm for 5 minutes and the supernatant maltene fraction was removed by pipette to a round bottomed flask. The asphaltenes were washed twice by resuspension in another 8ml of cold hexane followed by sonication, centrifugation, etc. The maltene fractions were pooled, evaporated to ca. 1 ml using a Buchi Rotavapor and transferred to a 10 ml vial. They were then evaporated under nitrogen to 200 µl and standards added: 5 µl deuterated (d8) carbazole (0.18 µg), 4 µl deuterated (d3) 2,4-dimethylphenol (0.74 µg), 4 µl 2 naphthol (0.47 µg), 4 µl deuterated (d6) phenol (0.20 µg).

2.2.2 SPE method for the isolation of hydrocarbon and polar fraction

Crude oils and reservoir extracts were first separated into hydrocarbon (aliphatic and aromatic hydrocarbons) and non-hydrocarbon fraction (including phenols and carbazoles) based on a solid-phase extraction (SPE) method. The Isolute C_{18} (non-end-capped) columns were flushed with 3ml of hexane and the column gently flushed with an air syringe. The maltene fraction after asphaltene precipitation was evaporated under a stream of nitrogen to ca. 100 µl (with internal standard) was transferred to a C_{18} non-endcapped (NEC) SPE cartridge (IST, Jones Chromatography, UK). It was then placed onto the frit of the column and allowed to adsorb onto the sorbant. The column tip was then rinsed with hexane (5 ml). A 10ml vial was placed under the

column and a small volume of hexane from the 5 ml was used to wash the sides of the column and the frit. The rest of the hexane was then poured in the column to separate the aliphatic/aromatic hydrocarbon fraction from the polar compounds. The column tip was then rinsed with hexane and the column gently flushed with an air syringe and the fraction collected. The fraction was then stored in a fridge for later separation. Another vial was placed under the column and DCM (5 ml) was added to extract the polar fraction. The DCM was removed from the column by gentle air flushing and the tip of the column was rinsed with the solvent (Bennett and Larter, 2000).

A *n*-phenylcarbazole standard solution (1 mg/10 ml in DCM) was added to the polar fraction then evaporated to around 500 µl in a nitrogen stream and stored in the fridge. About half the polar fraction was transferred to auto-sampler vials and directly analyzed by gas chromatographic-mass spectrometry (GC-MS) for fluorenone and carbazole compounds. The other half fraction which contains alkylphenols was derivatised with 100 µl of BSTFA for 1 hour at 60 °C prior to GC-MS analysis.

2.2.3 Ag^+ impregnated silica column SPE.

The saturated hydrocarbon and aromatic hydrocarbon fractions were obtained from a silver nitrate impregnated silica SPE columns. Details of the isolation of aliphatic and aromatic hydrocarbons using silver ion-silica solid phase extraction are given in Bennett and Larter (2000). The columns were not commercially available therefore had to be specially prepared. Kieselgel [60G] (30 g), sufficient to make 40 columns (Isolute FL columns), was put into a conical flask and distilled water was added (60 ml) into which silver nitrate (3 g) had already been dissolved. The solution was mixed well, and the flask covered in foil. This was left in a drying oven for two weeks until it was completely dry. Once dried the lumps need to be crushed using a pestle and mortar directly before use.

A frit was then placed into the base of an empty cartridge barrel. The silver nitrate impregnated silica was added (~550 mg), and compacted carefully using a glass rod. A second frit was then added and compacted further to a depth of 13-15 mm. The flask was returned to the oven when finished with.

The column was then cleaned with hexane (5 ml). Positive pressure was applied using a syringe and adapter for the solvent to pass through the column. The solvent was removed with gentle air flushing and the tip of the column was cleaned using hexane. The columns had to be used in the day they were prepared, as the silver nitrate is light sensitive.

The hexane fraction from C_{18} SPE was evaporated to around 1.0 ml in a stream of

dry nitrogen and add 10 µl of a combined standard containing 1,1'-binaphthyl (2.0953 µg), squalane (12.8386 µg), (d8)naphthalene (2.346 µg), (d10)phenanthrene (2.1712 µg) and (d10)fluorene (2.1712 µg). The hexane fraction (100 µl) was removed from the bulk amount using a syringe and carefully added to the frit of an Ag^+ impregnated silica column. The frit and barrel of the column were then washed twice with approximately 0.25 ml from the 2 ml of hexane. The remaining volume was added and the aliphatic hydrocarbon fraction was collected in a 10 ml vial. The solvent was removed from the frit by gentle air flushing, and the tip of the column was rinsed with hexane.

The vial was replaced and DCM (4 ml) was added to the column to extract the aromatic compounds. The solvent was again removed with gentle air flushing and the tip cleaned with DCM.

The aliphatic hydrocarbon fraction was evaporated to 1ml in a stream of dry nitrogen, and the aromatic fraction was reduced to a volume of 200 µl. The fractions were then transferred to auto-sampler vials prior to GC and GCMS analysis.

When using methods in the analytical scheme, procedural blank runs were performed using solvent, SPE sorbent and quantification standards, including a well characterized oil (such as Veslefrikk, A3) for reference purpose and replicate analyses.

2.2.4 TLC Separation

The TLC tank, lid and plates were cleaned using DCM and ethyl acetate, the plates were glass 20 cm by 20 cm. A mixture of Kieselgel 60G (35 g) and distilled water (65 ml) was prepared.

The plates were then coated in the silica gel solution at a thickness of 0.5 mm. The plates were left to dry, then cleaned with ethyl acetate and placed in the oven to activate. This took approximately four hours. The top 2 cm of the silica coating was removed with a spatula. The samples were then ready to be spotted. A TLC standard was also added to the plate so the different hydrocarbon fraction could be determined later.

The samples were transferred to the TLC plate (~15 mg) and placed into the tank, which contained an enough volume of petroleum ether to elute the samples up the plate. When the solvent front was nearing the top of the plate, the plate was removed, sprayed lightly with Rhodamine-6G and put under a UV light which enabled the compound bands to be detected, they were then marked.

Elution tubes, which were 20 cm in length, were prepared by plugging the narrow

end with a small amount of extracted cotton wool, adding a layer of activated alumina, enough to cover the wool, then the activated silica was added which was 3 cm in length. The different fractions were scraped off the TLC plate, and individually put into the prepared tubes. The fractions were then eluted with 10% DCM: Pet. Ether (30 ml) for the aliphatic hydrocarbon fraction, 20% DCM: Pet. Ether (30 ml) for the aromatic hydrocarbon fraction and 50:50 DCM: Methanol for the polar compounds.

The fractions were collected then concentrated by rotary evaporation, for GC and GC-MS analysis.

2.3 GC and GC-MS

2.3.1 Gas chromatographic analysis

Gas chromatographic analysis of the total hydrocarbon fractions was carried out on a Carlo Erba Mega 5160 GC fitted with a cold on-column injector, a flame ionisation detector (310 °C), and a DB-5 (J&W Scientific) fused silica capillary column (30 m length × 0.32 mm i.d. × 0.25 μm film thickness). Hydrogen was used as carrier gas at a flow rate of 1ml/min. The oven temperature was programmed from 40 °C to 300 °C at heating rate of 4 °C/min., with initial and final hold times of 2 min. and 20 min., respectively. A Labsystems Atlas 2000 data system was used for GC data acquisition and processing. Specific compounds were identified by comparison of retention time with those of a characterized sample and compound abundance ratios were determined on the basis of integrated peak areas assuming uniform response factors.

2.3.2 GC-MS analysis of the hydrocarbon fractions

Gas chromatographic-mass spectrometric analysis of the aliphatic and aromatic hydrocarbon fractions was performed on a Hewlett Packard (HP) 5890 Series II gas chromatograph (GC) fitted with a HP-5 fused silica capillary column (30 m length × 0.25 mm i.d. × 0.25 μm film thickness) and coupled to an HP 5972 MSD. Samples were analyzed in single ion monitoring (SIM) mode (ionisation energy 70 eV, filament current 220 μA, source temperature 190 °C, multiplier voltage 2000 V). The GC oven temperature program was 40 °C (initial hold time 5 min.), then heated using a heating rate of 4 °C/min to 300 °C (final hold time 20 min.). Helium was used as carrier gas at a flow rate of 1ml/min on a calculated pressure ramp. Ions monitored are shown in Table 2-1.

Specific compounds were identified by comparison of retention time with those from a previously characterized oil sample. Aliphatic hydrocarbon-based biomarker parameters and aromatic hydrocarbon ratios were calculated on the basis of integrated

peak areas. Internal standards, 10 μl (12.8386 μg) squalane and 10 μl (2.0953 μg) 1,1'-binaphthyl, were added to the hydrocarbon fraction prior to further separation into aliphatic and aromatic hydrocarbon fractions using a silver nitrate-silica gel SPE column, eluting with hexane and DCM, respectively (Bennett and Larter, 2000). The correction for relative response factors of individual compounds was applied for both fractions.

Table 2-1. Ions used in this study for the SIM gas chromatography-mass spectrometry analysis of the aliphatic and aromatic hydrocarbon fractions

m/z	Compound Class
	Aliphatic Hydrocarbon Fraction
123	Sesquiterpanes
191	Tricyclic and pentacyclic terpanes
217	Steranes
218	Isosteranes (αββ steranes)
231	Methylsteranes
183	Squlane
85	*n*- Alkanes
	Aromatic Hydrocarbon Fraction
128	Naphthalene
142	C_1-naphthalenes
156	C_2-naphthalenes
170	C_3-naphthalenes
184	C_4-naphthalenes + Dibenzothiophene
198	C_5-naphthalenes + C_1-dibenzothiophene
212	C_2-dibenzothiophene
178	Phenanthrene
192	C_1-phenanthrenes
206	C_2-phenanthrenes
220	C_3-phenanthrenes
154	Biphenyl
168	Methylbiphenyl + Dibenzofuran
166	Fluorene
202	Pyrene + Fluoranthene
231	Triaromatic steroid hydrocarbons
253	Monoaromatic steroid hydrocarbons + 1,1'-Binaphthyl

2.3.3 GC-MS analysis of carbazole and phenol fraction

Both the pyrrolic nitrogen compound enriched fraction and the alkylphenol enriched fraction were performed on a Hewlett-Packard 6890 Series II GC fitted with a split/splitless injector (310 °C) and linked to a Hewlett-Packard 5973MSD operated in SIM mode (electron voltage 70 eV, filament current 220 μA, source temperature 230 °C, multiplier voltage 2000 V, interface temperature 310 °C). Compound

separation was performed on an HP-5 fused silica capillary column (30 m length × 0.25 mm i.d. × 0.25 μm film thickness). Helium was used as carrier gas (flow 1ml/min, initial pressure of 50kPa, split at 30 ml/min, pressure programmed). The GC oven temperature program was 40 °C (initial hold time 3 min.), then at heating rate of 10 °C/min. to 200 °C, then 4 °C/min. to 310 °C (final hold time 14 min.).

5 μl (0.1860 μg) of d_8-carbazole used as internal standard (Chiron, Norway) for quantification of alkylcarbazoles and benzocarbazoles was added before transferring to a C_{18} non-endcapped (NEC) SPE cartridge (IST, Jones Chromatography, UK) which had been pre-cleaned using DCM, air-dried and conditioned with hexane before use. Ions of C_0, C_1, C_2-alkylcarbazoles (the C_0, C_1, C_2 prefixes refer to the number of alkylcarbons joined to the carbazole molecule) and benzocarbazole monitored are shown in Table 2-2. The identification of compounds was based on Li *et al.* (1992) and Bowler *et al.* (1997), and by comparison of retention time and mass spectrum with those of a standard oil from the Miller Field, North Sea. The detection limit of pyrrolic nitrogen compounds analysis was 0.01 μg alkylcarbazole/g oil.

Table 2-2. Ions used in this study for the SIM gas chromatography-mass spectrometry analysis of the alkylphenol enriched fraction.

m/z	Compound class
Alkylphenols	
166	Phenol
180	C_1-phenols
194	C_2-phenols
208	C_3-phenols
197	D3-2,4-Dimethylphenol
Alkylcarbazoles and benzocarbazoles	
167	Carbazole
181	C_1-carbazoles
195	C_2-carbazoles
217	Benzocarbazoles
267	Dibenzocarbazoles
243	N-Phenylcarbazole
175	D8-Carbazole

C_0, C_1, C_2, C_3-alkylphenols were analyzed as their trimethylsilylether derivatives and their identification was based on comparison with retention time characteristics of authentic standard compounds. 4 μl (0.7107 μg) of d3-2,4-dimethylphenol was used as internal standard for quantification of alkylphenols. Correction for relative response factors was not applied to the quantification of carbazole and phenol compounds, which were assumed to have the same response factor as the standard. The peak area data for both pyrrolic nitrogen compounds and alkylphenols was

calculated through integration of the appropriate peak in the respective molecular ion chromatograms.

2.3.4 Response factor (RF)

Response factors for aliphatic hydrocarbons were calculated relative to squalane and for aromatic hydrocarbons, relative to 1,1'-binaphthyl by dividing the percentage (w/w) of the compounds in the mixture of standards by their appropriate m/z response, which was then divided by squalane's or 1,1'-binaphthyl's percentage (w/w) to m/z response ratio. Reference standards of various aliphatic and aromatic hydrocarbon compounds were prepared and analyzed by GC and GC-MS to determine their relative response factors and to calibrate the squalane and 1,1'-binaphthyl-standards (Table 2-3). The response factors from GC for the various compounds are quite consistent, e.g., ranging from 0.95 to 1.08 for the squalane standard. Apparently, no significant bias occurs from the GC traces.

Table 2-3 Response factor (RF) calibration for squalane and 1,1'-binaphthyl-standards using GC and GC-MS methods.

Compound	Weight	GC			Full scan			SIM	
	(mg)	area	RF	Ion	area	RF/Sq	RF/1.1-Bn	area	RF
Naphthalene	5.584	851	0.95	128	10632437	27.93	1.78	9247870	1.87
n-C_{16}	5.051	792	0.97	85	1537884	4.47	0.29	982196	5.22
Phenanthrene	5.645	872	0.96	178	9856257	25.61	1.63	7803786	1.56
n-C_{19}	5.097	833	1.01	85	1585861	4.56	0.29	1237104	6.52
1,1-Binaphthyl	4.918	799	1.01	253	5252004	15.66	1.00	4366186	1.00
n-C_{24}	5.512	918	1.03	85	1755491	4.67	0.30	1176148	5.73
Squalane	5.309	855	1.00	183	361904	1.00	0.06	197616	1.00
5α-Cholestane	5.369	889	1.03	217	2531378	6.92	0.44	1488326	7.45
Ts	5.196	903	1.08	191	2180040	6.15	0.39	1411010	7.30
n-C_{30}	5.493	869	0.98	85	1599730	4.27	0.27	1089942	5.33
Diploptene	5.461	866	0.98	191	5079322	13.64	0.87	2796105	13.76
Hopane	5.221	908	1.08	191	1545361	4.34	0.28	1020301	5.25

The response factor bias observed in the full scan and SIM model appear to be pronounced because of fragmentation in the characterized ions of the mass spectrometer, i.e. with compounds that result in an ion current of different intensity originating from a single mass. The bias is remarkable between two internal standards.

The response factors of aliphatic hydrocarbons to squalane were calibrated with the model compounds *n*-C_{16}, *n*-C_{19}, *n*-C_{24}, *n*-C_{30}, 5α-cholestane, Ts, diploptene and C_{30} αβ hopane as listed in Table 2-3. The characteristic ion of m/z 85 for *n*-alkanes was 4.5 to 6.5 times more intense than the characteristic ion of m/z 183 for squalane. The response factors did not show large variation between *n*-C_{16} to *n*-C_{30}. Since my data are mainly acquired from SIM, the average response factors of *n*-C_{16}, *n*-C_{19}, *n*-

C_{24}, *n*-C_{30} was taken to calibrate the *n*-alkanes. Ts and C_{30} αβ hopane have a similar m/z 191 ion fragment intensity, which is 5-7 times higher than the characteristic ion for squalane, whereas diploptene has a very intense m/z 191 ion fragment. Tricyclic terpanes and pentacyclic terpanes calibrations were based on the response factors for Ts and C_{30} αβ hopane, and the molecular weight distribution was not taken into account. The concentrations of sterane compounds were calibrated using the response factor for 5α-cholestane.

Aromatic hydrocarbons were calibrated using the response factors of naphthalene, phenanthrene and 1,1'-binaphthyl. The characteristic ions for most aromatic hydrocarbons are their molecular ions because of their high intensity. The response factors between aromatic hydrocarbons and 1,1'-binaphthyl standard did not show such large differences as were seen for the aliphatic hydrocarbons. The response factors of the aromatic hydrocarbon fraction are highly dependent on molecular size, and decrease with increasing molecular weight. The molecular ion of naphthalene is 1.8 times stronger than that of 1,1'-binaphthyl and the molecular ion of phenanthrene is 1.6 times stronger than that of 1,1'-binaphthyl. In this regard, the calibrations of aromatic compounds are based on their molecular weight ranges, with response factor variations between 1.0 and 1.8.

3 GEOLOGICAL BACKGROUND AND OIL COMPOSITION

3.1Tectonic and stratigraphic settings

3.1.1 Structure characteristics

The tectonic development in China is mainly controlled by the southward compression of the Siberian Plate, the NEE compression and collision of the Indian Plate, and the NWW subduction and compression of the Pacific Plate (Fig. 3-1) (Niu and Hu, 1999). Since the Jurassic, rift basins developed along NE and NEE trends. Liaohe basin is one of the Tertiary basins located in the NE China, which mainly influenced by the Pacific Plate. It is one of the most important Cenozoic sedimentary basins in China, and is the third largest oil producing province. The basin consists of three main depressions: Western depression, Eastern depression and Damington depression. Three are three uplifts, i.e., Western uplift, Central uplift and Eastern uplift to separate these two depressions (Fig. 3-2).

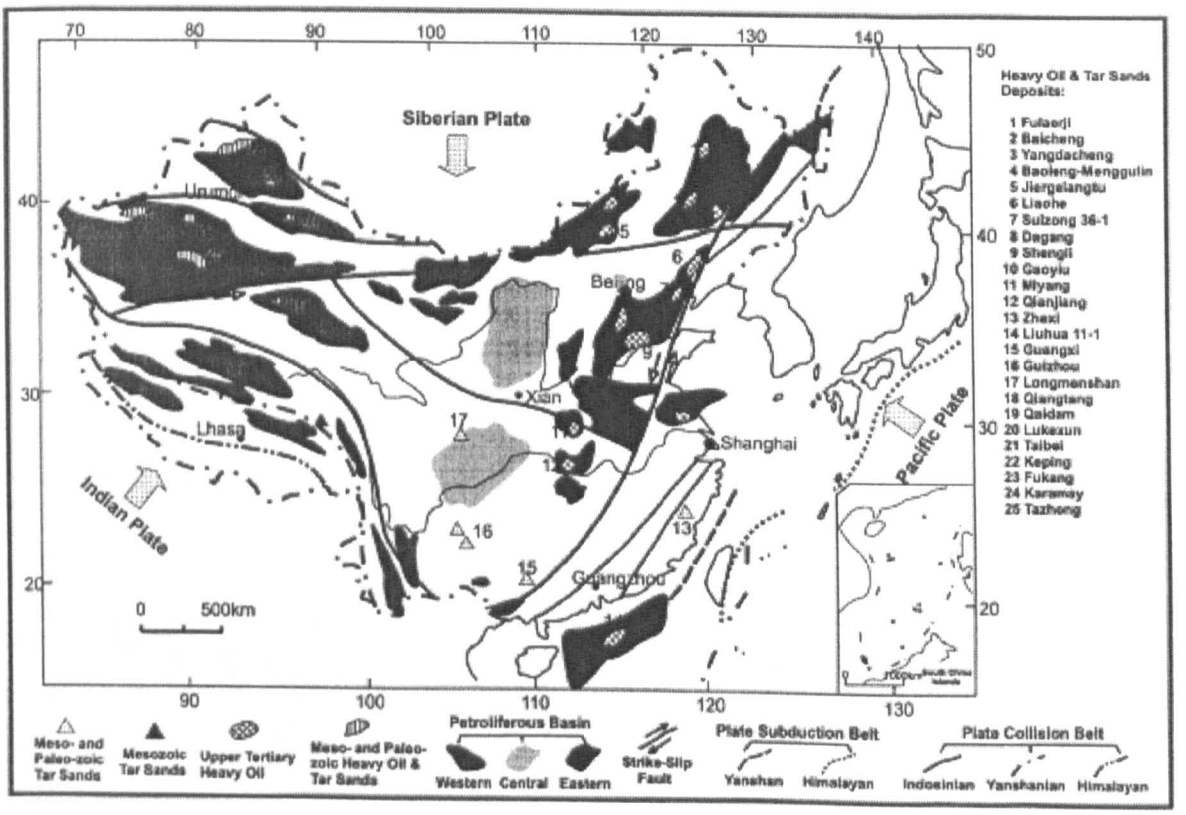

Fig. 3-1. Tectonic characteristics with distribution of heavy oil and tar sands in China (after Niu and Hu, 1999).

The Western depression, a NE-trending trough, is located between the Western uplift and Central uplift. During the late Paleocene, an initial rift started to develop in the Liaohe region. An extensional system was responsible for the formation of a hangingwall syncline basin during the Eocene. Alluvial-fan clasts are exclusively

derived from the hangingwall uplift and were deposited along a NE-trending syncline parallel to the depression border. With the development of extension episode, depocentres migrated south-westward. The early phase sediments accumulated in the northern part of the basin, mainly in the Damington depression and the depocentre moved further south to the Liaodong Bay offshore area. The east bordering extensional fault is a listric fault with high-angle at the top and low-angles downward. The west side of the depression is a gentle slope, which formed a half-graben shaped depression by the end of the Oligocene.

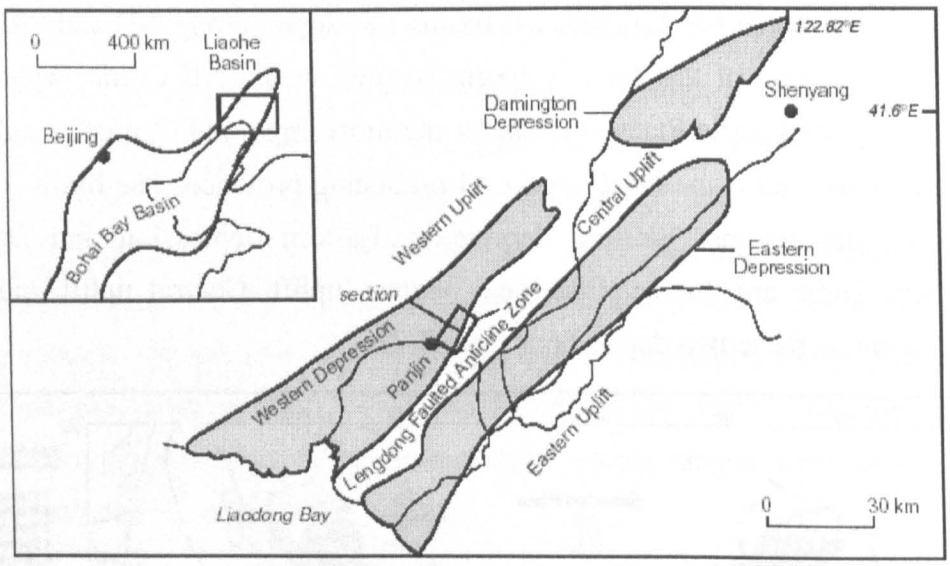

Fig. 3-2. Map of the Liaohe basin. The inset map shows the location of the Liaohe basin in NE China. The cross section displayed in Figure 3-3 is indicated (after Koopmans *et al.*, 2002).

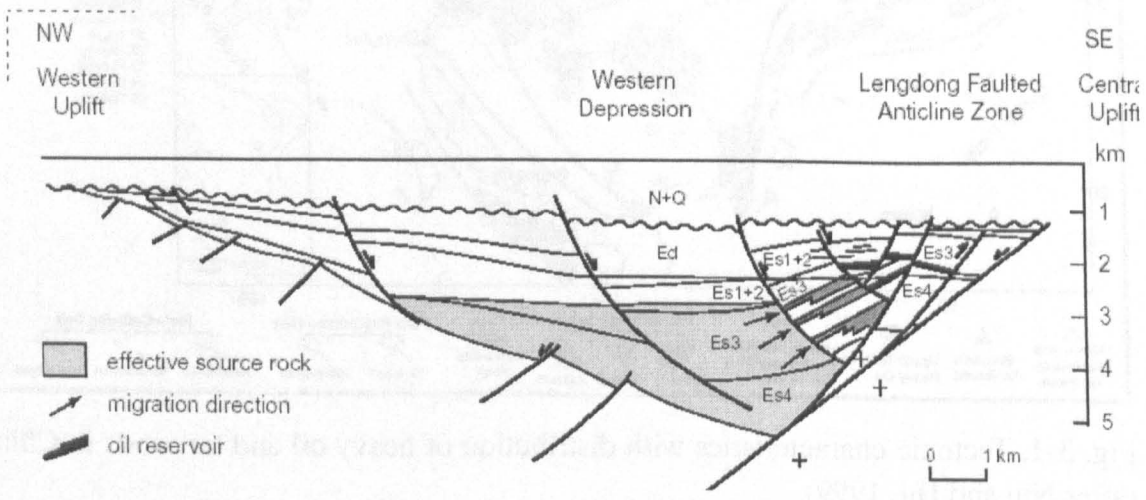

Fig. 3-3. Regional structural cross section. The heavy-oil field is located in the Lengdong faulted anticline zone (after Koopmans *et al.*, 2002). Es: Shahejie Formation of Eogene; Ed: Dongying Formation of Eogene; N+Q: Neogene + Quaternary.

Figure 3-3 shows a regional structural cross section of the Western depression. The EW tectono-stratigraphic cross section shows the lateral distribution of the producing units in the reservoir and the presence of normal faults in the NE-SW direction. The heavy-oil field sits in the Lengdong faulted westward dipping anticline zone on the east steep slope of the western depression, Liaohe basin. It is adjacent to the central uplift on the east and to the Chenjia sub-depression on the west. A detailed structural map of the study area shows in Figure 3-4. The NE-NNE trending fault system reflects the main extensional stress oriented in the SW-SSW direction. A reverse fault (i.e. inverted) by the end Oligocene tectonism indicates the influence of short period compressive stress (Fig. 3-5a). The well-connection cross profile shows the oil reservoir spatial distributions (Fig. 3-5b).

3.1.2 Stratigraphic characteristics

The Paleogene sequence can be divided into three formations: Fangshenpiao, Shahejie and Dongyin. The Fangshenpao Formation (Ef) is not present in the study area. The Shahejie Formation (Es) is widely distributed and contains the most important source rock and reservoir units in the entire basin. Based on lithology and fossil assemblages, it can be further subdivided into four members (Es4, Es3, Es2, and Es1, oldest to youngest). The sequence gains a regressive character towards the top, and is completed by the Dongying Formation of the Oligocene age. Three cycles can be divided: Es4-Es3, Es2-Es1 and Ed. There is a short erosion or hiatus in the beginning of each cycle. The Es4-Es3 cycle is the main phase of the depression development with high quality source rock deposit in this time. The sedimentary facies of the members Es3 and Es4 in the Western depression are displayed in Fig. 3-6.

Briefly, during the sedimentation of the Es4 member, the north part of the depression was a semi-closed lacustrine bay without inflow of water, while the south part was a freshwater paralic lacustrine environment. Marls are developed in slightly saline water sediments at this period. In the early Es3 member, drastic subsidence resulted in the development of an extensive deep lacustrine environment. Coarse grained clastics from the high on both sides slid into the bottom of the lake, forming turbidite and mudstone of deep lacustrine facies. However, abatement of rift activity and uplift of the north of the Western depression in the late Es3 member ultimately led to the shrinking of the water body in the lacustrine basin. Delta plain facies and submerged distributary channel facies are more prevail at this period.

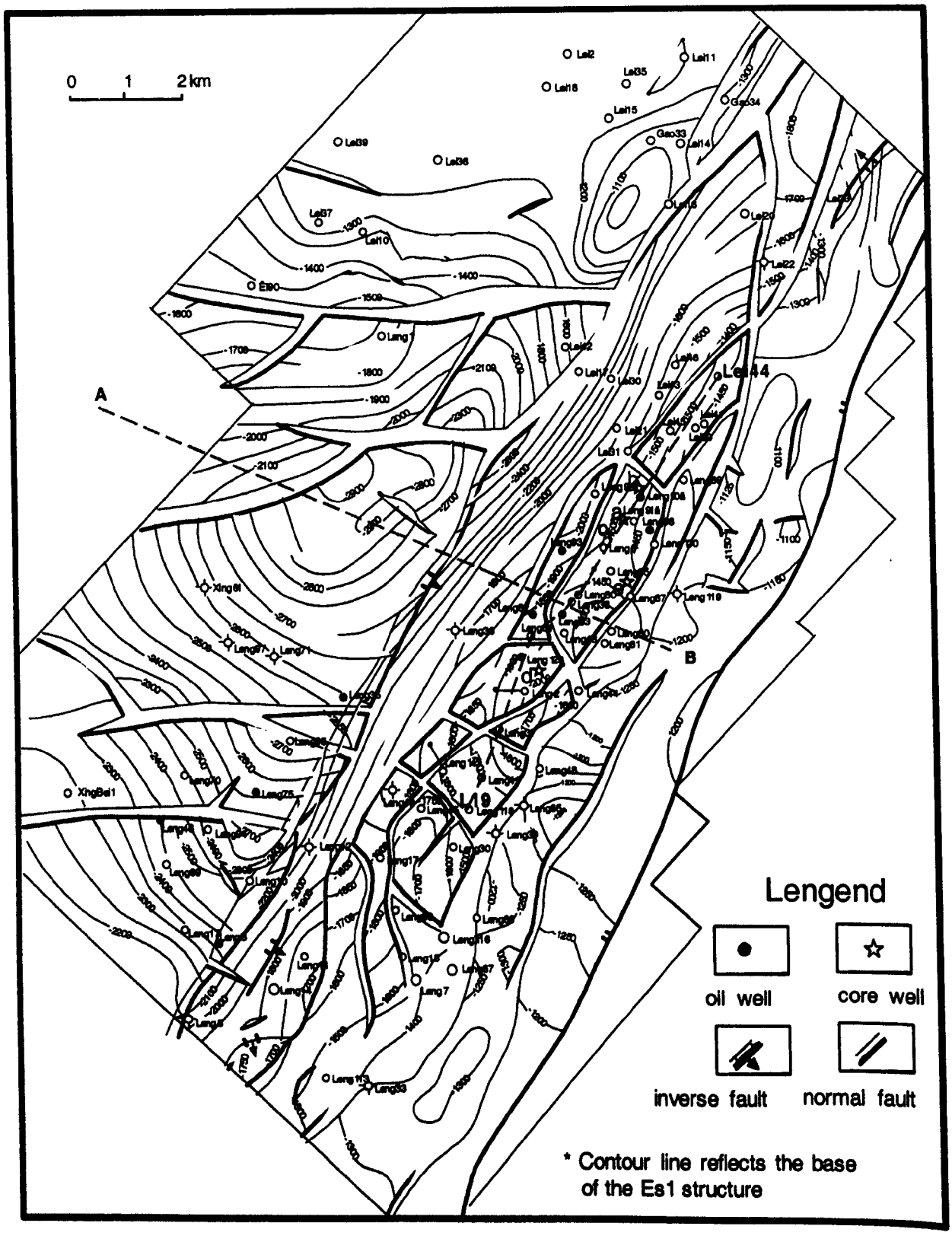

Fig. 3-4. Detailed structure map of the Lengdong oilfield.

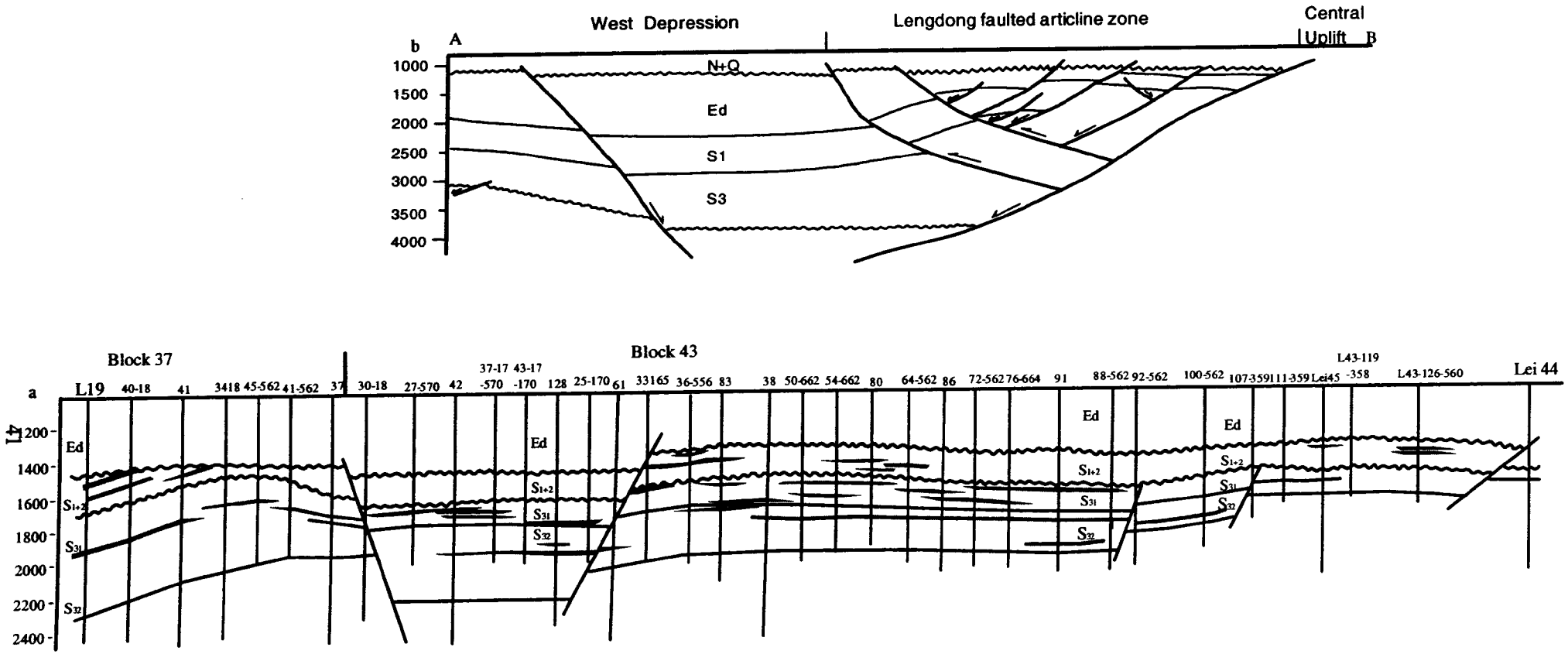

Fig. 3-5. Cross sections of the study area. a: Perpendicular to the main structure; b: Reservoir connected section parallel to the main structure (See Fig. 3-4 for location).

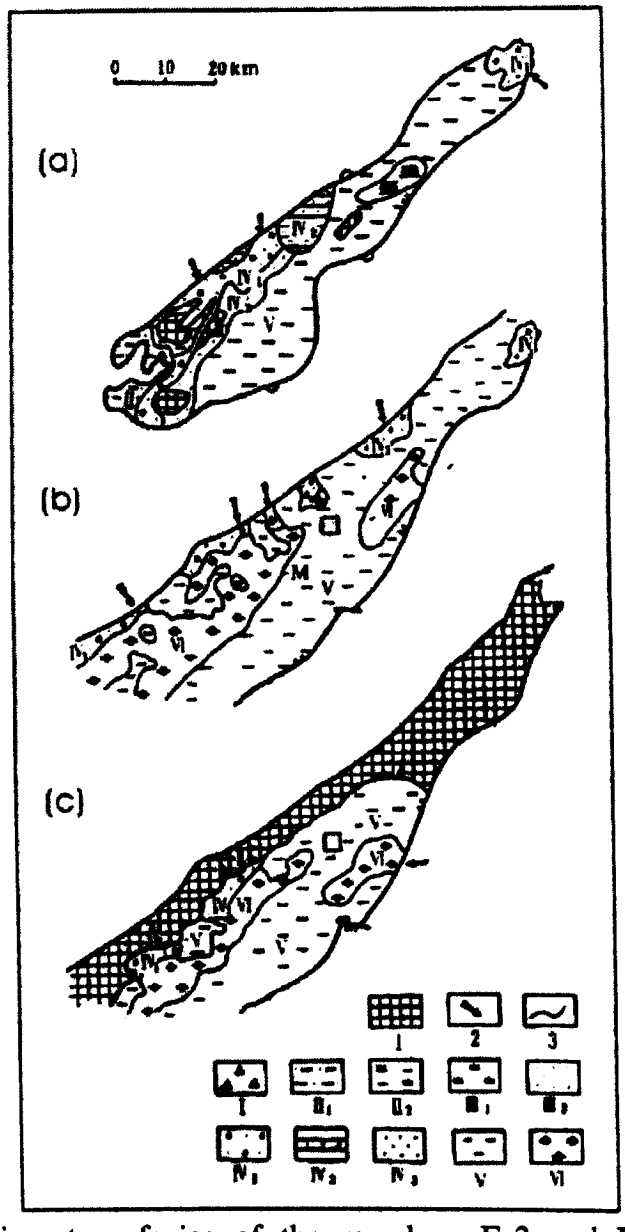

Fig. 3-6. The sedimentary facies of the members Es3 and Es4 in the Western depression (modified after Ge and Chen, 1993). (a)—Es4 member; (b)—Middle and lower Es3 member; (c)—Upper Es3 member. 1—Erosion area; 2—source direction; 3—facies boundary; I—alluvial fan facies; II—flood plain facies (II1—river channel and interchannel subfacies; II2—flood basin swamp subfacies); III—delta facies (III1—delta plain facies; III2—delta front facies); IV—fan delta facies (IV1—submerged distributary channel subfacies; IV2—interdistributary shoal subfacies); V—lacustrine facies; VI—turbidite facies.

A generalized stratigraphy for part of the basin is shown in Figure 3-7. Es4 was deposited during the initial rifting stage in isolated depressions. Dark mudstone, siltstone and interbedded sandstone are the typical lithologies. In the early Es3, drastic subsidence resulted in the development of an extensive deep lacustrine environment and this member consists of dark mudstones, shales and oil shales of deep freshwater lacustrine origin which contain excellent source rock intervals. Also during this period, coarse grained clastic sediments from highs on both sides slid into the bottom of the

lake forming turbidites which can comprise the main reservoir sandstones in some areas. The Es2 member was deposited during a contraction of the lake in the Liaohe basin because of tectonic uplift. It is very thin and hard to distinguish from overburden in the Es1 in study area. The Es1 is mainly composed of poorly sorted coarse sediments which comprise the second important petroleum reservoir in the basin. The Dongying Formation (Ed) typically consists of fluvial and shallow freshwater lacustrine grey mudstone and sandstone. The Guantao Formation (Ng) and Minhuazhen Formation (Nm) are comprised of widely distributed fluvial deposits unconformably overlying the Paleogene formations and providing overburden rocks to the petroleum system (Ge and Chen, 1993).

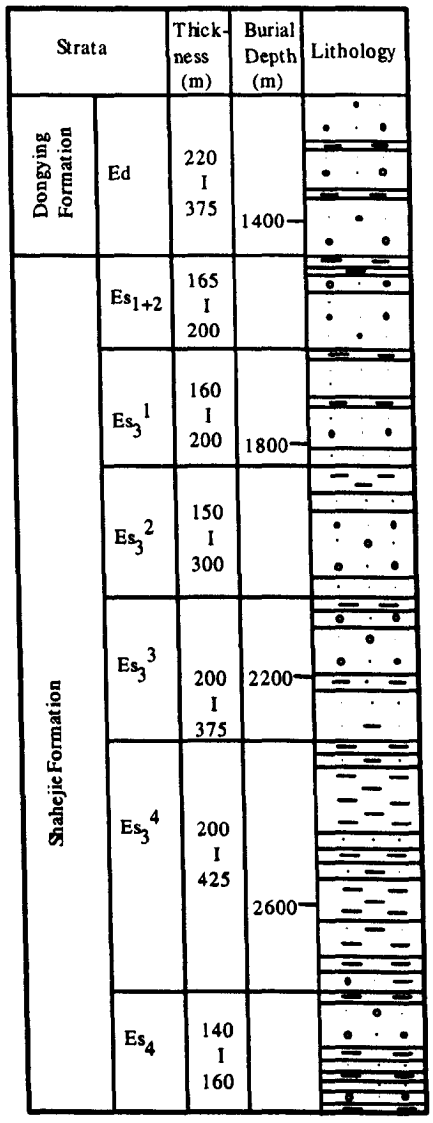

Fig. 3-7. Simplified stratigraphic column for the Lengdong oilfield.

3.1.3 Evolution history

The Lower Tertiary of the study area is controlled by periodic movement of the eastern boundary fault and paleogeography. From the Early Eocene time onwards, the Western depression is filled with strata generally thinning to the west. The restricted

basal sedimentary unit, the Fangshenpao Formation, deposited in initial rift phase does not occur in the study area. Before the deposition of the Es3, the small movement of the boundary fault occurs. Following the Es4 semi-deep lake deposition, the rift was developed to its maximum extend during the Es3 deposition period. During the deposition of the Es2-Es1 the boundary fault has more strong activity and some eastwards fall faults developed. During the deposition of the Dongying Formation the boundary fault activity tends to weak and most small sized faults start to activate. Because of uplift and compression by the end of the Ed deposition, some faults start to reverse. The geometries of the half-graben-controlling faults and the reactivated Tertiary faults may be consistent with the interpretation that transtensional motion controlled the rifting. Following the rifting, during the Late Tertiary, a widespread and continuous, but thin, layer covered the majority of the basin. The post-rift sedimentation has been under way since the Late Tertiary. These widespread Neogene and Quaternary units are equivalent to the 'thermal sag' stratigraphic succession.

3.2 Source rock characteristics and hydrocarbon generation history

3.2.1 Organic abundance and type

Of the essential elements of the petroleum system, the source rock is the most important in rift basins. Various analyses were used to estimate the kerogen type, maturation of source rocks and hydrocarbon potential. The quality and maturation of organic matter were determined by optical determination of vitrinite reflectance (Ro) and pyrolysis for maximum temperature (Tmax), oxygen index (OI), hydrogen index (HI), production index (PI), total organic carbon (TOC) and oil generation potential (S1 + S2).

Geochemical analyses carried out by Mei *et al.* (1994) showed that the Es4 member is rich in organic matter with TOC more than 5 wt.%. Oil generation potential is high. Microscopic analysis showed that the kerogen present consists mostly of alginate, suggesting an algae origin type I kerogen. The Es3 samples are also rich in organic matter (TOC ranged from 1.2 wt.% to 4.6 wt.%). Kerogen is of type I~II, with fair oil generation potential.

3.2.2 Thermal maturity

Thermal maturities of organic matter were evaluated with the reflectance of vitrinite (Ro%) and Rock-Eval maximum temperature (Tmax), which increase during thermal maturation. Some data analyzed by Mei *et al.* (1994) in a vertical sequence showed the level of maturation increasing steadily with depth. At 2500m Ro is 0.3%

and it rises to 0.37% at 3000m then reaches 0.49% at 3800m (Fig. 3-8). This vitrinite reflectance profile showed very low Ro values and implied immature source rock, which obviously contrary to the fact of discovered oil existence. The cause for low vitrinite reflectance is partially due to organic type Ro suppression, since most of these source rocks are Type I kerogen. It seems difficult in assessing thermal maturity using vitrinite reflectance data. Some marine origin yield vitrinite reflectance values, Kaiko and Tingate (1997) explained that the vitrinite reflectance is suppressed, and this suppression is related to the marine environment of deposition.

Tmax data obtained from Rock–Eval pyrolysis reveal an immature to mature level for organic matter (425 to 445 °C). At depth of 3000 m the Tmax values are greater than 435 °C and reach the oil generation window (Mei *et al.*, 1994). The Ro and Tmax profiles were illustrated in Figure 3-8. The modelling results (BasinMod 1-D, A Basin Analysis Modelling System, Platte River Associates, Inc. version 5.40) show slightly high values.

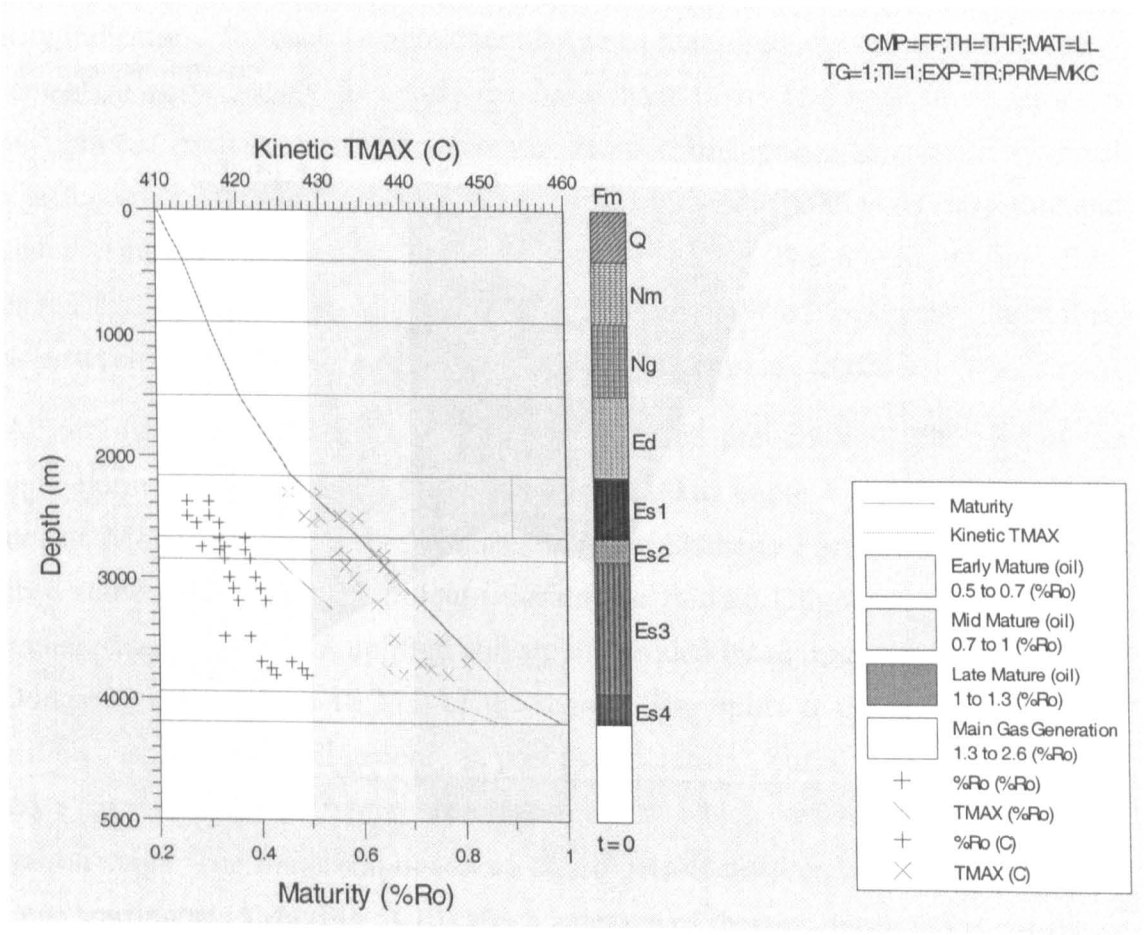

Fig. 3-8. Vitrinite reflectance, Tmax of samples from wells in the Western depression.

3.2.3 Petroleum generation history

To better understand the thermal evolution of the source rocks in the Chenjia sub-depression, an artificial well was submitted to one-dimensional thermal and kinetic

modeling. Burial reconstruction took into account measured thickness of formations drilled in the wells and seismic data and erosion estimates based on regional stratigraphic correlations (Ge and Chen, 1993). Absolute ages of depositional and erosional events were defined using the chronostratigraphic framework of the basin and the geologic time scale proposed by Ge and Chen (1993). Compaction history was described through a porosity–depth law in which porosity is a function of depth. An average porosity–depth curve was automatically calculated by the program for each formation by weighing the porosity law of each pure lithology (sandstone, shale, limestone, etc.) according to its relative proportion in the formation. Paleo-water depths were not incorporated to the model due to the lack of reliable estimates. The resulting geohistory plots (Fig. 3-9) shows two major subsidence phases (Middle Eocene/Middle Oligocene and Middle Miocene/Pliocene) and a major uplift event (Middle Oligocene/Middle Miocene). According to the burial reconstruction of the modeled well, the base of the Shahejie Formation reached its maximum depth at present time.

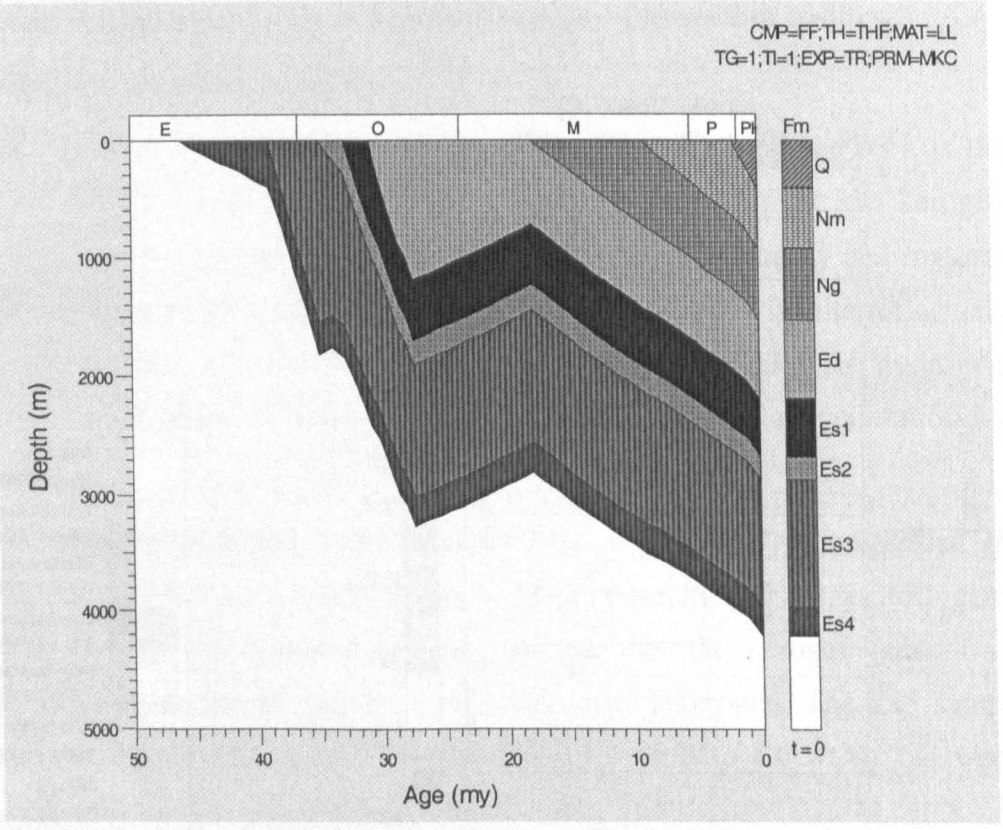

Fig. 3-9. Burial curves of the Chenjia sub-depression.

Maturation modeling requires several forms of input, including an understanding of both the stratigraphic and geothermal evolution of the basin. Many of these input parameters will not be known precisely so it is usual to specify most of them based on

some assumed knowledge regarding their nature and that of the problem as a whole (Ungerer, 1990). The burial history can be inferred from the stratigraphy using the backstripping and deconstruction technique (Fig. 3-9). Thermal conductivity of the sedimentary column was automatically calculated by the program taking into account the lithological composition, porosity decay and temperature of each formation. Due to the lack of measured data, thermal conductivity values are obtained by applying standard values (defaulted) according to lithology. The radiogenic heat contribution from the basement and the sediments was also included in the modeling by using default values of radiogenic heat production for pure lithologies available in the modeling program. The surface temperature is assumed to be 15 °C. Present-day bottom hole temperatures and borehole temperature logs were used to calibrate the simulation of the present-day temperature regime. Available geothermal information reveals that the basin has normal thermal gradient. The assessment of corrected bottom-hole temperatures (BHT) indicates that mean geothermal gradients vary between 29 and 35 °C/km across the Liaohe basin. Tmax is used to calibrate thermal maturity indicators. To reach an agreement between measured and calculated maturity assessment, it is necessary to adjust the basal heat flow. The heat flow variation follows general principles, which decreases from rifting phase to thermal reversal stage. After a number of trial-and-error simulations, the best fit between measured and calculated temperatures was obtained by using heat flow. The maximum heat flow values reached in the Eocene ranged between 60 and 70 mW/m^2 and present heat flow varies between 50 and 60 mW/m^2 (Hu *et al.*, 2001; Wang *et al.*, 2003).

According to the geohistory plot obtained for the pseudo-well, the base of the Shahejie Formation might have reached about 3000 m depth by the middle of the Oligocene. Modeling of kerogen indicates that the Shahejie Formation source rocks possibly started to generate petroleum during the middle Oligocene. However, the accumulated sediments were uplifted and slowly eroded by as much as 1000 m during the Dongying rifting (27.8-18 Ma) of the region. The uplift at the end of Dongying deposition suspended the oil generation process. Increasing burial during the Neogene caused a second stage of hydrocarbon generation, which is the main hydrocarbon generation stage. The major expulsion of liquid petroleum possibly began during the Miocene starting at 15Ma (Fig. 3-10). Such a degree of thermal evolution is consistent with the maturity of most of the oils and gases of the Liaohe basin, which are moderated mature at present time.

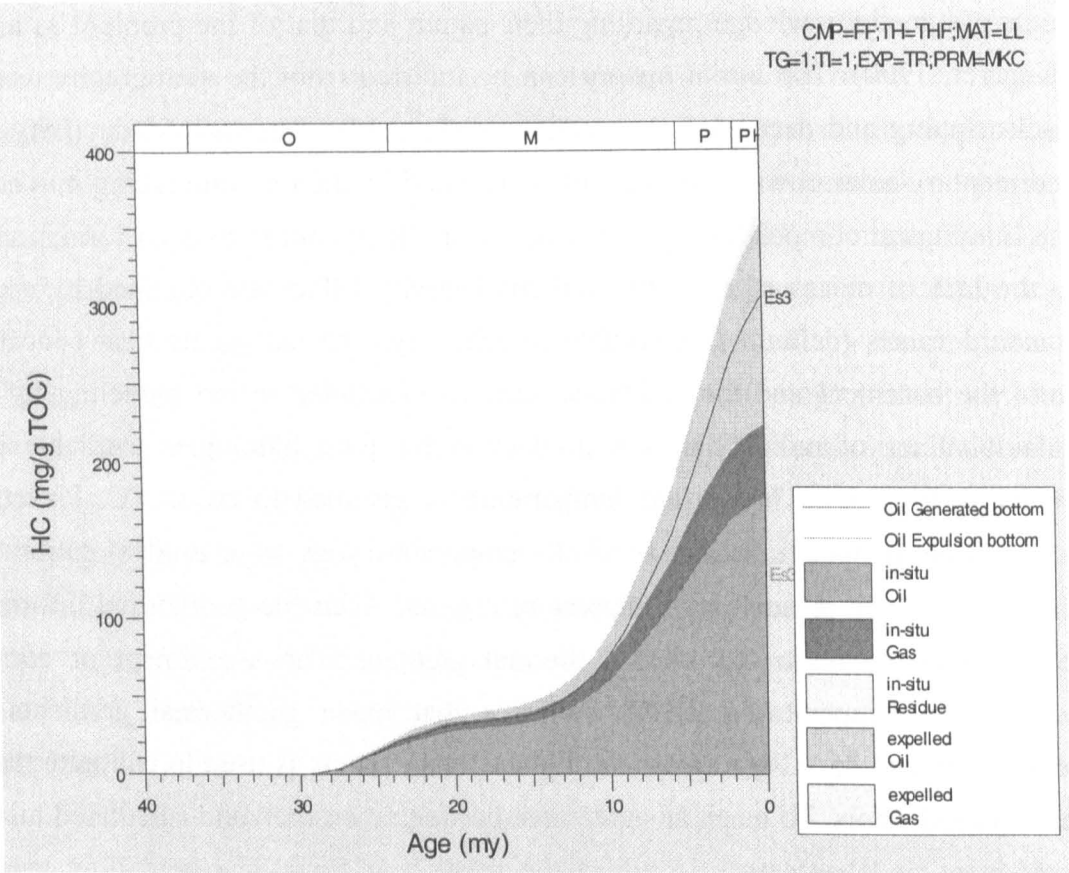

Fig. 3-10. Calculated oil generation, expulsion and accumulative hydrocarbon histories for the Es3 source rock.

3.3 Reservoir characteristics

3.3.1 Reservoir porosity and permeability

Due to their poorly sorted and shallow burial depths, the reservoirs in the Lengdong faulted block show strong heterogeneities with relatively high porosity and permeability. Porosities measured in the reservoirs range from < 5% to > 40% with an average of 15.8%. The permeability data show very large variations, ranging from < 1mD to > 5000 mD with a mean of 173 mD. There is a general positive trend between porosity and permeability in logarithm values (Fig. 3-11).

With the strong heterogeneities within the reservoir, the porosity shows a very broad decrease with increasing burial depths (Fig. 3-12). Loss of porosity is due to increasing depth and temperature by both compaction and cementation. The permeability almost has no clear relationship with burial depth (Fig. 3-13).

3.3.2 Reservoir temperature

One hundred eighty temperature data points were collected from 47 wells located in the Lengdong oilfield. The temperature data include drill stem test, continuous logging, bottom hole temperature (BHT), cable tests, temperature–pressure test, and

temperature test data when the oil-bearing strata is tested. These temperature data can be treated as minimum reservoir temperature since most measurements hardly reach equilibrium with strata and no calibration has been applied for any cooling effects of drilling mud circulation.

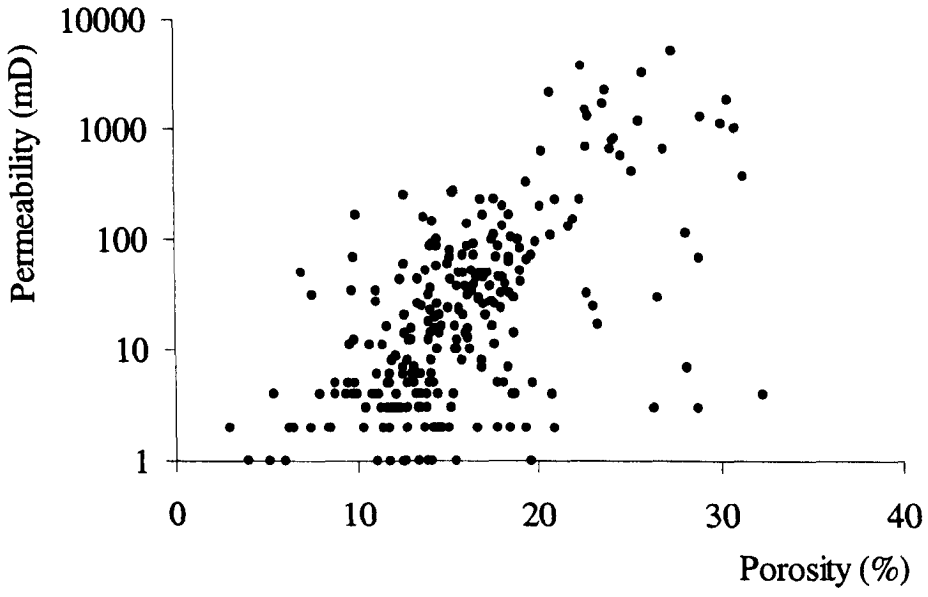

Fig. 3-11. The relationship between porosity and permeability of the Lengdong oilfield reservoir (data are provided by Liaohe Oil Company).

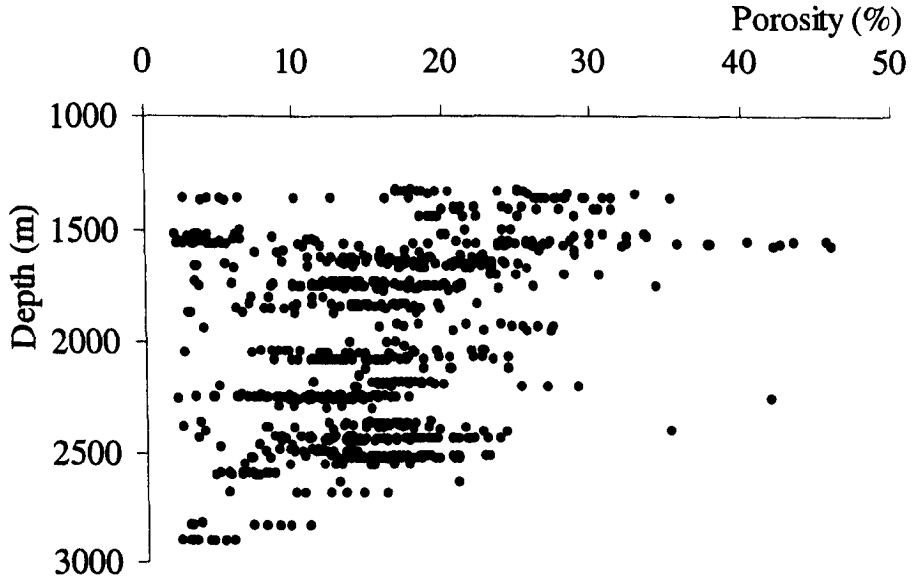

Fig. 3-12. The depth plot of the porosity for the Lengdong oilfield reservoir sandstones (data are provided by Liaohe Oil Company).

The depth range of temperature measurements is mainly between 1200 and 3500 m and a good linear relationship with depth has been observed (coefficient of regression r^2 is 0.82) (Fig. 3-14).

Present geothermal gradients are calculated to vary from 21 to 37 °C/km in the

Lengdong oilfield. Geothermal gradients may show a slight increase with depth (Fig. 3-15).

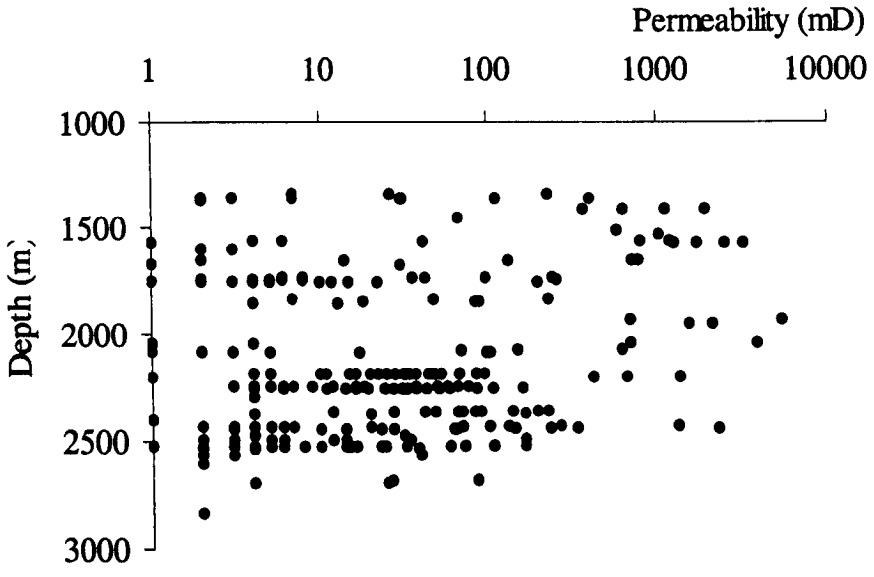

Fig. 3-13 Depth–permeability graph of the Lengdong oilfield reservoir (data are provided by Liaohe Oil Company).

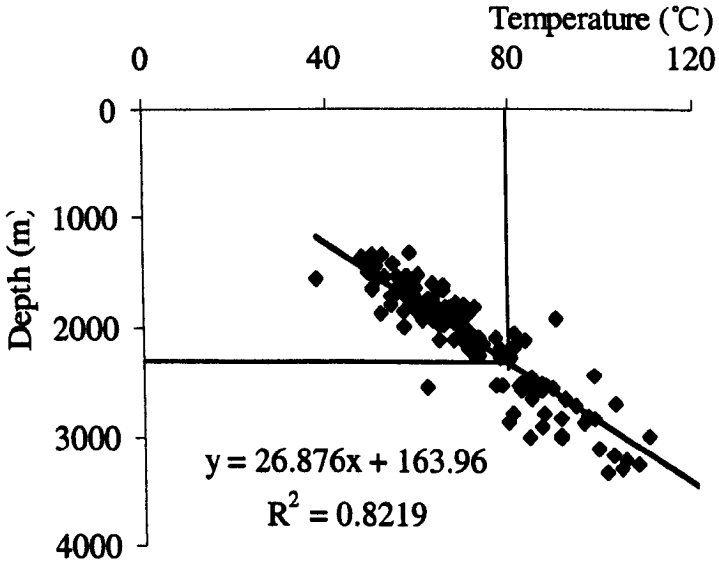

Fig. 3-14. Temperature depth data of the Lengdong oilfield reservoir and fitted by regression (data are provided by Liaohe Oil Company).

3.3.3 Reservoir pressure

The fluid pressures are mostly recorded by repeat formation tests (RFTs) and/or drill stem tests (DSTs) at specific depths in permeable rock layers. These data show very good relationship with burial depth (Fig. 3-16). Calculated pressure coefficients (measured pressures divided by hydrostatic pressures with assumed constant water gradient of 10.0 MPa/km) show the shallow-normally pressured and deep-slightly overpressured systems (Fig. 3-17). These measured high fluid pressures occur at depth more than 2000 m and near the sub-depression center. The biodegraded oils

below 2000 m are all in a normal or underpressured system. No overpressured biodegraded oil occurrences have been observed.

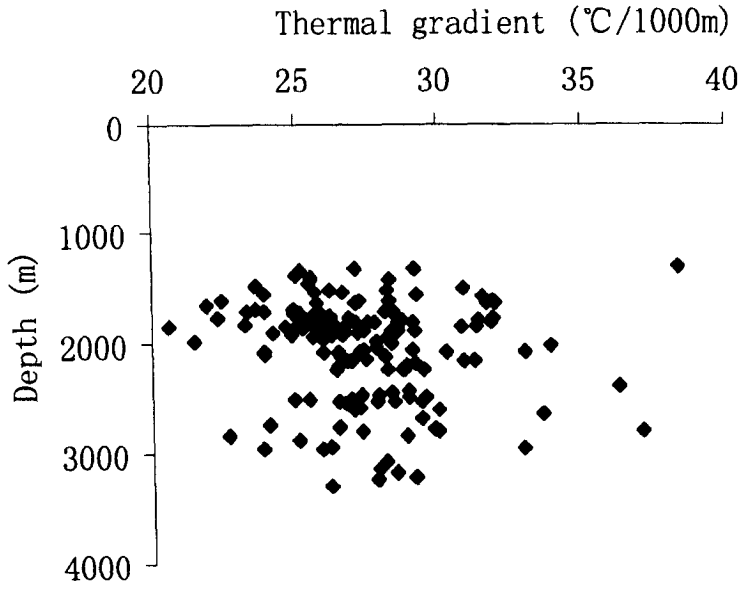

Fig. 3-15. Thermal gradient depth data of the Lengdong oilfield reservoir (data are provided by Liaohe Oil Company).

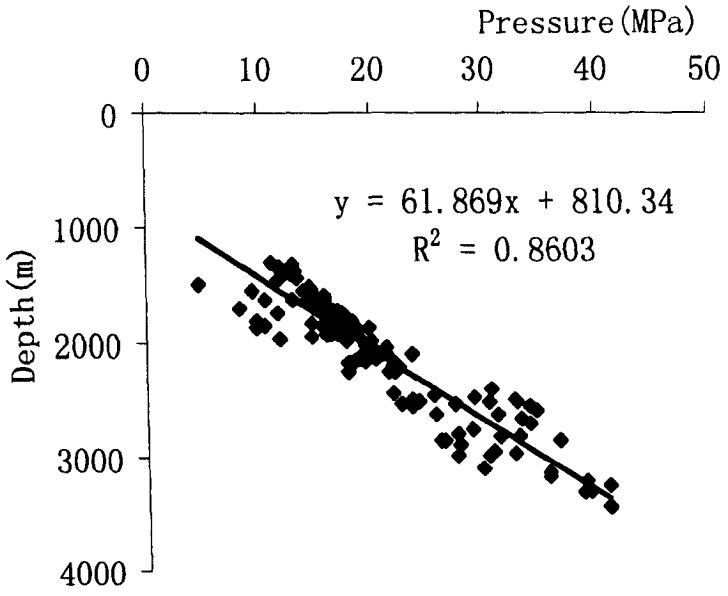

Fig. 3-16. Profiles of pressure with depth for the Lengdong reservoir (data are provided by Liaohe Oil Company).

3.3.4 Petroleum system events

A petroleum system encompasses a pod of active or once-active source rock, all related oil and gas, and all geologic elements and processes that are essential for petroleum accumulations to exist (Demaison and Huizinga, 1991; Perrodon *et al.*, 1992; 1995; Magoon and Dow, 1994). As previous sections discussed all elements and processes, the petroleum events chart presented in Fig. 3-18 indicates that the duration

of generation, migration and accumulation mainly occur since 15 Ma and the critical moment is 9 Ma. Trap development was associated with the Late Oligocene and Early Miocene uplift that resulted in significant erosion in the study area (about 300 m in depression center, see Figure 3-9). This structural and erosional event establish the time of development of the fault-fold and unconformity-related traps. The temporal relationships of the essential elements and processes controlling the petroleum system in the Lengdong area are summarized in Fig. 3-18.

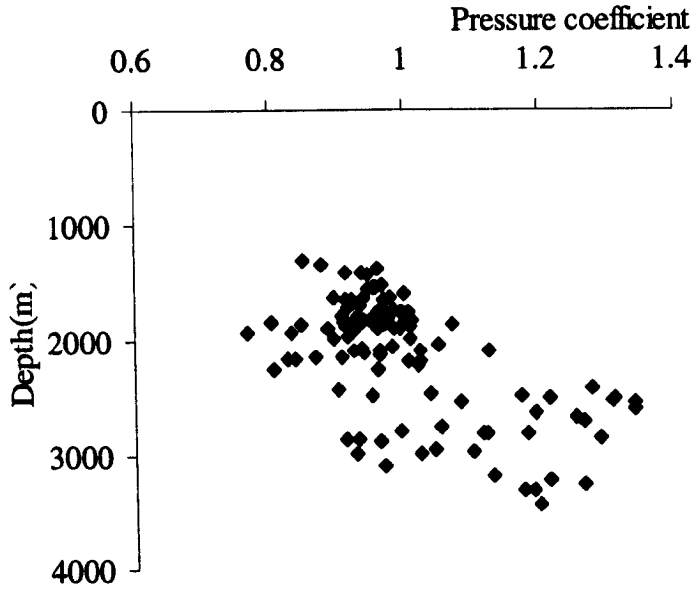

Fig. 3-17. Profiles of pressure coefficient with depth for the Lengdong reservoir (data are provided by Liaohe Oil Company).

3.4 Formation water

Water geochemistry provides a series of powerful tools for solving various oil field development and production problems. Specifically, naturally occurring chemical "tracers" in water can be used to identify the origin and track the movement of water in oil fields, as well as predict the precipitation of scales. These naturally occurring tracers include the absolute and relative abundance of the various dissolved salts (anions and cations) and the hydrogen and oxygen stable isotopic composition of the water itself.

The chemical analyses of the formation water measures the concentrations of the ions (e.g. Cl^-, SO_4^{2-}, HCO_3^-, CO_3^{2-}, Na^++K^+, Mg^{2+}, and Ca^{2+}). Salinity was calculated as the sum of dissolved species equivalent to TDS (total dissolved solids). The Na^+ and HCO_3^- are the major ions. The Na^+ +K^+ ion concentrations are positively correlated with TDS (Fig. 3-19), while other minor ions have no such kind of relationship. Based on chemical compositions all formation waters are ascribed to

$NaHCO_3$ type.

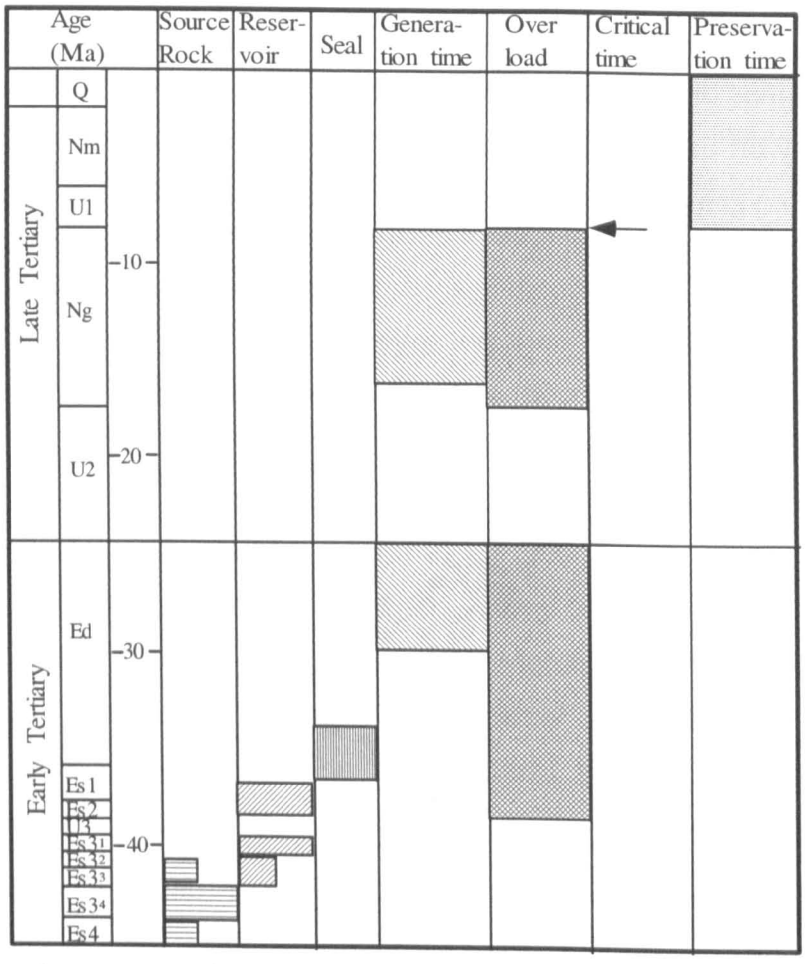

Fig. 3-18. Petroleum event chart in the Lengdong region summarising the timing of key elements and processes.

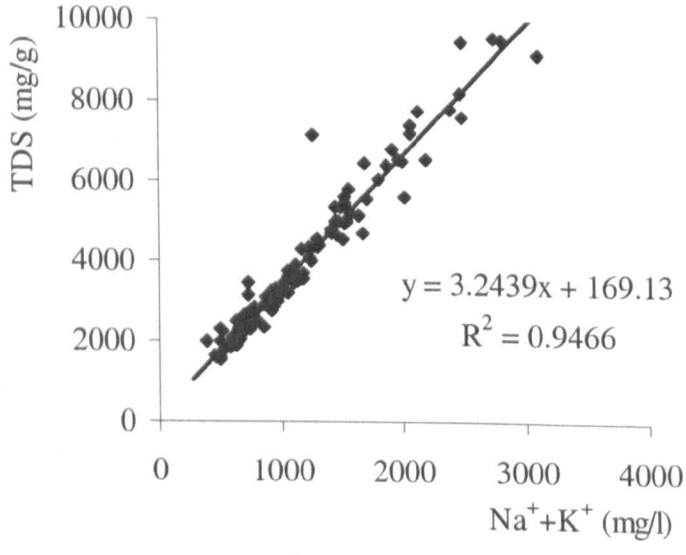

Fig. 3-19. Positive relationship between $Na^+ + K^+$ ion concentration with TDS (data are provided by Liaohe Oil Company).

The TDS vary greatly, ranging from 1500 to 9550 mg/l. Even though they are

very scatter against with depth, a slightly increase trend with depth is obvious, suggesting more saline water occur in the lower strata (Fig. 3-20).

The variations of TDS show a weak positive correlation with API gravity (Fig. 3-21). The heavy oil usually resides in relatively lower salinity water regime. Since no hydrogen or oxygen isotopic data are available, these low TDS water can not be ascribed to palaeometeoric origin.

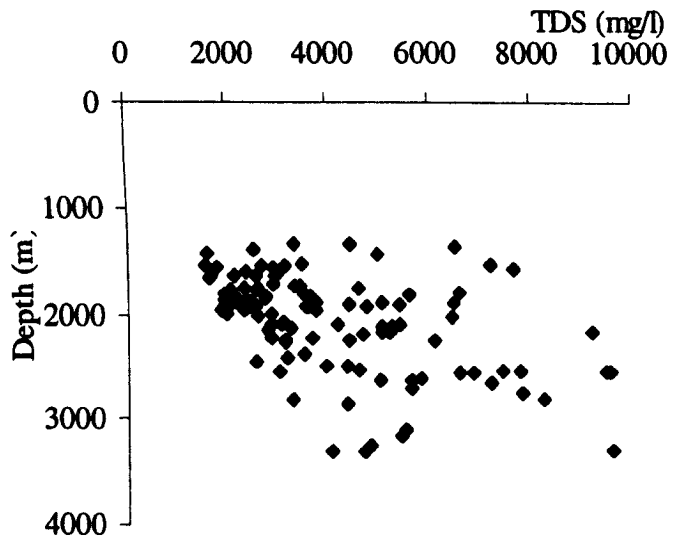

Fig. 3-20 Variation of TDS with reservoir burial depth (data are provided by Liaohe Oil Company).

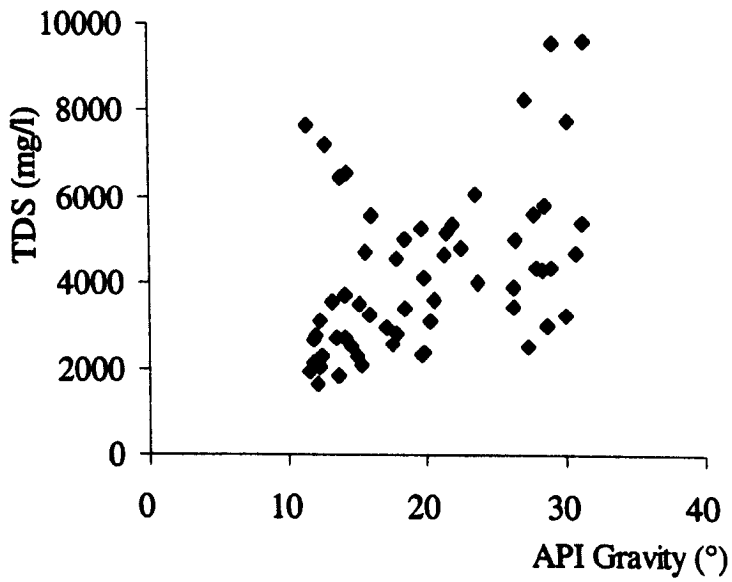

Fig. 3-21 Relationship between TDS of formation waters and API gravity of related oils (data are provided by Liaohe Oil Company).

3.5 Oil physical properties and chemical composition

The oils produced from the study area are mainly heavy to extremely heavy and

viscous, with small amounts of normal gravity oils being produced near the depression centre. Oils in the Lengdong oilfield with API gravities of a suite of oils ranging from about 9° to 33°, reflect oil classifications from normal to very heavy (Hunt, 1996). As shown in Figure 3-22a, a plot of API gravity against depth for the oils, high gravity oils occur at depths greater than 2200 m, while low API gravity oil occur at shallower depths. There is a positive trend between the burial depth and the API gravity at shallower reservoir and no significant change at deeper reservoir intervals. These heavy oils with API gravities less than 20° are highly viscous at room temperature and even under 50 °C, and viscosities show good correlation with the API gravities (Fig. 3-22b). Normal oils located in deeper reservoirs have viscosities lower than 100 mPa.s. It has been suggested that the heavy oils were formed by biodegradation of normal gravity oils (Lu *et al.*, 1990) sourced by the Es3 mature deep-water lacustrine sediments down-dip. Since biodegradation preferentially depleted *n*-alkanes (Connan, 1984; Peters and Moldowan, 1993), wax contents in these low API gravity oils decrease significantly (Fig. 3-22c). The effect of biodegradation can also be reflected in NSO contents, which increase with upward in shallower reservoirs (Fig. 3-22d).

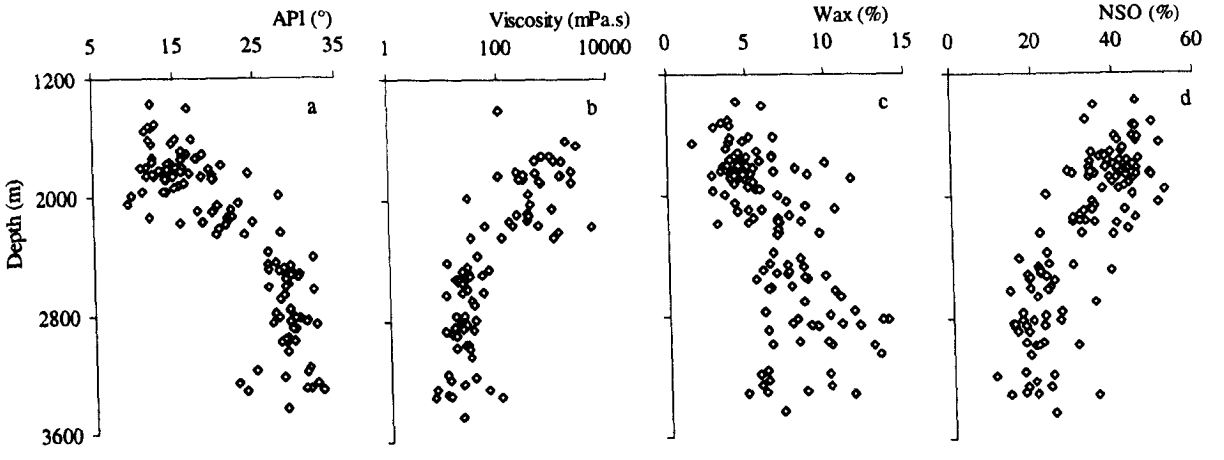

Fig. 3-22. Profiles of oil properties from the Lengdong oilfield. (a) API gravity; (b) Viscosity at 50 °C; (c) Wax content; (d) NSO compound content (data are provided by Liaohe Oil Company).

Sulfur contents of the Lengdong oils are very low; three data are 0.05, 0.16 and 0.22%. The low sulfur content suggests a fresh water depositional environment for the source rock.

3.5.2 Source facies indications

Biomarkers are useful tools to establish relationships between presently oils and their depositional environment since the carbon skeleton structures are inherited from

precursors in living organisms (Mackenzie, 1984; Peters and Moldowan, 1993). Reconstruction of the environmental conditions of organic matter deposition, based on biomarker data, is presently one of the most intensely studied subjects of organic geochemistry. The molecular composition and concentrations of particular organic compounds occurring in petroleum and bitumens may be helpful in: (1) reconstructing redox conditions in a basin (Didyk *et al.*, 1978; Peters *et al.*, 1986; Hughes *et al.*, 1995), (2) characterising salinity levels during deposition of organic matter (ten Haven *et al.*, 1988; Volkman, 1988; Volkman *et al.*, 1998), (3) determining the biological origin of deposited organic matter (Philp and Gilbert, 1986; Mello *et al.*, 1988; Moldowan *et al.*, 1995) as well as the degree of biodegradation (Connan, 1984; Peters and Moldowan, 1993).

Table 3-1 Biomarker indicators of source rock depositional environment of the Lengdong oils.

Well	Depth(m)	Age	Pr/Ph	$C_{29}H/C_{30}H$	$C_{35}H/C_{34}H$	γ-/$C_{30}H$	Hop/Ster	DBT/P	C_{27}%	C_{28}%	C_{29}%
Leng125*	1605.8-1678.8	Es_3	0.45	0.35	0.73	0.20	3.85	0.14	27	33	40
Leng83*	1701-1724	Es_3	0.56	0.42	0.74	0.16	4.91	0.12	27	31	41
Leng90*	1707.9-1738.9	Es_3	0.58	0.36	0.69	0.25	4.26	0.08	24	34	42
Leng61*	1790-1825	Es_3	0.59	0.37	0.73	0.27	4.28	0.11	24	34	41
Leng86*	1824-1843	Es_3	0.63	0.38	0.72	0.26	4.16	0.11	26	34	40
Leng93*	1846-1861	Es_3	0.46	0.39	0.73	0.33	3.83	0.14	26	34	40
Leng46	2496.6-2540.8	Es_3	0.70	0.52	0.69	0.05	4.28	0.14	35	23	43
Leng3	2805-2858	Es_3	0.93	0.45	0.70	0.04	5.15	0.13	34	25	41
Leng75	3121.1-3146.3	Es_3	0.80	0.47	0.69	0.05	4.55	0.14	33	24	43
Leng35	3126.4-3178	Es_3	0.74	0.50	0.69	0.05	5.16	0.15	32	24	44

*biodegraded

Pr/Ph: pristane/phytane; $C_{29}H/C_{30}H$: C_{29} 17α, 21β hopane/C_{30} 17α, 21β hopane; $C_{35}H/C_{34}H$: C_{35} 17α, 21β hopane (R+S)/C_{34} 17α, 21β hopane (R+S); γ-/$C_{30}H$: gammacerane/C_{30} 17α, 21β hopane; Hop/Ster: sum of C_{27}-C_{35} hopanes/sum of C_{27}-C_{29} steranes; DBT/P: dibenzothiophene/phenanthrene; C_{27}%, C_{28}%, C_{29}%: percentage of αααC_{27} (R+S), αααC_{28} (R+S), αααC_{29} (R+S).

The relative amounts of pristane and phytane, expressed as Pr/Ph ratios, have been used as an indicator of source depositional environment. According to Didyk *et al.* (1978) and ten Haven *et al.* (1987), low values (Pr/Ph < 2) indicate aquatic depositional environments including marine, fresh and brackish water (reducing conditions), intermediate values (2–4) indicate fluviomarine and coastal swamp environments, whereas high values (up to 10) are related to peat swamp depositional environments (oxidizing conditions). The (Pr/Ph) ratio is less than one for all oils from the Lengdong oilfield suggesting anoxic conditions of deposition.

The C_{29} 17α, 21β hopane/C_{30} 17α, 21β hopane ratio was used by Palacas *et al.* (1984) as a source rock parameter. In the case of the Lengdong oils C_{30}

17α, 21β hopane is much higher than C_{29} 17α, 21β hopane and the $C_{29}\alpha\beta$hopane/$C_{30}\alpha\beta$hopane ratios between 0.35 and 0.52. This ratio suggests the fresh water lacustrine origin of the Lengdong oils.

The C_{35}/C_{34}-homohopane ratios (C_{35} homohopane indices) are indicative of depositional environment (Peters and Moldowan, 1993). Increased concentrations of C_{35} homohopanes have been commonly noted in cases of organic matter deposited in anoxic and hypersaline conditions (Dahl *et al.*, 1994). Low C_{35} homohopane indices are consistent with deposition of the Lengdong oils in fresh water under weak reducing environments (Peters and Moldowan, 1991).

Of considerable importance for palaeoenvironmental interpretations is the presence of gammacerane – a specific C_{30}-triterpane. This compound is commonly cited as the main biomarker in many oils and bitumens traced back to hypersaline source environments (Moldowan *et al.*, 1992; Dahl *et al.*, 1994; Peters *et al.*, 1996). Abundant gammacerane is considered an indicator diagnostic of high salinity and water column stratification in the source rock depositional environment (Damsté *et al.*, 1995). Gammacerane has also been used as an indicator of carbonate or evaporate source rocks (Mello *et al.*, 1988; Peters and Moldowan, 1991). The gammacerane/C_{30} αβ hopane ratio in the Lengdong area is variable between two end member oil types. All biodegraded oils show high values between 0.16 and 0.33, while all non-biodegraded oils show very low values around 0.05. It was reported that Es4 source rock has a high relative abundance of gammacerane and Es3 source rock characterizes by low relative abundance of gammacerane (Lu *et al.* 1990; Li *et al.* 1994). Since gammacerane has high ability to resist biodegradation (Peters and Moldowan, 1993), the rise values in biodegraded oils may not relate solely with their depositional environment. Biodegradation actually masks the source distinction and may mislead the oil source correlation (Koopmans *et al.*, 2002).

The ratio of relative concentrations of hopanes to steranes can reflect differences in chemical characteristics of the organic matter deposited in different sedimentary environments. The hopane/sterane ratio is often used as a measure of the relative inputs of prokaryotic versus eukaryotic debris (Peters and Moldowan, 1993). Terpenoids with a hopane skeleton occur mainly in primitive bacterial organisms and in a few higher plants. The extended hopanes (pseudo-homologues: C_{31}-C_{35}) are derived directly from particular bacteriohopanepolyols (e.g. bacteriohopanetetrol) occurring in lipid membranes of many procaryotic organisms. Lower hopane pseudo-homologues (C_{30} and lower) may originate from precursors containing 30 carbon atoms, such as diplopterol or diploptene (Rohmer *et al.*, 1992; Peters and Moldowan,

1993; Farrimond *et al.*, 1998). In turn, steranes occurring in sedimentary organic matter can be traced to eucaryotic organisms. Sterols (e.g. Volkmann *et al.*, 1994) are sterane precursors, and are also widely noted in lipid membranes of modern microalgae. The tetracyclic sterol structure improves rigidity and strengthens a cell membrane in eucaryotic organisms (Peters and Moldowan, 1993).

The hopanes/steranes (hopanes consist of the C_{27} to C_{35} pseudo-homologues (including 22S and 22R epimers; steranes consist of the C_{27}, C_{28}, C_{29} (20S+20R) regular steranes) ratios are between 3.8 and 5.2 (Table 3-1). These high hopane to sterane ratios are indicative of the effects of terrestrial source.

It is agreed that the relative amounts of C_{27}-C_{29} steranes can be used to give indication of source differences. Huang and Meinschein (1979) proposed to plot the relative proportion of C_{27}-C_{28}-C_{29} sterols on ternary diagram in order to correlate the sterane composition with the type of depositional environment. The diagram is widely used to plot sterane abundance. In early publications it was commonly assumed that a predominance of C_{27} steranes in an oil or rock extract would signify an algal or marine input, whereas C_{29} steranes signified the presence of higher plant or terrestrial input. A number of significant and important advances have been made in the past two or three decades concerning interpretation of sterane distributions in oils and source rock extracts. It has now been clearly established that the presence of C_{29} steranes does not necessarily mean an input of higher plant material since C_{29} sterols can also have an algal source (Peters and Moldowan, 1993; Philp, 1994; Obermajer *et al.*, 1999).

The slightly higher relative amount of C_{29} steranes (40–43%) in the Lengdong oils as would be expected for organic matter of lacustrine origin (Curiale and Rui, 1991; Li *et al.*, 1994). The uniform distribution patterns in the Lengdong oils are indicative of their similarity in terms of organic matter type and paleoenvironment of deposition (Fig. 3-23).

The ratio of dibenzothiophene to phenanthrene and the ratio of pristane to phytane, when coupled together, provide a novel and convenient way to infer crude oil source rock depositional environments and lithologies (Hughes *et al.*, 1995). A cross-plot of dibenzothiophene/phenanthrene versus the pristane/phytane ratios can classify the oils and source rocks paleodepositional depositional environments. The classification scheme is based on the premise that these ratios reflect the different Eh-pH regimes resulting from the significant microbiological and chemical processes occurring during deposition and early diagenesis of sediments. The

dibenzothiophene/phenanthrene ratio assesses the availability of reduced sulphur for incorporation into organic matter and the pristane/phytane ratio assesses the redox conditions within the depositional environment. The dibenzothiophene/phenanthrene ratio alone is an excellent indicator of source rock lithology with carbonates having ratios > 1 and shales having ratios < 1. All dibenzothiophene/phenanthrene ratios from the Lengdong oils are less than 0.15, which coupling with relatively low Pr/Ph ratios indicates a typical fresh water lacustrine condition (Hughes *et al.*, 1995) (Table 3-1).

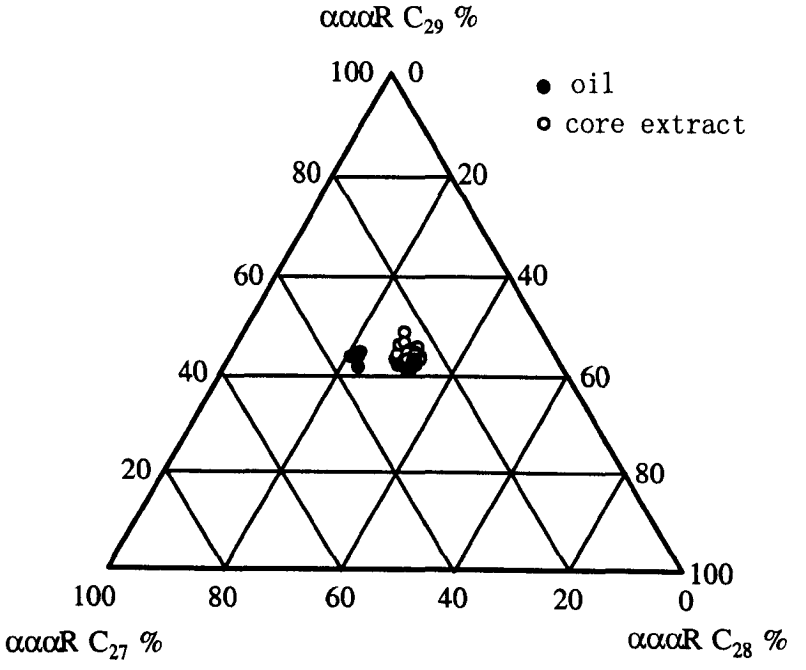

Fig. 3-23. Ternary diagram showing the relative abundance of C_{27}, C_{28} and C_{29} regular steranes in the Lengdong oils.

All above discussion suggests that oils in studied area have very similar biomarker distributions and have been generated from the same source rock faces at similar maturity levels. Large differences in fluid properties and oil quality are caused by secondary alteration processes, i.e., level of biodegradation.

3.5.3 Thermal maturity

A summary of the molecular maturity parameters measured in this study is shown in Table 3-2. Although some of the differences in these biomarker ratios are due to maturity effects, it is clear that part of these variations are due to the effect of differential levels of biodegradation on these samples. Consequently, it is necessary to analyze the data with caution.

The abundance of C_{27} 18α(H)-22,29,30-trisnorneohopane (Ts) relative to C_{27} 17α(H)-22,29,30-trisnorhopane (Tm) was used to indicate thermal maturity when it

was first proposed (Seifert and Moldowan, 1981). The biodegraded oils from the Lengdong oilfield exhibit a lower Ts/Tm values, 0.30-0.56, while the ratios of non-biodegraded oils are 0.63 to 0.80. The higher Ts content in these oils points to higher maturity but biodegradation effects can not be ruled out.

The ratio of 18α-(H)-30-norneohopane (C_{29} Ts) to $C_{29}\alpha\beta$ hopane is also a suitable maturity indicator (Moldowan *et al.* 1991). This ratio behaves in a similar manner to Ts/Tm, which increases with thermal maturity. The C_{29}Ts/ $C_{29}\alpha\beta$ hopane ratios in biodegraded oils (0.14–0.19) again lower than these of non-biodegraded oils, suggesting slightly high maturity for the non-biodegraded oils.

Table 3-2 Maturity ratios based upon steranes and triterpanes for the Lengdong produced oils.

Well	Depth(m)	Age	Ts/Tm	C_{29}Ts/C_{29}H	C_{31}S/S+R	Diast/St	C_{29}S/S+R	$C_{29}\beta\beta/\alpha\alpha+\beta\beta$
Leng125*	1605.8-1678.8	Es_3	0.30	0.16	0.56	0.11	0.41	0.31
Leng83*	1701-1724	Es_3	0.56	0.18	0.57	0.15	0.46	0.34
Leng90*	1707.9-1738.9	Es_3	0.46	0.18	0.57	0.13	0.45	0.34
Leng61*	1790-1825	Es_3	0.37	0.14	0.58	0.13	0.46	0.33
Leng86*	1824-1843	Es_3	0.37	0.16	0.57	0.13	0.45	0.34
Leng93*	1846-1861	Es_3	0.42	0.19	0.58	0.14	0.47	0.34
Leng46	2496.6-2540.8	Es_3	0.63	0.21	0.57	0.21	0.42	0.32
Leng3	2805-2858	Es_3	0.80	0.27	0.57	0.23	0.44	0.36
Leng75	3121.1-3146.3	Es_3	0.67	0.28	0.58	0.21	0.45	0.34
Leng35	3126.4-3178	Es_3	0.77	0.24	0.58	0.22	0.50	0.36

*biodegraded

Ts/Tm: C_{27} 18α(H)-22,29,30-trisnorneohopane (Ts)/C_{27} 17α(H)-22,29,30-trisnorhopane (Tm); C_{29}Ts/C_{29}H: 18α-(H)-30-norneohopane (C_{29} Ts)/$C_{29}\alpha\beta$ hopane; C_{31} S/(S+R): C_{31} 17α, 21β hopane 22S/22(R+S); Diast/St: C_{27}-C_{29}-diasteranes/C_{27}-C_{29} steranes; C_{29}S/S+R: $\alpha\alpha\alpha C_{29}$ steranes 20S/20(R+S); $C_{29}\beta\beta/\alpha\alpha+\beta\beta$: C_{29} steranes 14β(H), 17β(H)/[14α(H), 17α(H) +14β(H), 17β(H)].

The "S–R" indices are commonly applied to describe the thermal maturity of an oil. The isomerization happens at C-22 in hopanes resulting in an R to S conversion. The reaction leads to an S, R-equilibrium, which remains constant at higher maturity. The 22S/(22S+22R) C_{31} homohopane index was found to be 0.56-0.58 for all oils analyzed, indicating that the oils have reached the maximum of oil phase generation. The equilibrium value reported ranges from 0.57 to 0.62 (Seifert and Moldowan, 1986) and this isomerization ratio in the Lengdong oils are poor differentiators of oil maturity.

Diasteranes are more stable than the regular steranes, the diasteranes/steranes ratio increases with thermal maturity (Peters and Moldowan, 1993). Although the relative proportion of diasteranes may also be related to biodegradation, the higher

diasteranes/steranes ratio in non-biodegraded oils compared with biodegraded oils undoubtedly indicate higher maturity in these oils.

The ααα C_{29} sterane 20S/(20S+20R) ratio is one of the most widely applied molecular maturity parameters in petroleum geochemistry, and is based on the relative enrichment of the 20S isomer compared with the biologically-inherited 20R stereochemistry. This ratio reaches an equilibrium point of 50–55%. Another ratio is C_{29} sterane ββ/(αα+ββ) and reaches an equilibrium point of 70% (Mackenzie, 1984). Both indices, 0.41–0.50 and 0.31–0.36, respectively, show that none of the Lengdong oils has reached equilibrium values, which may be indicative of a low degree of maturity. The slight difference is owing to different charging history and these non-biodegraded oils resided in deeper reservoir are the products of the late generation.

A limitation of many of the aliphatic biomarker thermal maturity parameters is that they reach equilibrium before the main part of the oil window, and in some cases demonstrate inversion at high maturity levels. They are thus not effective at discriminating variations in thermal maturity for mid and high maturity oils (Farrimond *et al.*, 1999). The abundance and distribution of polycyclic aromatic hydrocarbons and their structural isomers, have also been widely used to assess the maturation of coals, source rock bitumens and oils. Aromatic hydrocarbon ratios can potentially be more useful in this regard as they are sensitive to maturity differences in the mid to late parts of the oil generation window (Radke, 1988). A variety of maturity parameters have been proposed based on the ratios of the relative concentrations of the more thermally stable aromatic isomers to the less stable ones (Radke and Welte, 1983; Alexander *et al.*, 1985; Radke, 1988; Budzinski *et al.*, 1995; van Aarssen *et al.*, 1999). The maturity parameters derived from methylated naphthalenes are based on the notion that naphthalenes with β-substituted methyl groups are more stable than those with α-substituents (Alexander *et al.*, 1985; Radke, 1988). Phenanthrene maturity parameters are based on greater stability of 3-MP and 2-MP compared to 9-MP and 1-MP (Radke and Welte, 1983). The alkylated dibenzothiophene isomers with methyl substituent in the 4-position are the most thermodynamically stable, whereas isomers with the methyl substituent in the 1-position have low stability (Radke, 1988; Chakhmakhchev *et al.*, 1997). Even though subtle changes in depositional conditions may complicate these rank estimates (Radke *et al.*, 1986; Budzinski *et al.*, 1995; Huang and Pearson, 1999), parameters derived from these compounds are broadly reliable and extensively used.

Table 3-3 Maturity ratios based upon polycyclic aromatic hydrocarbons for the Lengdong produced oils.

Well	Depth(m)	Age	TMNr	TeMNr	MDR	MPI1	Rc (%)	TA/(TA+MA)
Leng125*	1605.8-1678.8	Es_3	0. 49	0. 53	1. 66	0. 64	0. 78	0. 65
Leng83*	1701-1724	Es_3	0. 47	0. 49	2. 08	0. 60	0. 76	0. 66
Leng90*	1707.9-1738.9	Es_3	0. 61	0. 50	3. 06	0. 65	0. 79	0. 67
Leng61*	1790-1825	Es_3	0. 58	0. 48	2. 52	0. 63	0. 78	0. 67
Leng86*	1824-1843	Es_3	0. 49	0. 49	2. 55	0. 64	0. 78	0. 67
Leng93*	1846-1861	Es_3	0. 54	0. 37	2. 37	0. 64	0. 78	0. 66
Leng46	2496.6-2540.8	Es_3	0. 41	0. 54	1. 18	0. 42	0. 65	0. 60
Leng3	2805-2858	Es_3	0. 35	0. 42	1. 28	0. 52	0. 71	0. 63
Leng75	3121.1-3146.3	Es_3	0. 41	0. 48	1. 44	0. 52	0. 71	0. 65
Leng35	3126.4-3178	Es_3	0. 41	0. 51	1. 36	0. 48	0. 69	0. 67

*biodegraded

TMNr: 1,3,7-/(1,3,7- + 1,2,5-TMN); TeMNr: 1,3,6,7-/(1,3,6,7- + 1,2,5,6- + 1,2,3,5-TeMN); MDR: 4-MDBT/1-MDBT; MPI1: 1.5 × (2- + 3-MP)/(P + 1-MP + 9-MP); Rc: 0.6 × MPI1 + 0.4 (Radke and Welte, 1983); TA: triaromatic steroid hydrocarbons; MA: monoaromatic steroid hydrocarbons.

Variety of naphthalene-related parameters have been developed over the years and used to assess maturities of crude oils (Alexander *et al.*, 1985; Radke, 1988; van Aarssen *et al.*, 1999). In the case of the trimethylnaphthalenes (TMNs), the thermally stable isomers are 2,3,6-, 1,3,7-, 1,3,6-TMN and the less stable isomer is 1,2,5-TMN (van Aarssen *et al.*, 1999). Previous studies suggest that the abundance of 2,3,6-TMN is very low in many samples (van Aarssen *et al.*, 1999) and most TMN are easily affected by biodegradation (Fisher *et al.*, 1996). In addition, the 1,3,6-TMN has a direct natural product precursor in certain samples and its abundance in those cases might reflect source effects rather than maturity. Therefore, it is preferred to measure 1,3,7-TMN, to provide a more reliable parameter. The ratio of 1,3,7-TMN to the sum of 1,3,7-TMN and 1,2,5-TMN is called TMNr (van Aarssen *et al.*, 1999). TMNr values for the Lengdong oils range from 0.35 to 0.61 (Table 3-3). Interestingly, these deep reservoired oils have relatively low TMNr values compared to the shallower ones. Biodegradation may affect trimethylnaphthalene distributions. van Aarssen *et al.* (1999) proposed another alkylated naphthalene maturity parameter based on the tetramethylnaphthalene (TeMN) distributions. The ratio of 1,3,6,7-TeMN to the sum of 1,3,6,7-TeMN and (1,2,5,6 + 1,2,3,5)-TeMN is called TeMNr. TMNr values for the Lengdong oils range from 0.37 to 0.54 (Table 3-3). Both shallow and deep reservoired oils have the similar TeMNr values. Although no correlation between TMNr or TeMNr and vitrinite reflectance has been established, TMNr and TeMNr values in a set of normal maturity oils from the Barrow Sub-basin range from 0.5 to 1.0 (van Aarssen *et al.*, 1999) which are much higher than these from the Lengdong oilfield.

This again indicates marginal mature characteristics of the Lengdong oils.

The MDR (methyl dibenzothiophene ratio = 4-MDBT/1-MDBT) proposed by Radke *et al.* (1986) appears to be a more sensitive maturity index since it shows a better correlation with vitrinite reflectance and Rock-Eval Tmax in source rock bitumens (Radke, 1988). Table 3-3 shows MDR values in the Lengdong oils fall in a range from 1.18 to 3.06. Low MDR values with small variations also suggest their low maturity nature.

The relative abundance of triaromatic steroid hydrocarbons (TA) and monoaromatic steroid hydrocarbons (MA) is one of the most commonly-used maturity parameters (Mackenzie, 1981). The ratio TA/(TA+MA) increases with increasing thermal maturation. For the Lengdong oils this ratio is quite consistent in both biodegraded and non-biodegraded oils, indicating similar maturity throughout the whole oilfield.

The widely used methylphenanthrene index [MPI1 = 1.5 × (2-MP + 3-MP) / (P + 1-MP + 9-MP)] (Radke and Welte, 1983) is made under the assumption that 2-MP and 3-MP are derived from 1-MP and 9-MP by rearrangement. Due to its linear relationship with vitrinite reflectance, MPI1 is often used to calculate an alternative value of vitrinite reflectance (Rc) (Radke, 1988), and may be useful in source rock sequences where vitrinite reflectance values cannot be measured. MPI1 values cover the range of 0.42-0.65 in the Lengdong oils. Rc values for the Lengdong oils, calculated using the equation of Radke and Welte (1983) (= 0.6 × MPI1 + 0.4) are given in Table 3-3. The maturity ranges obtained for the Lengdong oils studied here are 0.65 to 0.79 %Rc.

4 BIODEGRADATION EFFECTS ON ALIPHATIC HYDROCARBONS

The samples used in this project were 54 core extracts from 5 wells and 10 oils from individual wells in the Lengdong oilfield. Sample locations are shown in Fig. 4-1 and details are listed in Table 4-1.

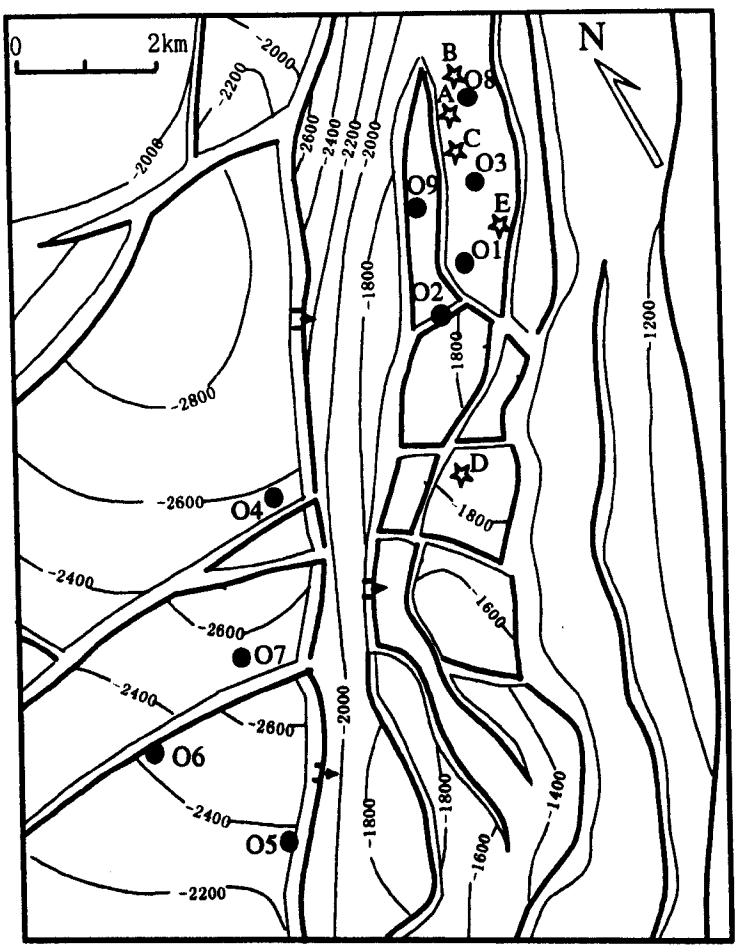

Fig. 4-1. Oil and core extract samples location in the Lengdong oilfield.
(Contour line is the base of the Es1 structure; ● oil sample; ☆ core sample)

The Es3 stratigraphy is characterized by deep lacustrine mudstone interbedded with turbidite. The dominant lithology of the reservoir is coarse grained conglomerate (see Chapter 3). The sampling interval of the Es3 column can be regard as a continuous column since no significant shale occurs in this interval and the whole column is saturated with oil. The oil-water contact is presently at ca. 1830 m depth in wells A, B and C. The Es1 is mainly composed of poorly sorted coarse sediments and Wells D and E are most likely separated by thin shale layer in somewhere even through detailed well log data for these two wells are not available.

4.1 Aliphatic hydrocarbon contents in reservoir oil

The bulk composition data (saturated hydrocarbons, aromatic hydrocarbons,

resins and asphaltenes) obtained by Iatroscan analysis enabled an assessment of the compositional changes occurring within each oil column. Variations in the abundance of residual oil and of the saturated hydrocarbon fraction in each extract of the Es3 column (Wells A, B and C) are illustrated in Figure 4-2. The residual oil abundance firstly increases and then decreases towards the oil water contact, while the saturated hydrocarbon contents show a progressively decreasing trend from 45% w/w at the top to about 25% w/w at the bottom (Fig. 4-2). This unusually well developed vertical gradient indicates a systematic loss of saturated hydrocarbon with increasing depth. Numerous studies have documented the occurrence of oil columns that contain compositional variation with depth. This can result for several reasons and examples include: gravity segregation, thermal diffusion, inadequate time for equilibrium processes, dynamic flux induced by active aquifer, biodegradation, and various mixing scenarios. These conditions, separate or in combination, can lead to significant variation in fluid composition in both vertical and lateral directions (Khavari-Khorasani *et al.* 1998; Larter *et al.*, 2003). This decrease in bulk saturated hydrocarbon content is also mirrored by systematic changes down reservoir in molecular parameters which unambiguously reflect the effects of biodegradation.

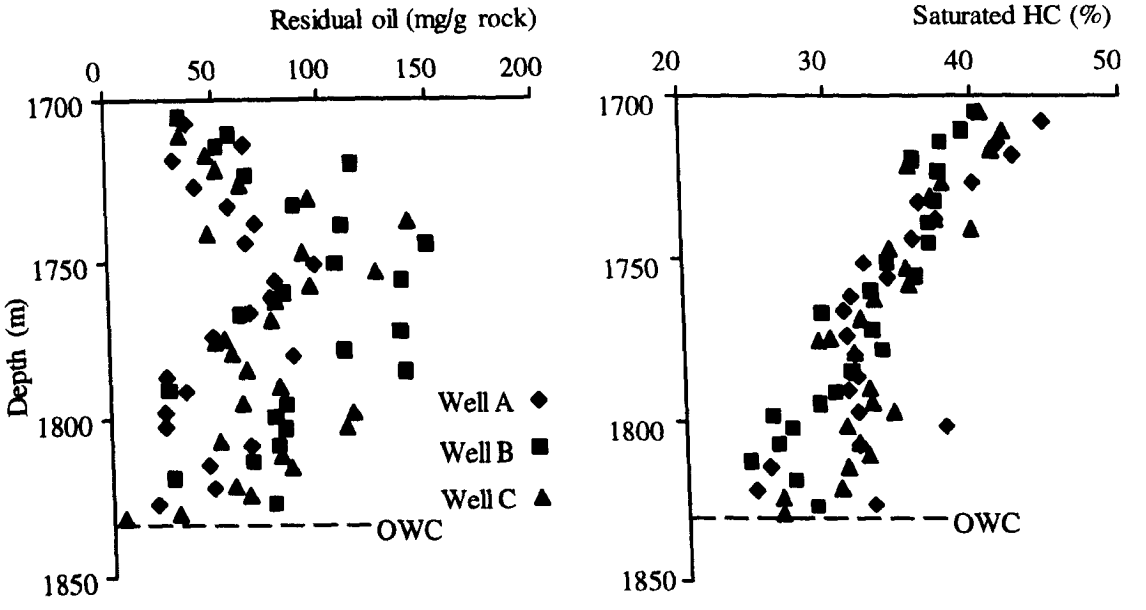

Fig. 4-2. Iatroscan data showing residual oil abundance and bulk composition changes within the Es3 oil column.

The results from Well D of the Es1 column are characterized by higher residual oil (extractable organic matter) abundances and lower saturated hydrocarbon contents. A slight trend of decreasing abundance with increasing depth can be observed in both parameters (Fig. 4-3).

Table 4-1 Oil and core extract sample list (see Fig. 4-1 for location).

No	Well name	Depth	Age	Type	No	Well name	Depth	Age	Type
L02	Well A	1707.8	Es3	core	L31	Well D	1490.8	Es1	core
L03	Well A	1727	Es3	core	L32	Well D	1516.7	Es1	core
L04	Well A	1738	Es3	core	L33	Well D	1535.7	Es1	core
L05	Well A	1751	Es3	core	L34	Well D	1561.9	Es1	core
L06	Well A	1761.5	Es3	core	L35	Well D	1583.6	Es1	core
L07	Well A	1773.5	Es3	core	L36	Well D	1608.7	Es1	core
L08	Well A	1786	Es3	core	L37	Well D	1624	Es1	core
L09	Well A	1797.5	Es3	core	L38	Well D	1645.5	Es1	core
L10	Well A	1808	Es3	core	25	Well E	1299.51	Es1	core
L11	Well A	1821.5	Es3	core	27	Well E	1310.85	Es1	core
L12	Well A	1826.5	Es3	core	28	Well E	1373.32	Es1	core
L16	Well B	1705	Es3	core	30	Well E	1379.7	Es1	core
L17	Well B	1720	Es3	core	35	Well E	1397.3	Es1	core
L18	Well B	1733	Es3	core	36	Well E	1406.4	Es1	core
L19	Well B	1745	Es3	core	41	Well E	1420.17	Es1	core
L20	Well B	1756	Es3	core	46	Well E	1459.33	Es1	core
L21	Well B	1772	Es3	core	47	Well E	1466.23	Es1	core
L22	Well B	1785	Es3	core	49	Well E	1488.95	Es1	core
L23	Well B	1799	Es3	core	50	Well E	1497.77	Es1	core
L24	Well B	1813	Es3	core	53	Well E	1516.04	Es1	core
L25	Well B	1827	Es3	core	57	Well E	1548.44	Es1	core
L39	Well C	1705.5	Es3	core	59	Well E	1563.35	Es1	core
L40	Well C	1717	Es3	core	61	Well E	1572.38	Es1	core
L41	Well C	1726.5	Es3	core	O1	Leng 83	1701-1724	Es3	oil
L42	Well C	1737.6	Es3	core	O2	Leng 61	1790-1825	Es3	oil
L43	Well C	1747	Es3	core	O3	Leng 86	1824-1843	Es3	oil
L44	Well C	1758	Es3	core	O4	Leng 35	3126.4-3178	Es3	oil
L45	Well C	1768	Es3	core	O5	Leng 3	2805-2858	Es3	oil
L46	Well C	1779	Es3	core	O6	Leng 46	2496.6-2540.8	Es3	oil
L47	Well C	1789.6	Es3	core	O7	Leng 75	3121.1-3146.3	Es3	oil
L48	Well C	1801.7	Es3	core	O8	Leng 90	1707.9-1738.9	Es3	oil
L49	Well C	1814.5	Es3	core	O9	Leng 93	1846-1861	Es3	oil
L50	Well C	1829.5	Es3	core	O12	Leng 125	1605.8-1678.8	Es3	oil

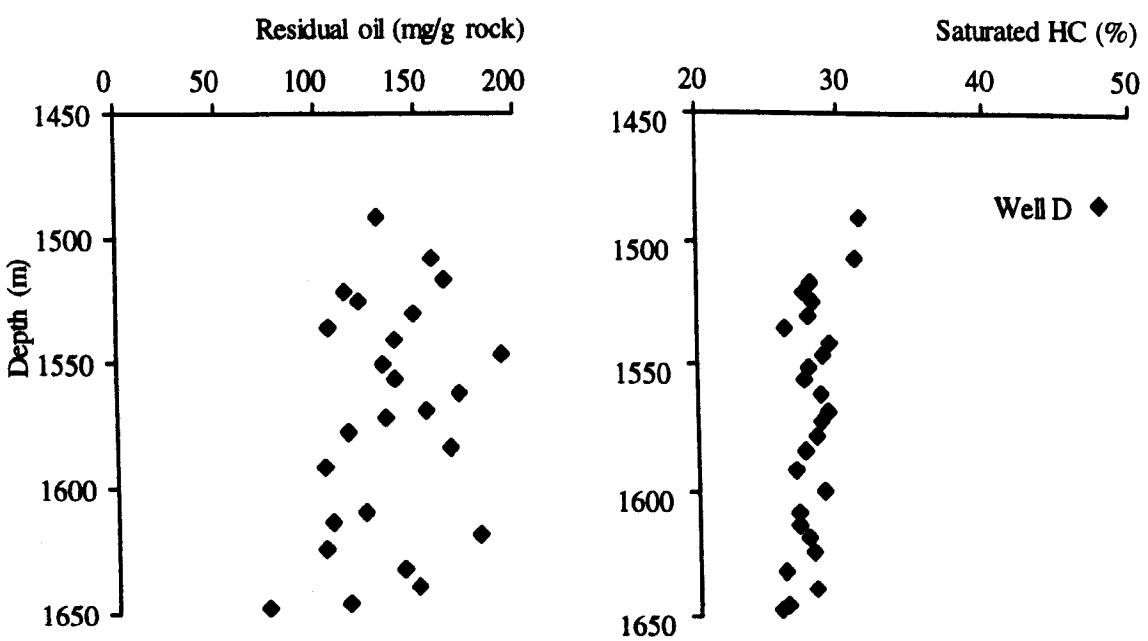

Fig. 4-3. Iatroscan data for Well D showing residual oil abundance and bulk composition changes within the Es1 oil column.

4.2 C_{15}+ *n*-alkanes and isoprenoid alkanes

4.2.1 Oil TIC

Representative reconstructed ion chromatograms (RIC) of the aliphatic hydrocarbon fraction from the Lengdong produced oils are shown in Figure 4-4 (sum of ions listed see Table 2-1). The alkane distribution patterns vary greatly depending on biodegradation degree. The unbiodegraded oils such as Leng 35 and Leng 46 are characterized by C_{12}-C_{30} *n*-alkanes with a smooth unimodal distribution, largely reflecting the composition of the original oil as generated from its lacustrine shale source rock at main stage of oil generative levels. The complete suite of *n*-alkanes is intact and *n*-alkanes are greater than adjacent isoprenoids (e.g. as monitored by pristane/*n*-C_{17} and phytane *n*-C_{18} ratios). The UCM of branched and cyclic compounds under the resolved peak envelope is small. The shallow reservoired oils such as Leng 90 and Leng 93, on the other hand, exhibit a completely different aliphatic hydrocarbon distribution pattern that reflects its alteration by microbial degradation. In Leng 90, *n*-alkanes are significantly depleted but isoprenoids are survived, while in Leng 93 all *n*-alkanes have been removed and the UCM hump is large. The C_{30} hopane and other polycyclic alkanes are predominated the GC signatures.

4.2.2 RIC from reservoir extracts

Representative RICs of the aliphatic hydrocarbon fractions from the Es3 column (Fig. 4-5) clearly illustrate the systematic changes in the composition of the residual oil throughout these columns. The least degraded samples were located at the top of the column and were characterized by a complete series of C_{15}-C_{30} *n*-alkanes with a maximum at *n*-C_{23}. With increasing depth within the oil column, the aliphatic hydrocarbons become progressively depleted. The *n*-alkanes also show a slight odd-even predominance. The sample from the middle of the Es3 column is significantly depleted in *n*-alkanes and isoprenoids, leaving the hopane series predominant in the chromatogram. The lowest sample near the OWC exhibits a complete removal of *n*-alkanes and isoprenoid alkanes, leaving the hopane series even more concentrated. No 25-norhopanes have been detected in the Es3 core extracts.

The extents of biodegradation in the Es3 column oils are light to moderate biodegradation, level 2 at the top of the Peters and Moldowan (1993) biodegradation scale (general depletion of *n*-alkanes), level 3 at the middle (> 90% *n*-alkanes removed) and level 4/5 at the bottom (*n*-alkanes disappear, > 90% isoprenoid alkanes removed). The systematic depletion of *n*-alkanes and isoprenoid alkanes is interpreted

as being attributable to biodegradation at the OWC and the consequent establishment of diffusion-controlled concentration gradients within the oil column.

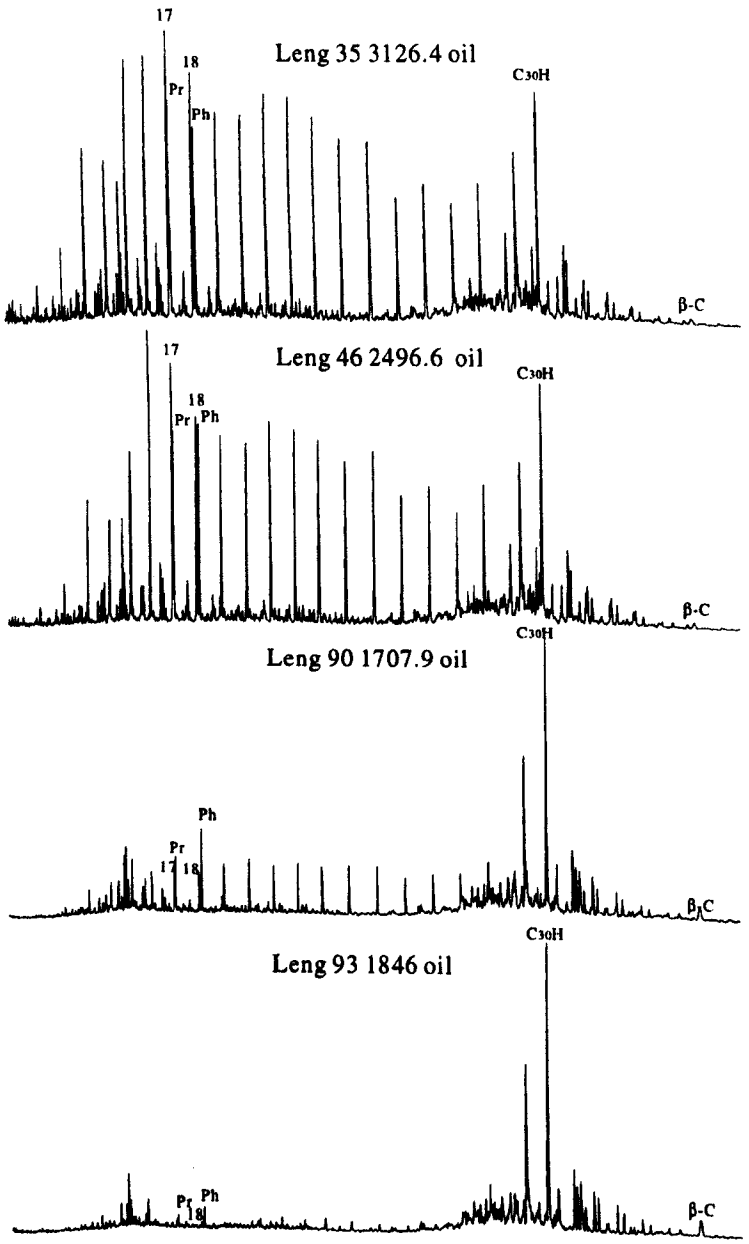

Fig. 4-4. Reconstructed ion chromatograms (sum of ions listed in Table 2-1) showing the aliphatic hydrocarbon distribution patterns in four representative oil samples. Numbers refer to *n*-alkane chain length; Pr: Pristane; Ph: Phytane; $C_{30}H$: C_{30} αβ hopane; β-C: β-carotane.

In the Es1 column the biodegradation of the oil is more severe than that in the Es3 columns since its burial depth is shallower. On the top of the Es1 column the RIC shows essentially complete loss of the *n*-alkanes (though minor amounts may indicates some minor recharging), a significant reduction in the abundance of acyclic isoprenoids and only trace amounts of the 25-norhopanes (Fig. 4-6). The biodegradation level is similar to that in the bottom of the Es3 columns. Towards the bottom of the column a significant amount of 25-norhopane homologues occur in the

RIC. The 25-norhopanes are often present in severely biodegraded oils and are generally considered to be the product of heavy biodegradation (Seifert and Moldowan, 1979; Rullkötter and Wendisch, 1982; Volkman *et al.*, 1983; Moldowan and McCaffrey, 1995; Peters *et al.*, 1996). Increasing oil biodegradation is evident from the increasing UCM hump. The biodegradation in the Es1 column oil has been extensive from level 5 near the top (*n*-alkanes and *iso*-alkanes removed) to level 8 near the bottom (> 50% C_{30} αβ hopane removed and significant 25-norhopanes produced).

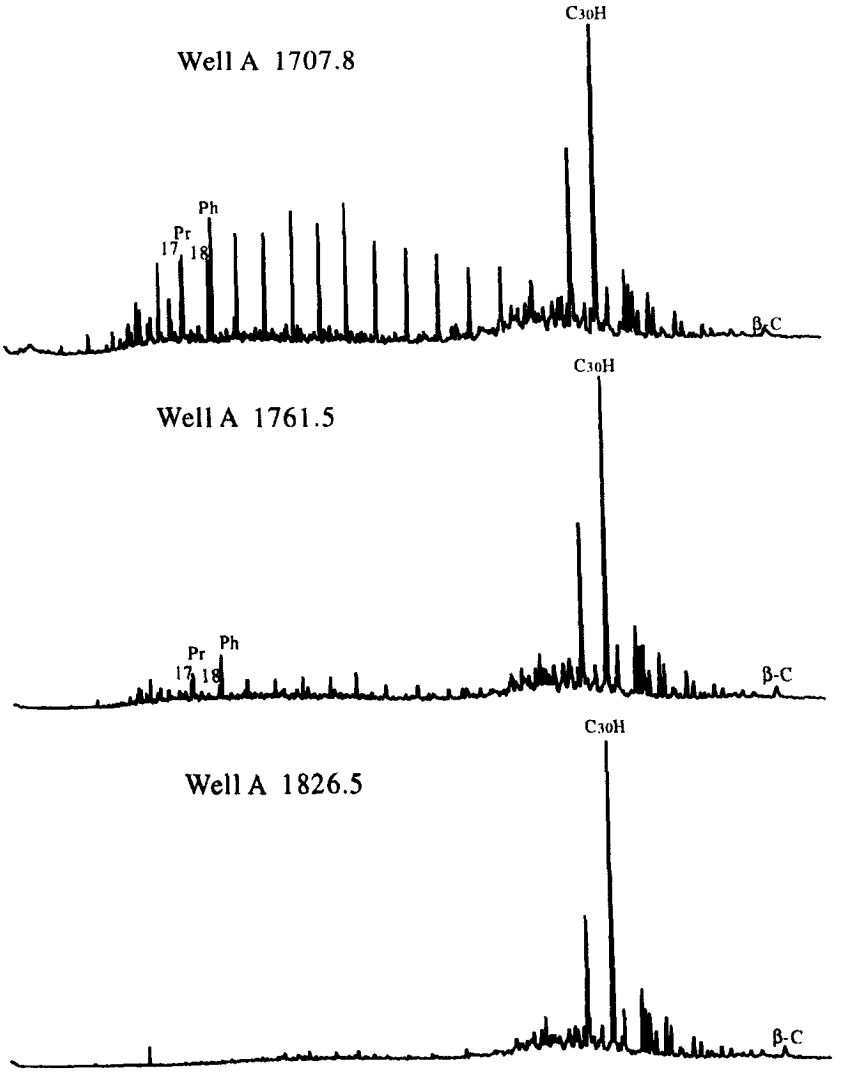

Fig. 4-5. Reconstructed ion chromatograms (sum of ions listed in Table 2-1) showing the aliphatic hydrocarbon distribution patterns in the representative oil samples of the Es3 column. Numbers refer to *n*-alkane chain length; Pr: Pristane; Ph: Phytane; $C_{30}H$: C_{30} αβ hopane; β-C: β-carotane.

4.2.3 Normal and isoprenoid alkane biodegradation index

The effects of biodegradation either from reservoir case studies (Connan, 1984; Peters and Moldowan, 1993) or from laboratory experiments (Goodwin *et al.*, 1983)

suggested that the short chain *n*-alkanes are removed faster than longer chain *n*-alkanes, which in turn are removed faster than branched and isoprenoid hydrocarbons. Thus, the ratios of pristane (Pr) to *n*-C_{17} and phytane (Ph) to *n*-C_{18} can provide a reliable means to monitor intrinsic biodegradation of oil. The depth-plot of (Pr+Ph)/(nC_{17}+nC_{18}) for the Es3 column shows systematic changes with depth but the maximum values do not occur at the base of the oil column (Fig. 4-7) and that indicates local effects do affect the column. It is apparent that both compound classes (*n*-alkanes and isoprenoid hydrocarbons) are affected by biodegradation, suggesting that this index may be reliably used to monitor oil biodegradation only in light to moderately biodegraded samples. Meanwhile since both biodegradation and mixing is going on in these study columns with these various oils, it is possible to have removed all isoprenoid alkanes at the base, while *n*-alkanes exist near the top of the column.

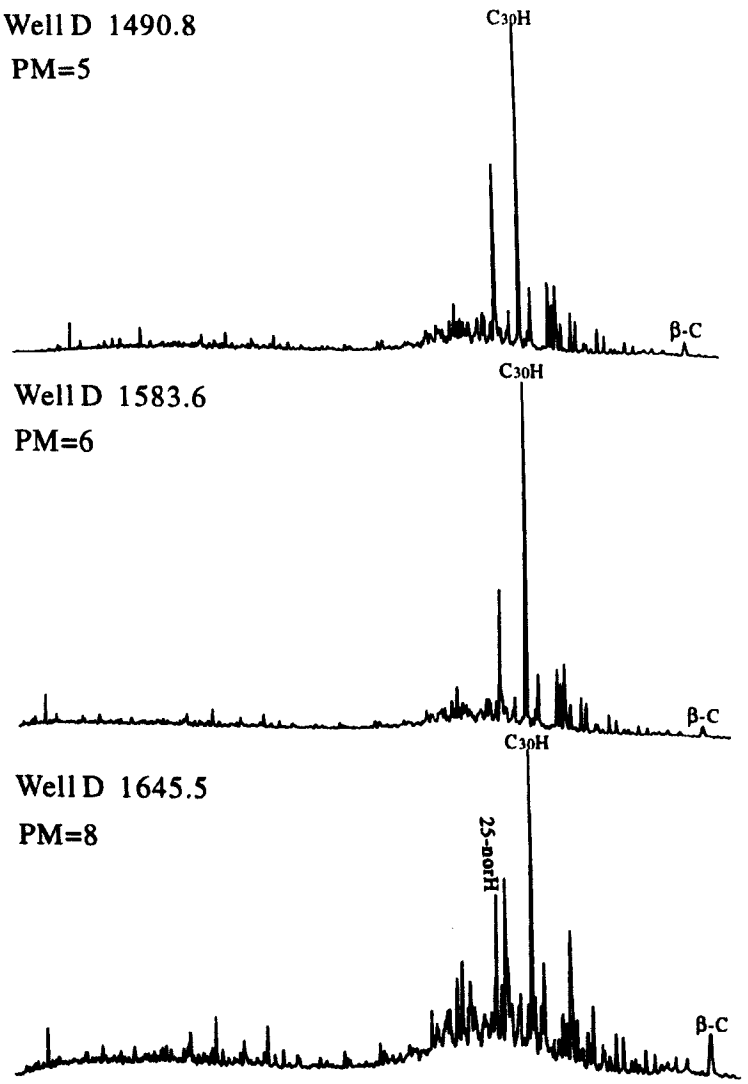

Fig. 4-6. Reconstructed ion chromatograms (sum of ions listed in Table 2-1) showing the aliphatic hydrocarbon distribution patterns in the representative oil samples of the Es1 column. Pr: Pristane; Ph: Phytane; $C_{30}H$: C_{30} αβ hopane; β-C: β-carotane.

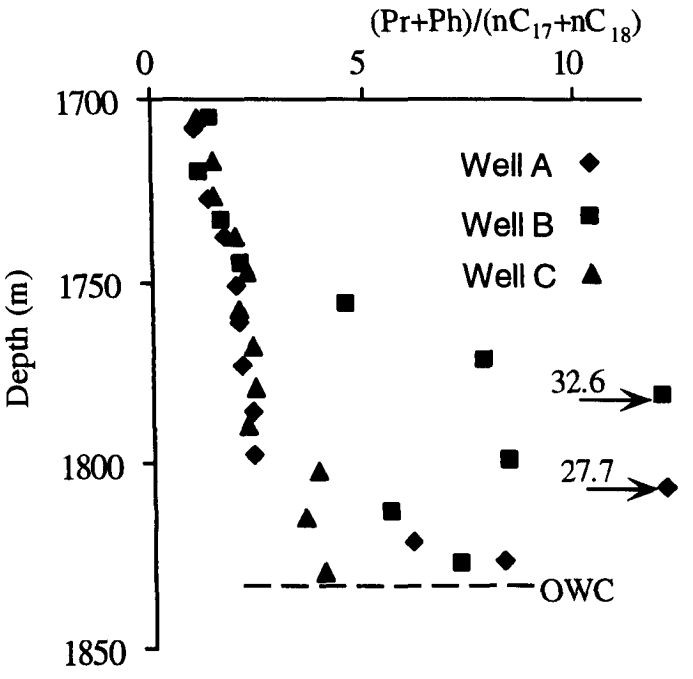

Fig. 4-7. Variation of the (Pr+Ph)/(nC_{17}+nC_{18}) ratios on the Es3 oil column.

4.3 Sesquiterpanes

The bicyclic sesquiterpenoids are a large biomarker class consisting of 30 main structures and at least 70 compounds. The principal source of the sesquiterpenoids preserved in geological samples is related to terrestrial organic matter (Philp *et al.*, 1981). Two typical compounds in this class are eudesmane and drimane (Fig. 4-8). In view of the abundance of the drimanes in the sediments older than Devonian, Philp (1994) proposed that they were associated with microbial input. In my sample suite, sesquiterpanes (m/z 123), ranging from C_{14} to C_{16}, are found in relatively low proportions, especially in reservoir extracts partially due to their volatile nature (Fig. 4-9). The distribution is dominated by drimane and homodrimane and is quite similar for all low biodegraded samples. These data suggest probably uniform source organic matter composition.

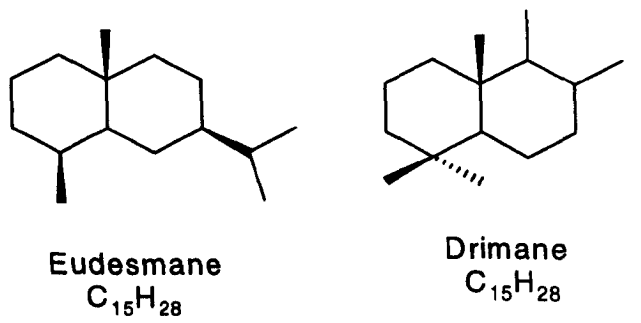

Fig. 4-8. Two typical bicyclic sesquiterpenoid structures.

The effects of biodegradation on bicyclic sesquiterpanes have been observed in both laboratory and field studies (Bailey *et al.*, 1973; Rubinstein *et al.*, 1977; Volkman *et al.*, 1983; 1984). Figure 4-10 shows total sesquiterpane concentration variation in the Es3 columns. The concentration of total sesquiterpanes decrease steadily from about 2000 μg/g EOM (extractable organic matter from reservoir rocks) at the top of the Es3 column to about 300 μg/g EOM near the OWC (Fig. 4-10a). Clearly, systematically decreasing sesquiterpane concentrations in the Es3 column is most possibly caused by biodegradation. In Es1 column the concentration of total sesquiterpanes is low but less dramatic change throughout the column (Fig. 4-10b).

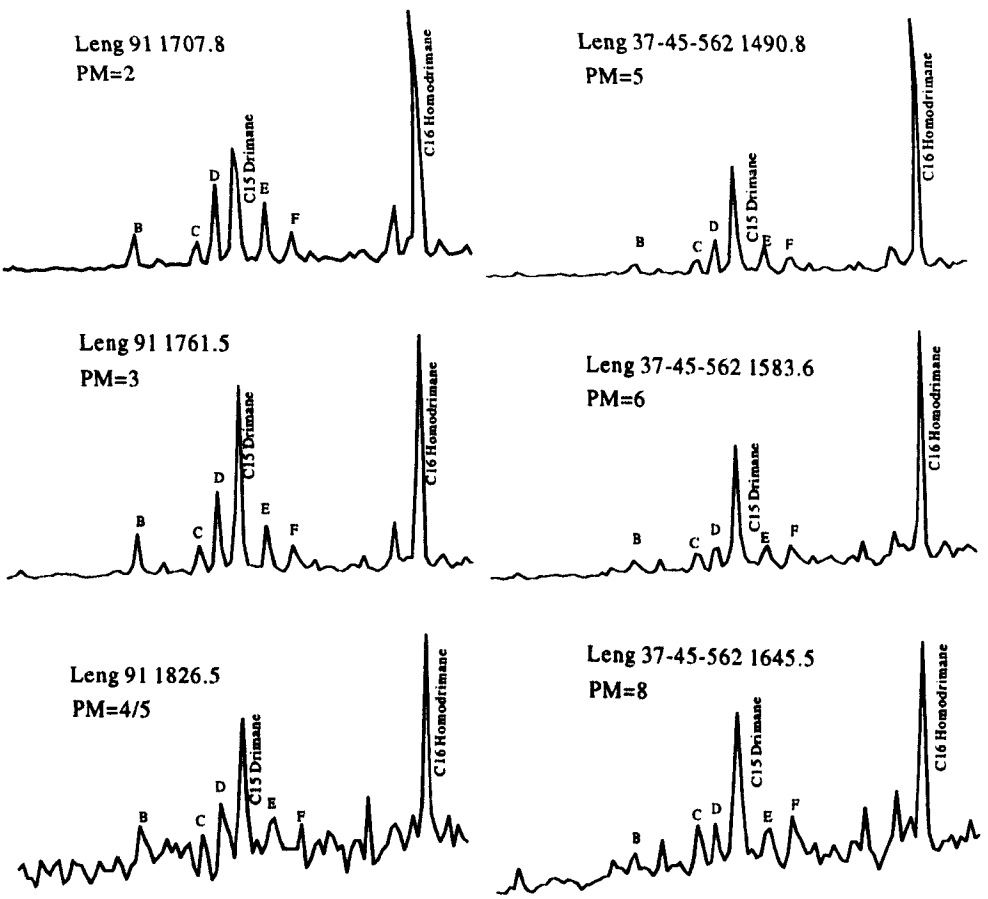

Fig. 4-9 Sesquiterpane (m/z=123) distribution patterns in the Es1 and Es3 columns.

As compared with acyclic isoprenoid alkanes, bicyclic sesquiterpanes appear to be more resistant to biodegradation. The ratios of total sesquiterpanes/(Pr+Ph) increase from 0.2 at the top of the Es3 column to about 1.5 at the bottom (Fig. 4-11a). In the more severely biodegraded Es1 column these ratios increase up to 8 (Fig. 4-11b).

Williams *et al.* (1986) found the bicyclic sesquiterpanes C, D and E to be more susceptible to degradation than F (see Figure 4-9 for identification). In the Es3 column the ratios of F/(C+D+E) increase from 0.2 to 0.4 (Fig. 4-12a) and in the Es1

column this ratio increase from 0.3 to 0.6 (Fig. 4-12b), indicating the bicyclic sesquiterpane distribution in the Lengdong oilfield is biodegradation related.

Williams *et al.* (1986) also reported that 8β(H)-homodrimane to be more susceptible to biodegradation than 8β(H)-drimane. However no clear trend as been observed on 8β(H)-drimane/8β(H)-homodramane for the Lengdong reservoir extract samples.

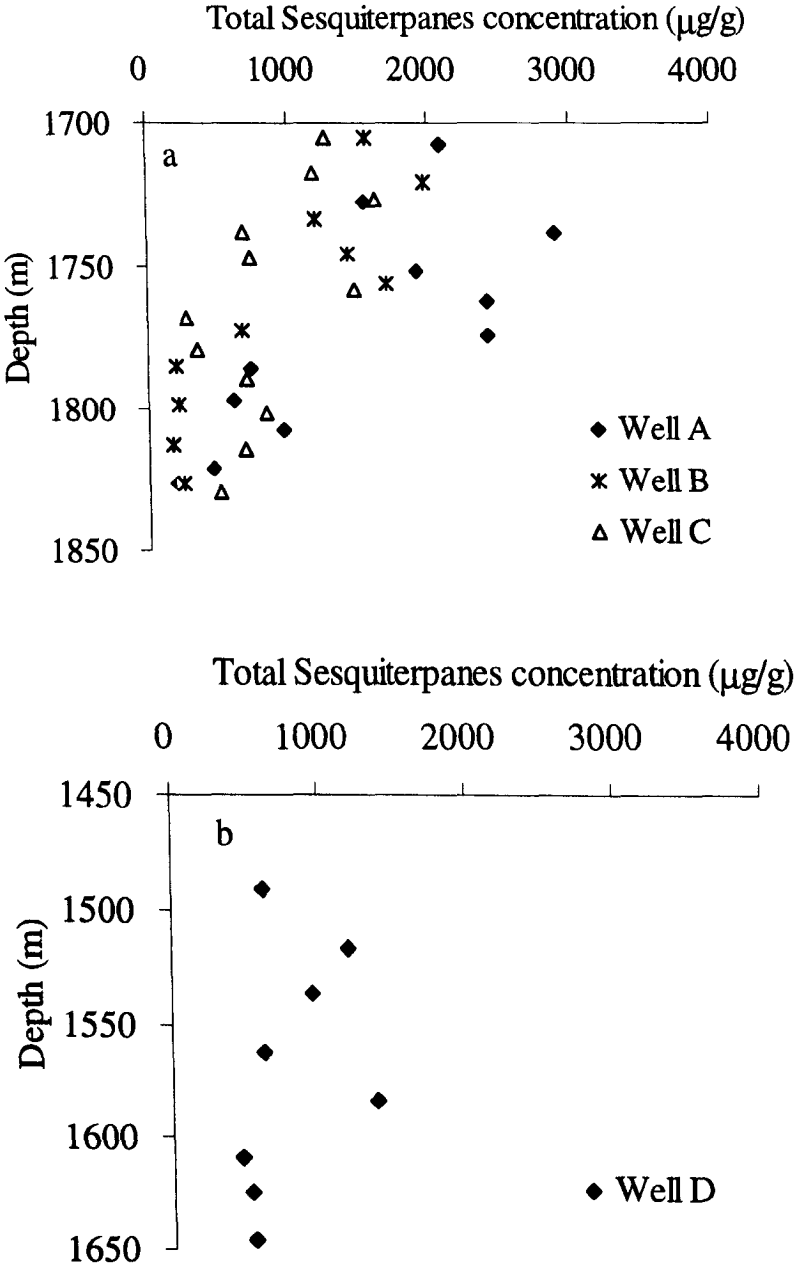

Fig. 4-10 Total sesquiterpane concentration variation in the Lengdong oilfield. (a) Es3 column; (b) Es1column.

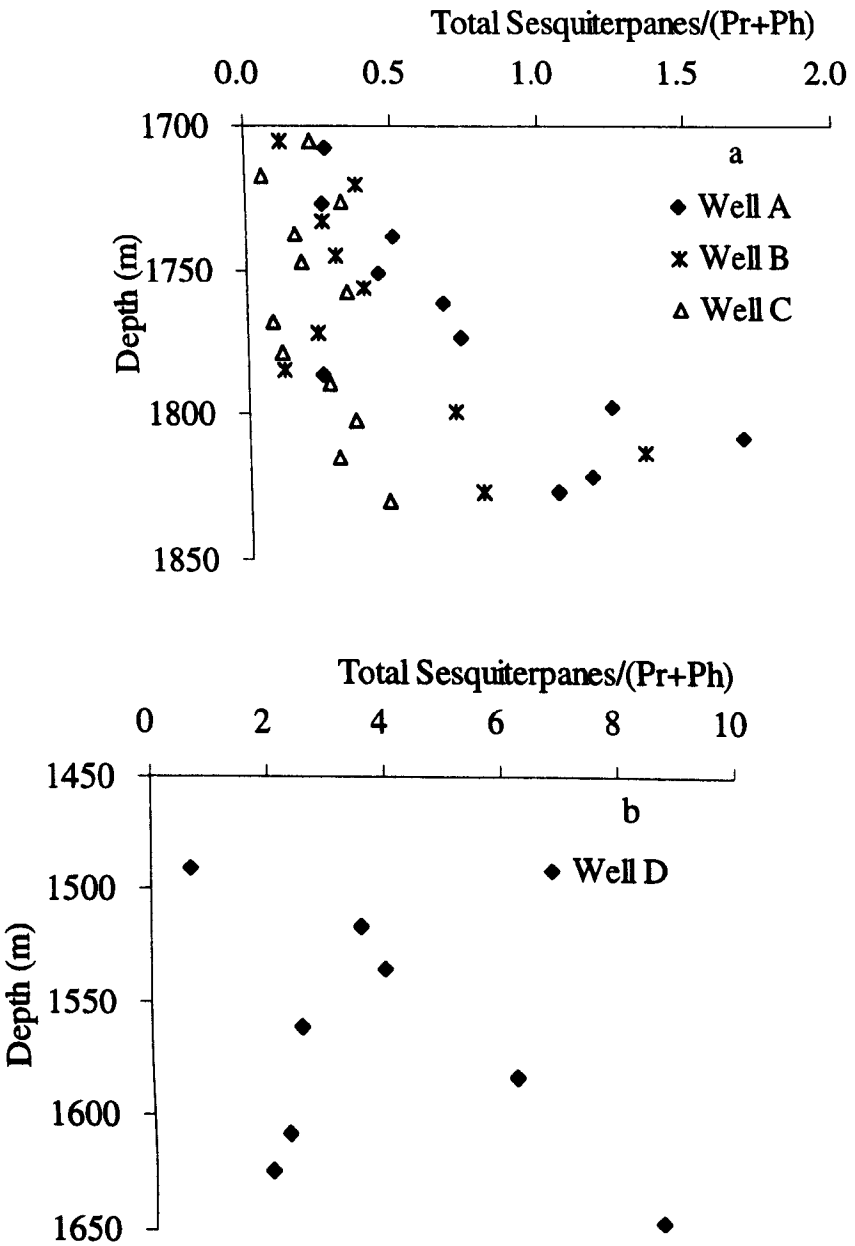

Fig. 4-11 The ratio of total sesquiterpane/(Pr+Ph) variation in the Es3 (a) and Es1 (b) columns of the Lengdong oilfield.

4.4 Tricyclic and tetracyclic terpanes

Tricyclic terpanes occur widely in petroleums and source rock extracts. Aquino Neto *et al.* (1983) systematically investigated the formation and distribution of tricyclic terpanes in oils and source rocks formed in a variety of depositional environments. De Grande *et al.* (1993) identified an extended series of tricyclic terpanes, from C_{19} up to C_{54}, in sediments and petroleums from Brazil, based on their chromatographic behavior and characteristic MS/MS transitions from molecular ions to m/z 191. They are widely used as indicators of multiple phases of oil filling into reservoirs (Talukdar *et al.*, 1986), thermal maturity in oils (Ekweozor and Strausz,

1983) and genetic characteristics of oils, even for samples affected by advanced biodegradation (Reed, 1977; Peters, 2000; Alberdi *et al.*, 2001).

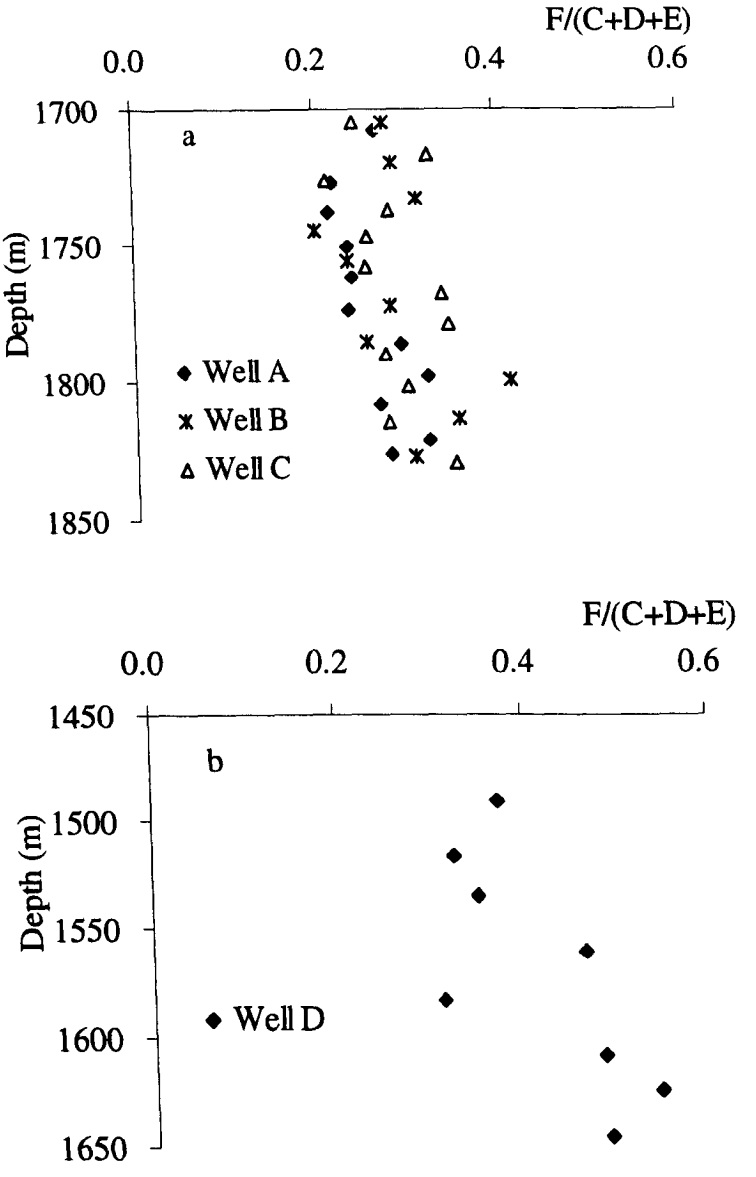

Fig. 4-12 The ratio of F/(C+D+E) sesquiterpane variation in the Es3 (a) and Es1(b) columns.

Tricyclic terpane distributions of the Lengdong reservoir extracts and peak characteristics are shown in Figure 4-13. The basic structure of tricyclic terpane is illustrated in Figure 4-14. The mass fragmentograms are characterized by the distribution in a wide range from C_{19} to C_{26} terpanes with C_{20}-C_{21} tricyclic terpanes slightly less than C_{23}. It differs from typical marine oil, in which C_{23} is the predominant component, indicating that the Lengdong oils were derived from lacustrine organic matter. The distribution pattern of the samples has no significant variations between each other, suggesting their similar origin. Some subtle differences are thought to be related with biodegradation.

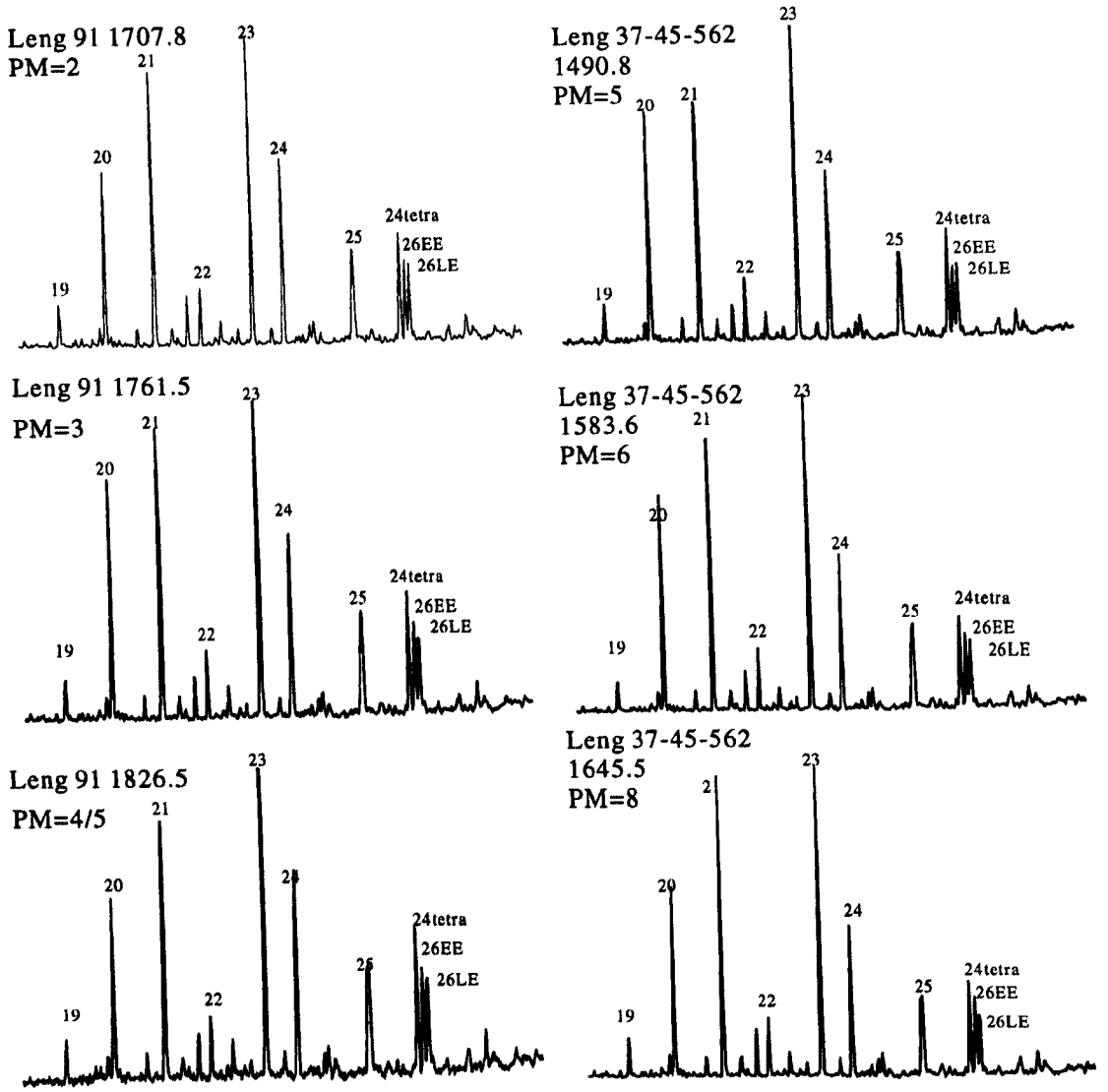

Fig. 4-13. Tricyclic terpane (m/z=191) distribution patterns of reservoir oils in the Es3 and Es1 columns. 24tetra: C_{24} tetracyclic terpane; EE: Early-eluting diastereomers; LE: late-eluting diastereomers; numbers refer to carbon number the compound contains.

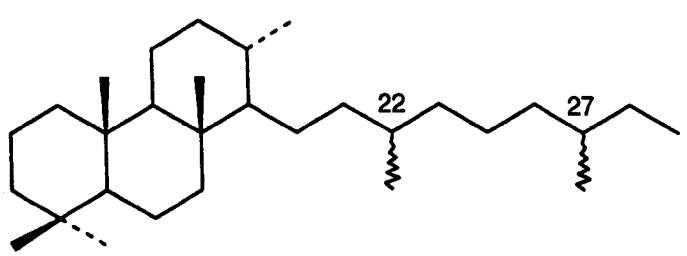

Tricyclic terpane

Fig. 4-14. Basic structure of tricyclic terpanes.

As a class, the tricyclic terpanes are quite recalcitrant. Their degradation typically occurs well after hopane removal, generally at the same time as the diasteranes (Reed, 1977; Seifert and Moldowan, 1979). The concentration of tricyclic terpanes show

little variation in the Es3 column. In Well A the concentration of tricyclic terpanes at about 2500 μg/g EOM is slightly higher that these in Well B and C at about 2000 μg/g EOM (Fig. 4-15a). In the Es1 column the concentration of tricyclic terpanes steadily increases from 2000 to 2600 μg/g EOM towards the bottom of the oil column, indicating their high ability to resist biodegradation (Fig. 4-15b).

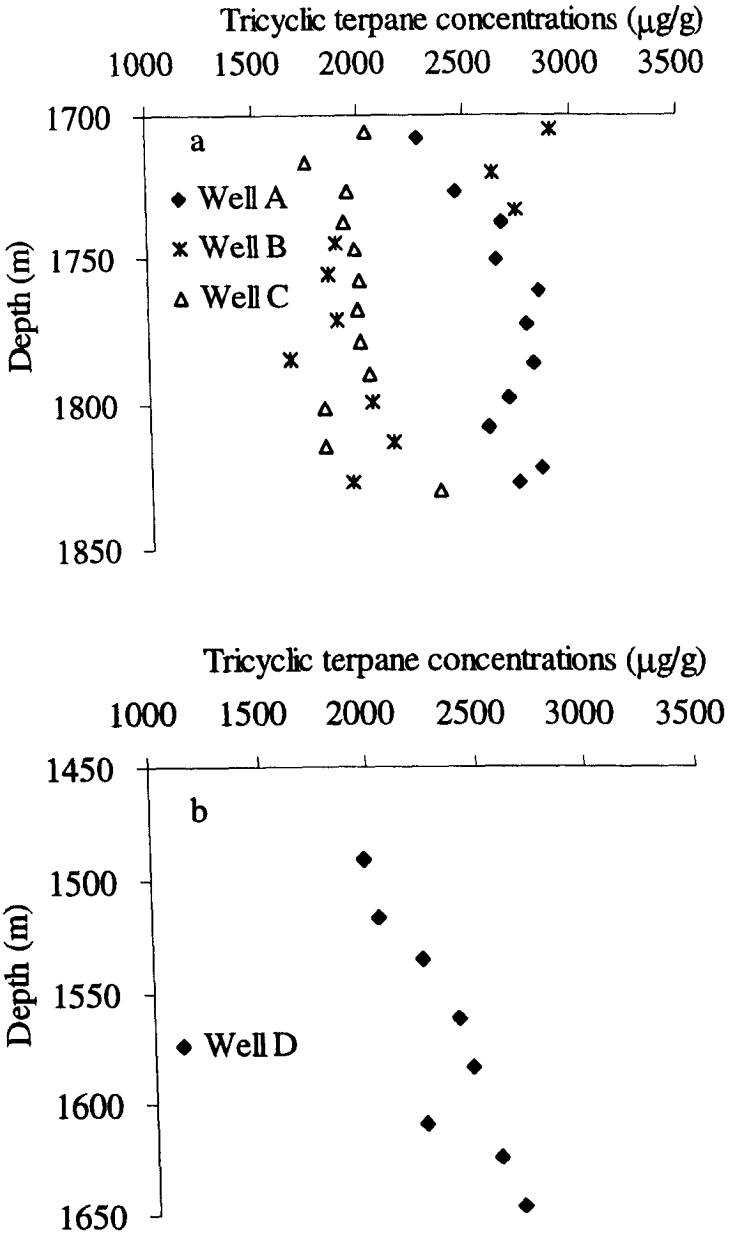

Fig. 4-15. Tricyclic terpane concentration variation in the Es3 (a) and Es1 (b) columns.

Although the tricyclic terpanes and the hopanes are derived from different precursors (and probably different source organisms) and their relative proportion is strongly dependent upon input and/or environmental factors, the ratio of tricyclic terpanes to hopanes increases with increasing maturity, thought to be due to the greater relative generation of tricyclic terpanes from the kerogen at high maturity

(Peters and Moldowan, 1993) and/or the higher thermal stability of the tricyclic terpanes (Farrimond *et al.*, 1999), although it is unlikely that at these temperatures any oil cracking occurs. The pentacyclic terpanes dominated all the oils and reservoir extracts in the Lengdong oilfield. The ratios of tricyclic terpanes/pentacyclic terpanes show a slightly decreasing trend in the Es3 column possibly revealing a subtle maturity difference between currently charging oil and the more deeply reservoired oils since the late charged more mature oil at the top of the column (Fig. 4-16a). In the Es1 column relative to pentacyclic terpane, tricyclic terpanes show a clearly increasing trend, suggest that pentacyclic terpanes are preferentially degraded relative to tricyclic terpanes (Fig. 4-16b).

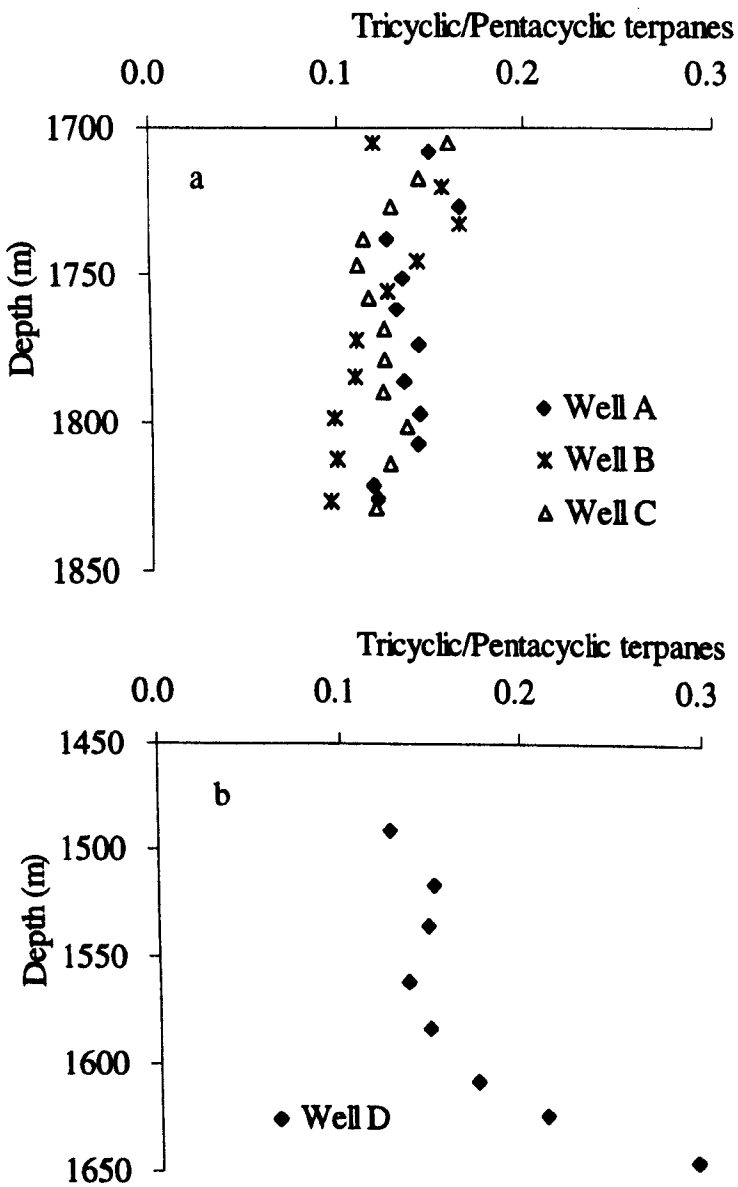

Fig. 4-16. Tricyclic/pentacyclic terpanes ratio variations in the Es3 (a) and Es1 (b) columns.

Changes in the carbon number distributions of the tricyclic terpanes have been employed in maturity assessment, based mainly on the C_{23} component (which is often dominant in a distribution) becoming relatively less prominent with increasing maturity. Specific parameters include the C_{23}/C_{21} ratio (Ekweozor and Strausz, 1983), C_{23}/C_{24} (Cassani *et al.*, 1988) and $(C_{20}+C_{21})/(C_{23}+C_{24})$ (Shi *et al.*, 1988). However, Farrimond *et al.* (1999) noticed the opposite trend, with the ratio of C_{23}/C_{21} tricyclic terpanes increasing through the 'oil window' within a single sedimentary horizon within the Dun Caan Shale Member in Scotland intruded by a 0.9 m thick Tertiary dolerite dyke. Their finding disagrees with the commonly observed decrease in the C_{23}/C_{21} ratio, previously ascribed to either thermal cracking of alkyl side chains (Ekweozor and Strausz; 1983; in an artificial heating study of an oil), or preferential generation of the C_{21} component from polar fractions and/or kerogen (Cassani *et al.*, 1988) under natural sediment burial. The recognition of compositional variability within sample suites of equal maturity indicates that environmental/diagenetic conditions also influence the carbon number distributions of tricyclic terpanes (e.g. Kruge *et al.*, 1990).

The ratios of $(C_{20}+C_{21})/(C_{23}+C_{24})$ tricyclic terpanes in the Es3 column show a weak increase trend (Fig. 4-17a). As slightly more mature oils are noticed to locate at the top of the column, therefore this result agrees with the Farrimond *et al.* (1999) conclusion that C_{23} tricyclic terpane is slightly more stable than other tricyclic terpanes. However, in the more severely biodegraded Es1 column, the ratios of $(C_{20}+C_{21})/(C_{23}+C_{24})$ remain constant (Fig. 4-17b), suggesting no obvious preferential component depletion to biodegradation among tricyclic terpanes.

For tricyclic terpanes with 25 carbon atoms or more, both 22S and 22R isomers occur. The C_{25} homologues coelute as a single broadened peak, but the C_{26} 22S and 22R isomers are resolved into a clear doublet (Fig. 4-13) which usually comprises approximately equal amounts of each isomer. However, the isomer identification has not confirmed yet. In this work these two isomers are referred to as early-eluting (EE) and late-eluting (LE). Farrimond *et al.* (1999) suggested their relative abundance possibly reflect isomerisation and can serve as a maturity parameter. Recently Alberdi *et al.* (2001) noticed stereoselective biodegradation of tricyclic terpanes in heavy oils from Venezuela. In the heavily degraded oils, LE stereoisomers seem preferentially removed during biodegradation. In the Lengdong sample suite only the C_{26} doublet is clearly identified. The C_{26} EE/LE ratios do show a slightly increase trend in the Es3 and Es1 columns (Fig. 4-18). However, this ratio is quite scattered and no specific correlation can be established with the degree of biodegradation.

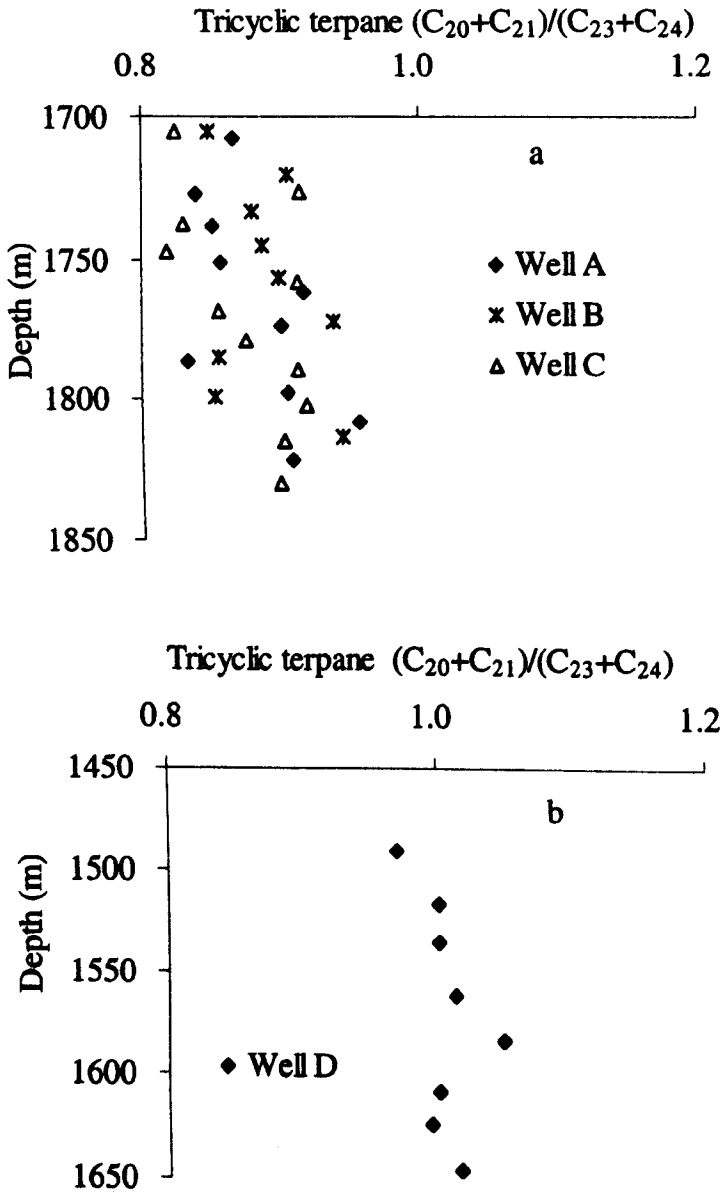

Fig. 4-17. Ratios of $(C_{20}+C_{21})/(C_{23}+C_{24})$ tricyclic terpanes in the study columns.

4.5 Pentacyclic terpanes

The carbon number distribution of pentacyclic terpanes in the Lengdong oils varies between C_{27} and C_{35} although Wang *et al.* (1996) demonstrated the presence of extended hopanes up to C_{44} in oils and extracts from the Liaohe basin. Pentacyclic terpanes provide information about organic matter type, maturity level, lithology of source rock and migration of hydrocarbons (Seifert and Moldowan, 1981; Blanc and Connan, 1992). Hopanes (Fig. 4-19) are a class of pentacyclic triterpane biomarkers that originate from hopanoids in bacterial membranes (Zundel and Rohmer, 1985; Farrimond *et al.*, 1998; 2000). In the Lengdong oils the C_{30} αβhopane is the dominating biomarker in all the crude oils which is characteristic for source rocks from lacustrine organic matter.

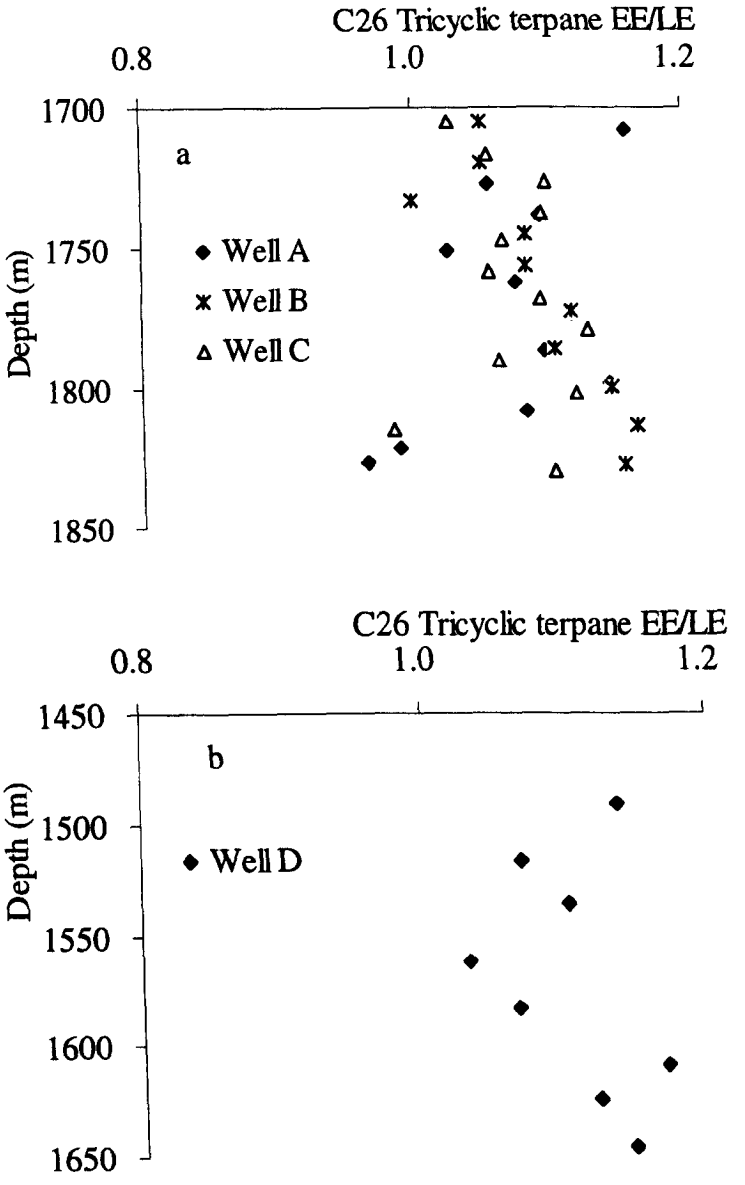

Fig. 4-18. Ratios of C_{26} tricyclic terpanes EE/LE in the Es3 (a) and Es1 (b) columns.

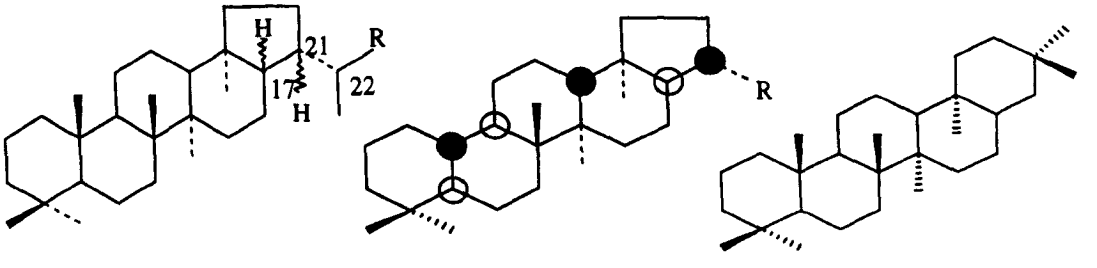

Hopane 25-nor-17(α) Hopane Gammacerane

Fig. 4-19. Some basic structures of pentacyclic terpanes.

Numerous studies show that C_{30} 17α(H), 21β(H)-hopane and its extended homologs (homohopanes) are biodegraded in the environment and laboratory (Goodwin *et al.*, 1983; Moldowan and McCaffrey, 1995; Peters *et al.*, 1996; Bost *et*

al., 2001). The microbially induced demethylation of extended hopanes to 25-norhopanes occurs mainly during biodegradation of petroleum in reservoirs (Seifert and Moldowan, 1979; Volkman *et al.*, 1983; Chosson *et al.*, 1991; Peters *et al.*, 1996).

4.5.1 Concentration variation in biodegraded columns

In the Es3 oil columns, the total pentacyclic terpanes concentrations show a continuously increase trend from approximately 40000 μg/g EOM at the top to 65000 μg/g EOM at the bottom (Fig. 4-20). The observation of a slight increase in pentacyclic terpane concentrations throughout the columns may be due to the fact that significant pentacyclic terpanes degradation has not yet begun in these samples and their relative enrichment is the result of depletion of other components (e.g., *n*-alkanes and isoprenoid alkanes). Less dramatic changes in Well C reflect its generally less severe degree of biodegradation. In the Es1 oil column, pentacyclic terpanes concentrations remain constant in the upper part of the column then show a sharp decrease in abundance in the lower part of the column at more advanced biodegradation stages. The concentration of 25-norhopanes starts to dramatically increase concurrently with an obvious depletion of hopanes (Fig. 4-21).

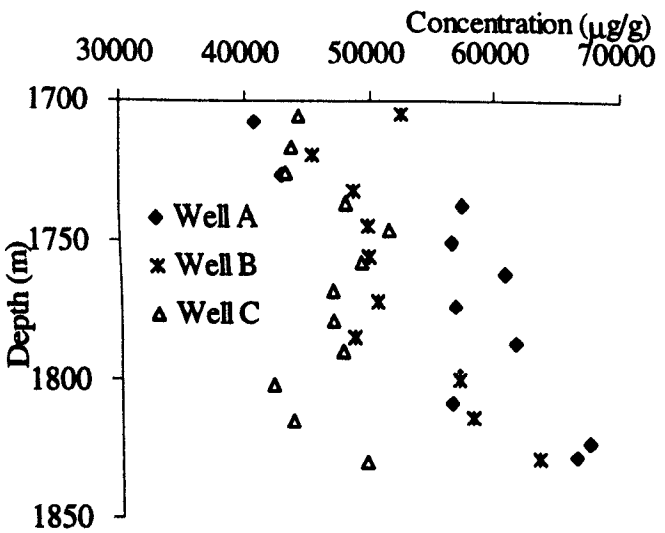

Fig. 4-20. Pentacyclic terpanes concentration variation in the Es3 column.

25-Norhopanes are generally considered to be the product of heavy biodegradation (Moldowan and McCaffrey, 1995; Peters *et al.*, 1996). However, large discrepancies between the loss of hopanes and the production of 25-norhopanes suggest that not all hopanes have been transformed into demethylated hopanes and preserved, other kinds of metabolites (such as hopanoid acids and demethylated hopanoid acids) may also exist (Aitken, 2004).

Representative pentacyclic terpane distribution are illustrated in Figure 4-22. Isomer distributions show clear relationship with degree of biodegradation the sample

has undergone.

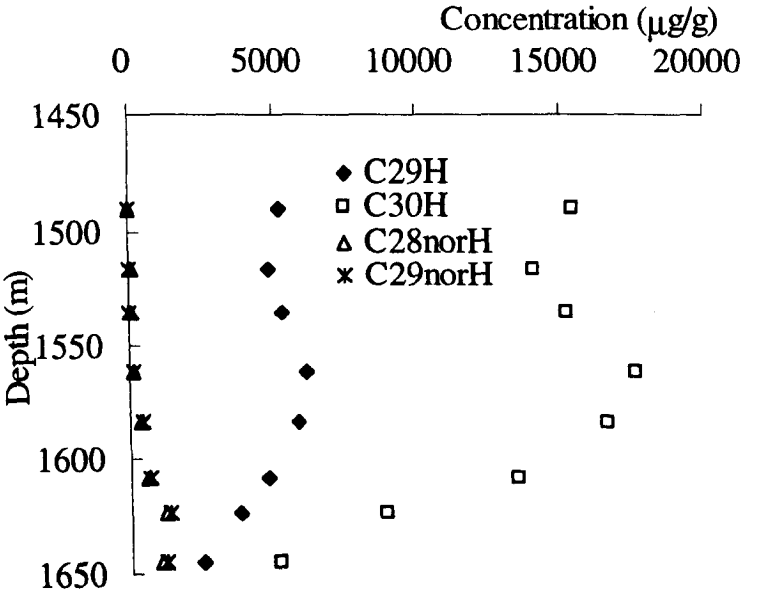

Fig. 4-21. Hopane and corresponding 25-norhopane concentration variation in the Es1 column. C29H: C_{29} 17α(H), 21β(H)-hopane; C30H: C_{30} 17α(H), 21β(H)-hopane; C28norH: C_{28}-25-norhopane; C29norH: C_{29}-25-norhopane.

4.5.2 Trisnorhopane and C_{29} Ts

Seifert and Moldowan (1981) discussed the two C_{27} trisnorhopanes, namely 18α(H)-22,29,30-trisnorneohopane (Ts), and 17α(H)-22,29,30-trisnorhopane (Tm), and suggested that they could be used as a maturity indicator based on the fact that Tm was proposed to be more thermally unstable than Ts. Moldowan *et al.* (1985) suggested their abundance was also controlled by depositional environment. The commonly occurring Ts and Tm in biodegraded oils appear to be relatively resistant to biodegradation even when normal hopanes appear to be relatively degraded (Seifert *et al.*, 1984; Brooks *et al.*, 1988; Lin *et al.*, 1989; Chosson *et al.*, 1991). Requejo and Halpern (1989) observed that in Monterey tar sands C_{28}-C_{34} hopanes are almost complete lost, but Ts and Tm remain stable. However, biodegradation of Ts relative to Tm was observed by Peters and Moldowan (1993).

In the Es3 column the Ts/Tm index shows a decreasing trend from 0.50 at the top to 0.38 at the bottom. The higher Ts/Tm ratio in the top reservoir oils points to a slightly higher maturity (Fig. 4-23a). This suggest that Ts/Tm ratio was not affected before PM level 4 and slightly higher ratios at the upper part of the column are due to a late charging and mixing process. In the Es1 column the Ts/ Tm ratios are less than those in the Es3 column, indicative of the lower maturity of the oil. The constant ratios throughout the Es1 column reflect that biodegradation has insignificant effect on these two components at present levels (Fig. 4-23b).

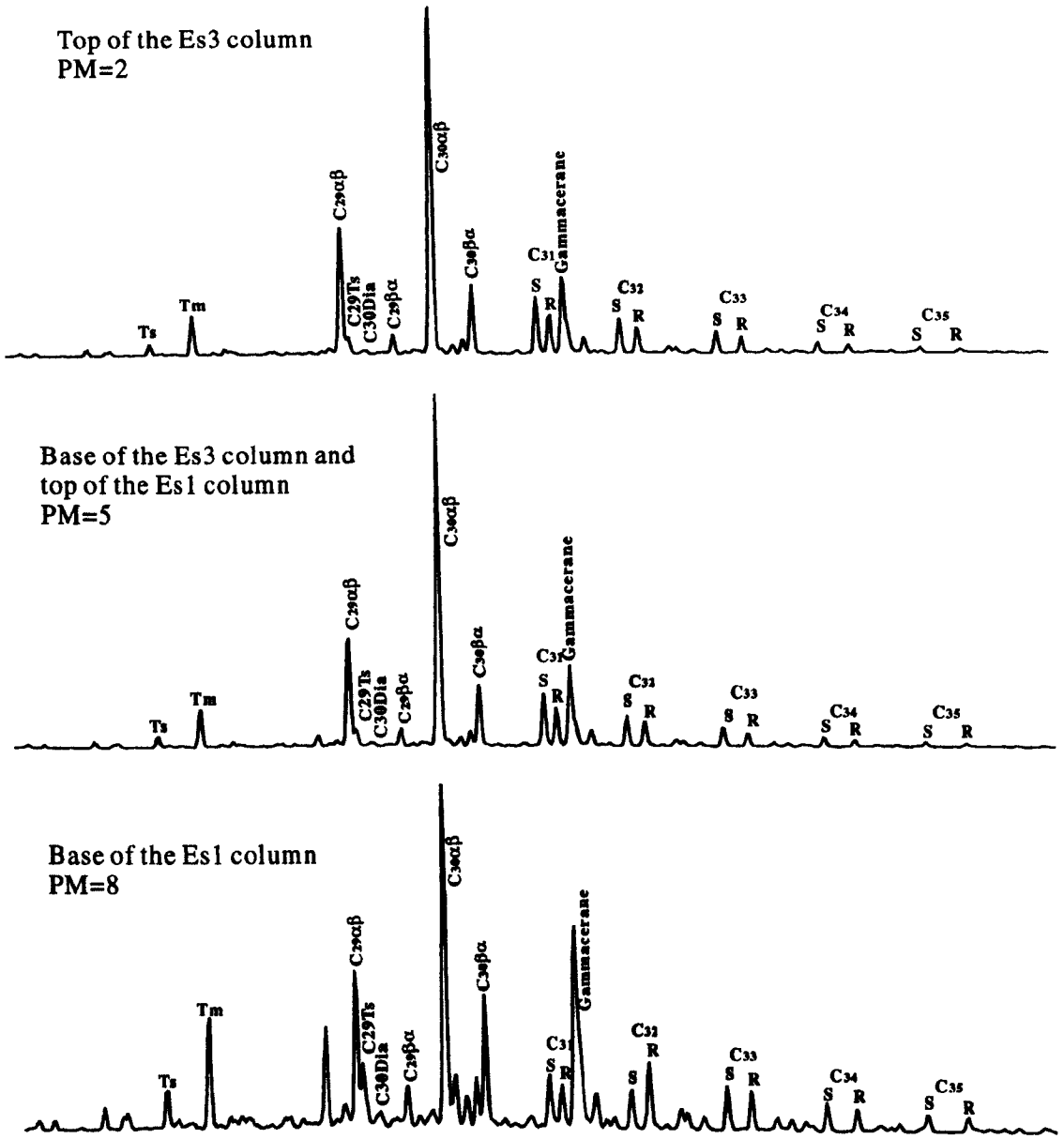

Fig. 4-22. Representative pentacyclic terpane (m/z=191) distribution in the Lengdong oilfield.

18-α(H)-30-Norneohopane (C_{29} Ts) is one of the most stable terpanes. The formation of C_{29} Ts takes place during diagenesis and the ratio of C_{29} Ts to C_{29} αβ hopane is a maturity indicator (Moldowan *et al.*, 1991). Biodegradation effects on C_{29}Ts have not been evaluated before. The similar variation of C_{29} Ts/C_{29} hopane to Ts/Tm indicates that maturity is the main control of these parameters in the Es3 column and slightly more mature oil appears in the top of the column (Fig. 4-24). While in the more heavily biodegraded Es1 column, variation of C_{29} Ts/ hopane ratios reflect biodegradation susceptibility. Similar trends of C_{29} Ts/C_{29} hopane and C_{29} Ts/C_{30} hopane suggest that C_{29} Ts is the most biodegradation-resistant terpane among the hopane series (Fig. 4-25).

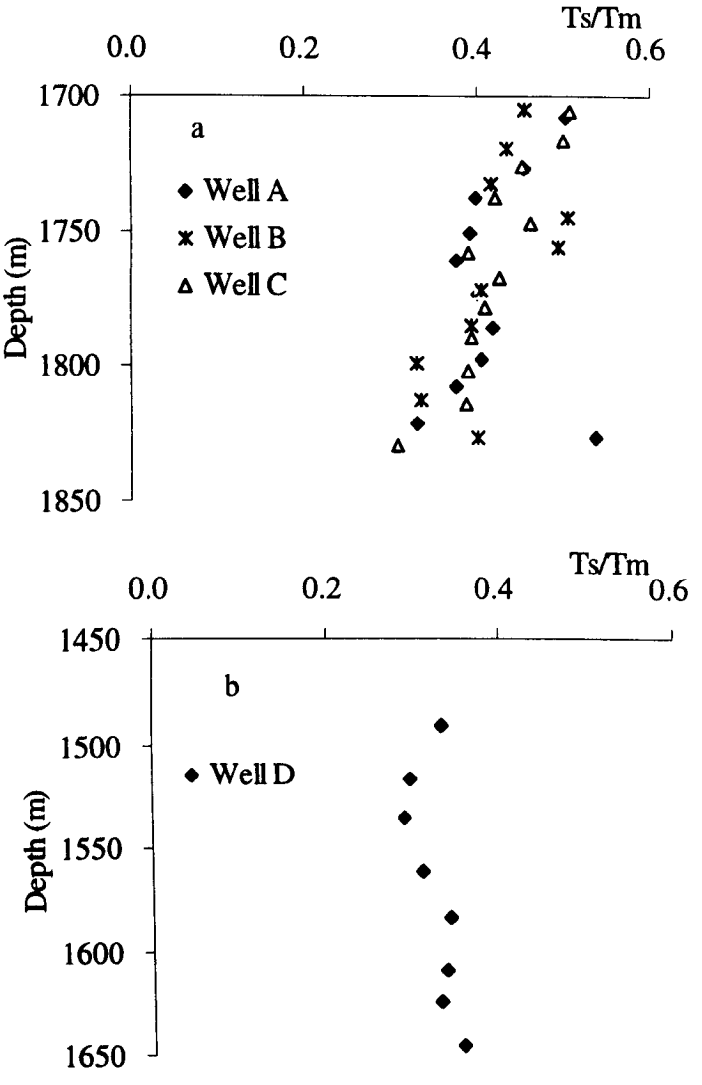

Fig. 4-23. Ts/Tm ratio variations in the Es3 (a) and Es1 (b) columns.

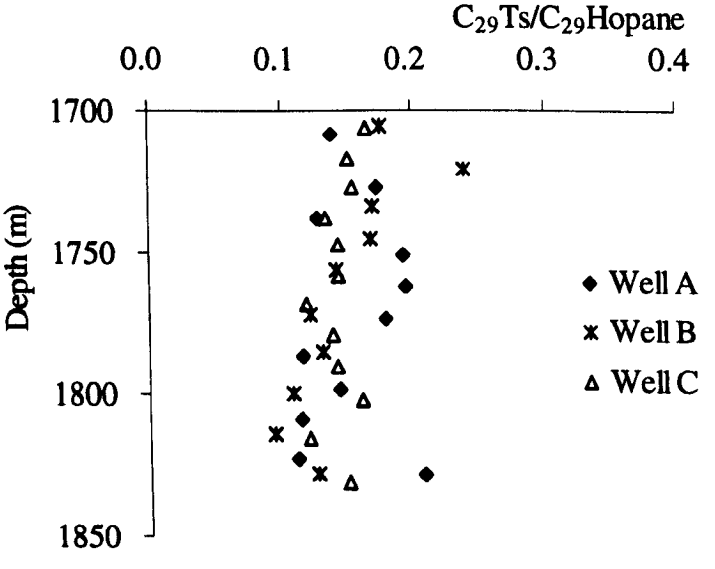

Fig. 4-24. C_{29} Ts/C_{29} hopane ratio variation in the Es3 column.

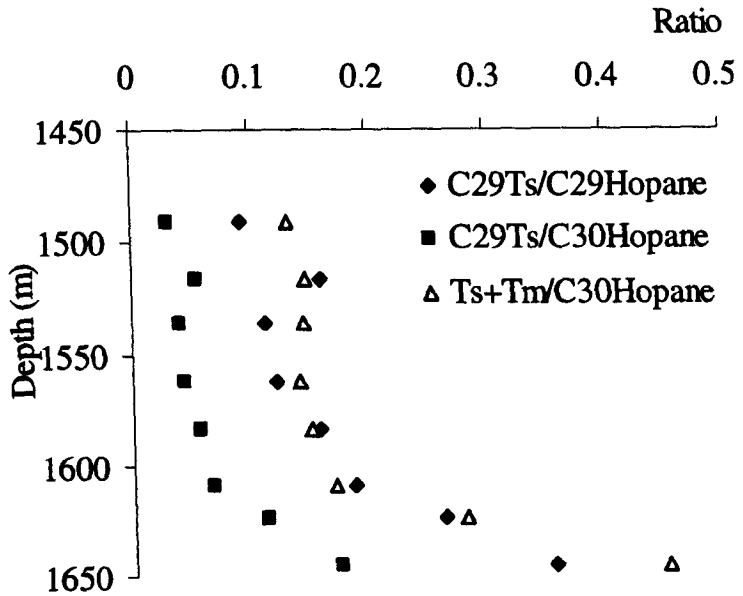

Fig. 4-25. Ratio variations of C_{29} Ts/C_{29} hopane, C_{29} Ts/C_{30} αβhopane and (Ts+Tm)/C_{30} αβhopane throughout the Es1 column.

4.5.3 Moretane/Hopane

The 17β(H), 21α(H) hopane (moretane)/ 17α(H), 21β(H) hopane ratio is affected by thermal maturity and decreases with increasing maturity. Goodwin *et al.* (1983) noticed that moretanes were more resistant to biodegradation than the 17α(H), 21β(H) hopanes. In the Es3 column hopane biodegradation did not start and moretane/hopane ratios show little variation throughout the column (not shown here). In the Es1 column both C_{29} moretane/C_{29} hopane and C_{30} moretane/C_{30} ratios hopane show the same increase trend toward the OWC, which is consistent with Goodwin's observation (Fig. 4-26).

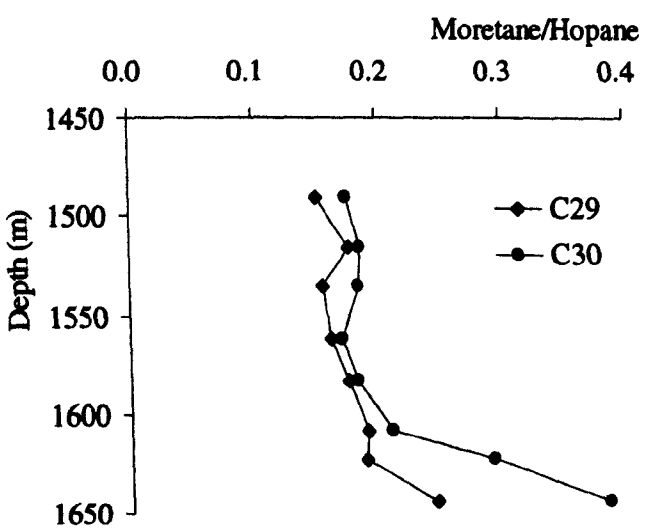

Fig. 4-26. Ratios of C_{29} and C_{30} moretane/hopane throughout the Es1 column.

4.5.4 Homohopane series

The distribution patterns of homohopanes are largely controlled by source depositional environment. C_{35} homohopanes are believed to be associated with highly reducing marine conditions during deposition (Moldowan *et al.*, 1985). In some Chinese evaporate lacustrine source rocks the elevated C_{35} homohopanes are quite obvious (Huang and Pearson, 1999). The decreasing trend from C_{31} to C_{35} homohopanes in the Lengdong oils analyzed indicates a fresh water suboxic source environment.

There are two opposite opinions about homohopane biodegradation order. From both laboratory studies and field observations, Goodwin *et al.* (1983) observed that heavier hopane homologues were more readily biodegraded than the lighter ones in a degradation sequence of $C_{35} > C_{34} > C_{33} > C_{32} > C_{31} > C_{30} > C_{29}$. Chosson *et al.* (1992) observed hopane degradation by pure cultures of *Nocardia, Arthrobacter*, and *Mycobacterium* species, and showed the same $C_{35} > C_{34} > C_{33} > C_{32} > C_{31} > C_{30}$ hopane degradation sequence as observed by Goodwin *et al.* (1983). However, Requejo and Halpern (1989) reported the preferential preservation of the C_{35} homohopanes in a biodegraded Monterey Tar and Moldowan and McCaffrey (1995) demonstrated degradation of the C_{30} through C_{34} hopanes with preservation of the C_{35} hopane in samples from a petroleum onshore site.

In the present study no preferential preservation of the C_{35} hopane can be observed but the order of alteration does not follow Goodwin's (1983) observation (Fig. 4-27). C_{31} 17α, 21β-homohopane/C_{30} 17α, 21β-hopane ratios are almost constant through all biodegradation level, implying that C_{30}-hopane had roughly the same biodegradation rate as C_{31}(R+S) homohopanes. C_{29} 17α, 21β-norhopane/C_{30} 17α, 21β-hopane and $C_{32\text{-}35}$ 17α, 21β-homohopane/C_{30} 17α,21β-hopane ratios increase in the advanced biodegradation level, revealing more extensive degradation of C_{30} hopane compared to C_{29} norhopane and $C_{32\text{-}35}$ homohopane. These changes are occurring after PM 6, while in the low level of the biodegradation all hopanes remain stable and no obvious changes can be observed. These results are in good agreement with the observation of a biodegraded West Siberian oil by Peters and Moldowan (1991) showed preferential preservation of the $C_{32\text{-}35}$ homohopanes. The results show that C_{30} and C_{31} hopanes are the most vulnerable components while $C_{32\text{-}35}$ homohopanes and C_{29} norhopane are highly resistant to biodegradation.

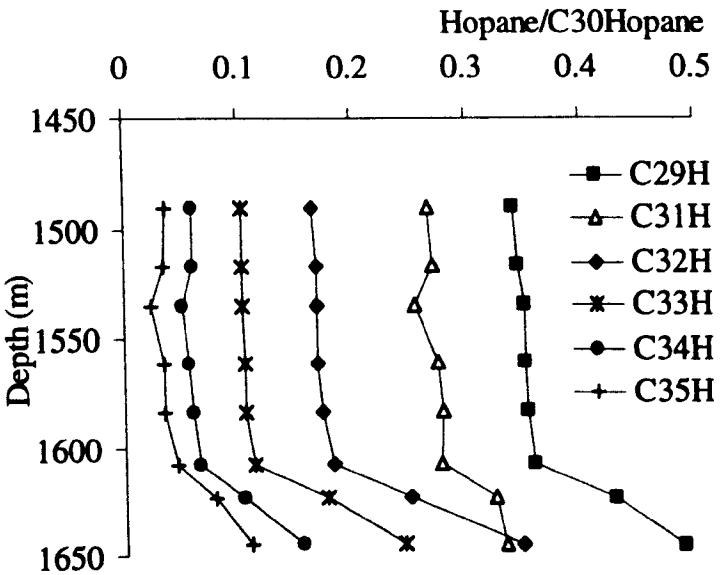

Fig. 4-27. Variations of C_{30} hopane compared to homohopane series the Es1 column.

4.5.5 R/S epimers

The preferential removal of 22R hopanes compared to 22S hopanes has been shown by Lin *et al.* (1989) in biodegradation of tar sand bitumens. Requejo and Halpern (1989) observed a slight decrease in the abundance of the 22R epimer of the C_{33} and C_{34} extended hopanes relative to the 22S epimer in Monterey tar sands. Peters *et al.* (1996) observed conservation of higher molecular-weight hopanes with preferential degradation of the 22R epimer. Subsequent molecular modelling of the R and S epimers of the C_{34}-C_{35} homohopanes revealed that the S epimer conformation may sterically protect the C-25 methyl group from microbial attack (Peters *et al.*, 1996). There is now wide agreement that the relative rate of biodegradation of hopanes, in the laboratory and reservoir, is 22R > 22S (Lu *et al.*, 1990; Chosson *et al.*, 1991; Blanc and Connan, 1992). Similar observations have been made by Volkman *et al.* (1983) and Goodwin *et al.* (1983), that bacteria degrade the 22R isomer of hopanes faster than the geologically-produced 22S isomer.

However, this concept did not fit the Lengdong situation. In the Es3 column, the homohopane 22S/22(R+S) ratios more or less similar for all samples, implying that biodegradation is not severe enough to affect the hopane distribution. In the Es1 column homohopane 22S/22(R+S) ratios did not increase with the degree of biodegradation but clearly decreased downward. For C_{31} and C_{33} components the homohopane 22S/22(R+S) ratios only slightly decrease from 0.58 to 0.56, while a dramatic decrease occur in the C_{32} component from 0.56 to 0.41 (Fig. 4-28). What caused the preferential removal of the 22S versus the 22R isomer in the extended hopanes in the Lengdong sample suite needs to be further investigated.

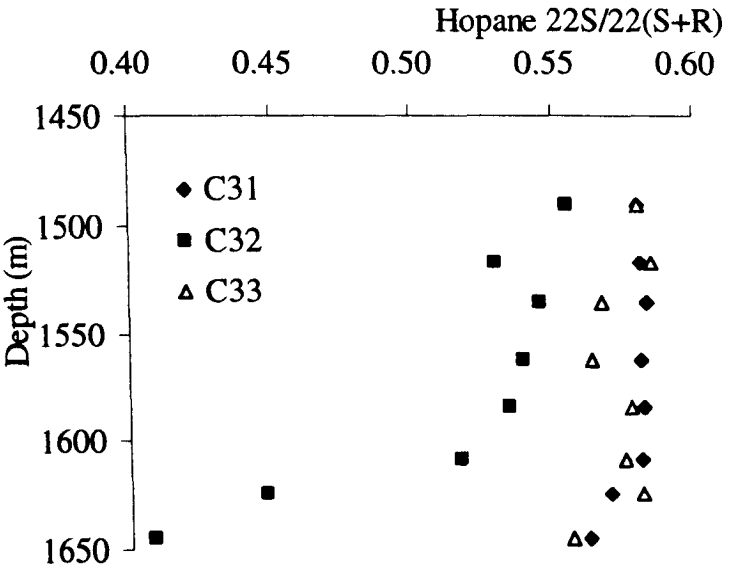

Fig. 4-28. Variation of homohopanes R and S epimers in the Es1 column.

4.5.6 Gammacerane

Gammacerane is derived from tetrahymanol, an indicator of water-column stratification in the source rock depositional environment. The occurrence of gammacerane appears to characteristic marker for high salinity and water column stratification in marine and nonmarine source rock depositional environments (ten Haven *et al.*, 1989; Peters and Moldowan, 1993; Damsté *et al.*, 1995). Gammacerane has also been used as an indicator of carbonate or evaporate source rocks (Mello *et al.*, 1988; Peters and Moldowan, 1991).

Blanc and Connan (1992); Brooks *et al.* (1988); Zhang *et al.* (1988) have all recognized that gammacerane is more resistant to biodegradation than hopanes. In the severely biodegraded sample, the regular αβ-hopanes have been removed, residually concentrating the more biodegradation-resistant tricyclic terpanes. In the ultra-severely degraded seep, even the tricyclic terpanes have been degraded, further concentrating the gammacerane and largely unidentified components in the tricyclic terpane range.

The gammacerane index (gammacerane/C_{30} αβ hopane) was quite constant throughout the Es3 column with a slight increase from 0.23 to 0.28 (Fig. 4-29a), reflecting a similar source depositional environment for oils in the Es3 reservoir. In the Es1 column the gammacerane index was still stable at 0.30 in the upper part of the column but a sharp increase occurred in the lower part of the column with the highest value of 0.91 (Fig. 4-29b). Significant increases in the gammacerane index reveal more extensive degradation of C_{30} hopane compared to gammacerane. Li *et al.* (1995)

reported that petroleums from Es3 source rocks can be differentiated from Es4 petroleums mainly by a low gammacerane index since gammacerane is rich in the Es4 sourced oils but poor in Es3 sourced oils. However, because of gammacerane's high ability to resist biodegradation, the oils that appear on biomarker ratios to originate from Es4 very possibly are actually biodegraded Es3 oils.

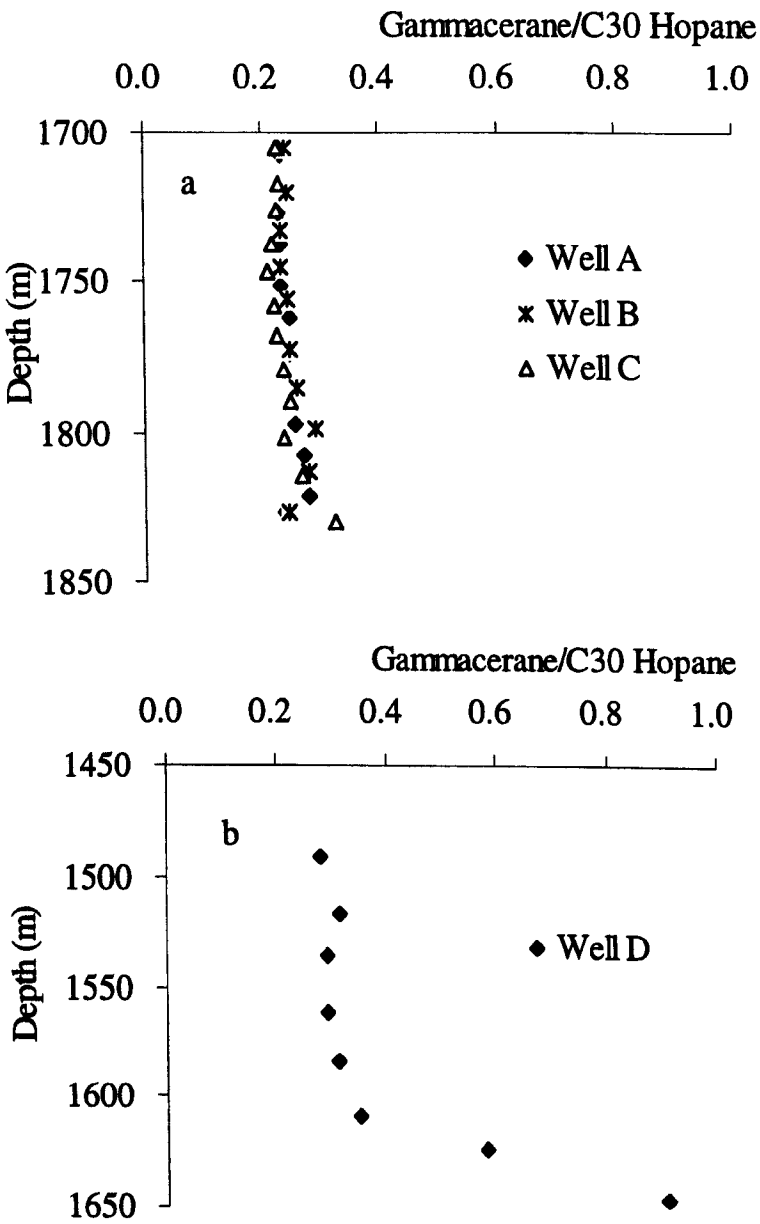

Fig. 4-29. Ratios of gammacerane/C_{30} αβ hopane in the Es3 (a) and Es1 (b) columns.

4.5.7 Hopane biodegradation pathway

25-Norhopanes have always been regarded as being indicative of heavy biodegradation of oil, although they are not found in all heavily biodegraded oils. Whether or not they are actually formed during the biodegradation process by microbial demethylation is a matter of debate. Two theories prevail for the common observation of abundant 25-norhopanes in biodegraded oils: (1) the biotransformation

of hopanes to 25-norhopanes through the microbial removal of the methyl group at C-10 in the hopane nucleus during the biodegradation of reservoired oil (e.g. Seifert and Moldowan, 1979; Moldowan and McCaffrey, 1995); (2) that 25-norhopanes are pre-existing biomarkers present in source rocks and non-biodegraded oils, which become concentrated during biodegradation through the selective removal of more easily biodegradable components (e.g. Blanc and Connan, 1992; Chosson *et al.*, 1992).

In the Es1 oil column of the Lengdong case study, there is an obvious increase in 25-norhopane/hopane ratio with depth, related to increased biodegradation at the base of the column. Here, this ratio is clearly driven by an increase in 25-norhopane concentration and an associated decrease in hopane concentration.

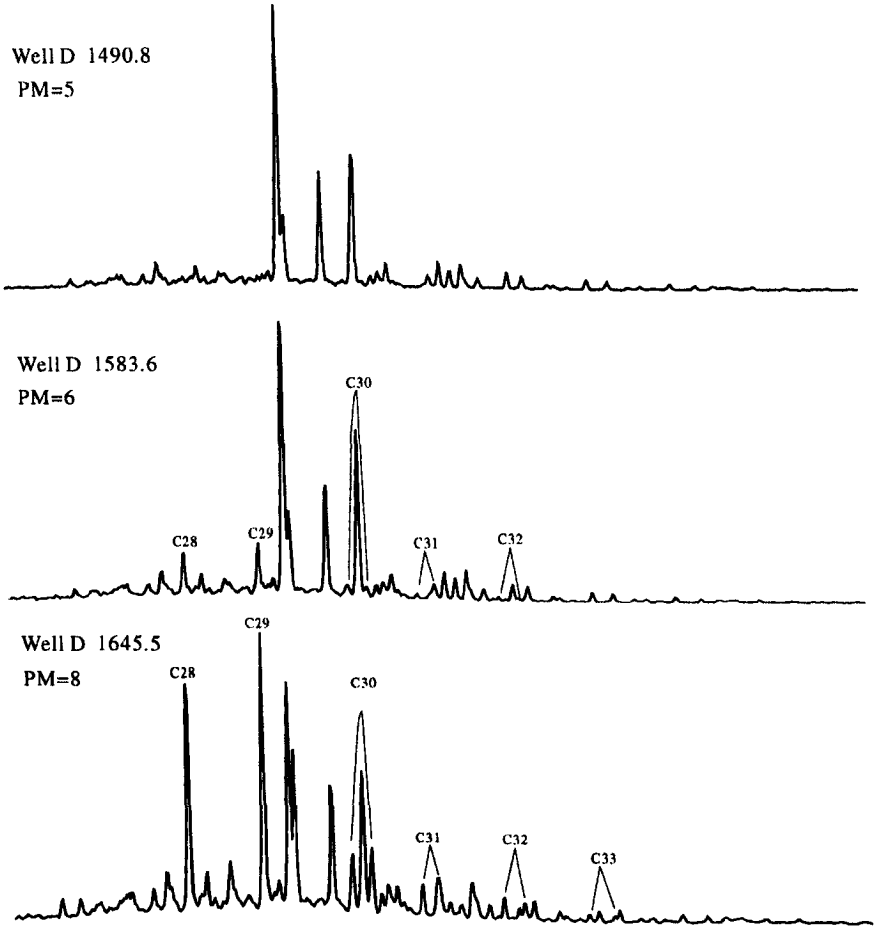

Fig. 4-30. GC-MS m/z 177 fragmentogram of 25-norhopanes in the Es1 column.

Since no significant amount of 25-norhopanes occur the Es3 column, the studies of this compound group are focused on the severely biodegraded Es1 column. Representative GC-MS fragmentograms of 25-norhopanes (m/z 177) are illustrated in Figure 4-30. The 25-norhopanes remain low in the upper part of the Es1 column. The average concentration of C_{28} 25-norhopane is 50μg/g EOM and that of C_{29} 25-norhopane is 70 μg/g EOM in the Es3 column and the upper part of the Es1 column. With increase of burial depth the 25-norhopane concentrations increase dramatically

in the Es1 reservoir. At the base of the column (near OWC) the concentration of C_{28} 25-norhopane reaches 1200μg/g EOM and that of C_{29} 25-norhopane is 1500 μg/g EOM (Fig. 4-31). This quantitative data with a 20-fold increase demonstrates that relative enrichment (Blanc and Connan, 1992) could not account for the 25-norhopane concentrations present in the biodegraded oil.

The $C_{28}\alpha\beta$-25-norhopane/$C_{29}\alpha\beta$hopane or $C_{29}\alpha\beta$-25-norhopane/$C_{30}\alpha\beta$hopane ratio was suggested as a suitable measure of the degree of biodegradation for the more severely biodegraded sample set since this ratio can distinguish different levels of biodegradation among heavily degraded oils where C-25 demethylation has occurred (Fig. 4-31). Quantitative measurements based on compositional changes at the molecular level indicate that the intrinsic level of biodegradation reaches a maximum at the bottom of the profile, near to the oil-water contact.

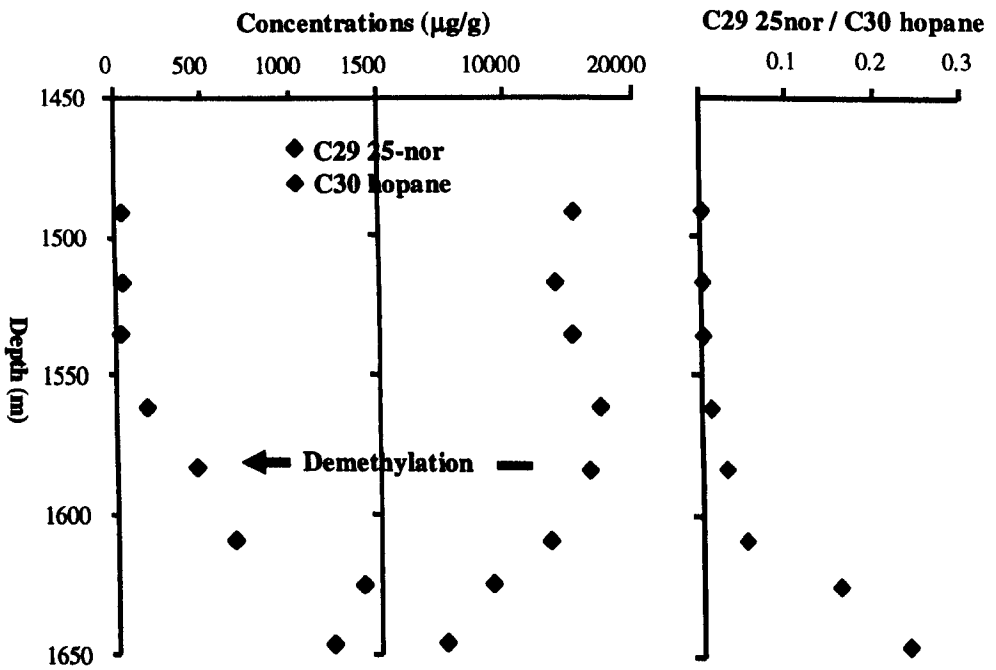

Fig. 4-31. C_{30} αβ Hopane and C_{29} αβ 25-norhopane concentration and their ratio variation in the Es1 column.

To calculate the "efficiency of demethylation", the different response factors of the $C_{29}\alpha\beta$ 25-norhopane (measured in m/z 177) and the C_{30} αβ hopane (measured in m/z 191) should be taken into account. The C_{30} αβ hopane undergoes two major fragmentations to give m/z 191 fragments, whilst the C_{29} 25-norhopane gives comparable fragments of m/z 177 and 191. Consequently, the $C_{30}\alpha\beta$ hopane is overestimated in the m/z 191 mass chromatogram compared with the response of the C_{29} 25-norhopane in m/z 177. Whilst no actual response factors has been calculated, an approximation of a factor of two (i.e. C_{30} αβ hopane needs to be divided by two) is about right (Farrimond, 2003, personal communication). With this approximate

response factor in mind, the concentration of $C_{30}\alpha\beta$ hopane falls from approximately 6000 μg/g EOM (modified by response factor) in parallel with an increase in C_{29} 25-norhopane concentration of around 1500 μg/g EOM – giving an indication that around 25% of the degraded hopanes are converted to 25-norhopanes. The remaining 75% must be degraded to other products.

Hopanoic acids have been previously reported in oils, where their presence may be due to contamination of the oil during migration through immature sediments (Jaffé *et al.*, 1988) or formation during biodegradation, either from bacterial oxidation of hopanes (Watson *et al.*, 1999) or from the biomass of the degrading bacteria (Meredith *et al.*, 2000). 25-Norhopanoic acids are potentially the products of two reactions associated with biodegradation – oxidation and demethylation (Fig. 4-32).

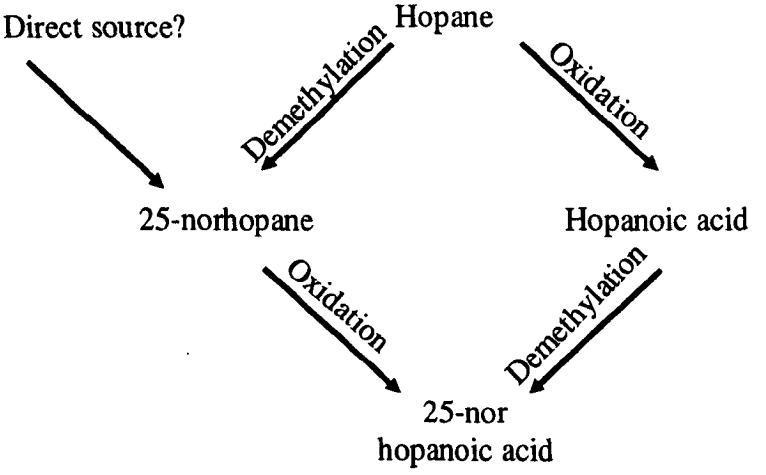

Fig. 4-32. 25-Norhopanoic acids formation pathways (Farrimond, unpublished result).

Since no detailed analysis of hopanoic acids in the Lengdong sample suite were made, the data from the Cheddar field (Bacchus unpublished data) may help to constrain this potential reaction scheme. Figure 4-33 shows a cross-plot of the demethylation parameters (25-nor/regular) for the hopanoic acids and hopanes (calculated using the C_{29} $\alpha\beta$ 25-norhopanoids and the C_{30} $\alpha\beta$ hopanoids from the Cheddar field, Bacchus unpublished data). The correlation between the two parameters indicates that the extent of demethylation of the hopanes is paralleled in the hopanoic acids.

The range of 25-nor/regular ratios seen in this field argues against the origin of 25-norhopanoic acids through the oxidation of pre-existing (i.e. derived from source) 25-norhopanes. Assuming constant rates of oxidation of hopanes and 25-norhopanes, the same 25-nor/regular ratio would be obtained for both hopanes and hopanoic acids. The data set shows a very wide variation in values of these parameters, which can only be explained by demethylation in the reservoir, or an extremely heterogeneous

oil charge (Farrimond, 2003, personal communication).

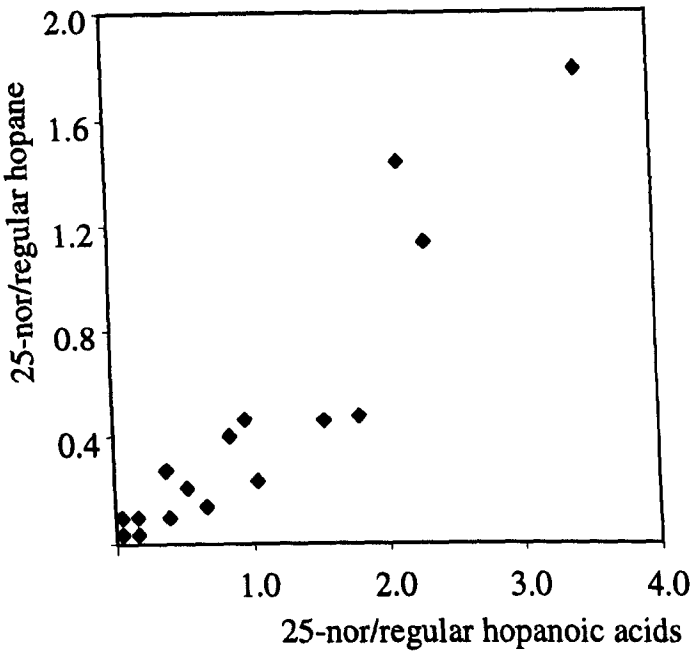

Fig. 4-33. Cross-plot of the demethylation parameters (25-nor/regular) for the hopanoic acids and hopanes (Bacchus unpublished data).

Even though hopanoic acids (and 25-norhopanoic acid) concentrations are normally 3 orders of magnitude lower than the hopanes, acids seem to be an important degradative product of hopanes. A correlation between the 25-nor/regular ratios for both hopanes and hopanoic acids indicates parallel demethylation of hopanes and hopanoic acids (Bacchus unpublished result).

4.6 Steranes

The structures of regular steranes and diasteranes are shown in Figure 4-34. In early publications it was commonly assumed that a predominance of C_{27} steranes in an oil or rock extract would signify an algal or marine input, whereas C_{29} steranes signified the presence of higher plant or terrestrial input. It has now been clearly established that the presence of C_{29} steranes does not necessarily mean an input of higher plant material since C_{29} sterols can also have an algal source (Moldowan *et al.*, 1985; Philp, 1994; Holba *et al.*, 2003). Biodegradation is an additional process that can alter the sterane distribution pattern in oil.

4.6.1 Concentration variation in biodegraded columns

In the Es3 oil columns, the total regular steranes concentrations show a continuously increasing trend from approximately 8500 μg/g EOM at the top towards the maximum value of 13000 μg/g EOM at the lower part of the column (Fig. 4-35). The observation of a slight increase in sterane concentrations in the main part of the

column is probably due to the fact of depletion of other components (e.g., *n*-alkanes and isoprenoid alkanes) at the base of the column near the OWC. A less dramatic trend in Well C reflects its less severe degree of biodegradation. In the Es1 oil column, regular sterane concentrations show a continuously decreasing trend from about 6000 to 2000 μg/g EOM throughout the column. Meanwhile the concentration of pregnanes, diasteranes and 4-methylsteranes remains constant or increase slightly throughout the column (Fig. 4-36).

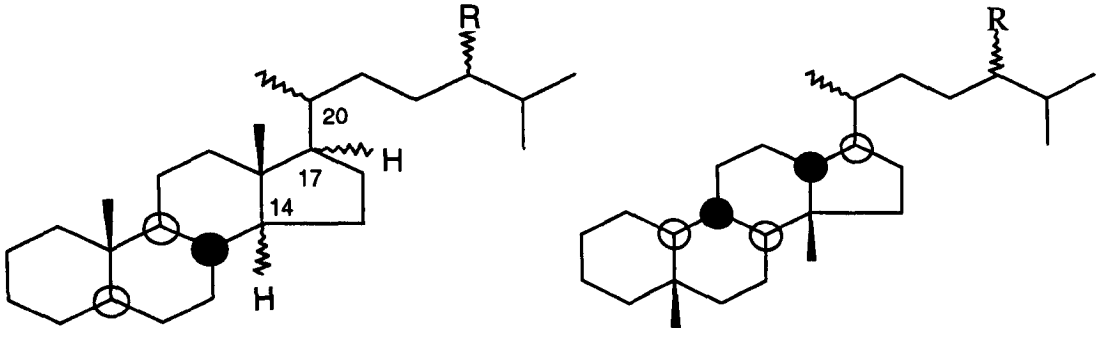

Sterane Diasterane

Fig. 4-34. Structures of regular steranes and diasteranes

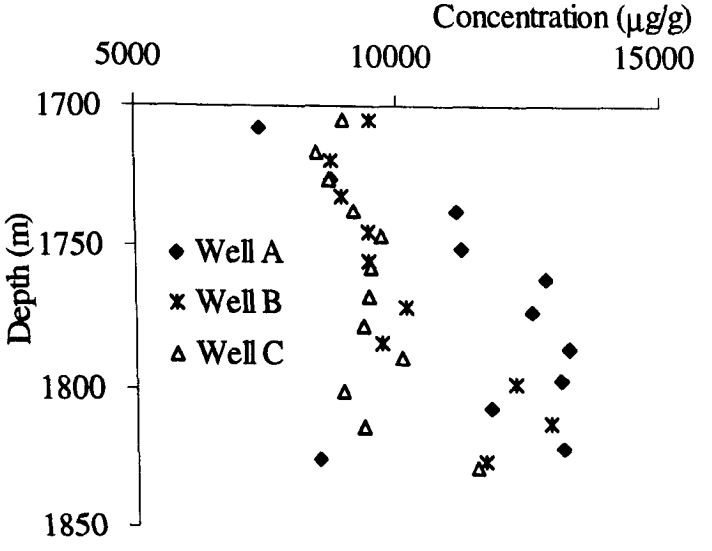

Fig. 4-35. Regular steranes concentration variations in the Es3 column.

4.6.2 Sterane carbon distribution

Representative GC-MS m/z 217 ion chromatograms are shown in Figure 4-37. In the top of the Es3 column where the biodegradation degree is relatively low, the sterane distribution pattern is characterized by predominantly regular steranes with low amounts of the lower molecular weight C_{21} and C_{22} steranes (pregnanes) and diasteranes. The relative proportion of regular steranes with increasing carbon number shows a consistent increase ($C_{27} < C_{28} < C_{29}$) with increasing depths. The epimer distributions are characterized by higher abundances of the biological 5α(H),14α(H),

17α(H) R configurations than the 5α(H), 14α(H), 17α(H) S and the 5α(H), 14β(H), 17β(H) configurations. Their similar distribution patterns in the Es3 column are indicative of their similarity in terms of organic matter type and paleoenvironment of deposition (Huang and Meinschein, 1979) in the source section. Furthermore, these oils have low abundances of C_{21} regular sterane and diasteranes. The epimerization ratios of C_{29} regular steranes are relatively low, indicating moderate thermal maturity.

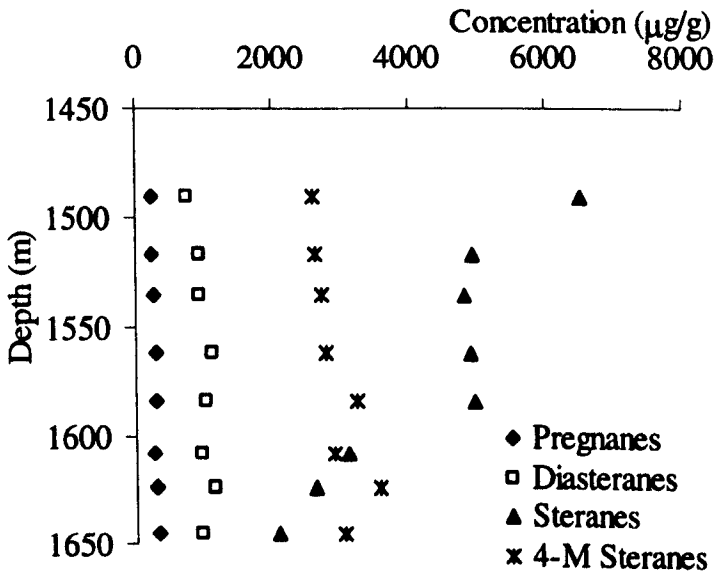

Fig. 4-36. Concentration variations of pregnanes, diasteranes, regular steranes and 4-methyl steranes in the Es1 column.

In Well A of the Es3 column the percentage of C_{27} steranes reduces from 25% to 22%, C_{28} steranes remain constant and C_{29} steranes increase from 44% to 47%, indicating their higher ability to resist biodegradation (Fig. 4-38a). This feature is clearer with increasing degree of biodegradation in the Es1 column with the C_{27} steranes percentage decreasing from 23% to 14% while that of C_{29} steranes increases from 43% to 54%. The percentage of C_{28} steranes also decreases slightly (Fig. 4-38b). All these data demonstrate that the sterane degradation proceeds in the order C_{27} before C_{28} before C_{29} steranes.

4.6.3 Epimer distribution

The isomerisation of regular steranes at the C-20 position is one of the classical maturity parameters (Mackenzie, 1984). Isomerisation at C-20 in stigmastane (C_{29} sterane) causes the C_{29} 20S/(20S+20R) ratio to rise with increasing maturity from 0 to about 0.5 over a maturity range of 0.3 to 0.7% equivalent vitrinite reflectance. However, the regular steranes are only moderately resistant to biodegradation and their distributions are distorted by biodegradation at a more advanced stage. There has been much discussion in the literature as to the order of sterane susceptibility to

degradation. The order of bacterial attack of the regular steranes in reservoirs, laboratories, seeps, and tars, is (from the most susceptible to the least susceptible) αααR > αββR > αααS > αββS with $C_{27} > C_{28} > C_{29}$ (Seifert and Moldowan, 1979; Connan, 1984; Seifert *et al.*, 1984; Peters and Moldowan, 1993). This order of attack shows that there is a bacterial preference for degrading biological configuration epimers and that maturity ratios using steranes are affected by this preferential degradation.

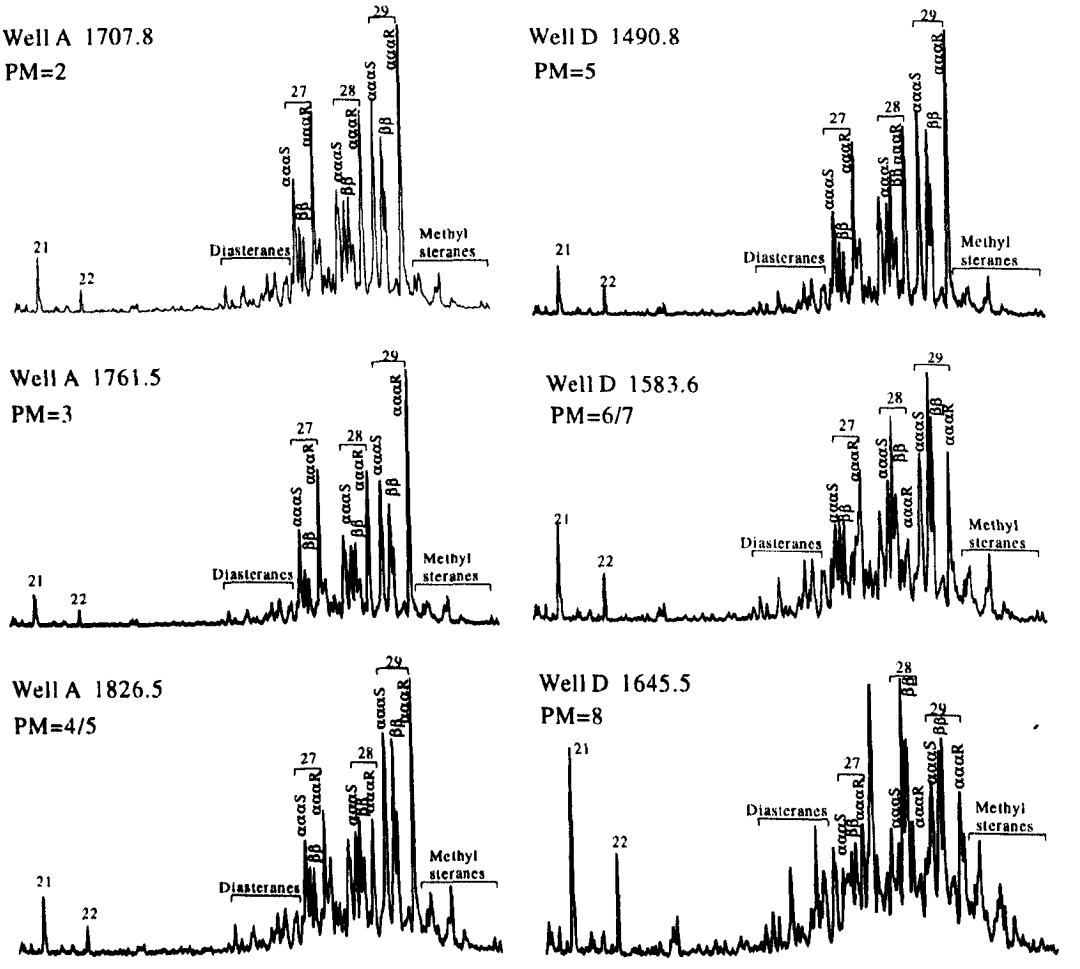

Fig. 4-37 Representative mass fragmentograms of m/z 217 for samples of Es3 and Es1 columns.

The profile of C_{29}-steranes ββ/(αα+ββ) and 20S/(20S+20R) ratios show slightly decreasing trends with depth in the Es3 column (Fig. 4-39). C_{29}-steranes ββ /(αα+ββ) ratios start from 0.32 at the top to 0.30 at the bottom and the 20S/(20S+20R) ratios decrease from 0.45 to 0.42 with a little scatter variation. Slightly high maturity signals at the top of the oil column suggest the top received more mature late arriving oil charge. At the bottom of Well A and B the ratios start to increase which may be caused by a biodegradation influence.

In the shallower, more degraded Es1 column the ratio of C_{29}-

sterane ββ /(αα + ββ) ratio shows a continuously increasing trend, which is unambiguously a biodegradation effect consistent with most other studies (Seifert *et al.*, 1984; Peters and Moldowan, 1993). However, the variation of the 20S/(20S + 20R) ratio is not consistent with previous studies. The proportion of 20S epimer increases from 0.43 to a maximum of 0.6 in the middle column then the trend is reversed and the ratio decreases to 0.45 near the OWC (Fig. 4-40). The reversal point is coincidental with a significant increase of 25-norhopanes. It seems 20S becomes more preferential to biodegradation at more advanced stage.

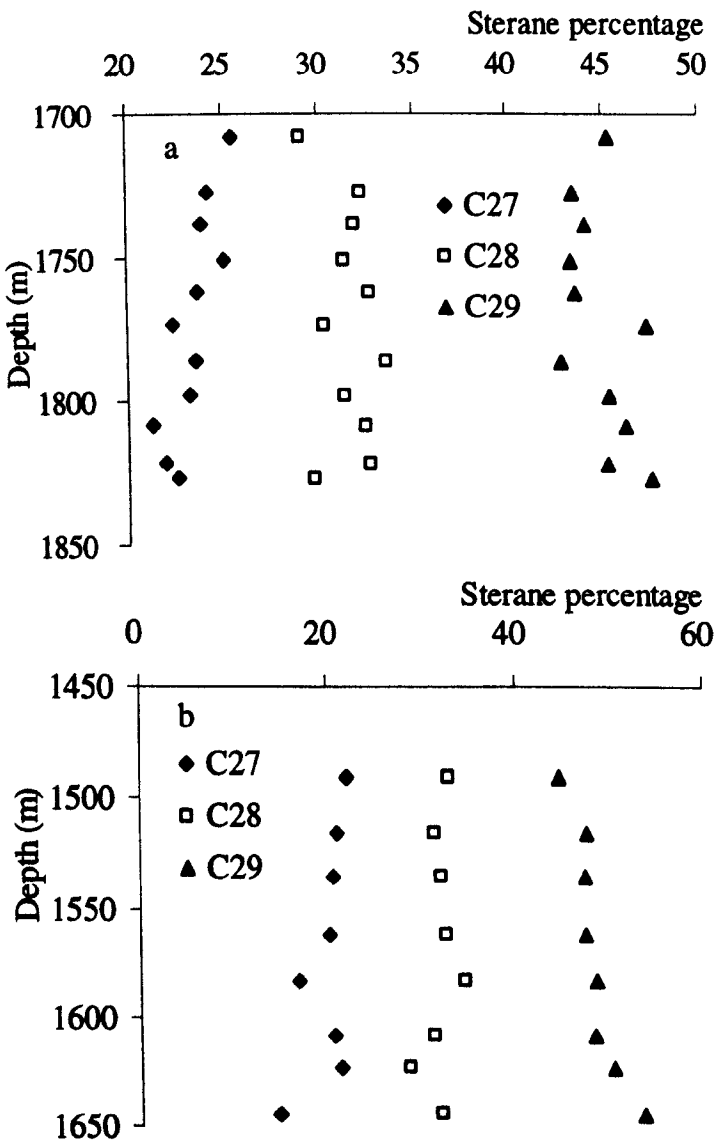

Fig. 4-38. Percentage variations of C_{27}, C_{28} and C_{29} regular steranes. (a): Es3 column of Well A; (b): Es1 column of Well D.

4.6.4 Pregnanes, diasteranes and methyl steranes

Since sterane biodegradation is not significant in the Es3 column, the comparison of biodegradation effects on different sterane compound groups is illustrated in the

Es1 column. There are a variety of studies on biodegradation effects on pregnanes, diasteranes and methyl steranes. The relative resistance of the diasteranes to biodegradation is greater than that of the steranes (Seifert and Moldowan, 1979; Seifert and Moldowan, 1981). Often the regular steranes are degraded at a considerably faster rate than the diasteranes (Goodwin *et al.*, 1983), with the steranes being completely removed in highly biodegraded oils, but leaving traces of the diasteranes (Seifert *et al.*, 1984).

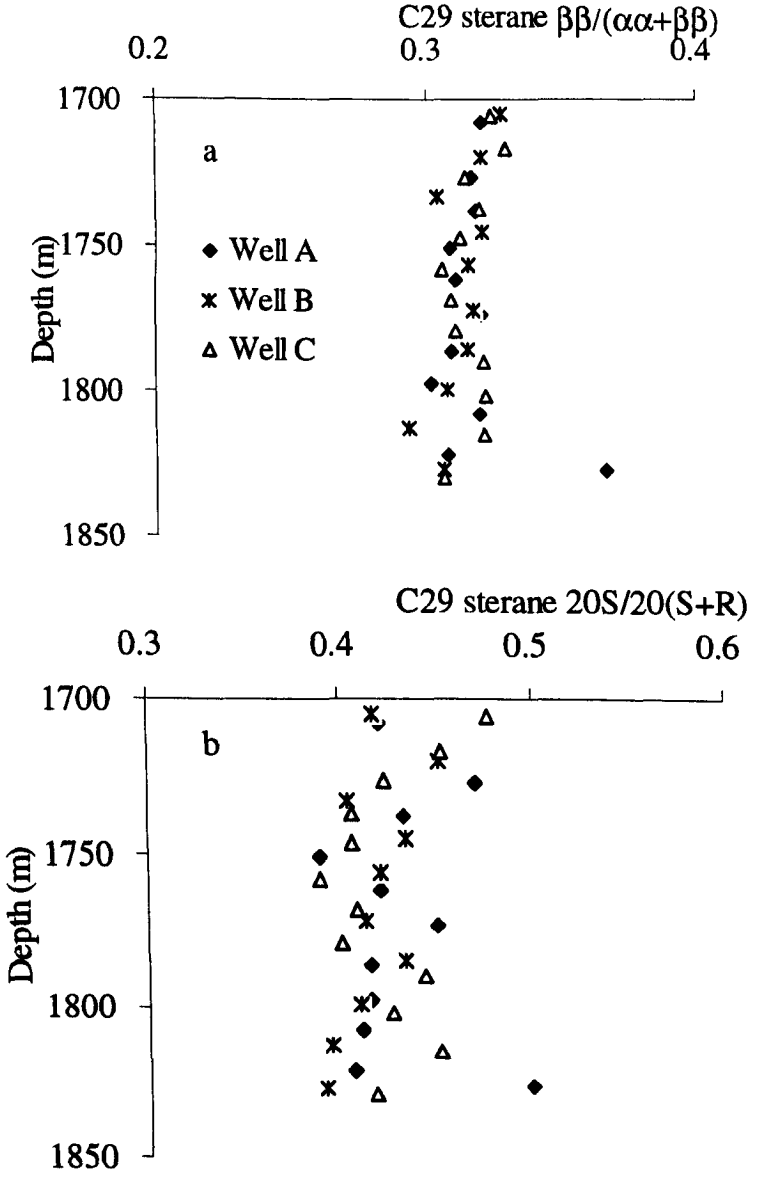

Fig. 4-39. The profile of C_{29}-steranes ββ/(αα+ββ) (a) and 20S/(20S+20R) (b) in the Es3 column.

The observation by Jiang *et al.* (1990), that in biodegraded oils the largest peaks seen in m/z 217 mass fragmentograms are the steranes with short side chains, especially C_{21}-C_{22} members, as well as the C_{28}-C_{29} diasteranes, appears to support the

above sequence of biodegradation. Brooks *et al.* (1988) reported that the short chain steranes (C_{21}-C_{22}) are more resistant to biodegradation than the diasteranes; these compounds also seem to be degraded only in extreme cases under reservoir conditions (Cassani and Eglinton, 1991). In laboratory simulations, Goodwin *et al.* (1983) demonstrated that bacteria degrade C_{27} diasteranes faster than C_{29} compounds. This agrees with the earlier observations of Seifert and Moldowan (1979) who noticed that the C_{29} diasteranes in biodegraded oils survive better than the C_{27} diasteranes. The 4-methylsteranes are more resistant to biodegradation than the C_{27}-C_{29} components (Lin *et al.*, 1989; Peters and Moldowan, 1993).

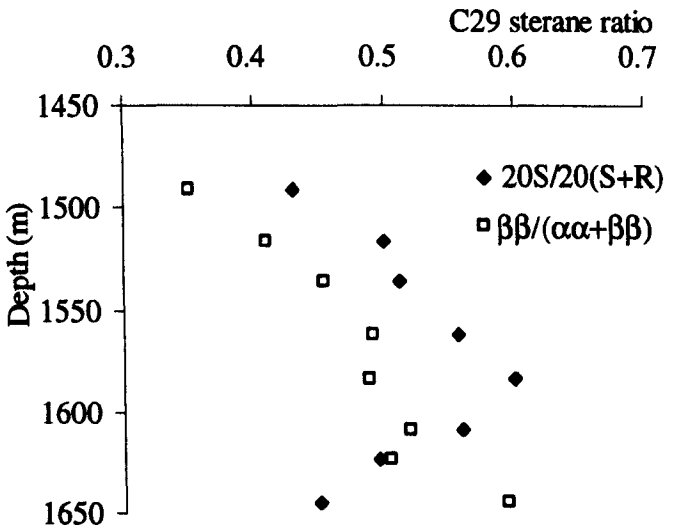

Fig. 4-40. The profile of C_{29}-steranes ββ/(αα+ββ) and 20S/(20S+20R) in Well D of the Es1 column.

The ratios of regular steranes to pregnanes, diasteranes and methyl steranes are show in Figure 4-41. All three ratios show the same increasing trend in the Es1 column i.e., regular steranes are preferentially removed, which is consistent with previous observations that pregnanes, diasteranes and methyl steranes are more resistant to biodegradation than regular steranes. Dramatic increase of 4-methyl steranes/steranes suggests that methyl steranes have even higher ability to resist biodegradation than that of pregnanes and diasteranes.

The degradation of steranes in the Lengdong reservoir oils showed that the C_{27} compounds were degraded first. The general order of bacterial attack of the regular steranes is 5α, 14α, 17α, C-20R (ααα**R**) > αββ**R** > ααα**S** > αββ**S** with $C_{27} > C_{28} > C_{29}$. This order of attack shows that there is a bacterial preference for biological epimers and maturity ratios using steranes are affected by this preferential degradation. However, the ααα**S** isomers are biodegraded prior to the ααα**R** compounds at more advanced stages of biodegradation (> PM level 6).

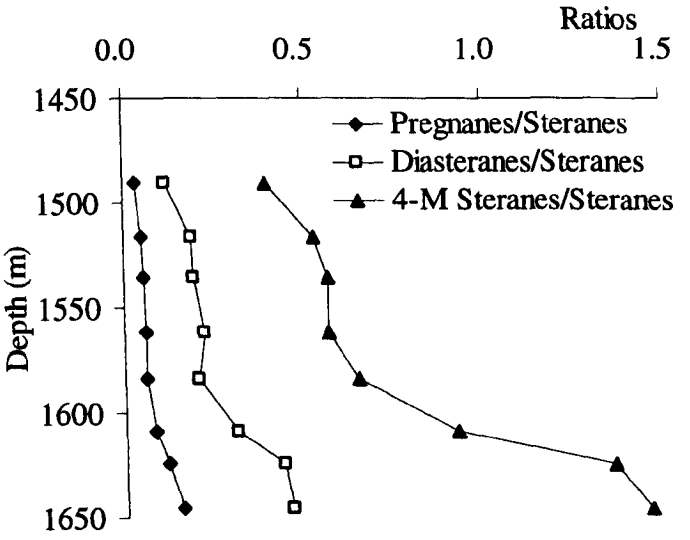

Fig. 4-41. Ratios of pregnanes/steranes, diasteranes/steranes and 4-methyl steranes/steranes in Well D of the Es1 column.

4.6.5 Hopanes vs steranes

There has been much discussion in the literature as to the order of sterane versus hopane degradation. Some studies indicated that microbial attack on steranes before the terpanes (Goodwin *et al.*, 1983; Seifert *et al.*, 1984; Brooks *et al.*, 1988), other observation suggested steranes decrease at the same time as hopanes (Philp, 1983; Zhang *et al.*, 1988), while hopanes loss prior to sterane depletion was also reported (Peters and Moldowan, 1991; Cassani and Eglinton, 1991).

Bigge and Farrimond (1998) reported conflicting data for two related oil seeps in Dorset (UK). Whilst one seep clearly showed only partial degradation of the ααα20R steranes and preferential loss of the αβ hopanes in the C_{29}-C_{33} range (with less marked removal of the C_{34} and C_{35} compounds), another nearby seep had a hopane distribution which appeared to be undegraded whilst the steranes had undergone extensive modification. Bigge and Farrimond (1998) assigned the differences between the relative extents of hopane and sterane degradation to two divergent pathways of biodegradation, the controlling factors of which were uncertain. Aerobic and anaerobic conditions may therefore control the effects of biodegradation on biological markers.

The steranes in the Lengdong samples were less abundant than the terpane compounds. High hopane concentrations are indicative of the incorporation of high levels of bacterial input (Tissot and Welte, 1984; Peters and Moldowan, 1993). In the Es3 column the ratios of C_{30}αβhopane/C_{29}αααR sterane are about 10 with very little variation except samples in Well A at the base of the Es3 column, which is affected by biodegradation (Fig. 4-42a). In the more severely biodegraded Es1 column, the

$C_{30}\alpha\beta$hopane/$C_{29}\alpha\alpha\alpha$R sterane ratio increases from 14 at the top of the column to the maximum value of 42 at the lower part of the column than decreases to 20 at the base near OWC (Fig. 4-42b).

The results presented here may offer an alternative explanation to the long-term controversy over the biodegradation preference of steranes and hopanes. At intermediate degradation stages (PM level 4-7) biodegradation probably affects the steranes before the hopanes, at more advanced stages (> PM level 7) hopanes become more vulnerable. Some of the previous studies may actually have been limited to narrow biodegradation level ranges and revealed only part of the picture.

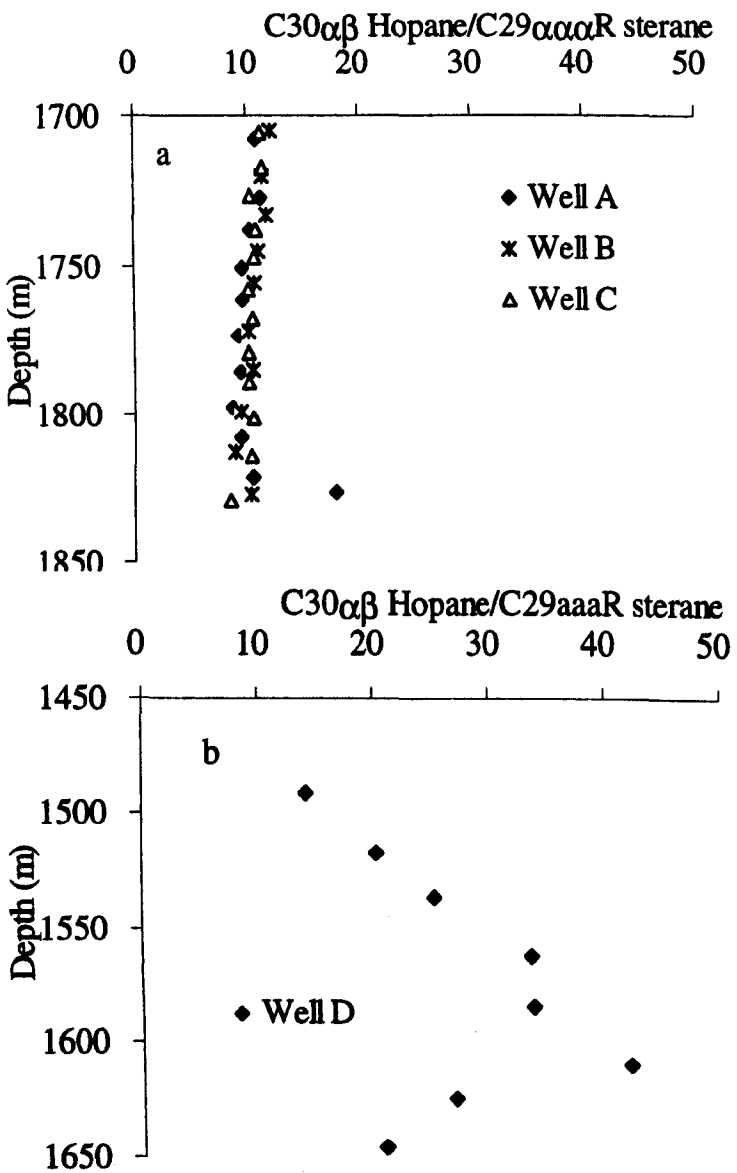

Fig. 4-42. Ratios of $C_{30}\alpha\beta$ hopane/$C_{29}\alpha\alpha\alpha$R sterane in the Es3 (a) and Es1 (b) columns.

5 BIODEGRADATION EFFECTS ON AROMATIC HYDROCARBONS

Some basic structures of aromatic hydrocarbon compounds are illustrated in Figure 5-1. As previous discussed in Chapter 1, the biodegradation of PAHs is highly dependent on the number of aromatic rings, number of alkyl substituents and position of alkyl substituents (Volkman *et al.*, 1984; Fisher *et al.*, 1996; George *et al.*, 2002). The rate of biodegradation decreases with increasing number of aromatic rings and alkyl substituents. Within compound classes, however, some isomers are more susceptible to biodegradation than others, and that is controlled by the position of the alkyl substituents (Volkman *et al.*, 1984; Rowland *et al.*, 1986; Fisher *et al.*, 1996; Budzinski *et al.*, 1995; Fisher *et al.*, 1998; George *et al.*, 2002). Aromatic steroid hydrocarbons are highly resistant to biodegradation, being degraded only in some extreme conditions (Wardroper *et al.*, 1984; Lin *et al.*, 1989; Cassani and Eglinton, 1991).

5.1 Overall distribution patterns and concentration variations

5.1.1 RIC

Representative reconstructed ion chromatograms (RICs) (sum of ions listed in Table 2-1) of the core extract aromatic hydrocarbon fractions from the Es1 and Es3 columns (Fig. 5-2) clearly show systematic changes in the composition of the residual oil. The alkylnaphthalenes, alkylphenanthrenes and triaromatic steroid hydrocarbons (TAS) are the three most abundant classes of aromatic compounds in the samples from the top of the Es3 column. Such a molecular composition may be considered as characteristic of a lightly degraded oil. In the middle of the Es3 column alkylphenanthrenes are abundant but the relative amounts of alkylnaphthalenes, alkylbiphenyls, and alkylfluorenes are significantly decreased in abundance, relative to the least degraded top samples. Downwards to the bottom, the relative amounts of alkylphenanthrenes are also significantly depleted, exhibiting more intensive biodegradation. In the Es1 column all alkylnaphthalenes and alkylphenanthrenes are heavily removed and aromatic steroid hydrocarbons are predominant the RICs showing extensive biodegradation.

5.1.2 Concentration

Concentrations of the C_{3+}-alkylbenzenes are generally very low (less than a few hundred μg/g EOM) in the sample set due to losses during sample storage prior to analysis. Complete series of long chain alkylbenzenes occur only in oils at the top of

the Es3 column and concentrations decrease rapidly at slightly lower depths. No alkylbenzenes were observed in core extracts from the Es1 column, suggesting that higher molecular weight monoaromatic compounds are susceptible to biodegradation as also noted by Blanc and Connan (1992).

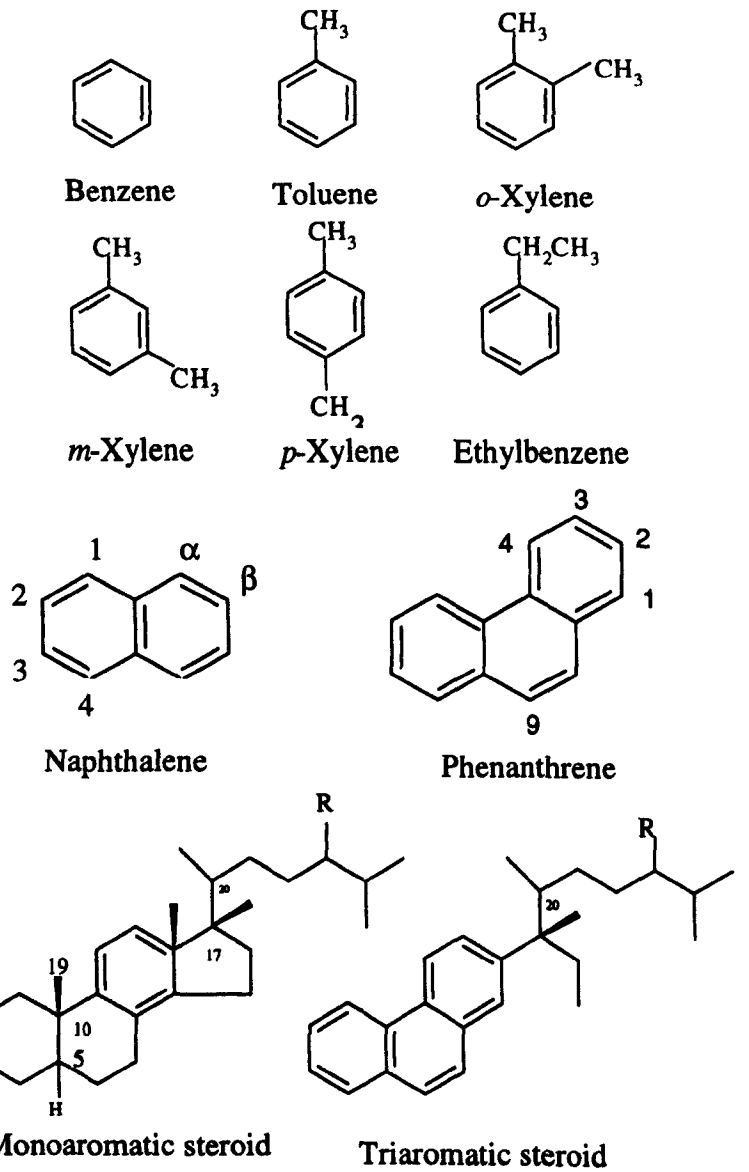

Fig. 5-1. Some basic structures of aromatic hydrocarbon compounds.

The variations in the concentrations of the $C_{0\text{-}5}$-alkylnaphthalenes, $C_{0\text{-}3}$-alkylphenanthrenes, C-ring monoaromatic steroid hydrocarbons (C_{21}, C_{22}, C_{27}-C_{29}-MAS) and triaromatic steroid hydrocarbons (C_{20}, C_{21}, C_{26}-C_{28}-TAS are quite distinct (Fig. 5-3). The concentration indicates the average value for samples with the same biodegradation level on Peters and Moldowan's (1993) scale. Obviously, normal alkanes are depleted first and then the isoprenoid hydrocarbons before PM level 4. Meanwhile, 25-norhopane starts to increase its concentration continuously. These components make a constraint for the assessment of biodegradation influence on aromatic hydrocarbons. The concentrations of $C_{0\text{-}5}$-alkylnaphthalenes decrease

gradually from about 750 μg/g EOM at PM level 3 to 220 μg/g EOM at PM level 5, and thereafter decrease more slowly. The concentrations of the C_{0-3}-alkylphenanthrenes show a slightly different variation trend. In the very early stages of biodegradation (PM level 2) they comprise the major components of the aromatic fraction in the Lengdong oils. Their concentrations increase slightly from 1900 μg/g EOM at PM level 2 to 2000 μg/g EOM at PM level 3 then decrease sharply to about 700 μg/g EOM at PM level 5. The concentrations of MAS and TAS show the opposite variation trend, increasing steadily with increasing degree of biodegradation. All of these systematic changes suggest that biodegradation is the primary control on the concentrations of aromatic hydrocarbons in the Lengdong oils.

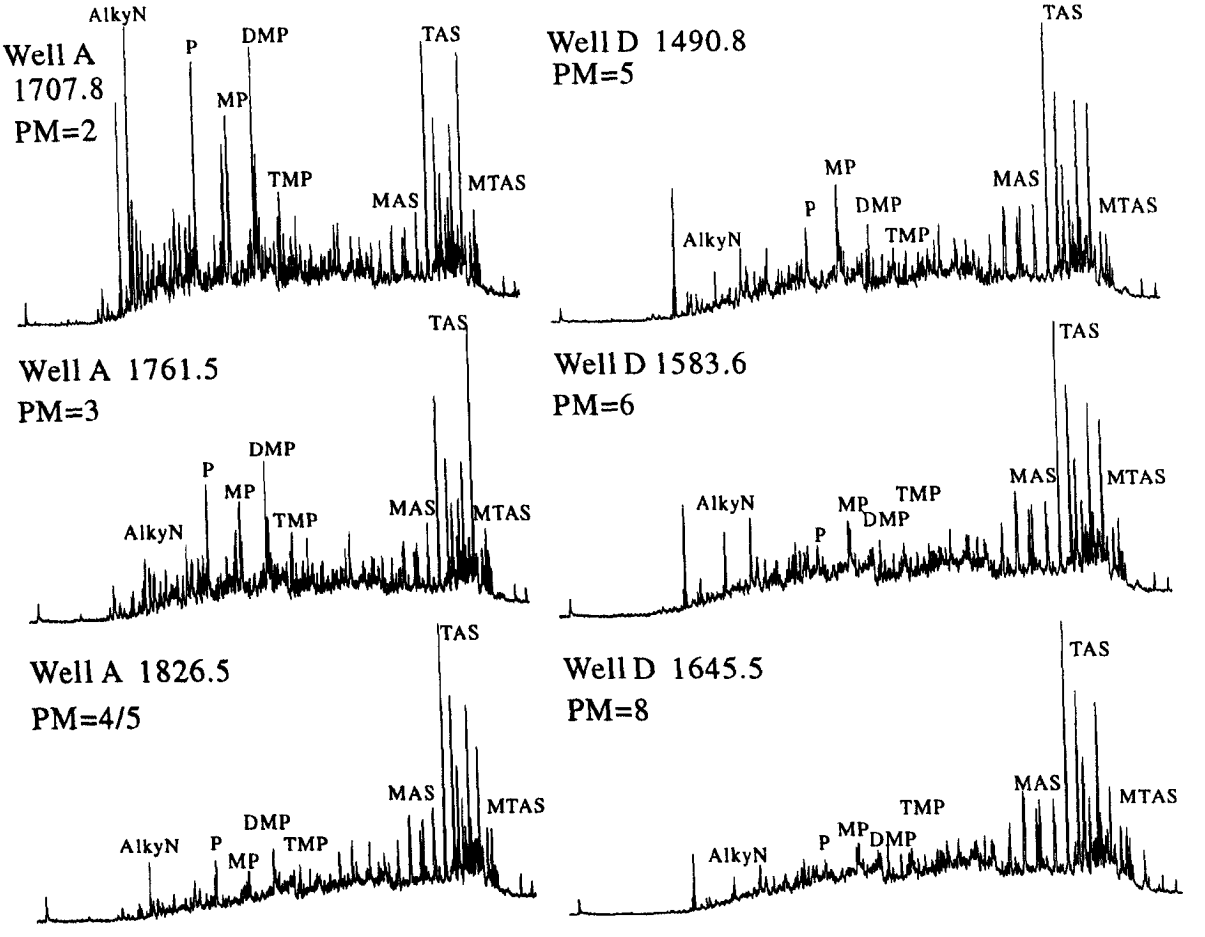

Fig. 5-2. Representative RICs (sum of ions listed in Table 2-1) showing aromatic hydrocarbon distributions in the Lengdong reservoir core extracts at various levels of biodegradation. AlkyN: alkylnaphthalenes; P: phenanthrene; MP: methylphenanthrenes; DMP: dimethylphenanthrenes; TMP: trimethylphenanthrenes; MAS: monoaromatic steroid hydrocarbons; TAS: triaromatic steroid hydrocarbons.

5.2 Alkylnaphthalenes

5.2.1 Degree of alkylation

There are three main controls on the susceptibility of aromatic hydrocarbons to

biodegradation; they are the number of aromatic rings, the degree of alkylation, and the position of alkylation (Volkman *et al.*, 1984; Peters and Moldowan, 1993; Fisher *et al.*, 1996; Ahmed *et al.*, 1999; George *et al.*, 2002). It is widely accepted that the more alkylated aromatic hydrocarbons are the less susceptible to biodegradation. Ahmed *et al.* (1999) compared alkylation ratios in coals with biodegradation level and concluded that methylnaphthalenes (MNs) are more susceptible to biodegradation than ethylnaphthalenes (ENs), dimethylnaphthalenes (DMNs) are more susceptible than trimethylnaphthalenes (TMNs) and TMNs are more susceptible than tetramethylnaphthalenes (TeMNs). During the course of crude oil biodegradation experiments, Mazeas *et al.* (2002) noticed that for phenanthrene and dibenzothiophene compounds, the degradation rate decreases with increasing degree of alkylation.

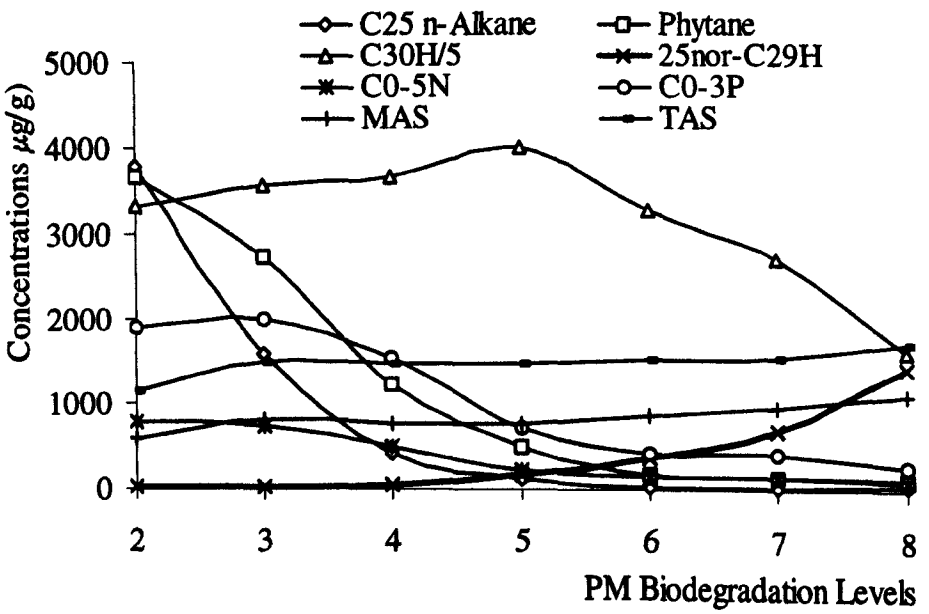

Fig.5-3. Variation the average concentrations of the $C_{0\text{-}5}$-alkylnaphthalenes; $C_{0\text{-}3}$-alkylphenanthrenes; (C_{21}, C_{22}, $C_{27\text{-}29}$) C-ring monoaromatic steroid hydrocarbons (MAS); (C_{20}, C_{21}, $C_{26\text{-}28}$) triaromatic steroid hydrocarbons (TAS); *n*-C_{25}; phytane (Ph); $C_{30}\alpha\beta$hopane/5 (C30H/5) and 25-nor-$C_{29}\alpha\beta$hopane (25nor-C29H) with biodegradation levels.

This study of the Lengdong reservoir oils reveals several exceptions to the observations noted above. Indeed, the percentages of the C_2-, C_3-, C_4- and C_5-alkylnaphthalene homologues (C_2-alkylnaphthalenes i.e., total amount of EMNs and DMNs, the same rule applied for other notation) show considerable variation with increasing degree of biodegradation (Fig. 5-4). The relative abundances of the C_4- and C_5-naphthalenes increase with increasing degree of biodegradation while those of the lower alkylhomologues decrease, in agreement with previous reports. However, the rate of increase or decrease differs for each homologue group. For example, the

proportion of C_2-naphthalenes decreases from 15% to 13% through the entire biodegradation range, whereas the proportion of the C_3-naphthalenes decreases from 47% at PM level 2 to 28% at PM level 8. Furthermore, it is interesting to note that the C_3-naphthalenes are depleted more rapidly than the C_2-naphthalenes, in contrast to some of the more 'classic' observations. The ratio of C_2-naphthalenes /C_3-naphthalenes actually increases with increasing degree of biodegradation and this may be related to demethylation of the C_3-naphthalenes during the advanced stages of biodegradation.

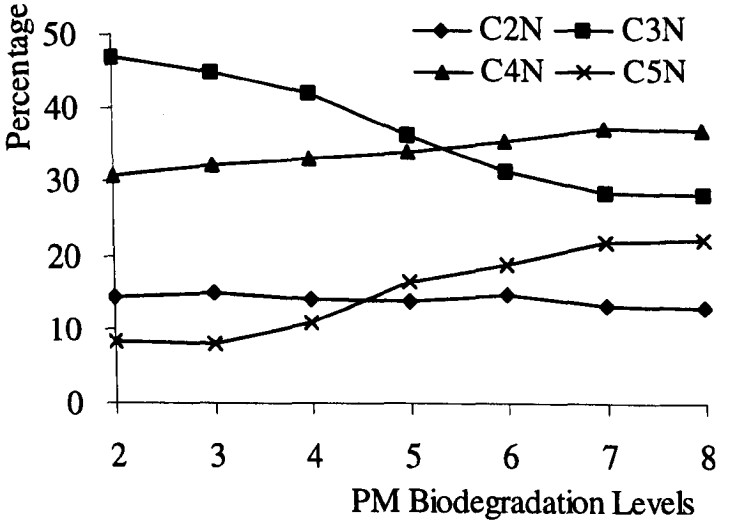

Fig. 5-4. Relative abundance of C_2-, C_3-, C_4- and C_5-alkylnaphthalene homologues (as percentage of $\sum C_{2\text{-}5}$-naphthalenes) in oils at different levels of biodegradation from the Es3 and Es1 oil columns of the Lengdong oilfield. N: alkylnaphthalenes.

5.2.2 Methynaphthalenes

Methylated naphthalenes are ubiquitous constituents of sedimentary organic matter (Tissot and Welte, 1984). They have been reported to occur in crude oils with up to six methyl groups attached to the naphthalene carbon skeleton (Bastow *et al.*, 1998, and references therein). The distributions of methylated naphthalenes are highly variable between samples as they are controlled by the effects of source, thermal stress and biodegradation.

Relative to *n*-alkanes and isoprenoid alkanes, alkylated naphthalenes would be expected to be biodegraded more slowly. Under reservoir conditions dimethylnaphthalenes with β substituents are readily biodegradable (Volkman *et al.*, 1984). However, during storage of samples before analysis volatile methylnaphthalenes are lost and thus these concentrations are very low in the studied sample set. The ratios of 2-MN/1-MN are therefore not accurately represented, scattered with a weak declining trend in the Es3 column (Fig. 5-5).

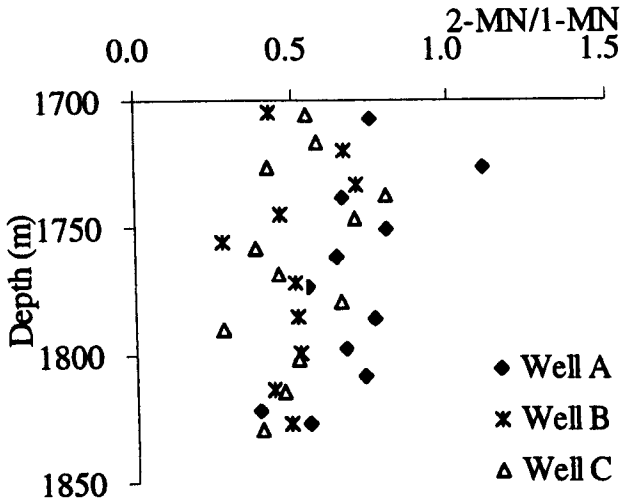

Fig. 5-5. Ratios of 2-MN/1-MN in the Es3 column.

5.2.3 C_2-naphthalenes

The DMNs, TMNs, TeMNs and PMNs are common constituents of oils and source rock extracts. The distributions of multiply methylated naphthalenes are highly variable between samples as they are controlled by the effects of source, thermal stress and biodegradation but source and maturity are constant here. The presence of abundant 1,6-DMN, 1,2,5-TMN, 1,2,7-TMN, 1,2,5,6-TeMN, 1,2,3,5-TeMN and 1,2,3,5,6-PMN in low maturity sedimentary organic matter has led to the suggestion that these compounds originate from terpenoids derived from microbial and land plant sources (van Aarssen *et al.*, 1999 and reference therein). However, with increasing maturity the relative abundances of these isomers are diminished and at high maturity the isomer distributions reflect their relative stabilities (Alexander *et al.* 1985) with β-isomers becoming dominant. The effects of biodegradation on the distribution of methylated naphthalenes were first described by Volkman *et al.* (1984) and Fisher *et al.* (1996) extended this research to TMNs and TeMNs. Obviously, Fisher's contaminated coast sand samples are biodegraded under aerobic condition and most reservoir biodegradation is most likely an anaerobic process (Larter *et al.*, 2003). The actual biodegradation susceptibility for multiple alkylated naphthalenes under reservoir conditions is thus not fully established yet.

There are varieties of studies of biodegradation effects on dimethylnaphthalene isomers. Dimethylnaphthalenes with methyl substituents that are adjacent (i.e. 2,3- and 1,8-dimethylnaphthalene), are most resistant to biodegradation because the proximity of the adjacent methyl groups, which inhibit attack, perhaps due to steric hindrance. 1,6-Dimethylnaphthalene is less resistant than other isomers while ethylnaphthalenes are considerably more resistant to biodegradation than most of the

dimethylnaphthalenes (Volkman *et al.*, 1984; Fisher *et al.*, 1996; Bastow *et al.*, 1999).

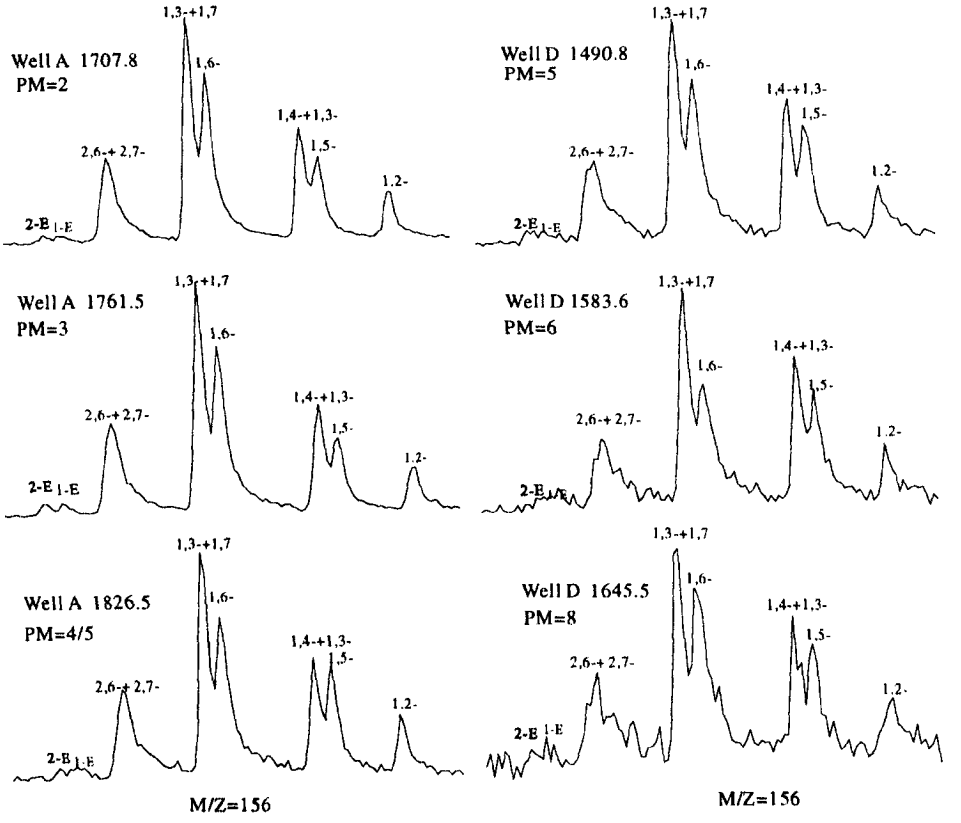

Fig. 5-6. Representative C_2-naphthalene distributions from the Lengdong oil columns.

Representative distributions of C_2-naphthalenes form the Lengdong oilfield are shown in Figure 5-6. Two ethylnaphthalene isomers are very low in all sample sets and do not show significant variation with increasing degree of biodegradation. 1,6-dimethylnaphthalene shows a slight decreasing until PM level 6 and then remain relatively high at PM level 8. This seems not in consistent with previous observation (Volkman *et al.*, 1984; Fisher *et al.*, 1996). 1,2-Dimethylnaphthalene has two adjacent methyl groups and shows a weakly increasing trend with increasing degree of biodegradation. The relative percentages of C_2-naphthalene isomers are shown in Fig. 5-7. The susceptibility to biodegradation of C_2-naphthalene isomers is hard to rank. Most C_2-naphthalene isomers did not show systematic variation. This study reveals that C_2-naphthalene isomer distributions are not very good biodegradation indicators.

5.2.4 Trimethyl naphthalene isomers (TMNs)

Representative mass chromatograms showing the distributions of TMNs, TeMNs and PMNs in oils at different levels of biodegradation are shown in Figure 5-8. Based on thermodynamic considerations, the most thermally stable TMN isomer is 2,3,6-TMN (peak 4) and one of the least stable isomers is 1,2,5-TMN (peak 7), which is often abundant in low maturity oil samples (van Aarssen *et al.*, 1999). In the Lengdong sample set, however, the variations in TMN distributions are more

dependent on biodegradation since the oils originate from a common source and have a similar thermal maturity (Koopmans *et al.*, 2002; Huang *et al.*, 2003). The variation in the relative abundance of individual TMN isomers with level of biodegradation, shown in Figure 5-9, reflects their susceptibility to biodegradation. With increasing degree of biodegradation, 2,3,6-TMN shows the most rapid decrease and 1,3,6-TMN (peak 2) follows a similar trend, while 1,2,3-TMN (peak 8) and 1,2,4-TMN (peak 6) gradually increase in relative abundance. The susceptibility of the TMN isomers in the Lengdong oils to biodegradation has the following order (from most susceptible to least susceptible):

2,3,6-TMN > 1,3,6-TMN > 1,3,7-TMN; 1,2,5-TMN; 1,2,7- + 1,6,7- + 1,2,6-TMN > 1,3,5- + 1,4,6,-TMN > 1,2,3-TMN; 1,2,4-TMN.

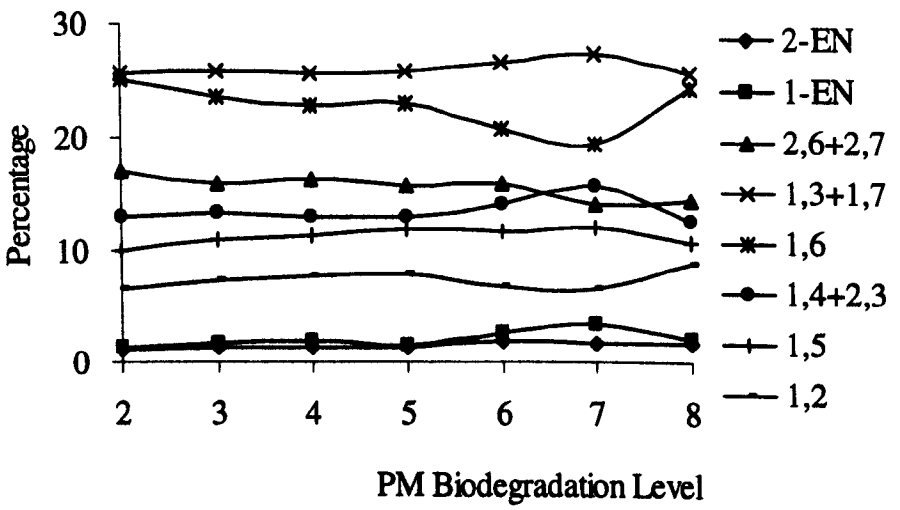

Fig. 5-7. Relative concentration of C_2-N isomers at different level of biodegradation.

5.2.5 Tetramethyl naphthalene isomers (TeMNs)

As described by van Duin *et al.* (1997), in the case of TeMNs the most abundant isomer in petroleum is usually 1,3,6,7-TeMN and one of the least abundant isomers is often 1,2,5,6-TeMN. Under the chromatographic conditions used here, 1,2,5,6-TeMN co-elutes with 1,2,3,5-TeMN, which is in fact very similar in stability to each other. Therefore, throughout this paper, the abundances of 1,2,5,6- and 1,2,3,5-TeMN will be measured as one sum referred to as 1,2,5,6-TeMN + 1,2,3,5-TeMN. Often 1,2,5,6-TeMN is the most abundant isomer in samples of low maturity. On this basis a ratio is proposed which describes the extent to which the distribution of isomers approaches equilibrium. van Aarssen *et al.* (1999) defined the ratio of 1,3,6,7-TeMN to the sum of 1,3,6,7-TeMN and (1,2,5,6 + 1,2,3,5)-TeMN as TeMNr.

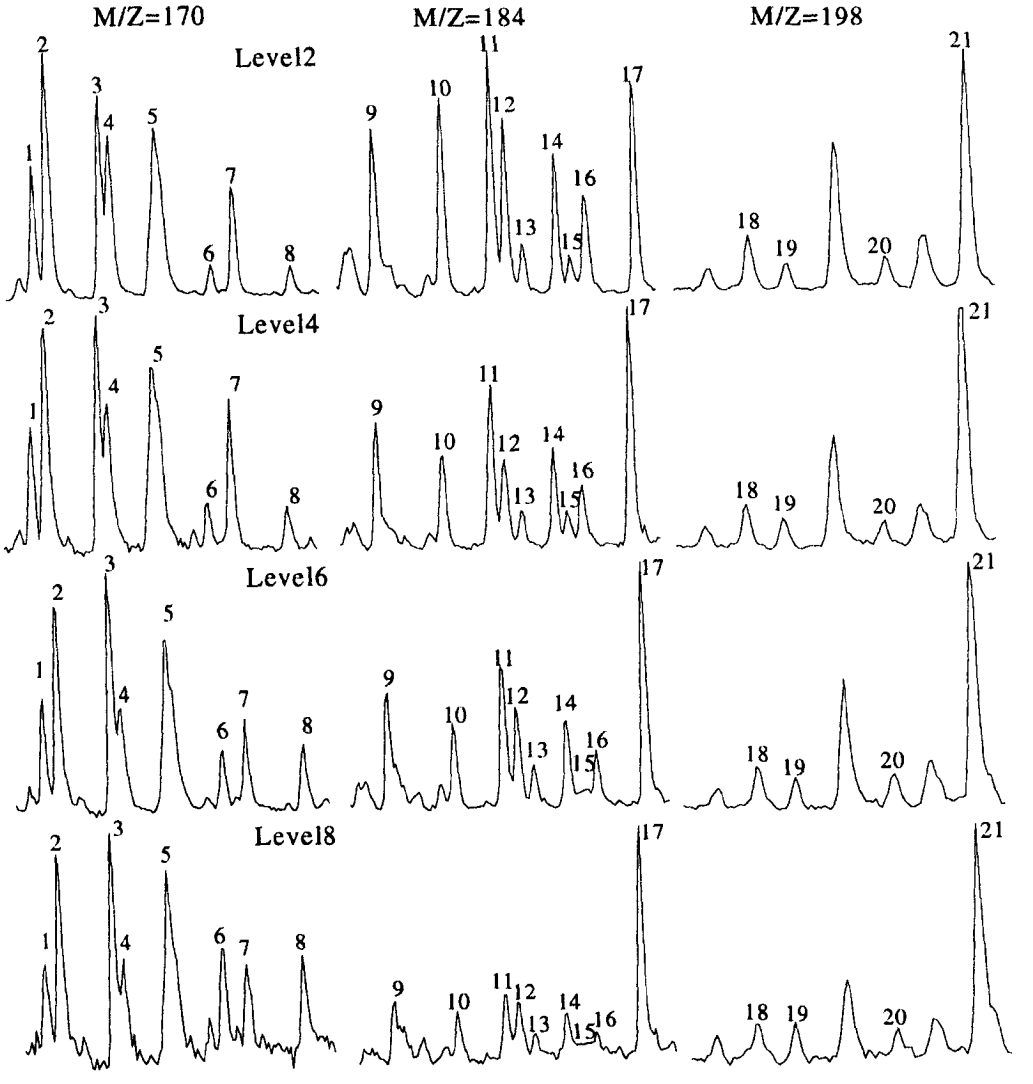

Fig. 5-8. Representative mass chromatograms of TMNs, TeMNs and PMNs in oils at different levels of biodegradation from the Es3 and Es1 oil columns of the Lengdong oilfield.

Among the tetramethylnaphthalenes, 1,3,6,7-TeMN (peak 10 in Fig. 5-8) is the most thermally stable isomer whereas 1,2,5,6-TeMN is the least thermally stable and usually the most abundant isomer in samples of low maturity (van Aarssen *et al.*, 1999). Under the GC conditions used in our analysis 1,2,5,6-TeMN co-elutes with 1,2,3,5-TeMN (peak 17 in Fig. 5-8). According to Fisher *et al.* (1996), 1,3,6,7-TeMN is only slightly more susceptible to biodegradation than 1,2,5,6-TeMN. For the oils from the Lengdong oilfield, this seems to apply only at low levels of biodegradation (< PM level 4) (Fig. 5-10). At more advanced stages, the relative abundance of

1,2,5,6-TeMN increases dramatically with increasing degree of biodegradation, reflecting its high resistance to biodegradation. The relative abundances of 1,2,3,7-TeMN (peak 15 in Fig. 5-8), 1,2,3,6-TeMN (peak 16 in Fig. 5-8) and 1,3,6,7-TeMN (peak 10) show a consistent decrease with increasing degree of degradation, while 1,3,5,7-TeMN (peak 9 in Fig. 5-8), 1,2,6,7-TeMn (peak 14 in Fig. 5-8) and 2,3,6,7-TeMN (peak 13 in Fig. 5-8) seem to be more-or-less stable. The order of susceptibility of the tetramethylnaphthalene isomers to biodegradation, at least for the Lengdong oils, is as follows (from most susceptible to least susceptible):

1,3,6,7-TeMN; 1,2,3,6-TeMN > 1,2,5,7-TeMN; 1,2,3,7-TeMN; 1,2,4,6- + 1,2,4,7- + 1,4,6,7-TeMN > 1,3,5,7-TeMN; 1,2,6,7-TeMN; 2,3,6,7-TeMN > 1,2,5,6-TeMN + 1,2,3,5-TeMN.

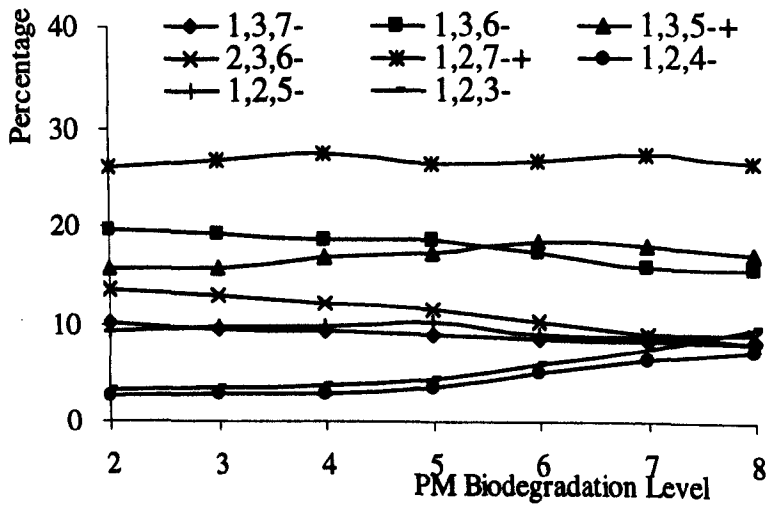

Fig. 5-9. Relative abundance of TMN isomers (as a percentage of the sum of C_3-naphthalenes) in oils at different levels of biodegradation from the Es3 and Es1 oil columns of the Lengdong oilfield. Compounds with co-eluting isomers are labeled '+'. See Figure 5-8 for details.

5.2.6 Pentamethyl naphthalene isomers (PMNs)

In the PMNs, the most thermally stable isomer is 1,2,4,6,7-PMN (peak 18) and the least thermally stable isomer is 1,2,3,5,6-PMN (peak 21) (van Aarssen *et al.*, 1999). In the Lengdong oilfield 1,2,3,5,6-PMN is the predominant PMN isomer, accounting for more than 60% of the total PMNs and indicative of the relatively low maturity of the oils in the study area. To the best of my knowledge, the effect of biodegradation on PMNs has not been studied. In the Lengdong sample suite no dramatic changes were observed among PMN isomers but 1,2,4,6,7-PMN appears to be slightly more susceptible to biodegradation than 1,2,3,5,6-PMN (Fig. 5-11). The order of susceptibly of the pentamethylnaphthalene isomers to biodegradation is (from most susceptible to least susceptible): 1,2,4,6,7-PMN > 1,2,3,6,7-PMN; 1,2,3,5,7-

PMN > 1,2,3,5,6-PMN.

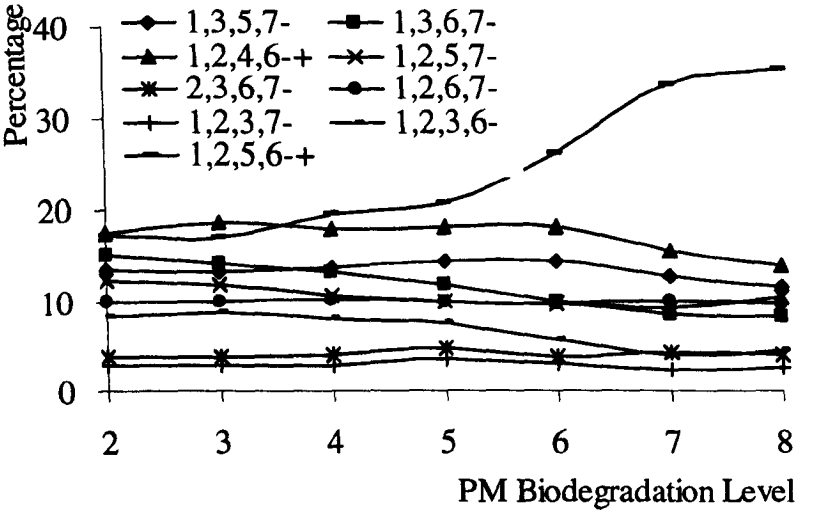

Fig. 5-10. Relative abundance of TeMN isomers (as percentage of the sum of C_4-naphthalenes) in oils at different levels of biodegradation from the Es3 and Es1 oil columns of the Lengdong oilfield. Compounds with co-eluting isomers are labeled '+'. See Figure 5-8 for details.

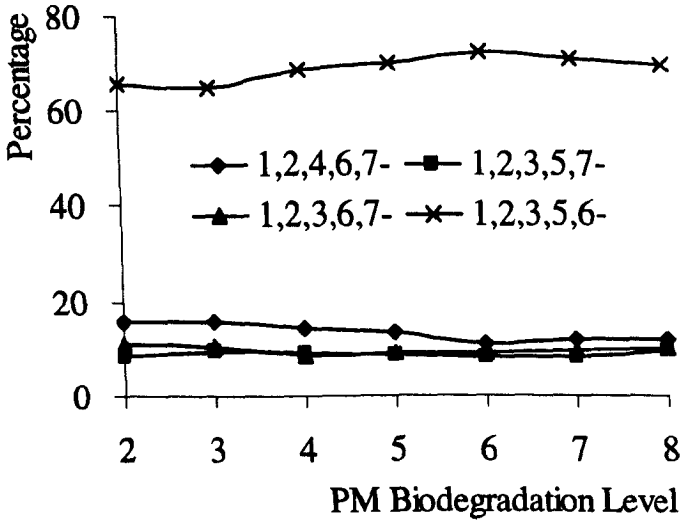

Fig. 5-11. Relative abundance of PMN isomers (as percentage of the sum of C_5-naphthalenes) in oils at different level of biodegradation from the Es3 and Es1 oil columns of the Lengdong oilfield.

5.3 Alkylphenanthrenes

5.3.1 Degree of alkylation

The relative abundance of phenanthrene (P) and the C_1-, C_2- and C_3-alkylphenanthrenes in the oils also varies with degree of biodegradation (Fig. 5-12). At low levels of biodegradation (< PM level 4) the relative amounts of phenanthrene, C_1-, C_2- and C_3-phenanthrenes remain constant although their absolute concentrations

begin to decrease with increasing degree of biodegradation. After PM level 4 there is a sharp increase in the proportion of C_3-phenanthrenes and decreases in the relative abundances of the less-alkylated homologues. The percentage of the methylphenanthrenes decreases from 26% at PM level 2 to 9% at PM level 8 while that of phenanthrene decreases from 11% to 5%, indicating that methylphenanthrenes are more readily biodegraded than phenanthrene.

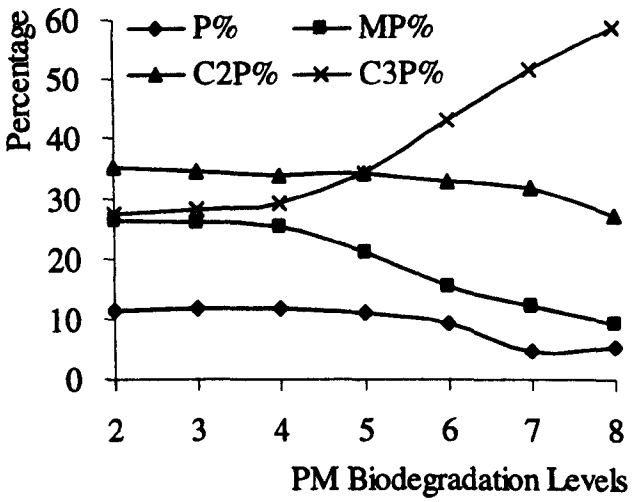

Fig. 5-12. Relative abundance of phenanthrene, C_1-, C_2- and C_3-phenanthrenes (as percentage of the sum of $C_{0\text{-}3}$-phenanthrenes) in oils at different levels of biodegradation from the Es3 and Es1 oil columns of the Lengdong oilfield.

5.3.2 Methylphenanthrenes (MPs)

The distribution of the methylphenanthrene isomers is a common maturity indicator (Radke and Welte, 1983). Taking into account the fact that the aromatic hydrocarbons especially phenanthrene derivatives, are more resistant to biodegradation than aliphatic hydrocarbons (Stojanovic *et al.*, 2001), maturity parameters calculated on the basis of the distribution of methylphenanthrene isomers are generally more reliable. However, Volkman *et al.*, (1984) noticed that when 25-norhopanes present, almost all of the alkylnaphthalenes and alkylphenanthrenes had been removed from the oil by biodegradation. Nadalig *et al.* (2000) studied the degradation of a mixture of phenanthrene (P), 2-methylphenanthrene (2MP) and 9-methylphenanthrene (9MP) by a bacterial community. The results obtained show a difference of degradation rates between the three compounds. P and 2MP were more rapidly degraded than 9MP. They also investigated the degradation of methylphenanthrenes in petroleum, but no selectivity of degradation was observed between the methylphenanthrenes. Other naturally degraded oil (Rowland *et al.*, 1986) and laboratory experiments (Budzinski *et al.*, 1998) indicate that of the methylphenanthrenes 9-MP is more resistant to biodegradation than the other MP

isomers.

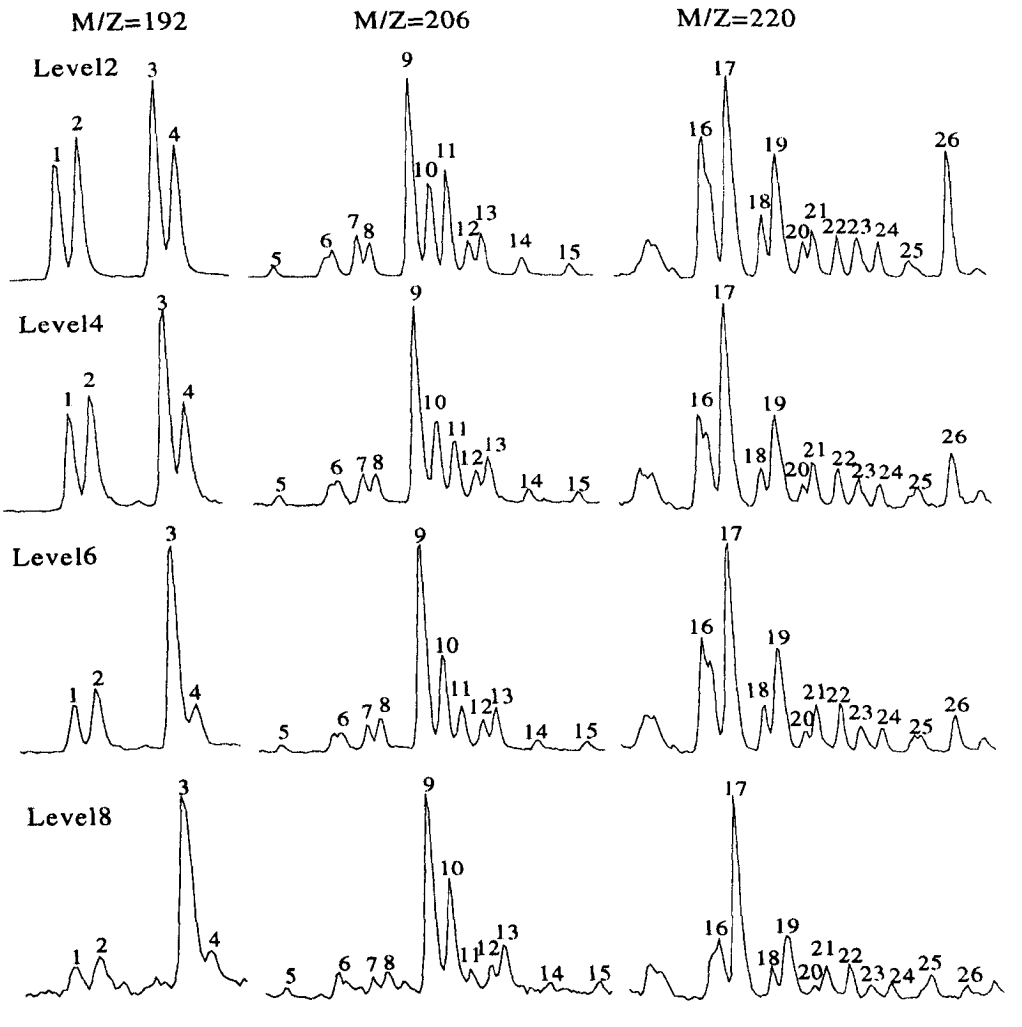

1	3-MP	10	2,5-+2,9-+1,6-DMP	18	1,3,9-+2,3,6-TMP
2	2-MP	11	1,7-DMP	19	1,6,9-+1,7,9-+2,3,7-TMP
3	9-MP	12	2,3-DMP		
4	1-MP	13	1,9-+4,9-+4,10-DMP	20	1,3,8-TMP
5	3-EP	14	1,8-DMP	21	2,3,10-TMP
6	9-,2-,1-EP+3,6-DMP	15	1,2-DMP	22	TMP
7	3,5-+2,6-DMP	16	1,3,6-+1,3,10-+2,6,10-TMP+2-E-5-	23	1,6,7-TMP
8	2,7-DMP			24	1,2,6-TMP
9	1,3-+3,9-+2,10-+3,10-DMP	17	1,3,7-+2,6,9+2,7,9-+7-E-1-MP	25	1,2,7-+1,2,9-TMP
				26	1,2,8-TMP

Fig. 5-13. Representative mass chromatograms of C_1-, C_2- and C_3-phenanthrenes in oils at different levels of biodegradation from the Es3 and Es1 oil columns of the Lengdong oilfield.

Representative mass chromatograms showing the distributions of the C_1-C_3 alkylphenanthrenes in the Lengdong oils are given in Figure 5-13. The distribution patterns of all three series of homologues show clear systematic variations with increasing degree biodegradation. The results clearly show the more refractory nature of 9-MP compared to the other methylphenanthrenes. The relative abundance of 9-MP shows a consistent increase with increasing degree of biodegradation, with the most pronounced changes occurring between PM levels 5 and 7 (Fig. 5-14). The changes in relative abundance of the isomers occur later than the variations in alkylphenanthrene

concentrations (Fig. 5-3), but it is quite clear from the Lengdong data that maturity parameters based on the methylphenanthrenes are not valid above PM level 4. Cassani and Eglinton (1991) observed a preferential alteration of 1-MP and 2-MP, which is a more subtle variation than seen in the present case study. In the Lengdong oil samples the order of susceptibility of the methylphenanthrenes to biodegradation is: 2-MP > 1-MP; 3-MP > 9-MP.

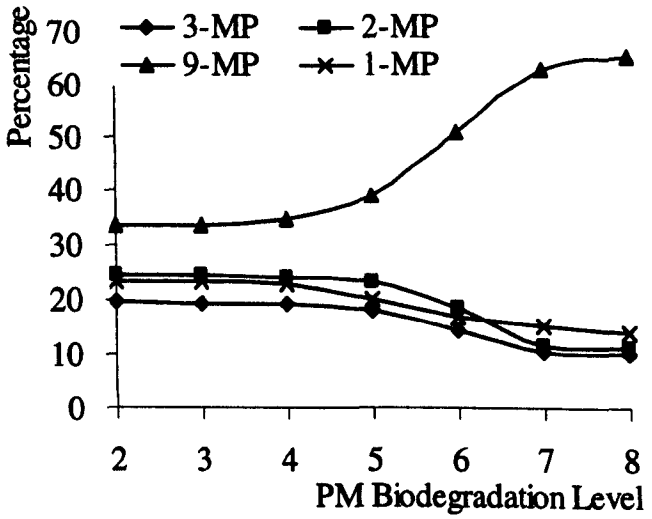

Fig. 5-14. Relative abundance of MP isomers (as a percentage of the sum of methylphenanthrenes) in oils at different levels of biodegradation from the Es3 and Es1 oil columns of the Lengdong oilfield

5.3.3 Dimethylphenanthrenes and ethylphenanthrenes (C_2-P)

Most studies indicate that the dimethylphenanthrenes (DMPs) are generally more resistant to biodegradation than phenanthrene and the methylphenanthrenes, but the relative susceptibility of dimethylphenanthrene isomers has not been established. Recent aerobic biodegradation experiments have indicated that among the dimethylphenanthrenes the most easily degraded isomer is 2,6-DMP and the least degraded is 1,7-DMP (Budzinski *et al.*, 1998; Mazeas *et al.*, 2002). No order of susceptibility relating to in-reservoir biodegradation has been reported to the best of my knowledge.

Representative mass chromatograms (m/z = 216) showing the distribution of C_2-alkylphenanthrenes (Fig. 5-13) and a plot of the relative abundance of C_2-P isomers (Fig. 5-15) indicate systematic changes in DMP composition with increasing degree of biodegradation. The 1,7-DMP isomer (peak 11) and to a lesser extent 2,6-DMP (peak 7) decrease in relative abundance during biodegradation. This is in contrast to observations of aerobic biodegradation carried out in the laboratory by Budzinski *et al.* (1998) and Mazeas *et al.* (2002), and probably reflects differences in redox conditions

and microbial consortia. The most recalcitrant 'component' of the DMNs is the 1,3- + 3,9- + 2,10- + 3,10-DMP complex (peak 9), which shows a continuous increase in relative abundance with increasing degree of biodegradation. A similar trend can be observed for 2,5- + 2,9- + 1,6-DMP (peak 10), but in this case the greatest increase occurs at a more advanced stage of biodegradation. The overall susceptibility of the DMN isomers is consistent with previous observations in that isomers with substituents at the 9 or 10 position are more resistant to biodegradation than isomers with substituents at other positions (Rowland *et al.*, 1986). A provisional order of susceptibility to biodegradation for the DMNs (from most susceptible to least susceptible) is inferred to be: 1,7-DMP > 2,6-+3,5-DMP; 2,7-DMP > 1,8-DMP; 2,3-DMP > 3-EP; 9- + 2- + 1-EP + 3,6-DMP; 1,2-DMP > 1,9- + 4,9- + 4,10-DMP > 2,5- + 2,9- + 1,6-DMP; 1,3- + 3,9- + 2,10- + 3,10-DMP.

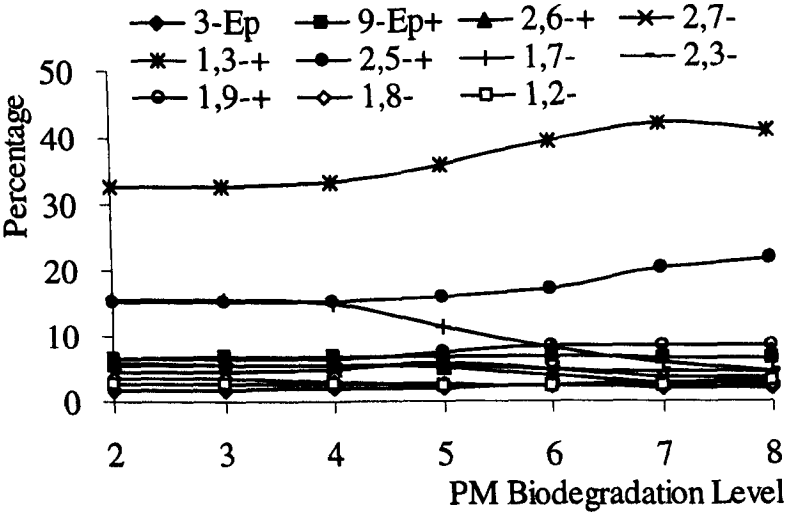

Fig. 5-15. Relative abundance of C_2-phenanthrene isomers (as percentages of the sum of C_2-phenanthrenes) in oils at different levels of biodegradation from the Es3 and Es1 oil columns of the Lengdong oilfield. Compounds with co-eluting isomers are labeled '+'. See Figure 5-13 for details.

5.3.4 Trimethylphenanthrenes and ethyl-methylphenanthrenes (C_3-P)

The isomer distributions of the C_3-alkylphenanthrenes in oils are very complex and the identification of individual isomers in the mass chromatograms is still tentative (Kruge, 2000). Although the TMPs have a high resistance to biodegradation compared to less-alkylated phenanthrene homologues, no geochemical indicators have been developed on the basis of their distribution patterns. Representative mass chromatograms (m/z = 220 in Fig. 5-13) showing the distribution of TMPs and a plot of the relative abundance of TMP isomers (Fig. 5-16) show systematic variations during biodegradation. The least-resistant component is 1,2,8-TMP (peak 26), which is quite abundant in the less-biodegraded samples (< PM level 3) and becomes

continually more depleted between PM levels 3 to 6. The relative abundance of Peak 16, comprised of (1,3,6- + 1,3,10- + 2,6,10-TMP + 2-E-5-MP), also decreases but the depletion begins at a more advanced stage of biodegradation (> PM level 5). The most recalcitrant component is peak 17 (1,3,7- + 2,6,9- + 2,7,9-TMP + 7-E-1-MP) which increases in relative abundance from PM level 4. A tentative order of susceptibility to biodegradation for the C_3-P (from most susceptible to least) was inferred to be:

1,2,8-TMP > 1,3,6- + 1,3,10- + 2,6,10-TMP + 2-E-5-MP > 1,6,7-TMP; 1,3,8-TMP > 1,3,9- + 2,3,6-TMP; 1,6,9- + 1,7,9- + 2,3,7-TMP; 1,2,6-TMP > 1,2,7- + 1,2,9-TMP; 2,3,10-TMP > 1,3,7- + 2,6,9- + 2,7,9-TMP + 7-E-1-MP.

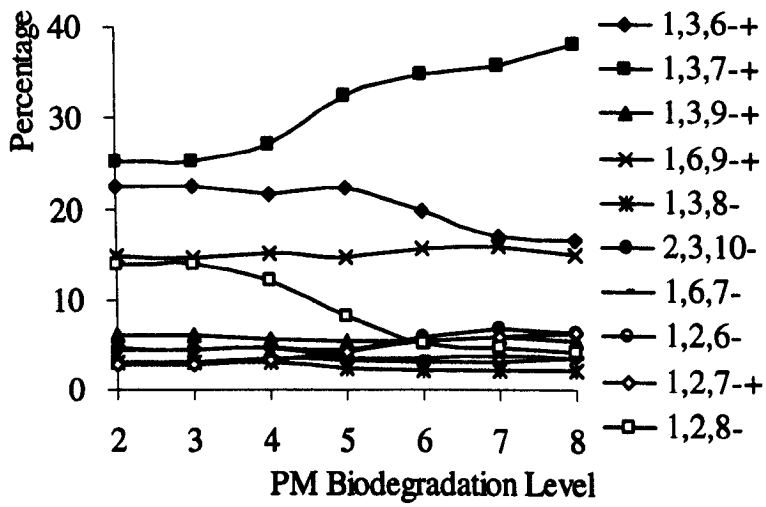

Fig. 5-16. Relative abundance of C_3- phenanthrene isomers (as percentage of the sum of C_3-phenanthrenes) in oils at different levels of biodegradation from the Es3 and Es1 oil columns of the Lengdong oilfield. Compounds with co-eluting isomers are labeled '+'. See Figure 5-13 for details.

5.4 Tetracyclic aromatic hydrocarbons

Three common tetracyclic aromatic hydrocarbon compound structures are shown in Figure 5-17. Biodegradation effect on tetracyclic aromatic hydrocarbons has been studied by a variety of environmental and biological experiments (Kiehlmann *et al.*, 1996). Sepic *et al.* (1998) reported the findings from a biodegradability study of fluoranthene using two pure bacterial strains, *Pasteurella sp.* IFA (B-2) and *Mycobacterium sp.* PYR-1 (AM). Two metabolites (9-fluorenone-1-carboxylic acid and 9-fluorenone) were identified. Dean-Ross *et al.* (2002) investigated the ability of sediment bacteria to utilize polycyclic aromatic hydrocarbons (PAHs). Cometabolism of fluoranthene in these strains was confirmed by the isolation of metabolites of fluoranthene and by kinetic analysis of the rate of utilization of the growth substrate in the presence of fluoranthene. Metabolism of fluoranthene occurred by attack on the

fused ring of the fluoranthene molecule, producing 9-fluorenone-1-carboxylic acid. In a *Rhodococcus sp.*, a second metabolite, a-(carboxymethylene)fluorene-1-carboxylic acid, was identified, indicating that this strain has the capacity to metabolize fluoranthene via *ortho* as well as *meta* cleavage. Caldini *et al.* (1995) noticed a *Pseudomonas* fluorescence strain isolated from exhausted-oil-polluted soil could degrade chrysene as a sole carbon source. Bogan *et al.* (2003) discovered a strain GTI-23 has considerable ability to mineralize a range of polycyclic aromatic hydrocarbons such as phenanthrene, fluoranthene, or pyrene as a sole source of carbon and energy, both in liquid and soil environments. Chang *et al.* (2002) used the known concentrations of phenanthrene, pyrene, anthracene, fluorene and acenapthene added to soil samples to investigate the anaerobic degradation potential of polycyclic aromatic hydrocarbon (PAH). Relative degradation rates observed were phenanthrene > pyrene > anthracene > fluorene > acenaphthene. Biodegradation was also measured under three anaerobic conditions; results showing the high-to-low order of biodegradation rates to be sulfate-reducing conditions > methanogenic conditions > nitrate-reducing conditions.

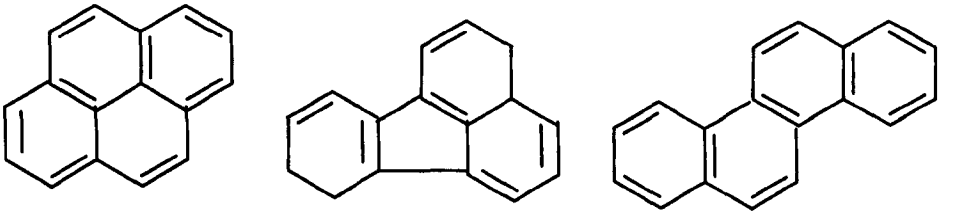

pyrene fluoranthene chrysene

Fig. 5-17. Three common tetracyclic aromatic hydrocarbon compound structures.

However, the biodegradation behaviour of tetracyclic aromatic hydrocarbons in reservoir oil has not yet been reported. Representative mass chromatograms at m/z = 202 with fluoranthene and pyrene are shown in Fig. 5-18. It is clearly seen that fluoranthene is more vulnerable to biodegradation than pyrene. With increasing degree of biodegradation, the relative concentration of fluoranthene decreases and that of pyrene increases.

The susceptibility to biodegradation between pyrene and chrysene is hard to compare in this sample set. In the Es3 column the ratios of pyrene to chrysene range from 0.5 to 1.0 with no clear trend throughout the column (Fig. 5-19a), while in the Es1 column, this ratio first increases from 0.63 to 1.11 at the mid part of the column than decreases to 0.63 at the base of the column (Fig. 5-19b). It is uncertain whether this variation is controlled by biodegradation or some other unknown factors. Both pyrene and chrysene are clearly more resistant to biodegradation than fluoranthene.

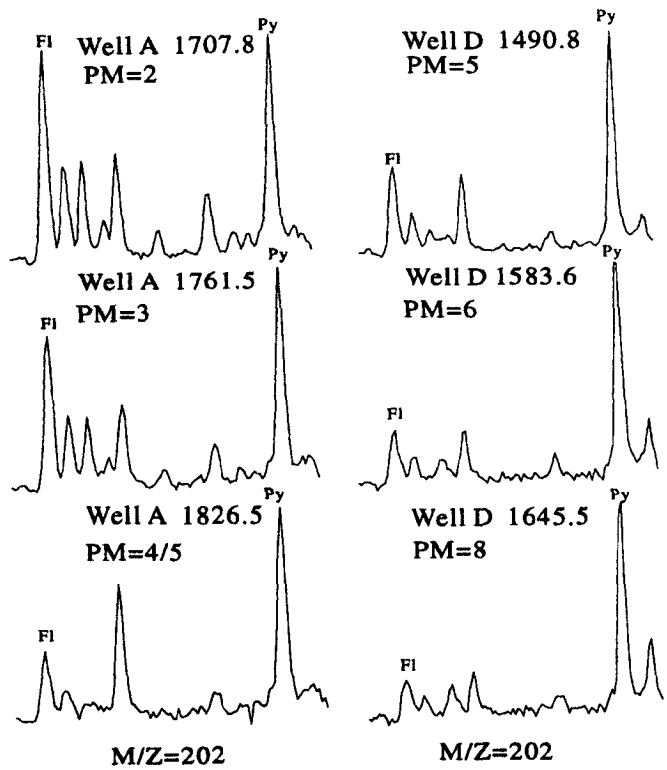

Fig. 5-18. Representative mass chromatograms at m/z=202 for fluoranthene (Fl) and pyrene (Py).

5.5 Aromatic steroid hydrocarbons

The distribution of aromatic steroid hydrocarbons provides a good maturity assessment tool (Riolo *et al.*, 1986). There are two widely used parameters. One is the ratio of short side-chain triaromatic steroid hydrocarbons to long side-chain components [$C_{21}/(C_{21}+C_{28})$], which increase with increasing maturity (Mackenzie *et al.*, 1981). The other is the steroid hydrocarbon aromatization parameter [TA/(TA+MA)] (TA is total triaromatic steroid hydrocarbons and MA is total monoaromatic steroid hydrocarbons), which based upon the decrease in monoaromatic relative to triaromatic steroid hydrocarbons with increasing maturity. Biodegradation has little effect on aromatic steroid hydrocarbons (Connan, 1984; Peters and Moldowan, 1993). However, in severely biodegraded oils, the C_{20}-C_{22} compounds appeared to have been depleted (Wardroper *et al.*, 1984; Lin *et al.*, 1989; Cassani and Eglinton, 1991).

Series of C-ring monoaromatic steroid hydrocarbons (C_{21}, C_{22}, $C_{27\text{-}29}$) (Fig. 5-20) and triaromatic steroid hydrocarbons (C_{20}, C_{21}, $C_{26\text{-}28}$) (Fig. 5-21) were recognized in the aromatic hydrocarbon fraction of the Lengdong oils. As previously discussed the concentration of aromatic steroid hydrocarbons shows an increasing trend with increasing degree of biodegradation. The aromatization parameter [TA/(TA + MA)]

varies little in these two studied columns indicating a narrow maturity span for this case sample suite. However, subtle but systematic variations still can be observed from these two columns. In the Es3 column slightly higher values occur at the top of the column suggests a more mature late oil charge in the top of the Es3 column (Fig. 5-22a). It slight decrease towards the bottom occurs in the Es1 column and may be a biodegradation influence although monoaromatic steroid hydrocarbons appear to be more resistant to biodegradation than the triaromatic steroid hydrocarbons (Fig. 5-22b). The monoaromatic steroid aromatization parameter is unaffected by heavy biodegradation as observed in this case study, which can be used to determine the maturity of biodegraded oils and seep oils prior to alteration (Moldowan, *et al.*, 1992).

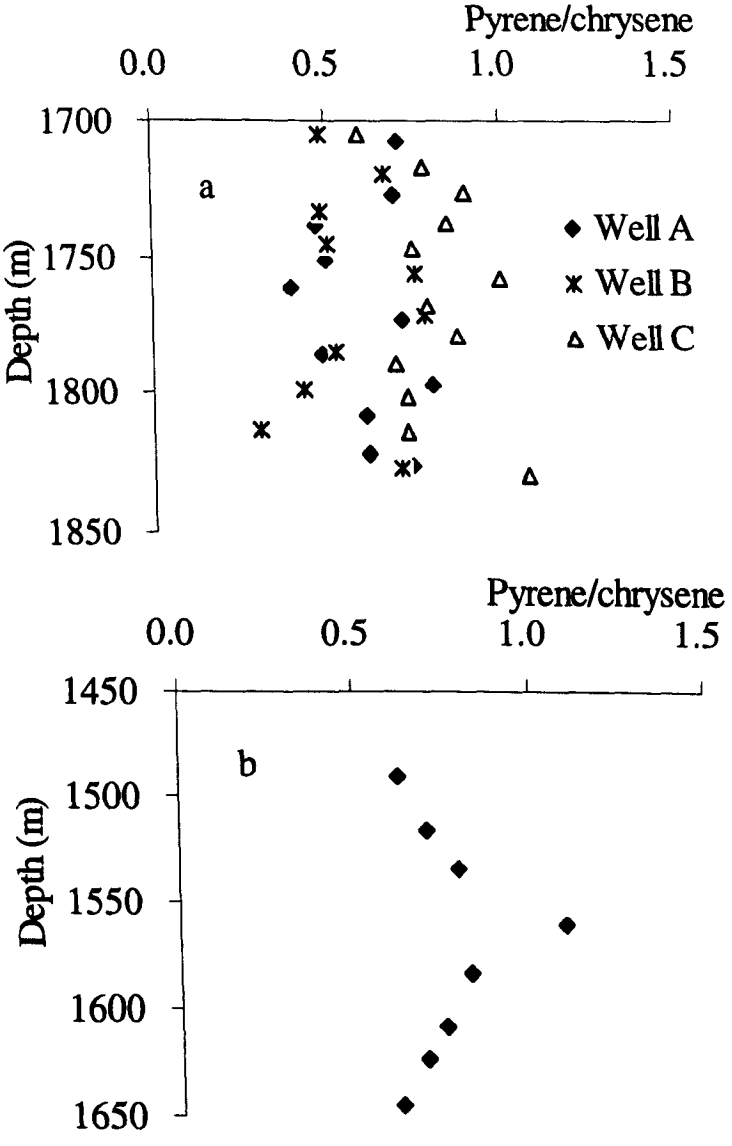

Fig. 5-19. Pyrene/chrysene ratio variations in the Es3 (a) and Es1 (b) columns.

The preferential degradation of the C_{26} homologues compared with the higher homologues in the Lengdong sample set seems quite clear in the Es3 column which $C_{26}S/C_{28}S$ show systematical decrease trend. While in the Es1 this ratio is slightly

higher than that in the Es3 column but did not show much variation throughout the column (Fig. 5-23).

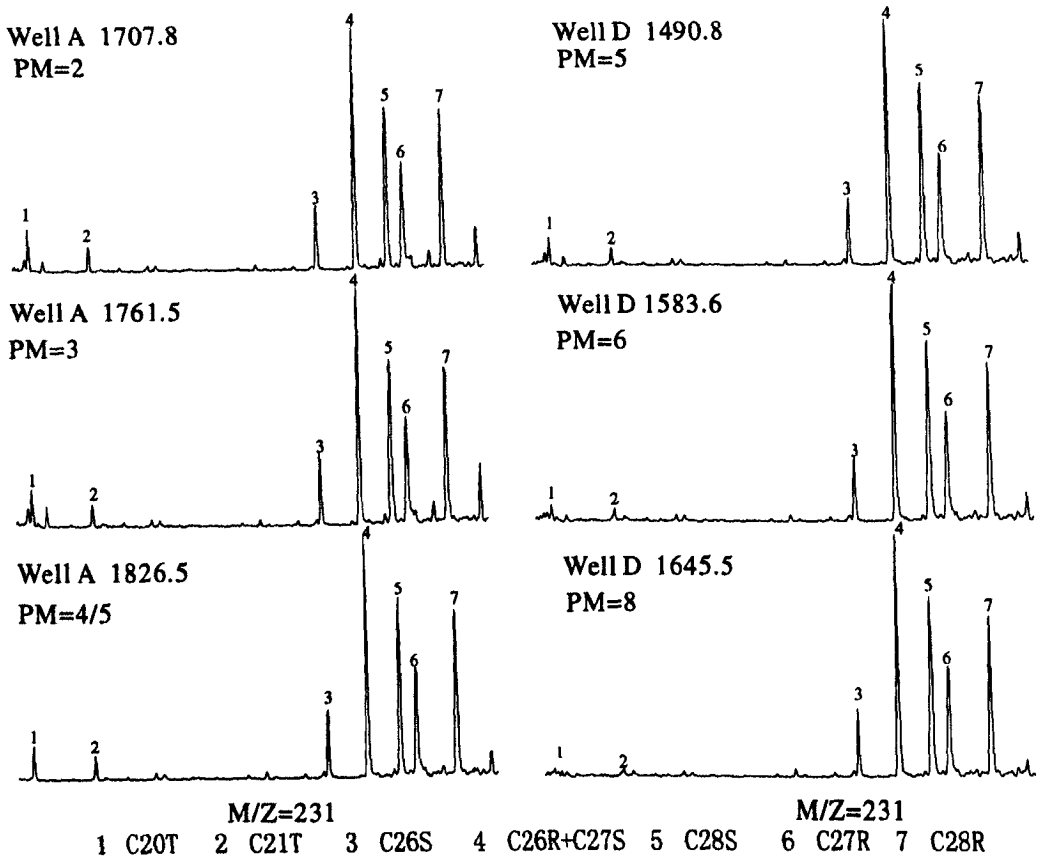

Fig. 5-20. Representative mass chromatograms of triaromatic steroid hydrocarbons at m/z 231 in the Es3 and Es1 columns.

Biodegradation seems to result in the preferential removal of the short side-chained triaromatic steroid hydrocarbons compared to the long-chained counterparts (Wardroper *et al.*, 1984; Lin *et al.*, 1989; Cassani and Eglinton, 1991), whereas the short side-chained C_{21}-C_{22} pregnanes become more enriched with increasing biodegradation compared to long side-chained regular steranes (Brooks *et al.*, 1988). Monoaromatic steroid hydrocarbons appear to be more resistant to biodegradation than the triaromatic steroid hydrocarbons (Lin *et al.*, 1989). However, the effect of biodegradation on the C_{21}, C_{22}-MAS has not been reported. Whether it is similar to the effect on the triaromatic steroid hydrocarbons or the steranes will provide further insight into biodegradation mechanisms and processes.

Consistent with previous studies, there is an increase in the ratio of the $C_{21\text{-}22}$-pregnanes to $C_{27\text{-}29}$-steranes and a decrease in the ratio of $C_{20\text{-}21}$-triaromatic steroid hydrocarbons to $C_{26\text{-}28}$ triaromatic steroid hydrocarbons with increasing degree of biodegradation in the Es1 column. However, there is no obvious trend for the ratio of $C_{21\text{-}22}$-monoaromatic steroid hydrocarbons to $C_{27\text{-}29}$ monoaromatic steroid

hydrocarbons between PM levels 5 to 8 (i.e. over the biodegradation range of the Es1 column) (Fig. 5-24). This suggests that monoaromatic steroid hydrocarbons do have a high resistance biodegradation and that their behavior during biodegradation is different from both the triaromatic steroid hydrocarbons and the regular steranes.

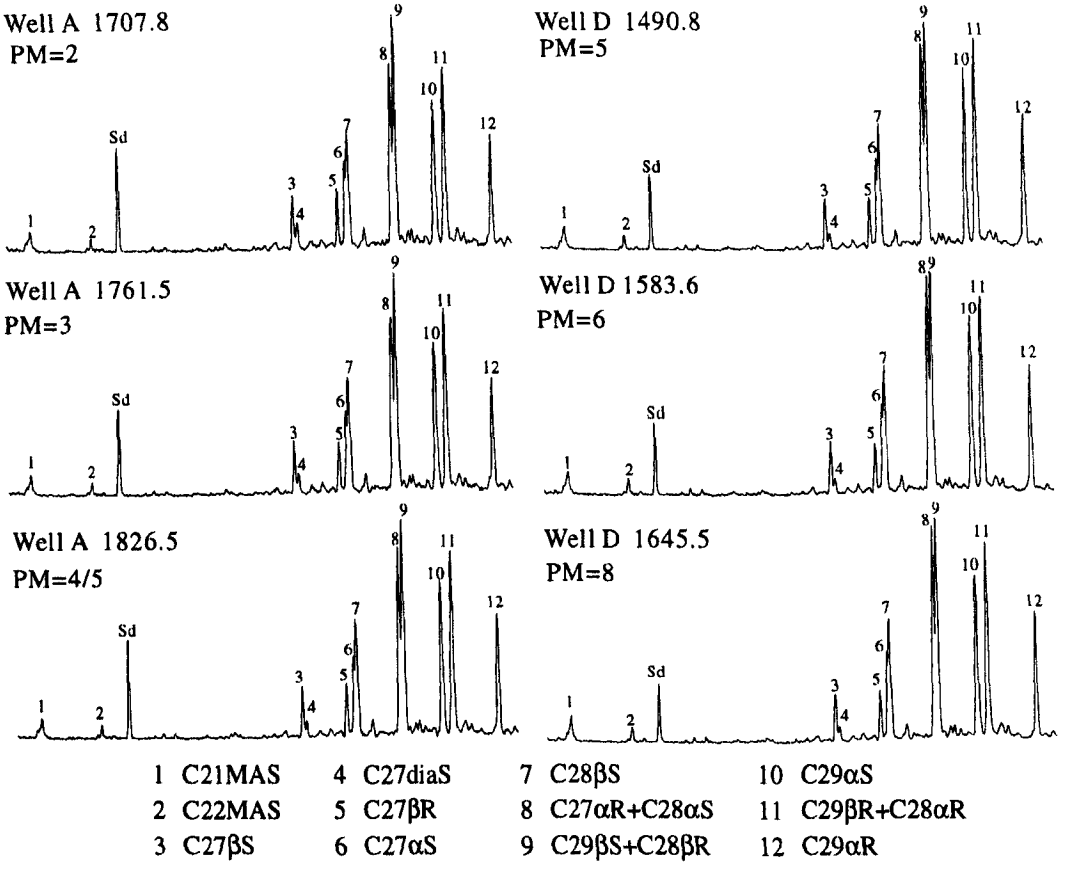

Fig. 5-21. Representative mass chromatograms of monoaromatic steroid hydrocarbons at m/z 253 in the Es3 and Es1 columns. sd: 1,1'-binaphthyl standard.

5.6 Alkyldibenzothiophenes

Numerous organosulfur compounds are present in petroleum, making sulfur the third most abundant element in a typical crude oil, after carbon and hydrogen. The organosulfur compounds comprise thiols, sulfides, and thiophene moieties. Among the most commonly found sulfur heterocycles are thiophenes. These may have alkyl side chains or may be condensed with one or more benzene ring(s) to form benzothiophenes, dibenzothiophenes, naphthothiophenes or benzonaphthothiophenes. Most studies of organosulfur compounds have focused on those compounds found in the aromatic fraction of petroleum, namely, the benzothiophenes and dibenzothiophenes.

The origin and thermal stability of aromatic sulfur compounds has attracted much research in the last two decades. In particular, benzothiophenes and dibenzothiophenes have been found especially useful because they are common in a

variety of both oils and source rocks and their distribution are sensitive to thermal stress. In low maturity oils and source rocks the abundance of benzothiophenes is often found to be greater than that of their dibenzothiophene counterparts and the relative distributions of benzothiophenes and dibenzothiophenes have thus been employed as maturation parameters (Ho *et al.*, 1974; Radke and Willsch, 1994; Santamaria *et al.*, 1998). Furthermore, the thermal stability of alkylated dibenzothiophenes varies with the position of substitution, and maturity parameters based on the isomer ratios MDR (4-MDBT/1-MDBT) and EDR (4,6-DMDBT/4-EDBT) have been used as maturity indicators for both oils and source rocks in a number of studies (Chakhmakhchev *et al.*, 1997; Santamaria *et al.*, 1998).

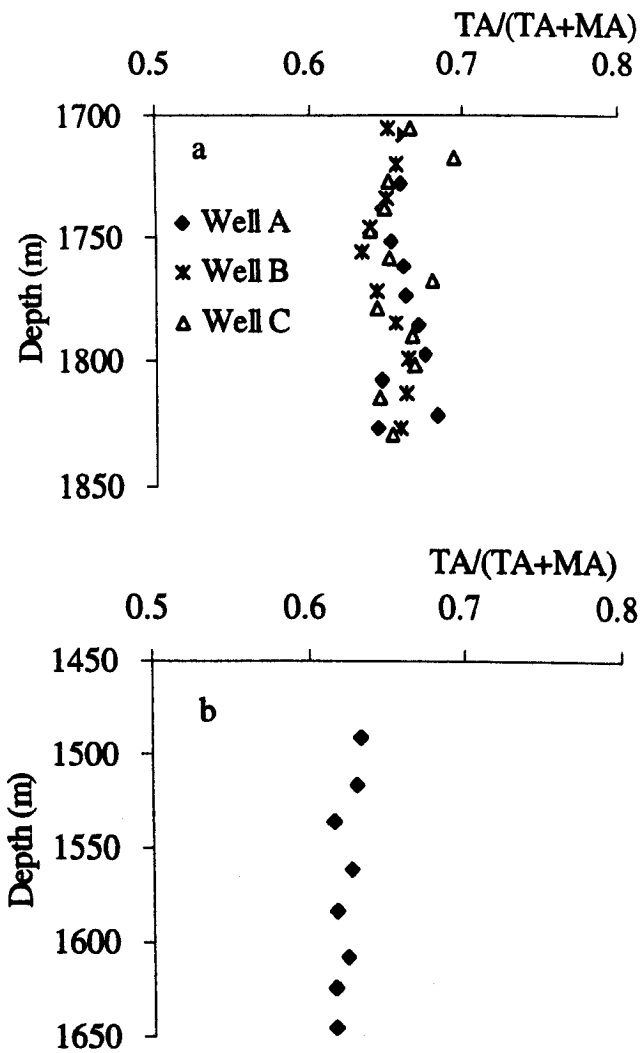

Fig. 5-22. Aromatization parameter [TA/(TA + MA)] profile. a: Es3 column; b: Es1 column.

Huang and Pearson (1999) suggested that paleoenvironment is another important control for thiophene concentrations and distribution in crude oils. Lowest methyldibenzothiophene ratios (MDR) are found in high sulfur oils of hypersaline derivation, whilst high wax oils of freshwater derivation tend to have very high ratios.

Wang and Fingas (1995) proposed that relative distributions of C_1-DBTs in various samples could be used for oil source identification and biodegradation studies. Petrochemists are interested in aromatic sulfur compounds since they want to develop a process for biodesulfurization of fossil fuels (Bressler *et al.*, 1997; Setti *et al.*, 1999), while environmental scientists are more concerned about bioremediation processes for organosulfur compounds in petroleum or creosote contaminated environments. Most aromatic sulfur compound biodegradation studies have been carried out in laboratory cultures (Kropp *et al.* 1997) and in contaminated environments (Hostettler and Kvenvolden 1994). Bahrami *et al.* (2001) studied anaerobic microbial biodegradation of dibenzothiophene by thermophilic bacteria obtained from crude oil. Some work has been done on aromatic sulfur compound biodegradation in petroleum reservoirs (Fedorak and Westlake, 1984).

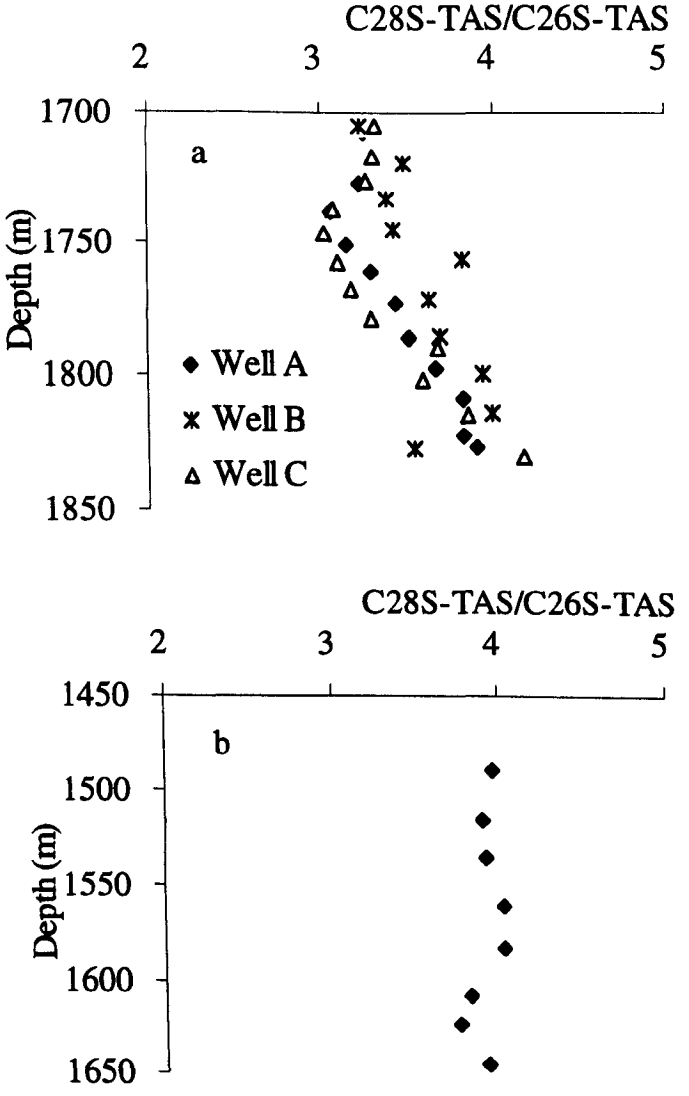

Fig. 5-23. Ratio of C_{28}S-TAS/C_{26}S-TAS in the Es3 (a) and Es1 (b) columns.

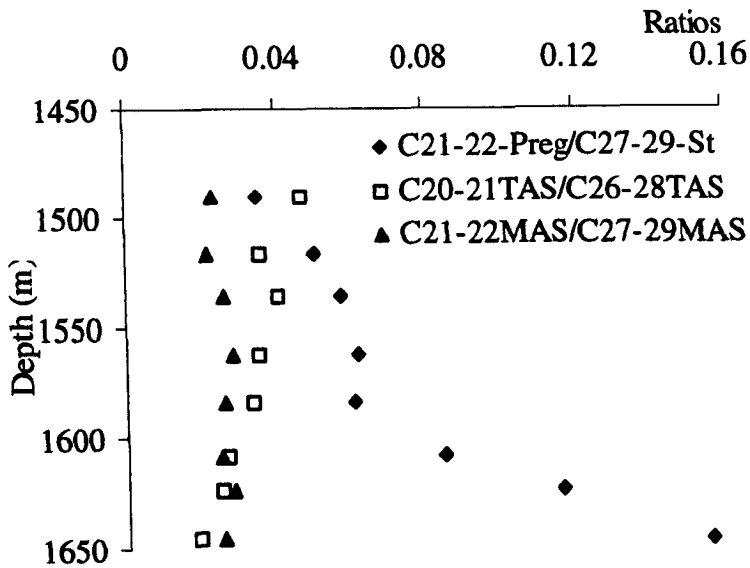

Fig. 5-24. Ratio profile of short chain steranes, MAS and TAS compared with their long chain counterparts in the Es1 column.

The sulfur-bearing aromatics, especially dibenzothiophenes, are depleted in reservoired oils by water washing (Lafargue and Barker, 1988), a feature that led to Palmer (1993) using the benzothiophene distributions as an indicator of water washing. Palmer (1993) noted that the relative amount of *n*-paraffins was not significantly depleted in the oil/water transition zone, while benzothiophene and C_1-dibenzothiophenes were; therefore it seems that the oils had been water washed and only slightly biodegraded. The alkyldibenzothiophenes were also enriched with C_2 and C_3 homologues by water washing (Palmer, 1984).

Palmer (1993) commented that the heterocompounds such as alkyldibenzothiophenes are generally believed to be resistant to mild biodegradation, however, Lin *et al.* (1989) observed that benzothiophenes as well as other aromatic compounds are readily removed as a result of in-reservoir biodegradation. The preferential degradation of the sulfur-containing aromatics relative to the aromatics and alkanes in biodegraded oil samples analyzed by Philp *et al.* (1988) suggested an anaerobic degradation pathway as the process was related back to sulfur-decomposing (anaerobic) bacteria. However decomposition of sulfur-containing compounds (by aerobic bacteria) observed in some outcrops implies that an aerobic degradation pathway cannot be ruled out. Kropp and Fedorak (1998) reviewed the biodegradation of benzothiophene, alkylbenzothiophenes, DBT, alkylDBTs, and naphthothiophenes with a focus on the identification of metabolites detected in laboratory cultures.

5.6.1 Degree of alkylation

It is generally accepted that biodegradation of alkyl-substituted polycyclic

aromatic hydrocarbons strongly depends on the number of the substituents. The more substituents the aromatic compound has, the less degraded it will be at any degradation level (Volkmans *et al.*, 1984; Philp *et al.*, 1988; Peters and Moldowan, 1993). Fedorak and Westlake (1984) showed that the susceptibility of DBTs in Prudhoe Bay crude oil to biodegradation decreased with increasing alkyl substitution. This is normally true in most of the present study samples, but some exceptions do exist in the alkylnaphthalenes and alkylphenanthrenes as described before (section 5.2 and 5.3). The relative percentage of alkyldibenzothiophenes at different biodegradation levels is shown in Fig. 5-25. C_3-DBTs show a continuous increase in relative concentration with increasing degree of biodegradation since they are highly alkylated. All DBT, C_1-DBTs and C_2-DBTs decrease in relative concentration with advancing biodegradation. The relative percentage of DBT is low in all study samples but it did not show a great decrease with increasing degree of biodegradation. However, the decrease of MDBTs seems more significant and suggests that it is more susceptible to biodegradation than DBT.

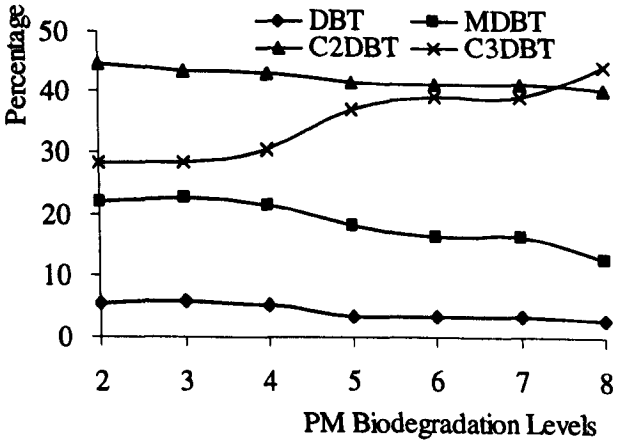

Fig. 5-25. Relative percentage of alkyldibenzothiophenes at different biodegradation levels.

The degradation of PAH compounds is generally initiated by dihydroxylation of one of the polynuclear aromatic rings, this being followed by cleavage of the dihydroxylated ring (Sabate *et al.*, 1999; Vila *et al.*, 2001; Dean-Ross *et al.*, 2002). Lu *et al.* (1999) isolated strain TZS-7 from crude oil which could degrade dibenzothiophene and 4,6-DMDBT and they found that 4,6-DMDBT was degraded through a ring-destructive pathway by resting cells of strain TZS-7. However, the current study demonstrates that demethylation - similar to that seen in the microbial demethylation of extended hopanes to form 25-norhopanes (Peters *et al.*, 1996) - may also be an important step in aromatic hydrocarbon biodegradation. Although demethylation has been proposed as one of the mechanisms for the formation of the lower alkylhomologues, no specific positional preference has been identified. As

discussed in the previous sections (section 5.2 and 5.3) that the DMNs can be partially derived by cleavage of a methyl group from TMNs and the ratio of phenanthrene to the methylphenanthrenes increase with increasing degree of biodegradation, the faster decrease of MDBTs compared to DBT may also be due to microbial demethylation although the situation is complicated by the possibility of the simultaneous biodegradation of parent compound and alkylated compounds. Although there is no direct evidence that demethylation is occurring, it may explain the observed trends. Further work is clearly called for.

5.6.2 Methyldibenzothiophenes

Representative distributions of MDBTs and C_2-DBTs are shown in Fig. 5-26. The MDBT ratio used to be a good maturity indicator based upon the principle that 4-methyldibenzothiophene is more stable than the 1-methyl isomer (MDR= 4-MDBT/1-MDBT, Radke, 1988). As biodegradation proceeded, not only did the absolute concentrations of C_1-dibenzothiophenes decrease, but the three isomers of methyldibenzothiophenes showed great alteration in their relative proportions with increasing degree of biodegradation. MDR from the Lengdong sample set are shown in Fig. 5-27. In the Es3 column the MDR shows a 'S' type variation. At the upper part of the column higher MDR values are probably due to late charged more mature fluid as most other biomarker indicators implied and the decline trend in the lower part of the column is caused by biodegradation. The decrease of MDR suggests that 1-MDBT is slightly more resistant to biodegradation than 4-MDBT. A weak decreasing trend in the Es1 column further confirms the slightly more vulnerable nature of the 4-MDBT.

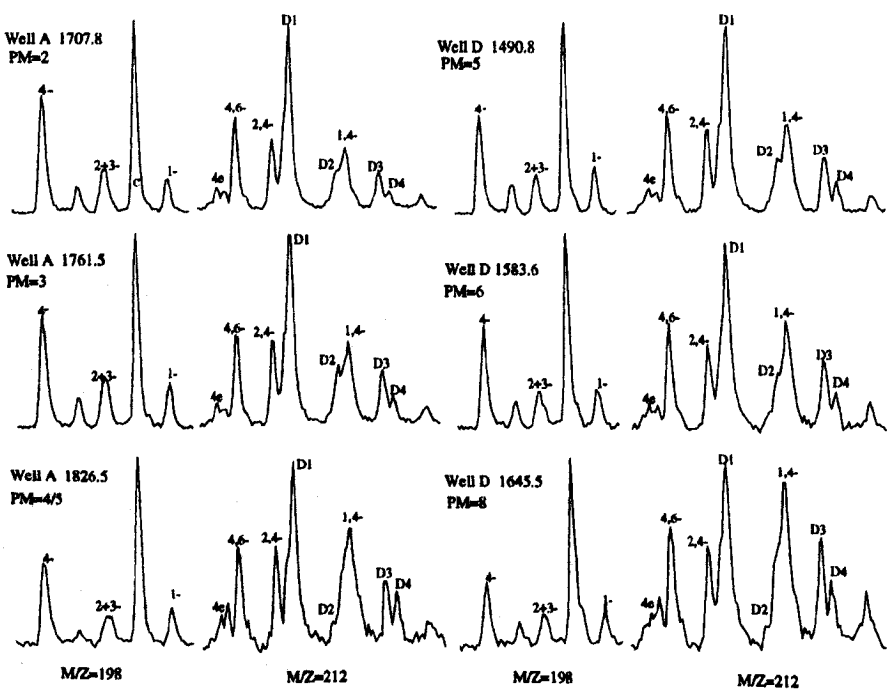

Fig. 5-26. Representative distribution of MDBTs and C_2-DBTs in studied columns.

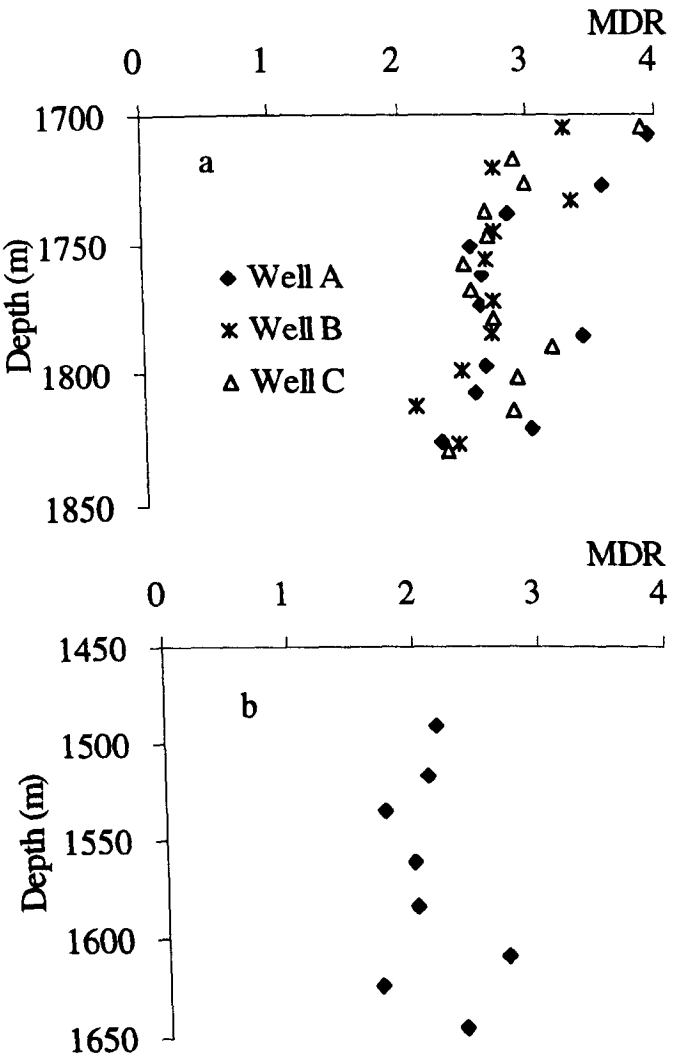

Fig. 5-27. MDR (4-MDBT/1-MDBT) ratios variation in the Es3 (a) and Es1 (b) columns.

For the ratios of 4-MDBT/ (2- + 3-MDBT) in the Es3 column different trend can be observed with slightly increase in the lower part of the column (Fig. 5-28). This is consistent with observations by Wang and Fingas (1995) that 2- and 3-methyl-DBT were more easily degraded than 1- and 4-methyl-DBT. In the Es1 column this trend is not very clear since two samples near the bottom show decrease trend. The order of biodegradation susceptibility of methyldibenzothiophene isomers is (from most susceptible to least susceptible):

2-+3-MDBT > 4-MDBT > 1-MDBT

5.6.3 C_2-dibenzothiophenes

No reservoir petroleum biodegradation study for C_2-DBT has been reported. Theoretically, the relative recalcitrance of the symmetric DMDBTs should reflect that previously reported for the MDBTs. 2,8-DMDBT bears the methyl groups on both benzene rings at the same position to the thiophene ring as in 2-MDBT. 4,6-DMDBT

bears the methyl groups on both benzene rings at the same position to the thiophene ring as in 4-MDBT. The ease biodegradation of 3,4-DMDBT is because it has an unsubstituted benzene ring that is preferentially attacked by aromatic hydrocarbon-degrading bacteria. The lab work carried out by Kropp *et al.* (1997) with pure and mixed cultures suggested that the susceptibility of the isomers of DMDBTs to bacterial degradation was dependent upon the positions of the methyl groups. 4,6-DMDBT is only slight lost in petroleum-degrading mixed cultures. A Pseudomonas spp. was able to oxidize and cleave a methyl-substituted ring of 2,8-DMDBT, while the 3,4- isomer was oxidized by all three aromatic hydrocarbon-degrading Pseudomonas spp. Thus, the order of susceptibility of these three isomers to degradation appear to be: 3,4-DMDBT > 2,8-DMDBT > 4,6-DMDBT.

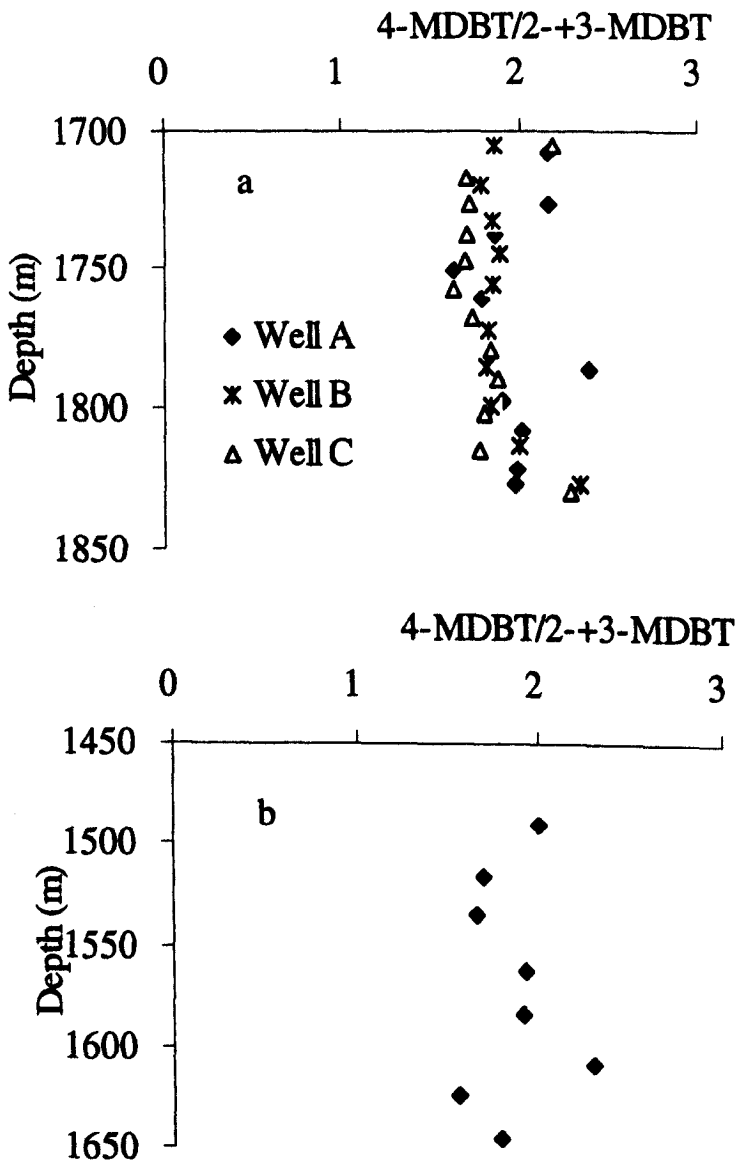

Fig. 5-28. Ratios of 4-MDBT/2-+3-MDBT variation in the Es3 (a) and Es1 (b) columns.

The relative percentage of C_2-DBTs at different biodegradation levels from the Lengdong sample set is shown in Fig. 5-29. Since some of the isomers are still unknown, they were simply labeled as DMDBT1, 2 and 3. DMDBT1 is the most abundant component and its relative concentration shows a continuous decline with increasing degree of biodegradation. 2,4-DMDBT that bears the methyl groups on one ring also shows a decrease with increasing biodegradation level, however, 1,4-DMDBT shows a increasing trend even though only one ring was substituted. 4,6-DMDBT does not increase in its relative concentration as one might expect.

The susceptibility of C_2-dimethyldibenzothiophenes to biodegradation appears to be of the order: DMDBT1 > 2,4-DMDBT > 4,6-DMDBT > 4-EDBT > DMDBT2, DMDBT3, DMDBT4 > 1,4-DMDBT.

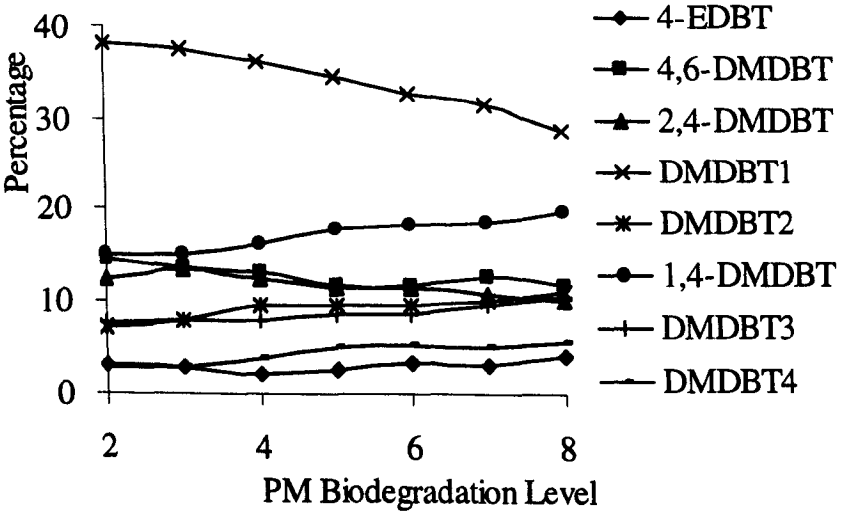

Fig. 5-29. Relative distribution of C_2-DBT at different biodegradation levels.

5.7 Implication of biodegradation effects on PAHs

A variety of PAH maturity parameters are widely used to assess the thermal maturation of source rock bitumens and oils. Each parameter is based on the same principle, namely the increase in abundance of thermodynamically more-stable isomers relative to less-stable ones with increasing maturity. However, biodegradation can have a significant impact on the validity of these aromatic hydrocarbon maturity parameters, this being determined by the susceptibility of individual components in each parameter to microbial attack. Interestingly, this study shows that the thermally most-stable isomers in the studied PAHs are more susceptible to biodegradation than thermally less-stable ones, suggesting that biodegradation and selective depletion is not controlled by thermodynamics but is related to the stereochemical structure of individual compounds.

Our previous work in this field study area indicates that oil maturity lies within a very narrow range although subtle differences do exist (e.g., slightly more mature oil at the top of the Es3 column), attributed to variation in the burial depth/average temperature of the source rock from which the oils were expelled (Huang *et al.*, 2003, 2004). Eight commonly used maturity parameters based on the distributions of trimethylnaphthalene isomers (TNR, TNR2, Radke, 1987; TMNr, van Aarssen *et al.*, 1999), tetramethylnaphthalene and pentamethylnaphthalene isomers (TeMNr, PMNr, van Aarssen *et al.*, 1999), methylphenanthrene isomers (MPI1, Radke and Welte, 1983), and mono- and tri-aromatic steroid hydrocarbons (C_{20+21}/C_{28}S-TAS, TA/(TA+MA), Mackenzie *et al.*, 1981) show distinct variations with increasing degree of biodegradation (Fig. 5-30). Some parameters containing both the most- and the least- susceptible components, such as TNR, TeMNr and MPI1, show dramatic decreases in values with increasing degree of biodegradation, while parameters involving similarly susceptible components, such as TNR2 and PMNr, show less variation. Biodegradation can therefore have a significant effect on the validity of aromatic hydrocarbon maturity parameters. For many of the parameters, the effect of biodegradation is most notable after PM level 4, although for the TNR parameter values begin to decrease from PM level 2. The ratio of short side-chained tri-aromatic steroid hydrocarbons to long side-chained components (C_{20+21}/C_{28}S) begins to decrease at PM level 6, while the mono-aromatic steroid aromatization parameter [TA/(TA + MA)] does not exhibit any variation, even at PM level 8, and therefore provides a valid maturity assessment for oils in the study area.

It is possible that the susceptibility of the different PAHs to biodegradation depends not only on stereochemistry and thermodynamic considerations but also on, for example, oil composition, nutrient availability, redox conditions and species composition of the microbial population. The results of our study of the Lengdong oils may not, therefore, be directly transferable to biodegraded oils from other reservoirs and fields – and they are probably not reflected in aerobic microbial degradation situations such as oil seeps and surface spills. However, present study suggests that maturity assessments of in-reservoir biodegraded oils using PAH-based maturity parameters should be made with caution and should include consideration of the relative susceptibilities of the parameter components, especially where the oils are moderately to severely biodegraded. The situation obviously becomes more complex in reservoirs containing a mixture of biodegraded and undegraded oils.

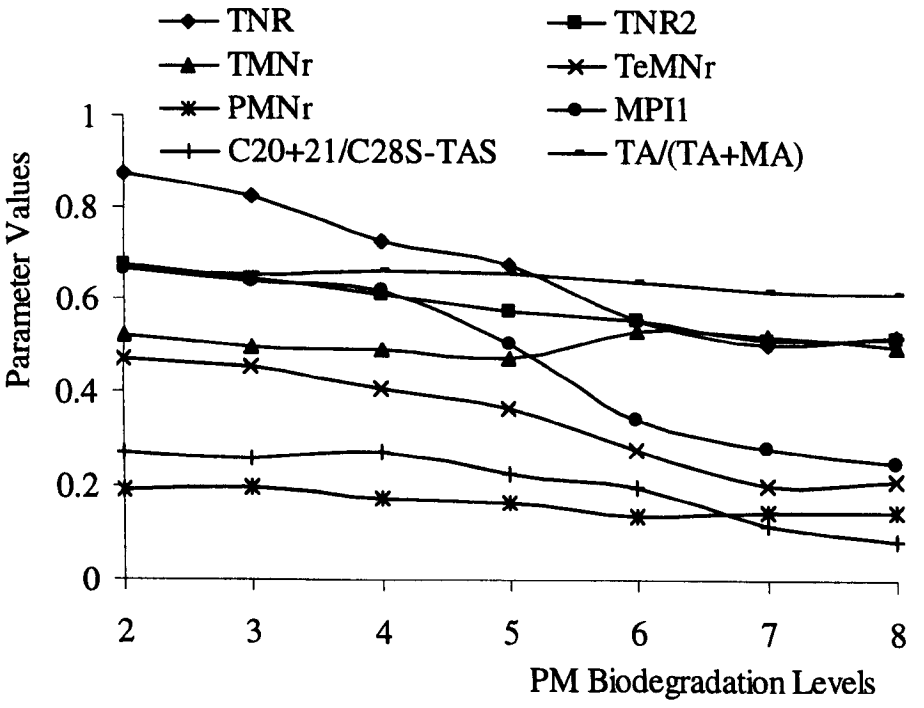

Fig. 5-30. Variation in values obtained for some commonly used PAH maturity parameters with degree of biodegradation.

6 BIODEGRADATION EFFECTS ON NON-HYDROCARBONS

Although polar compounds (NSO compounds) are often a large fraction of oils, geochemists have mainly collected data relevant to saturated and aromatic hydrocarbon compounds. The molecular parameters defined by using the analytical data of these two hydrocarbon fractions can supply important indications about origin and maturity of oils, but NSO compounds can probably be an important complementary source of information.

Recent developments in the characterization of heteroatomic (N and O containing) compounds in petroleum have introduced the possibility that geochemical parameters may be used to estimate petroleum migration distances and the relative volumes of interacting petroleum and water in a petroleum system (Larter and Aplin, 1995). The role of secondary petroleum migration in controlling the composition of petroleum has received increasing attention through both field and laboratory-based studies. The principle has been used by several authors in attempts to monitor migration range and to assess the volumes of oil transported during secondary migration. The application of polar oxygen and nitrogen containing petroleum compounds to the modelling of natural fluid flow may prove possible because these compounds may interact with formation water and rock surfaces (either mineral or organic matter), thereby constantly modifying their distribution and/or concentration within a petroleum as it interacts with increasing volumes of water and mineral surfaces during secondary migration (Taylor *et al.*, 1997).

Biodegradation of NSO compounds also attracted geochemists for a long time especially for environmental concerns. Atlas (1981) provided some early general observations about the ability of microbes to metabolize compound groups typically associated with petroleum. He indicated that heteroaromatic NSO compounds with a small number of rings may be biodegradable, as may monoaromatic compounds and PAHs with two to four rings. Mueller *et al.* (1989) provided an overview of biodegradation for a similar range of compounds, with reference to environmental contamination by creosote. They cited several laboratory studies where biodegradation of PAHs, heteroaromatic and phenolic compounds has been demonstrated and where specific strains of microbes able to utilize these compounds have been isolated from environmental samples. However, they pointed out that of these three groups, much less is known about biodegradation processes for the heteroaromatic carbazoles. Dyreborg *et al.* (1997) demonstrated biodegradation of

nitrogen-, sulfur- and oxygen-heteroaromatics under a variety of redox conditions. Johansen *et al.* (1997) demonstrated biodegradation for the range of compounds (phenols and aromatic hydrocarbons) that were present in creosote-contaminated groundwater under nitrate-reducing conditions. Here some detailed observations on biodegradation effects on alkylcarbazoles, benzocarbazoles and alkyphenols in reservoir condition are presented.

6.1 Carbazole compounds

The nitrogenous compounds found in crude oils fall into two classes - the 'nonbasic' molecules include pyrroles and indoles, but are predominantly mixed alkyl derivatives of carbazole, while the 'basic' molecules are largely derivatives of pyridine and quinoline. The total nitrogen content of crude oils averages around 0.3%, of which the nonbasic compounds comprise approximately 70-75% (Wilhelms *et al.*, 1992; Benedik *et al.*, 1998; Merdrignac *et al.*, 1998). Some basic structures of carbazole compounds are shown in Figure 6-1. Among the alkylated carbazoles, the shielded isomers (where the alkyl groups are directly adjacent to the N-H functional group) have been found to be enriched in crude oils whereas the non-shielded isomers are more abundant in residual source rock bitumens. It has been proposed that the isomeric abundances of C_1- and C_2-alkylcarbazoles are controlled by interactions between the functional group and mineral surfaces during primary migration (Li *et al.*, 1995). Larter *et al.* (1996a) suggested that in source-related oils the concentrations and the ratios between two benzocarbazole isomers, benzo[a] and benzo[c]carbazole, may be used as an indicator of oil secondary migration distance, with the benzo[a] isomer being removed preferentially (by sorption on to mineral and organic surfaces) during migration. Such approaches have been confirmed by laboratory and field studies (Larter *et al.*, 2000; Terken and Frewin, 2000).

The influence of thermal maturation must also be considered as a factor in determining carbazole distributions (Larter *et al.*, 2000). Clegg *et al.* (1998a) provided convincing evidence of source maturity control on alkylcarbazole and benzocarbazole concentrations and distributions in petroleums from the Sonda de Campeche area, Gulf of Mexico and Harrison *et al.* (1997) showed similar observations for coals. Similarly, Li *et al.* (1997) demonstrated this for the Duvernay Formation of the Western Canada Basin. Bennett *et al.* (2002) reported that the benzocarbazole concentrations in source rocks from the North Sea clastic petroleum system increase up to ca. 0.85% VRE (vitrinite reflectance equivalent) and then decrease at higher maturity levels, although the benzocarbazole [a]/([a]+[c]) ratio did not show a good maturity-related variation. The current view suggests that carbazole and

benzocarbazole ratios cannot be considered as exclusive indicators of migration, and that other factors (e.g. facies, maturity) may also contribute to the changes in carbazole and benzocarbazole distributions observed in migrated oils. In circumstances where facies and maturity effects are minimal due to geological conditions, then spectacular migration-related fractionation of benzocarbazoles has been observed (Terken and Frewin, 2000).

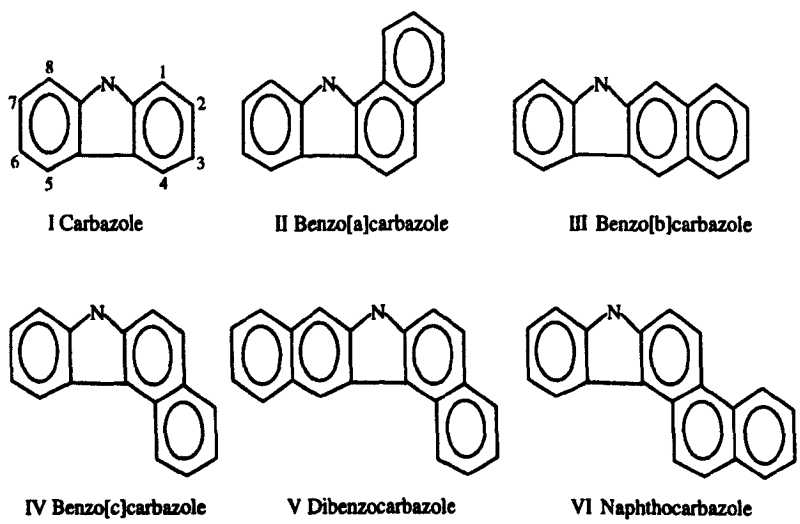

Fig. 6-1 Basic structure of carbazole, benzocarbazole and naphthocarbazole.

While previous studies have focused on migration and maturity issues, carbazoles are also known to be altered during biodegradation (Atlas, 1981; Fedorak and Westlake, 1984; Zhang *et al.*, 1999). However, carbazole distributions have not been investigated within the geological framework of a single biodegraded oil column which might allow further insight into the processes controlling their occurrence. The effects of in-reservoir biodegradation on the occurrence of carbazoles and benzocarbazoles in reservoir core extracts from the Lengdong oil field have been investigated. The intention was to assess the extent of biodegradation within the oil columns and to relate this to the abundance and distribution of carbazole compounds in the reservoir petroleums. It is important that the effects of biodegradation are recognized so that carbazole data can be interpreted accurately for other geochemical applications.

6.1.1 Concentrations and relative abundance of carbazole compound groups

The concentrations of carbazole compounds varying in the study columns are clearly related with degree of biodegradation as indicated by both aliphatic and aromatic hydrocarbons. Previous study by Zhang *et al.* (1998) observed a continuous decrease in alkylcarbazole concentrations with increasing degree of biodegradation in

a set of biodegraded oils from the same area. In the Es1 column, alkylcarbazole concentrations (total amount of carbazole, methylcarbazoles, dimethylcarbazoles, trimethylcarbazoles i.e., C_0-C_3 alkylcarbazoles) show a linear trend of depletion from 99 μg/g EOM at the top of column to 23 μg/g EOM at the bottom of the column (Fig. 6-2a).

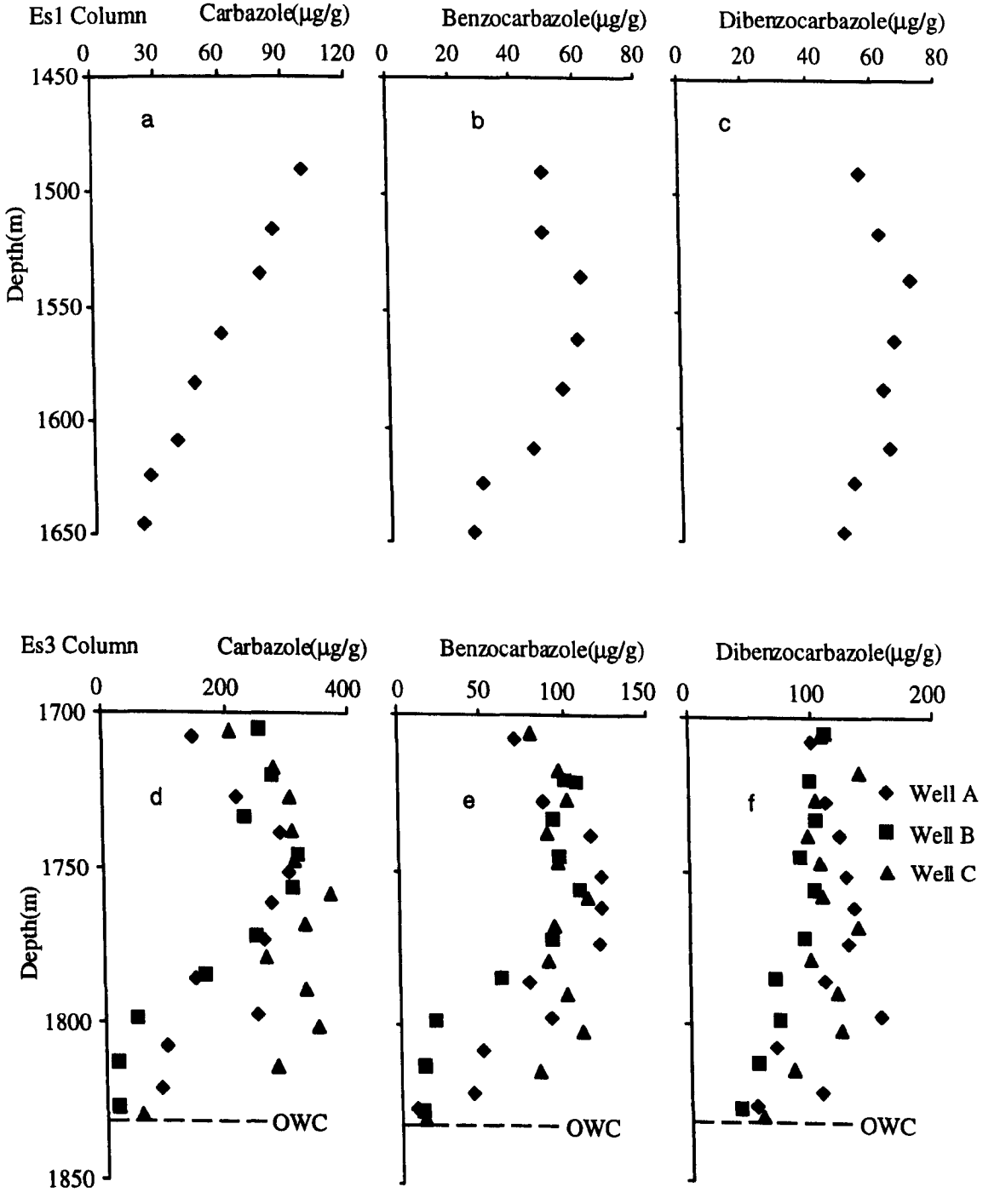

Fig. 6-2. Variation in the concentrations of C_0-C_3 alkylcarbazoles, C_0-C_1 alkylbenzocarbazoles and dibenzocarbazoles or naphthocarbazoles with depth in the Es1 and the Es3 oil columns.

Alkylated benzocarbazole concentrations (total amount of benzocarbazole and methylbenzocarbazoles i.e., C_0-C_1 alkylbenzocarbazoles) show similar changes, with

values decreasing from 62 μg/g EOM to 27 μg/g EOM (Fig. 6-2b). Dibenzocarbazoles or naphthocarbazoles (m/z 267) concentrations show a slight decrease from 72 to 50 μg/g EOM with increasing depth (Fig. 6-2c), suggesting that these compounds may be more resistant to microbial attack.

In the Es3 columns, the C_0-C_3 alkylcarbazole concentrations firstly increase from approximately 200 μg/g EOM at 1700m in the least degraded oil to 350 μg/g EOM at 1750m and then decrease sharply to around 50 μg/g EOM below 1800m (Fig. 6-2d). The C_0-C_1 alkylbenzocarbazole concentrations show similar but less dramatic changes, firstly increasing from approximately 90 μg/g EOM at the top of the oil columns to 110 μg/g EOM at the middle of the columns and then decreasing sharply to around 20 μg/g EOM near the bottom of the columns (Fig. 6-2e). These changes are comparable with the variation in bulk composition and may reflect an intrinsic connection. The observation of a slight increase in alkylated carbazoles and benzocarbazoles concentrations in the upper part of the columns may be due to the fact that significant carbazole and benzocarbazole degradation has not yet begun in these samples and their relative enrichment is the result of depletion of other components (e.g., hydrocarbons). Their sharp decrease in abundance in the lower part of the columns may be the result of biodegradation. Dibenzocarbazoles or naphthocarbazoles show less drastic variations in the Es3 columns, with concentrations decreasing from 100 μg/g EOM to 50 μg/g EOM with increasing column depth (Fig. 6-2f).

In all of these profiles it is important to consider that degradation is unlikely to be proceeding to different degrees throughout the oil column; the observed trends most probably reflect biodegradation at the base of the oil column and mixing of the resulting disturbed column by diffusion and advection related to charging (Larter *et al.*, 2003).

The relative abundance of the carbazole compound groups in the extracted oils also shows systematic variations. In the Es1 column, the proportion of C_0-C_3 alkylcarbazoles decreases linearly from 57% to 28%; the C_0-C_1 alkylbenzocarbazoles firstly increase and then decrease towards oil water contact, while the dibenzocarbazoles or naphthocarbazoles show little variation in the upper part of the oil column and then steadily increase in the lower part. In the Es3 columns, the least degraded samples at the top of the oil column are characterized by a predominance of alkylcarbazoles relative to the C_0-C_1 alkylbenzocarbazoles and dibenzocarbazoles or naphthocarbazoles. With increasing depth, the relative proportions of alkylcarbazoles, benzocarbazoles and dibenzocarbazoles or naphthocarbazoles remain constant in the

upper part of the columns and then show dramatic changes in the lower part, with decreases in the alkylcarbazoles and C_0-C_1 alkylbenzocarbazoles concentrations and an increase in the dibenzocarbazoles or naphthocarbazoles.

6.1.2 Relative abundance of the alkylcarbazole homologue groups

Within the C_0-C_3 alkylcarbazoles, the relative proportion of carbazole and methylcarbazoles in the Es1 column is very low and little variation is observed through the column, with mean values around 5% of the total C_0-C_3 alkylcarbazoles (Fig. 6-3a). The predominant alkylcarbazoles are the trimethylcarbazole isomers; interestingly, they decrease slightly in relative abundance from 70% in the upper part of the column to 65% toward the bottom of the column while the relative abundance of dimethylcarbazoles increases from 25% to 30% (Fig. 6-3b,c). The concentrations of all compounds decrease towards the base of the oil column, however, suggesting that all compounds are being degraded to some extent.

In the Es3 oil columns, biodegradation has resulted in a significant reduction in total carbazole abundance and in the preferential depletion of C_0 and C_1 alkylated compounds at the base of the oil column. As found for the Es1 oil column, the alkylcarbazoles are dominated by the trimethylcarbazoles, while the relative abundance of the C_0 and C_1 alkylcarbazoles is low, with average values of 10%, and no significant variation is observed throughout most of the three columns. The obvious decreases in abundance occur in the lower part of the Es3 columns, below 1800m (Fig. 6-3d-f). Dimethylcarbazole isomer distributions show some scatter, especially in the lower part of the columns, and there is no clear relationship between dimethylcarbazole abundance and the degree of biodegradation (< level 5). However, when Zhang *et al.* (1998) compared the relative proportion of carbazole and methylcarbazoles with dimethylcarbazoles, they noted that the dimethylcarbazoles have a higher resistance to biodegradation than the less alkylated homologues. The trimethylcarbazoles are more abundant than the other alkylcarbazoles and concentrations increase slightly towards the bottom of the columns.

6.1.3 Methylcarbazole isomer distributions

In common with most aromatic hydrocarbons, the positions of alkyl groups on an alkylcarbazole molecule have a significant effect on its biodegradation behaviour. 1-methylcarbazole is the predominant component in most crude oils and source rocks (Li *et al.* 1997; Clegg *et al.*, 1998a, 1998b; Horsfield *et al.*, 1998). Representative mass chromatograms of the methylcarbazoles (MCs) and dimethylcarbazoles (DMCs) in samples at different columns are shown in Fig. 6-4; a marked variation can be

observed in samples at different biodegradation levels. Methylcarbazoles deplete faster than dimethylcarbazoles, meanwhile their distributions show great variations. There is a decrease in the proportion of 1-methylcarbazole (1-MC) with increasing degree of biodegradation from level 2 to level 6, suggesting that 1-MC, the partially shielded isomer, is more susceptible to microbial attack than the other three methylcarbazole isomers.

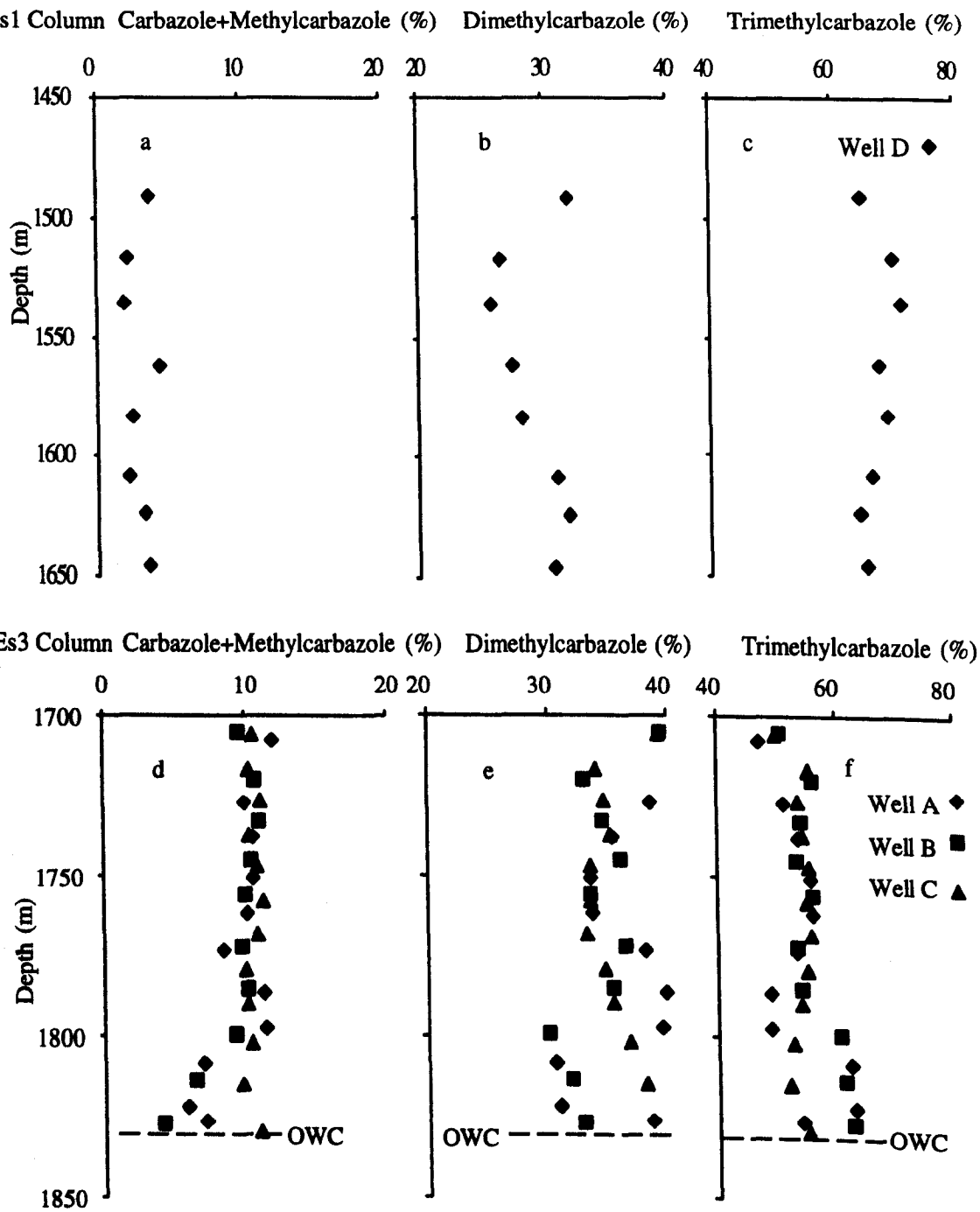

Fig. 6-3. Relative abundance of C_0+C_1-alkylcarbazoles, C_2-alkylcarbazoles and C_3-alkylcarbazoles as a percentage of the summed total of these compound classes in the Es1 and the Es3 columns.

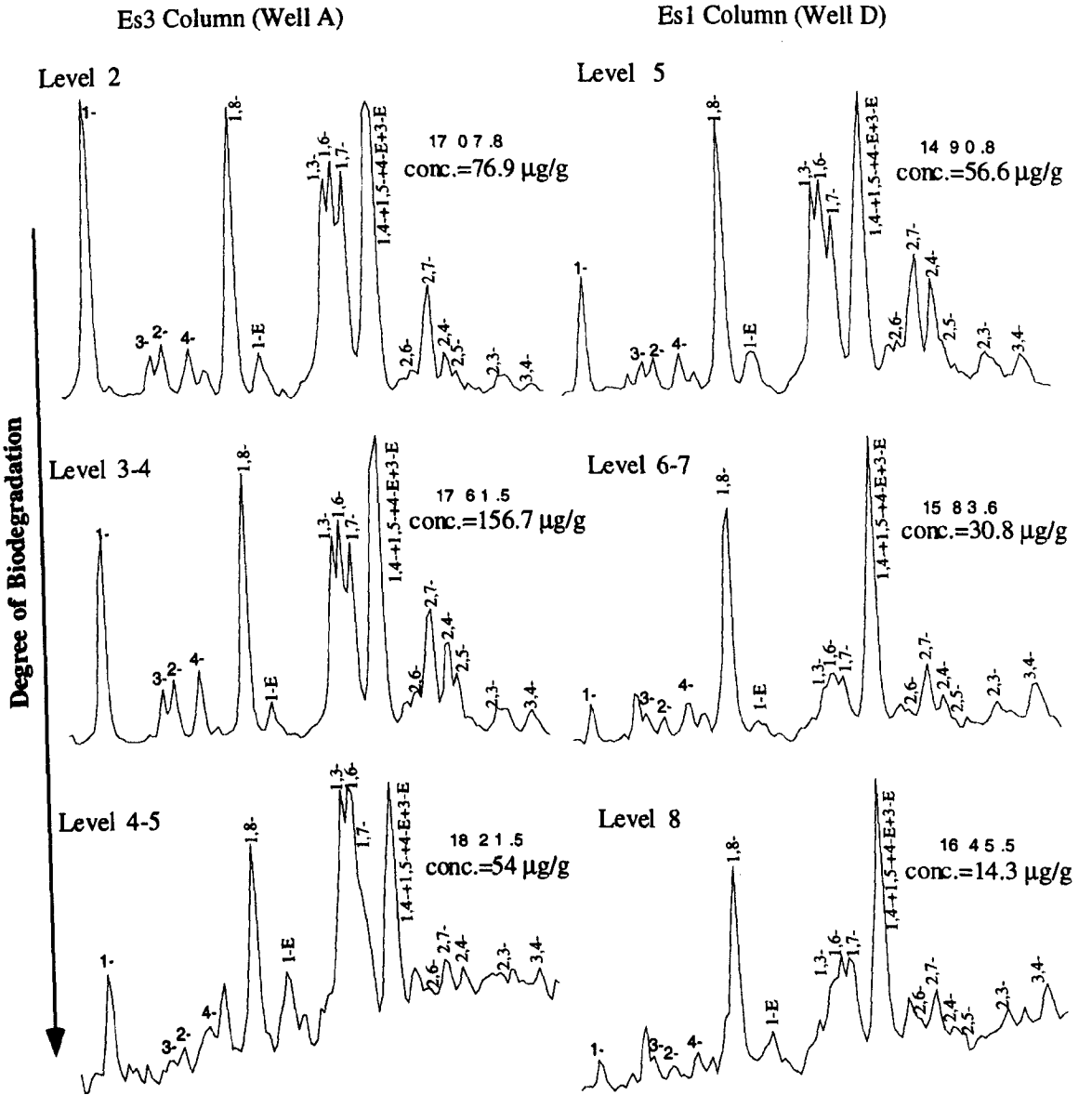

Fig. 6-4. Mass chromatograms of m/z 181 and 195 (carbazole fraction) showing the variation in methylcarbazole and dimethylcarbazole isomer distribution with increasing level of biodegradation in samples from Es3 and Es1 oil columns. Individual isomers are labeled. 'Level' refers to Peters and Moldowan level of biodegradation (see text). Conc.: concentration of total isomers identified.

If biodegradation is the primary control on the distribution of carbazoles in the oil column, then a negative correlation would be expected between the relative abundance of the 1-methylcarbazole to 4-methylcarbazole and the degree of biodegradation. A comparison of aliphatic hydrocarbon 'biodegradation responsive ratios' and methylcarbazole ratios indicates that the 1-MC/4-MC ratio does show a general decrease with biodegradation. Fig. 6-5 shows the correlation between the ratios 1-MC/4-MC and $C_{30}\alpha\beta$Hop/(Pr+Ph) in the Es3 columns (Fig. 6-5a) and between the ratios 1-MC/4-MC and $C_{29}\alpha\beta$-25-Norhop/$C_{30}\alpha\beta$Hop in the Es1 columns (Fig. 6-5b). Zhang *et al.* (1998) noticed in moderate to heavily biodegraded oil samples that the 1-MC/4-MC ratios decreased from 1.54-1.93 to 0.85-0.95 with

increasing degree of biodegradation. This data suggests that among the methylcarbazoles, the 1-MC isomer is the most susceptible to biodegradation. For certain oil suites, therefore, the relative abundance of partially shielded and non-shielded alkylcarbazole isomers may be useful in refining the degree of petroleum biodegradation within the Peters and Moldowan range 2 to 6.

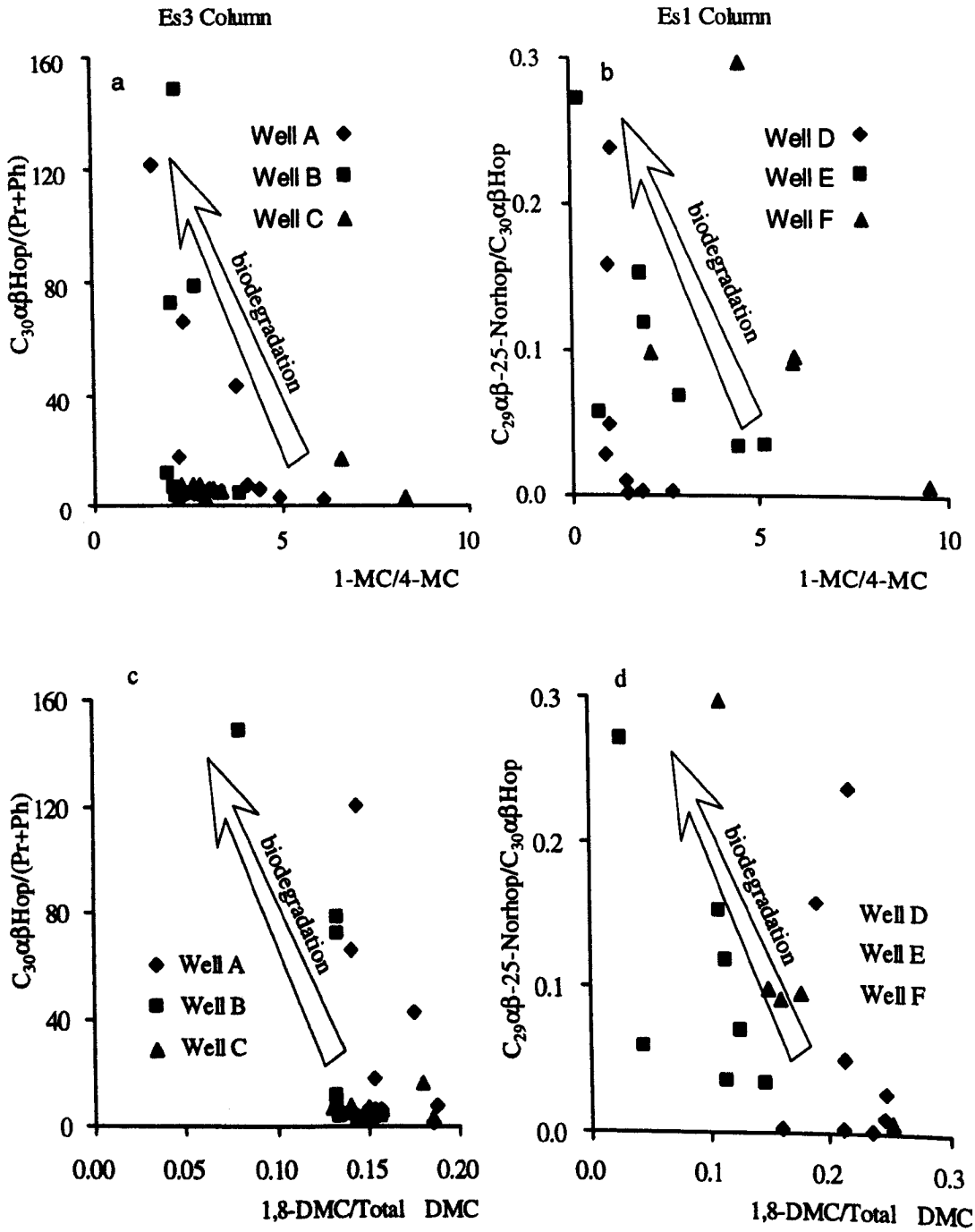

Fig. 6-5. Relationship between carbazole isomer abundance and biodegradation indicators. (a) 1-MC/4-MC vs $C_{30}\alpha\beta$Hop/(Pr+Ph) in the Es3 columns; (b) 1-MC/4-MC vs $C_{29}\alpha\beta$-25-Norhop/$C_{30}\alpha\beta$Hop in the Es1 column; (c) 1,8-DMC/Total DMC vs $C_{30}\alpha\beta$Hop/(Pr+Ph) in the Es3 columns; and (d) 1,8-DMC/Total DMC vs $C_{29}\alpha\beta$-25-Norhop/$C_{30}\alpha\beta$Hop in the Es1 columns. (For abbreviations see text). Arrow indicates increasing degree of biodegradation.

6.1.4 Dimethylcarbazole distributions

The dimethylcarbazoles can be classed into three isomeric groups. The shielded isomers have two methyl groups, at the 1- and 8- positions; partially shielded isomers have one of the alkyl groups present at the 1- position; and exposed isomers have no substitution at the 1-position (Fig. 6-4, see Fig. 6-1 for structures).

In the Es3 oil column, the shielded isomer (1,8-dimethylcarbazole (1,8-DMC)) shows a relative decrease in abundance with increasing degree of biodegradation (Fig. 6-5c), especially in the lower part of the columns, suggesting that it is more susceptible to biodegradation than other isomers. In this moderately biodegraded column the 1,3-DMC, 1,6-DMC and 1,7-DMC (i.e., partially shielded isomers) show a relative increase with increasing degree of biodegradation (Fig. 6-4). However, this observation for the dimethylcarbazoles is subject to some uncertainty.

In the Es1 sample set, the relative abundance of 1,8-DMC shows more scatter along the profile. Samples from Wells E and F show a decrease in the relative proportion of 1,8-DMC with increasing degree of biodegradation. In Well D there is no obvious trend and in some heavily biodegraded samples 1,8-DMC remains higher than the other dimethylcarbazoles (Fig. 6-4 and 6-5d), suggesting that biodegradation may affect the dimethylcarbazole distribution in different ways. Zhang *et al.* (1998) suggested that partially shield dimethylcarbazoles are more susceptible to biodegradation than both shielded and exposed counterparts. However, as we are looking at a dynamic system with continuous mixing and transport of compounds, care should be exercised in interpreting sequences of events. The Bacchus unpublished data from other areas show that in some cases 1,8-DMC is removed preferentially as a result of biodegradation while in other cases 1,8-DMC remains relatively constant. Although clear conclusions as to the relative susceptibility of the various dimethycarbazole isomers to biodegradation cannot be drawn from this data, nitrogen shielded isomers generally do not appear to be enriched during biodegradation as one may have expected.

6.1.5 Benzocarbazole distributions

Benzocarbazole has three isomers i.e., benzo[a]carbazole, benzo[b]carbazole and benzo[c]carbazole. Benzo[a]carbazole and benzo[c]carbazole are usually the main isomers in crude oils and source rocks. It has been proposed that benzocarbazole concentrations in migrated crude oil change as a function of migration distance, and that the (benzo[a]carbazole/benzo[a]carbazole+benzo[c]carbazole) ratio (BC ratio) can be used as a migration distance index (Larter *et al.*, 1996a). In a case history from

Oman, Terken and Frewin (2000) showed that for an essentially iso-mature oil suite, large reductions in the BC ratio were due to migration effects. Molecular dynamics calculations (van Duin and Larter, 1998) indicate a greater preference for the benzo[a] isomer to partition into the water-phase prior to solid phase sorption compared with the benzo[c] isomer, which may explain the observed changes in benzo[a]carbazole/benzo[c]carbazole ratios observed in migrating petroleum (Larter *et al.*, 1996a). Other studies have indicated that the BC ratio increases with increasing oil maturity in some (but not all) petroleum systems (Clegg, 1998a, 1998b; Li *et al.*, 1997; Larter *et al.*, 2000; Bennett *et al.*, 2002).

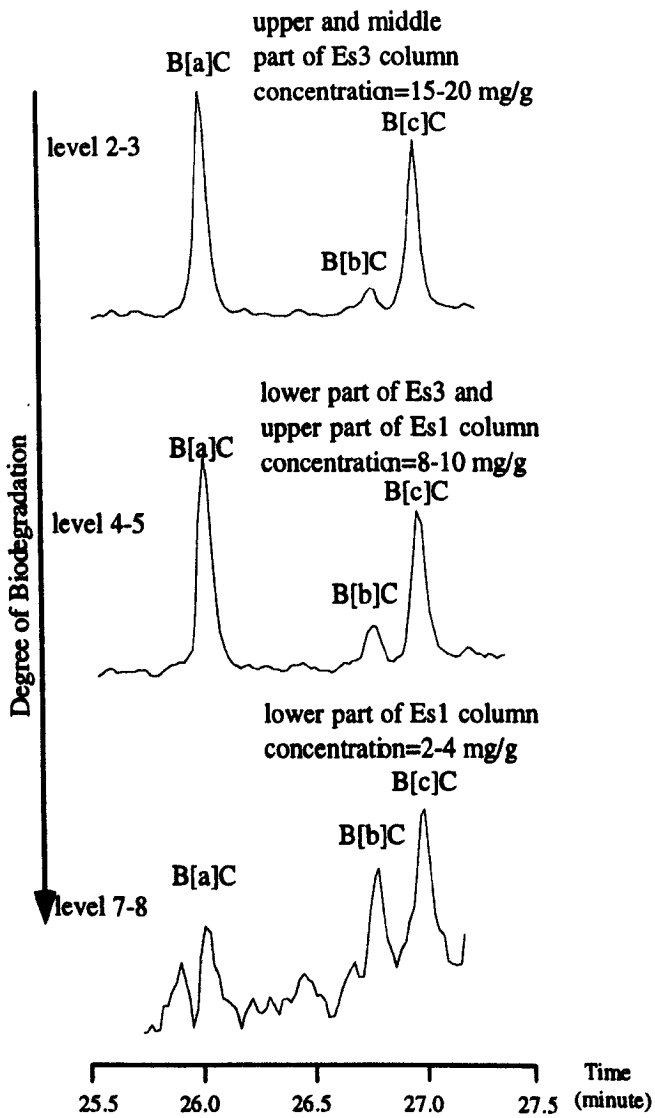

Fig. 6-6. Mass chromatograms of m/z 217 (carbazole fraction) showing the response of the benzocarbazole isomer distribution to increasing biodegradation in samples from the Es3 and Es1 oil columns. 'Level' refers to Peters and Moldowan scale of biodegradation (see text).

Representative distributions of the benzocarbazoles in residual oil samples at different levels of biodegradation in the Es3 and Es1 oil columns are shown in Fig. 6-

6. At the top of the Es3 column, benzo[b]carbazole occurs in relatively minor abundance compared to benzo[a]carbazole and benzo[c]carbazole. There is an obvious increase in the relative abundance of benzo[b]carbazole with increasing level of biodegradation, strongly suggesting that the benzo[b] isomer has a higher resistance to biodegradation than the other two isomers. There is a progressive decrease in abundance of benzo[a]carbazole with depth such that in severely biodegraded samples benzo[b]carbazole and benzo[c]carbazole are the main isomers in the oil.

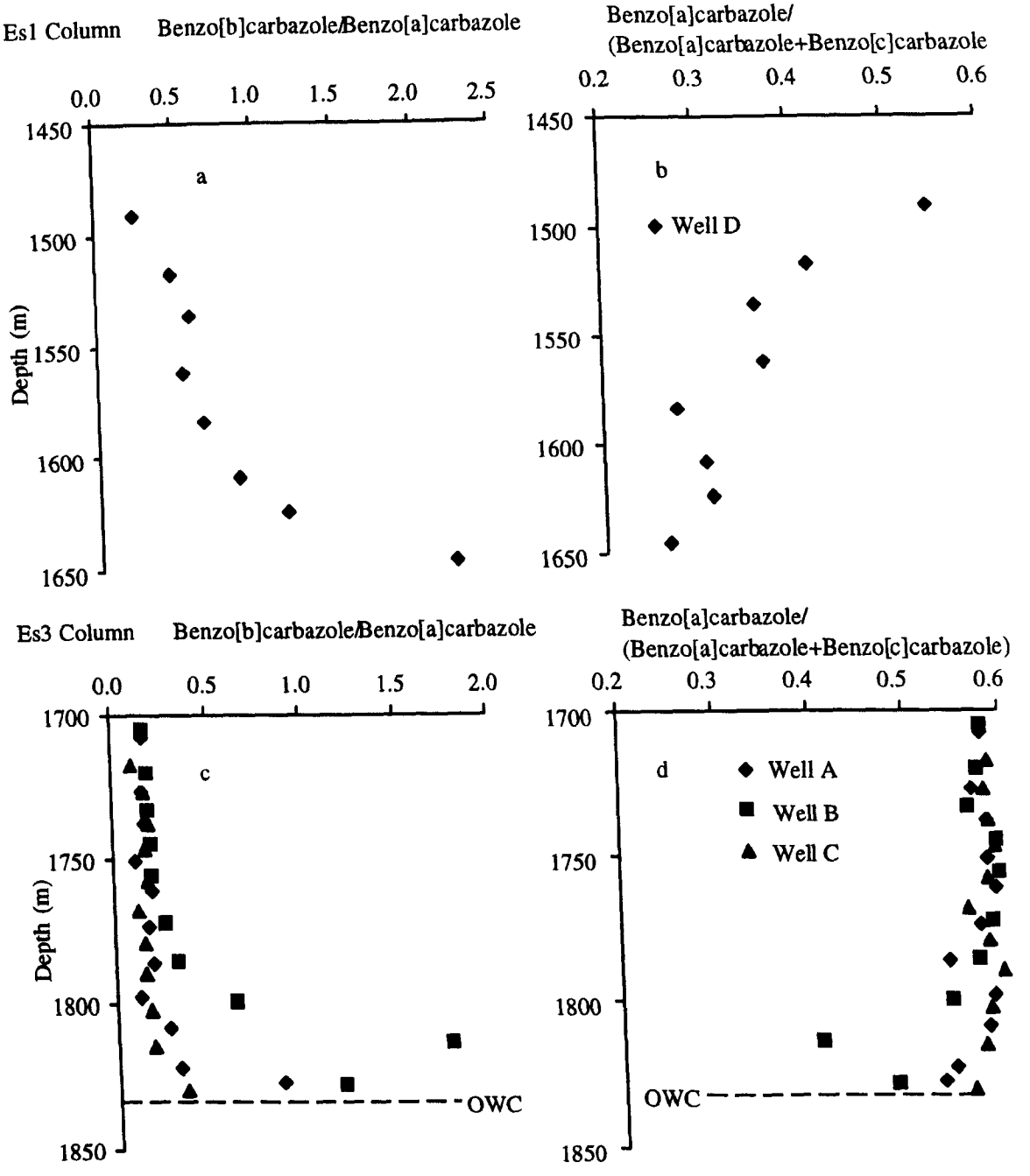

Fig. 6-7. Variation in the ratios benzo[b]carbazole/benzo[a]carbazole and benzo[a]carbazole /(benzo[a]carbazole + benzo[c]carbazole) (BC ratio) with depth in samples from the Es1 and Es3 oil columns.

A notable feature of the Lengdong reservoir extracts is the trend for BC ratios to decrease with increasing degree of biodegradation (Fig. 6-7). The order of susceptibility to biodegradation for benzocarbazole is benzo[a]carbazole > benzo[c]carbazole > benzo[b]carbazole. The ratio benzo[b]carbazole /benzo[a]carbazole may therefore be a sensitive indicator of biodegradation at levels of biodegradation above level 4. An inverse linear relationship between the ratio $C_{30}\alpha\beta$Hopane/(Pr+Ph) and the ratio benzo[b]carbazole/benzo[a]carbazole in the Es3 columns (Fig. 6-8a) and between the ratio $C_{29}\alpha\beta$-25-Norhopane/$C_{30}\alpha\beta$Hopane and benzo[b]carbazole/benzo[a]carbazole in the Es1 columns (Fig. 6-8b) was observed, again suggesting that benzocarbazole ratios may be useful in detecting differential effects of biodegradation at advanced levels of biodegradation.

Biodegradation of the benzocarbazoles seems to occur before the steranes and at advanced biodegradation levels (> PM level 4), concomitant with isoprenoid degradation. Although Oldenburg *et al.* (1999) have reported relatively high abundances of benzo[b]carbazole in some oils from the Haltenbanken area, offshore mid-Norway, suggested to be sourced by the coal-rich Åre Formation, the uniform benzocarbazole distributions dominated by benzo[a] and benzo[c] isomers in less biodegraded Liaohe oils suggest that here, the increase in the relative concentration of the benzo[b] isomer is related to the effects of biodegradation rather than any source rock depositional environment factor.

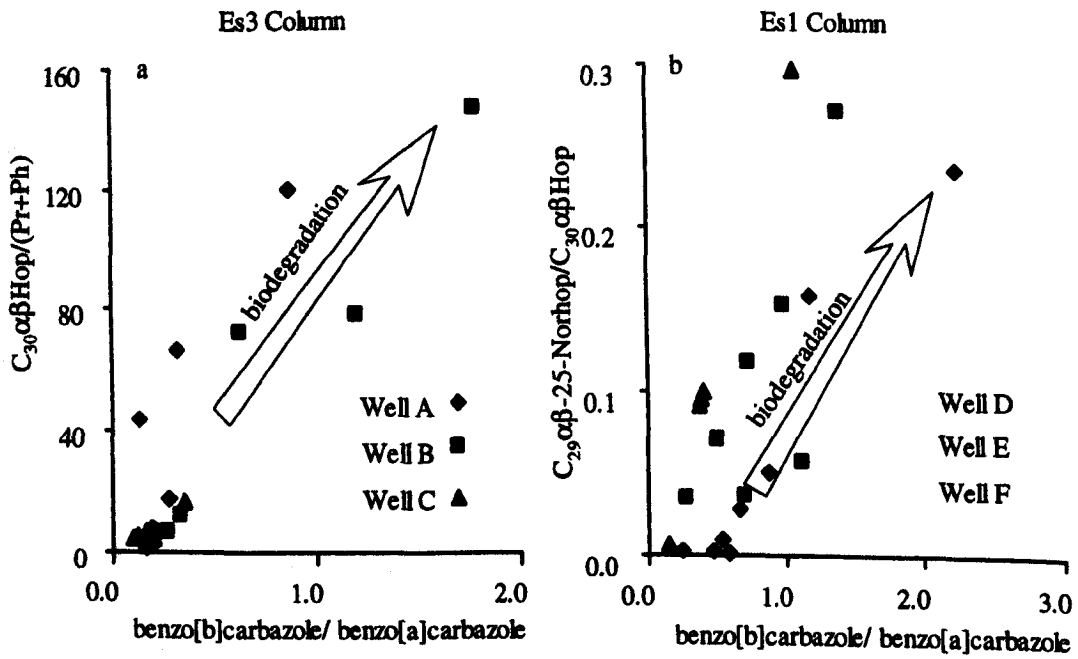

Fig. 6-8. The relationship between (a) the ratios benzo[b]carbazole /benzo[a]carbazole and $C_{30}\alpha\beta$Hop/(Pr+Ph) (biodegradation parameter) in the Es3 columns and (b) the ratios benzo[b]carbazole/ benzo[a]carbazole and $C_{29}\alpha\beta$-25-Norhop/$C_{30}\alpha\beta$Hop (biodegradation parameter) in the Es1 columns.

6.1.6 Pathways of carbazole biodegradation

Relatively little work has been done on the mechanisms of carbazole compound biodegradation and most of it has been carried out under aerobic conditions. Carbazole biodegradation studies have been based largely on metabolite identification and comparison of products with other aromatic compound biodegradation pathways. It appears that under aerobic conditions there are three different modes of initial oxidation: (i) a naphthalene-like attack, in which one of the aromatic rings is oxidized to a dihydrodiol; (ii) an angular dioxygenase attack, in which the carbon bonded to the nitrogen and the adjacent carbon in the aromatic ring are both oxidized; and (iii) a five-membered ring attack, in which the nitrogen atom is directly oxidized (Bressler and Fedorak, 2000).

Some details are known; for example, in an angular dioxygenase attack, the initial enzymatic degradation of carbazoles is considered to give a dihydroxylated intermediate which is spontaneously converted to 2'-aminobiphenyl-2,3-diol (an unstable intermediate). These intermediates then follow either a *meta-* or an *ortho-* pathway (named according to the location of the initial ring cleavage), leading to intermediates which enter the central metabolic pathways such as the TCA cycle (Benedik *et al.*, 1998). The extradiol dioxygenase attacks the hydroxylated ring at the *meta* position to form 2-hydroxy-6-oxo-6-(2'-aminophenyl)hexa-2,4-dienoic acid. Hydrolysis of the *meta*-cleavage compound yields 2-hydroxy-4-pentenoate and anthranilic acids, which are further converted to tryptophan or catechol. Catechol is metabolized through the β–ketoadipate pathway (Ouchiyama *et al.* 1993).

Carbazole biodegradation in deep petroleum reservoirs is more complicated than that observable in controlled experiments in the laboratory. Clearly, in a deep (ca. 2 km) reservoir anaerobic processes will be dominant and thus it can be inferred from the observed degradation of carbazoles and related compounds in this and other studies that rates for anaerobic biodegradation of these compounds exist. Structural preferences are seen in the degradation of both carbazoles and benzocarbazoles, and factors such as water solubility or compound abundance are clearly less important than chemical structure as, for example, 1-methylcarbazole is more rapidly degraded than the more water-soluble methylcarbazole isomers. Water solubility doubtless has some control, as carbazole and alkylcarbazoles are more rapidly degraded than, for example, the more water-soluble benzocarbazoles.

Biodegradation of carbazoles and alkylcarbazoles appears to begin at biodegradation levels where isoprenoid alkanes are being actively degraded and occurs largely at degradation levels 3 to 4 and greater. While the specific degradation

products are not known, it is likely that at Peters and Moldowan biodegradation levels greater than PM 3 petroleum nitrogen compounds may comprise a nutrient source to the petroleum degrading biosphere at the base of the oil column. Conversely, it would appear that at the economically most significant levels of biodegradation (PM level 1-3), where normal and isoprenoid alkanes are being removed, the sources of nitrogen for biomass growth are not petroleum nitrogen compounds but are more likely to be ammonium ions in formation water or gaseous nitrogen.

6.2 Alkylphenols

6.2.1 Factors control phenolic compound occurrence

Phenolic compounds are common components of living organisms and sedimentary organic matter, including petroleums. In the plant kingdom they are not usually present in a free state but are generally found as simple combinations of esters or glycosides or as more complex polymeric structures such as lignins and tannins (Ribéreau-Gayon, 1972). Phenolic compounds frequently occur in many families of angiosperms and gymnosperms as constituents of heartwoods, seeds, fruits, leaves, pigments of some flowers and essential oils. Phenolic compounds have been also identified in fungi (Ribéreau-Gayon, 1972). Alkylphenols have been reported to occur in a wide range of petroleums but their origin and fate are still not clearly explained (Ioppolo *et al.*, 1995; Taylor *et al.*, 1997). The presence of alkylphenols in petroleums that do not manifest an obvious structural relationship to a natural precursor compound led Taylor (1994) and Ioppolo *et al.* (1995) to propose that the occurrence of phenols in petroleum is controlled initially by the alkylation and isomerisation of precursors in source rocks during diagenesis, catagenesis and petroleum generation.

Factors reported in the literature to control the concentrations and distributions of alkylphenols in petroleums are migration, biodegradation, water washing and phase fractionation (Larter *et al.*, 1996b; Taylor *et al.*, 2001). The ability of alkylphenols to form H-bonds with water molecules results in a relatively hydrophilic nature, favouring their partition out of petroleum into water under both surface and subsurface conditions (Bennett *et al.*, 1996; Taylor *et al.*, 1997). Thus, alkylphenols readily interact with water and exhibit high partition coefficients in oil/water systems (Ioppolo *et al.*, 1995; Bennett *et al.*, 1996; Taylor *et al.*, 1997), and it has been shown that oilfield waters and oils are in equilibrium with regard to alkyphenol distributions and concentrations (Dale *et al.*, 1995). This particular characteristic has been proposed as a potential control on alkylphenol concentrations and distributions in petroleum fluids (Dale *et al.*, 1995; Larter *et al.*, 1996b; Taylor *et al.*, 1997). In addition to their affinity for water, alkylphenols have also been shown to interact

strongly with the mineral matrix and organic matter in rocks (Sandvik *et al.*, 1992). As water, minerals and organic matter are ubiquitous and highly variable components of carrier rocks, the controls on the occurrence and distribution of alkylphenols in a petroleum during secondary migration are unlikely to be simple (Lucach *et al.*, 2002).

The concentration of alkylphenols observed in the crude oils most probably reflects partitioning of phenols into the solid phases (organic and mineral) of the fine-grained carrier bed lithologies of this area during migration. Evidence for a (sorption-related) decrease in the total concentration of alkylphenols with increasing migration distance (i.e. with increased exposure to organic (kerogen) and inorganic components (minerals) of the rock matrix) has been previously reported by Taylor (1994), Taylor *et al.* (1997), Chen (1995), and Larter *et al.* (1996b).

After expulsion from the source rock, the concentrations and relative abundance of alkylphenol isomers is determined mainly by 3-phase partitioning between petroleum, water and solid phases (both mineral and organic) during migration and within the reservoir. Larter *et al.* (1996b) proposed the utilisation of alkylphenols as geotracers, a geotracer being defined as "a chemical component in a petroleum system which distributes systematically and hence predictably between carrier phases". Using an example from the Tampen Spur, North Sea, Larter *et al.* (1996b) showed a migration distance-related decrease in total alkylphenol concentration in a suite of source-related crude oils. Taylor *et al.* (1997) noted that, as expected, during secondary migration the total concentration of the alkylphenols in the oil decreases. They claimed a consistency of the alkylphenol distribution in oils migrated along different distances. To explain this consistency, chiefly observed on a complex parameter defined as hindered/nonhindered ratio, an oil-water-rock partition process of alkylphenols is required. Alternatively, Galimberti *et al.* (2000) observed a noticeable variability in some ratios between the concentration of the most water-soluble alkylphenol isomers (e.g. phenol and cresols) in oils migrated different distances. Based on the different solubility of alkylphenol isomers, these authors defined the molecular migration index (MMI) using the concentration ratio *o*-cresol/phenol.

In addition, the increasing concentration of petroleum-derived phenols in formation waters in the vicinity of oil and condensate accumulations has been proposed as a petroleum proximity indicator tool for use in exploration (e.g. Macleod *et al.*, 1993). The presence of phenols in subsurface waters was the consequence of oil/water interactions occurring in the trap or occurred during migration. The analyses of some water samples of dry wells have shown high phenol content in those wells

drilled on the structure flanks in consequence of the presence of a shallower oil-water contact, verified by wells successively testing an up-dip position. On the contrary, a complete absence of phenols was found in produced water of wells properly drilled on the top of the structures and dry because no oil accumulation occurred.

Although alkylphenols have been proposed to have some utility as geochemical markers, our understanding of their detailed systematics is far from complete. Biodegradation takes important role in alkylphenol concentrations and isomer distributions (Taylor *et al.*, 2001). Theoretically, biodegradation may either diminish or enhance alkylphenol concentrations in a reservoired oil depending on the local factors. Phenol and alkylphenols can be mineralised under both aerobic and anaerobic conditions (Howard *et al.*, 1991; van and Young, 2000). Gibson (1991) identified four routes for the microbial oxidation of toluene, two of which lead to the generation of alkylphenol intermediates. *Pseudomonas mendocina kr* oxidises toluene to *p*-cresol (with subsequent oxidation of the methyl group to form *p*-hydroxybenzoate, which is in turn hydroxylated to 3,4-dihydroxybenzoate). *Pseudomonas cepacia g4* oxidises toluene to 3-methyl catechol via *o*-cresol. The fact that these pathways involve cresols as intermediates suggests that alkylated phenols may be present in environments in which aromatic hydrocarbons are being aerobically biodegraded. Kaphammer *et al.* (1990) have also reported a pathway for the hydroxylation of toluene and benzene to *m*-cresol and phenol respectively, by *Pseudomonas pickettii*. Taylor *et al.* (2001) noticed that biodegradation resulted in significant reduction in total alkylphenol abundance and preferential depletion of C_3- and C_2-alkylated compounds. These effects were most pronounced in oils in which the methylated naphthalenes had been biodegraded (PM level 4 or 5). Water washing preferentially removed the phenol and cresols leaving relatively enhanced C_2- and C_3-alkylphenol distributions.

It is clear that alkylphenol concentrations in oils are affected by a combination of biodegradation, water washing and migration history (Larter et al., 1996b; Taylor *et al.*, 2001; Lucach *et al.*, 2002). Therefore, it is important that the effects of biodegradation be recognised so that alkylphenol data can be interpreted accurately for calibration of sedimentary basin fluid flow models. The alkylphenol distributions of the different oil samples allow interpretations to be drawn on the mechanisms of in-reservoir alteration in the Lengdong oilfield.

Since the alkylphenol concentrations are extremely low in the reservoir extracts of the four wells (Well A, B, C of the Es3 column and Well D of the Es1 column) described before, here discussions are focused on oils and core samples from Well E. The oils have undergone varying degrees of biodegradation as indicated by RIC traces

of the aliphatic fractions (Fig. 6-9). The extent of biodegradation in oil samples seems depth-related. All oils with buried deeper than 2000 m show no sign of biodegradation, which is consistent with the temperature limited of 80 °C to cease the biodegradation as observed by Connan (1984) and Palmer (1993). The oil shallower than that depth experienced different degree of biodegradation, which is controlled by the distance from the OWC. No sterane and hopane alteration can be observed from these oil samples. The depletion of *n*-alkanes and acyclic isoprenoid alkanes in the oil sample set corresponding to level 2 to 4 on the biodegradation scale of Peters and Moldowan (1993).

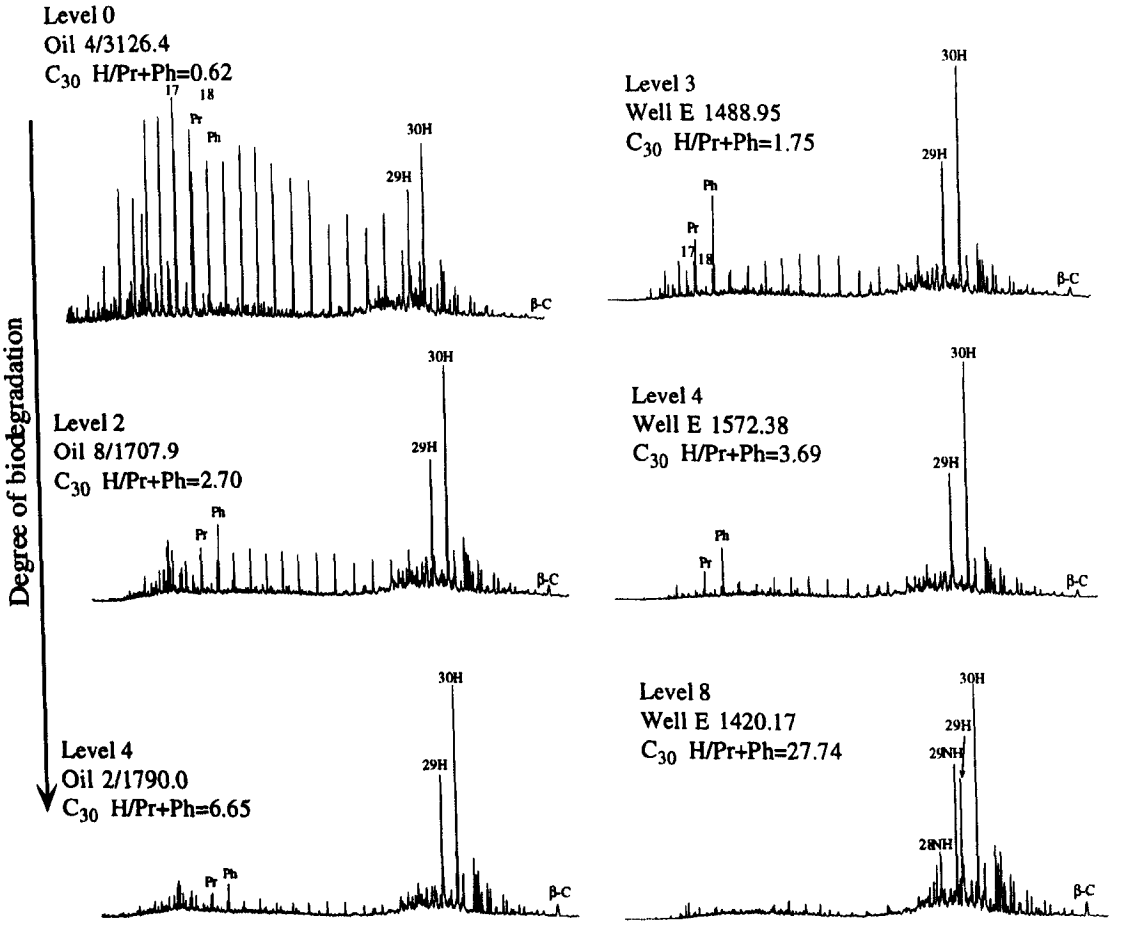

Fig. 6-9. RIC of oils and reservoir extracts from the Liaohe basin at different biodegradation level. Numbers indicate the carbon number for *n*-alkanes. Pr: Pristane; Ph: Phytane. Sample details see Table 4-1.

The biodegradation pattern on the reservoir extracts from Well E is more complicated. Since it is not a continuously oil saturated column no obvious single gradient can been observed. The upper part of the column experienced severe biodegradation in which the *n*-alkanes and isoprenoids have been removed, the steranes have been affected, and a significant fraction of the hopanes have been converted to their demethylated hopane homologues and there is a characteristic UCM indicative of heavy biodegradation (Fig. 6-9). According to the scheme of

Peters and Moldowan (1993), the level of hydrocarbon biodegradation in this part of the column ranges from PM level 5 (removal of acyclic isoprenoids) to PM 8 (hopane biodegraded, 25-norhopanes enriched). Conversely, in the lower part of the studied column, the oil has been moderately biodegraded, with the *n*-alkanes and acyclic isoprenoid alkanes remain observable and no 25-norhopanes being present. Their biodegradation level is between PM 2 (*n*-alkane depleted) to PM 4 (*n*-alkanes absent and isoprenoids affected).

These two intervals show distinct different biodegradation regimes. The upper part of the reservoir has higher oil saturation and a thick water leg, while the lower part of the reservoir has lower oil saturation and a thin water. Water volume beneath the oil body seems to exert the main control on the degree of biodegradation of oil above it (Fig. 6-10). This is again interpreted as being attributable to biodegradation at the oil-water contact and the consequent establishment of diffusion-controlled concentration gradients within the oil column (Larter *et al.*, 2003; Huang *et al.*, 2004). Thin water legs can not sustain a large quantity of microbial consortia leading to less biodegraded oils in oil leg above.

Biodegradation indicators based on the ratios $C_{30}\alpha\beta$hopane/(Pr+Ph) and $C_{29}\alpha\beta$-25-norhopane/$C_{30}\alpha\beta$hopane coupled with column structure clearly reflect biodegradation intensity of the oil suffered and the possible control factor.

6.2.2 Concentrations

The concentrations of $C_{0\text{-}3}$-alkylphenol compounds are less than 6 μg/g EOM and show a weak decline trend towards the bottom of the Es3 column (Fig. 6-11a). In the Es1 columns, the $C_{0\text{-}3}$-alkylphenol concentrations are even lower ranging from 2 to 4 μg/g (Fig. 6-11b). There is no clear relationship between the extent of hydrocarbon degradation and alkylphenol abundance in the Es3 column. This may be due to the fact significant alkylphenol degradation has not yet begun in these samples and/or that late-stage migration of fresh oils, that can be clearly observed in the hydrocarbon GC traces at the top cloumn, have supplemented the alkylphenols present in the reservoir. Total phenol concentrations decrease from the Es3 column to the Es1 column suggests that the biodegradation of phenols is contemporaneous with the microbial utilisation of the hydrocarbons in these oils. Caution should be taken when interpreting these data since such a low value is easily affected by a variety of other factors. Biodegradation effects were investigated in following section using the sample with more abundant alkylphenols.

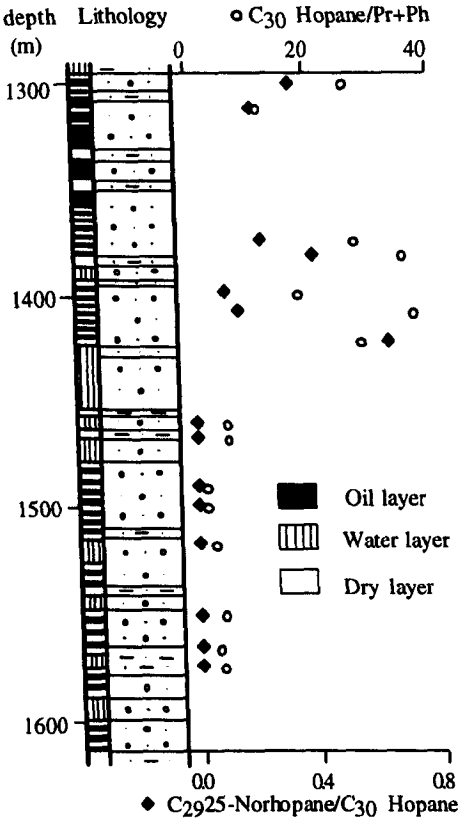

Fig. 6-10 Simplified study oil column with biodegradation degree indicators. Obviously the upper part of the column has experienced more severely biodegradation.

The alkylphenols are quite abundant in the Lengdong oils and significant variations are observed. In non-biodegraded oils the total phenol concentrations range from 22.1 to 50.0 μg/g EOM and that of biodegraded oils from 8.9 to 19.1 μg/g EOM with one exception of 37.7 μg/g EOM. Slightly higher concentrations in one biodegraded sample may be due to the production of some alkylphenols during early biodegradation stage. The overall decreasing trend is quite clear once oil experiences a certain degree of biodegradation.

Among reservoir extracts two intervals show distinct differences of the total phenol concentrations. The total phenol concentration in the upper part of the column is very low, ranging from 2.9 to 8.8 μg/g EOM and that of lower part of the column remains very high, ranging from 18.5 to 62.9 μg/g EOM. Since the similarities in the source facies characteristics and maturity level of the oils, as indicated by the hydrocarbon and aromatic compound analyses, the reservoir extracts exhibit quite considerable variation in the distribution and concentrations of the alkylphenols, which mainly caused by the biodegradation. There is a clear relationship between the extent of hydrocarbon degradation and the concentration of the $C_{0\text{-}3}$-alkylphenols in studied samples (Fig. 6-12). A reverse trend can be observed for both oils and reservoir extracts. The relatively low total phenols concentrations in biodegraded oils

and reservoir extracts confirm the main conclusion proposed by Taylor *et al.* (2001) that biodegradation generally reduces the abundance of alkylphenols in oil. Fig. 6-12 shows total alkylphenol concentrations versus degree of biodegradation and indicates that the most extensive phenol biodegradation in the samples occurred between level 2 and level 4 of the Peters and Moldowan (1993) biodegradation scale i.e. after the removal of the *n*-alkanes. At more advanced biodegradation levels the total concentration of alkylphenols become very low and no significant depletion occur.

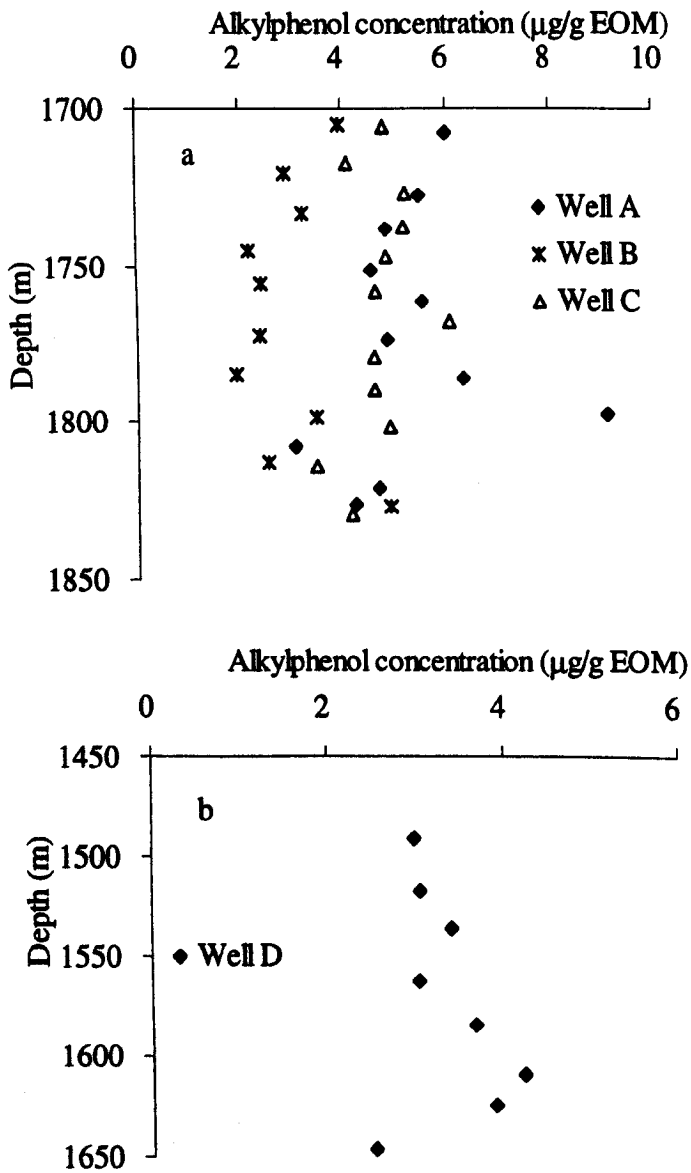

Fig. 6-11. Variation in C_0-C_3 alkylphenol concentrations in the Es3 (a) and Es1 (b) columns.

6.2.3 General distribution of alkylphenols

Taylor *et al.* (1997) noticed the isomeric distributions of alkylphenols in non-biodegraded crude oils are broadly similar, irrespective of source facies. The relative abundance of C_0+C_1 compounds, C_2 compounds and C_3 compounds in 25 non-

degraded oils were 37 ± 10% (mean ± one standard deviation) 41 ± 7% and 22 ± 5% respectively. This feature leads them to suggest that the source-organic matter type of an oil is a less important factor controlling the alkylphenol distributions in oils than processes such as alkylation, isomerisation of alkylphenols during diagenesis and thermal maturation or partitioning of phenols between petroleum, water and solid phases during primary and secondary petroleum migration. The differences in absolute and relative abundance of the different homologue groups in the Lengdong oils suggest migration may also have some effects upon alkylphenol occurrence.

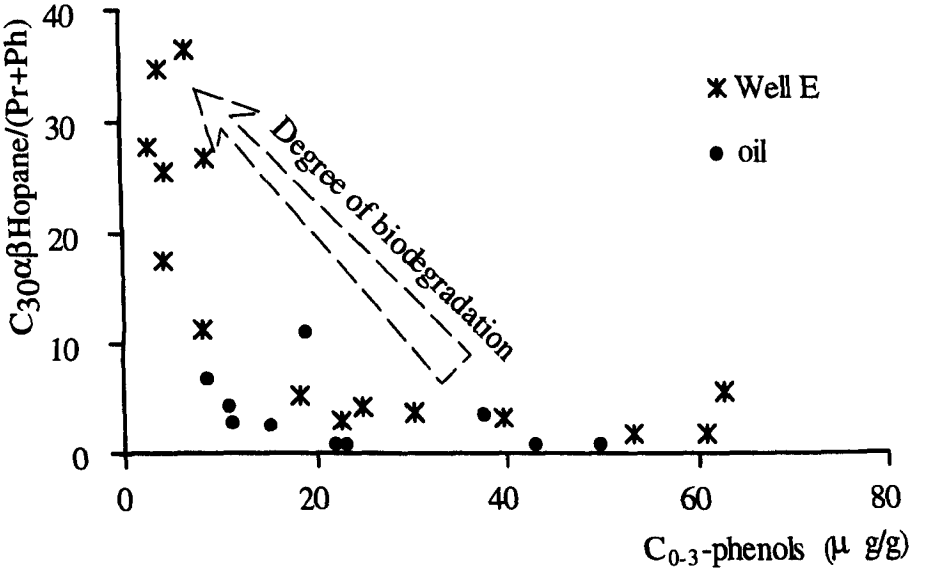

Fig. 6-12. The relationship of the total C_0-C_3 alkylphenol concentrations and C_{30} αβ hopane in the suite of Liaohe oils and reservoir extracts analysed.

In non-biodegraded Lengdong oils alkylphenols are rich in higher homologues while in biodegraded samples the alkylphenol distributions in both crude oils and reservoir extracts are generally dominated by low molecular alkylphenols such as phenol and cresols. For instance, in 4 non-biodegraded oils the average percentage of C_0- + C_1-, C_2- and C_3-phenols are 22.2%, 41.2 % and 36.0%, respectively. In 5 biodegraded oils C_0-+C_1-, C_2- and C_3-phenols are 34.0%, 40.0% and 26.0%, respectively. The ratio of phenol/C_3-phenols in study oils clearly increase with degree of biodegradation (Fig. 6-13). This is accordance with the Taylor *et al.* (2001) observation that both naturally and experimentally biodegraded samples show an alkylphenol distribution enhanced in phenol and cresols.

In the Well E reservoir extracts, the phenol distribution patterns greatly differ from these in oil regardless of their biodegradation degree. From moderate (level 2) to extremely heavily biodegraded (level 8) samples the alkylphenol distributions are dominated by phenol and cresols and the concentrations of C_2-C_3 alkylphenol isomers are very low. There is broad increase trend in the phenol/C_3-phenols ratios with

increasing degree of biodegradation (Fig. 6-13).

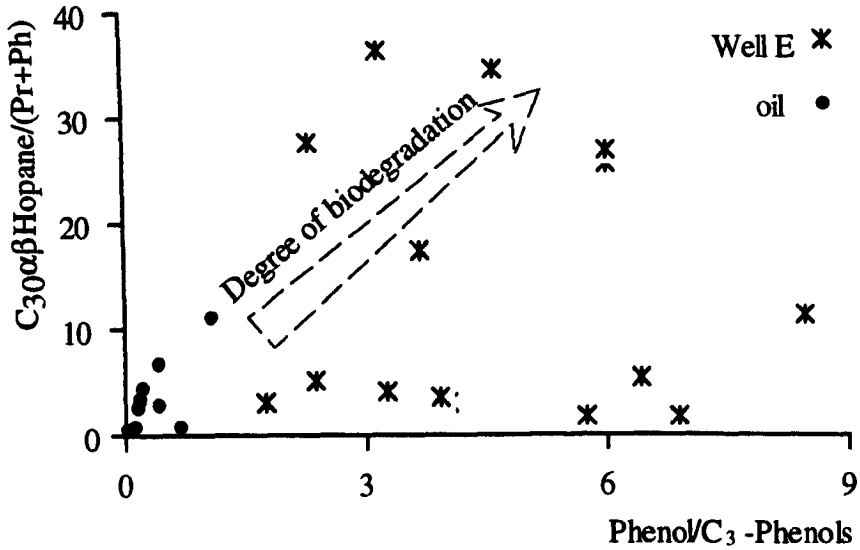

Fig. 6-13. Changes in the molecular distribution of C_0-C_3 phenols in response to increasing biodegradation.

In the Es3 column the phenol/C_3-phenols also did not display clear trend throughout the column. However, different well sites do show different phenol/C_3-phenols ratios (Fig. 6-14a). Relatively low ratios occur in the Well A and B, while Well C has relatively higher ratios. As I discussed previously the main difference between these wells are the water leg sizes. Thicker water legs occur in the Well A and B, while Well C has no water leg. The low ratios in the Well A and possibly indicate more intensive oil-water interaction occurring in these two wells even though water washing is not the main cause in studied column since Taylor *et al.* (2001) noticed when water washing occurs alkylphenols become enriched in C_3-isomers. This ratio in the Well D of the Es1 column shows a clearly increasing trend, which suggests that biodegradation is the predominant control on alkylphenol occurrence (Fig. 6-14b). The predominance of the most water-soluble species (phenol and cresols) in the most degraded oils suggests that biodegradation is the predominant control on alkylphenol occurrence.

6.2.4 Cresol distributions

Cresol has three isomers among which *o*-cresol is dominated component in most non-biodegraded oils. Ioppolo-Armanios *et al.* (1995) explained this distribution related with catalytic alkylation/isomerisation of unknown alkylphenol precursors in source rocks, rather than selective removal of *meta*- and *para*-substituted alkylphenol isomers from petroleum by water washing. In non-biodegraded Liaohe oils the phenol distributions is also dominated by *o*-cresol with trace amount of *p*-cresol (Fig. 6-15).

With the increase of biodegradation relative proportion of *p*-cresol get enriched and three cresol isomers reach the similar amount in moderate biodegraded oil (O4, level 4) (Fig. 6-15).

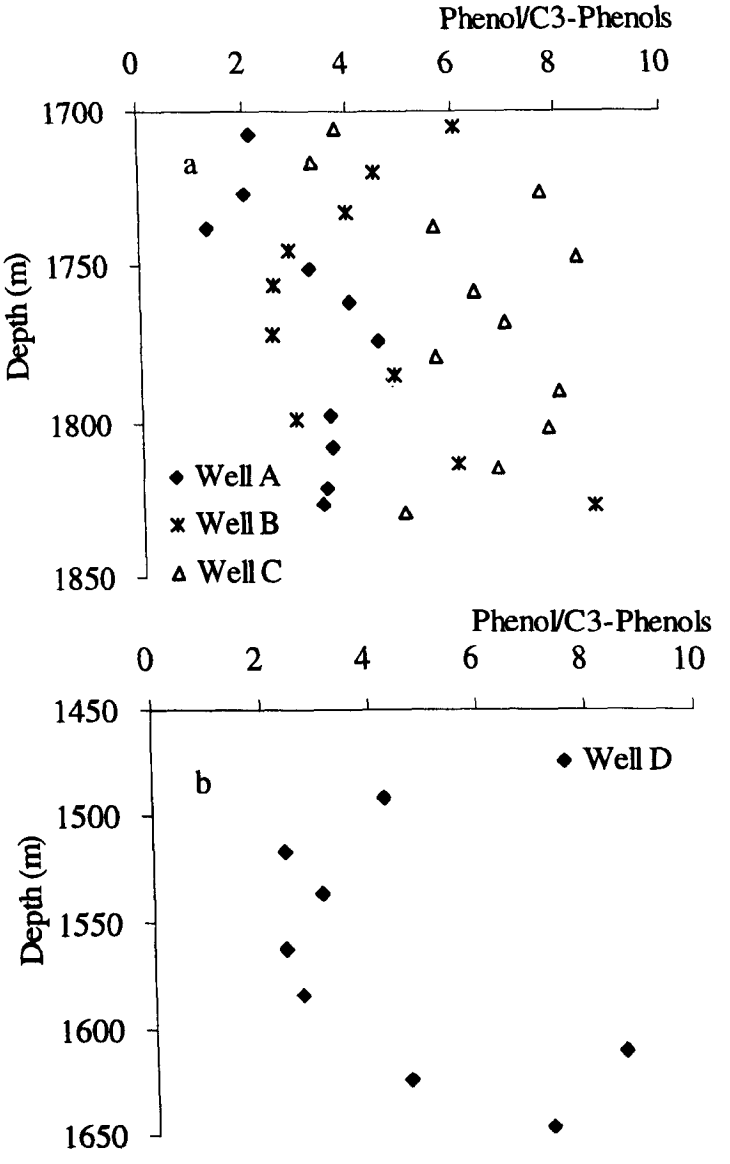

Fig. 6-14. The ratios of Phenol/C_3-Phenols in the Es3 (a) and Es1 (b) columns.

The cresol distributions in the reservoir extracts show significant differences from these in oils. In moderate biodegraded sample (1489 m/level 3) the predominant component is *m*-cresol with trace amount of *o*-cresol. With increasing degree of biodegradation *p*-cresol and *o*-cresol get enriched. It is not clear why *m*-cresol has such high relative concentration in reservoir extracts, but this isomer seems the most susceptible component to biodegradation. The ratios of *p-/m*-cresol for both oils and reservoir extracts increase with the degree of biodegradation (Fig.6-16). The relative concentrations of *o*-cresol show clear trends to increase in reservoir extracts while slightly decrease in oil samples with increasing degree of biodegradation. From steric

hinderance consideration, *para*-substituted phenols should be biodegraded faster than *ortho*-substituted phenols and this phenomena has been observed in contaminated underground water samples (Broholm and Arvin, 2000). There is no obvious reason to explain why *p*-cresol has slightly higher ability to resist biodegradation. It must be mechanistic in origin.

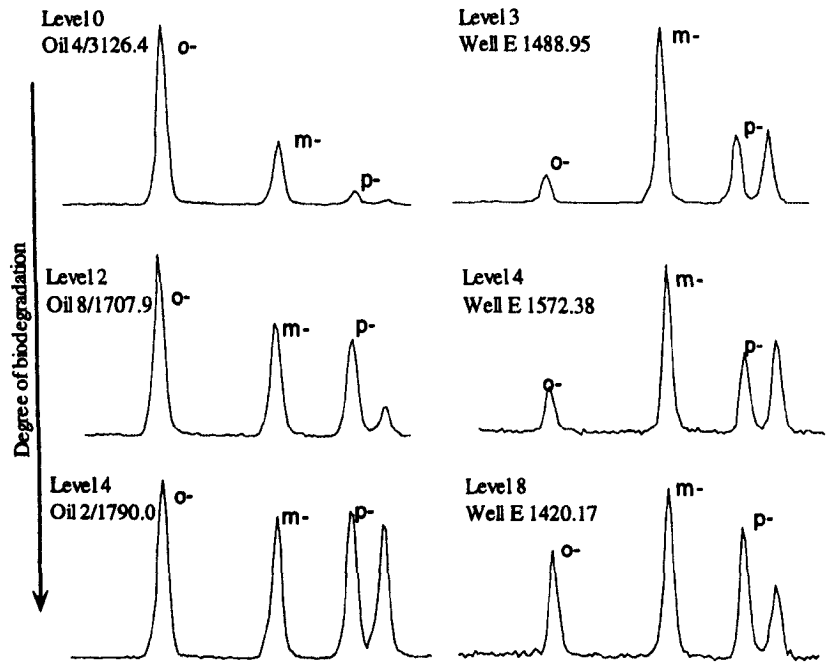

Fig. 6-15 Cresol distributions in different degree of biodegradation samples.

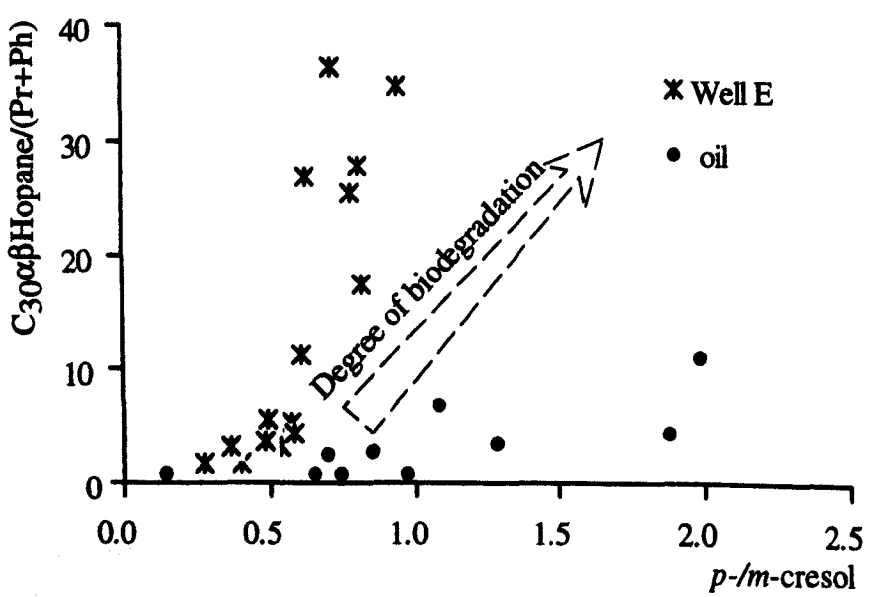

Fig.6-16. The relationship of the ratios between *p*-/*m*-cresol and $C_{30}\alpha\beta$Hopane/(Pr+Ph).

6.2.5 C_2-phenol distributions

In non-biodegraded oil 2,5-xylenol, 2,4-xylenol+3-ethylphenol (EP) and 2,6-xylenol are three major peaks in C_2-phenols. The concentrations of 3,5-xylenol, 3,4-

xylenol, 2-ethylphenol and 4-ethylphenol are usually very low. Benzoic acid was identified by mass spectra comparisons to co-elute with 2,3-xylenol in the suite of the Lengdong samples (Fig. 6-17). Consequently, this compound has not been considered for the interpretation of alkylphenols distributions and concentrations in this suite of samples. Once biodegradation starts 2,5-xylenol depletes first, meanwhile 2,6-xylenol shows an accompanying depletion especially pronounced in the oil sample suite. Although this isomer has a higher oil-water partition coefficient than other dimethyl phenols because of steric hindrance (Taylor *et al.*, 1997), no increase in the relative proportions of 2,6-xylenol can be observed. On the contrary, a noticeable decrease of 2,6-xylenol/3,4-xylenol ratios was seen with increasing degree of biodegradation in oil samples (Fig. 6-18).

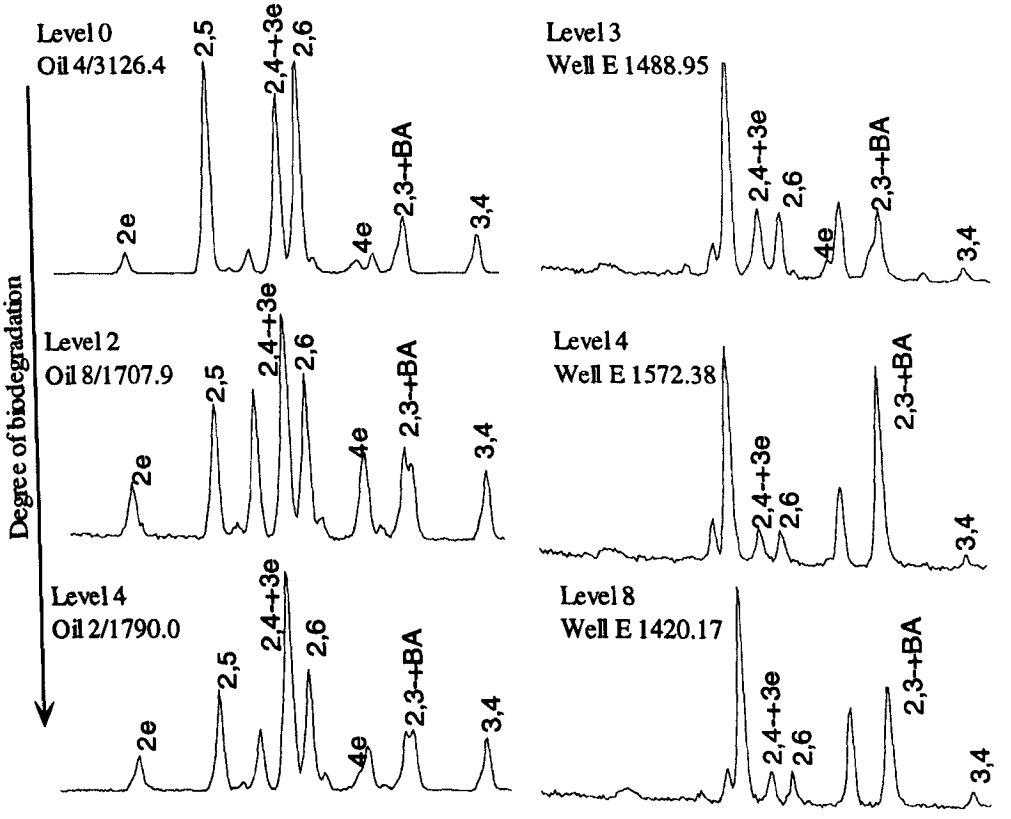

Fig. 6-17 C_2-phenol distributions in different degree of biodegradation samples. BA: benzoic acid.

In the Well E reservoir extracts C_2-phenols are very low even though 2,4-xylenol+3-EP and 2,6-xylenol remains the major identifiable peaks. Some low abundance noisy peaks and benzoic acid become predominant. It remains unclear whether the benzoic acid was produced or it has high ability to resist biodegradation as compared with alkylphenols (Wilkes *et al.*, 2000). In the case of 2,6-xylenol, methyl groups substituted in both sides of hydroxylation function group make it OH-shielded. Theoretically this isomer has the highest ability to resist biodegradation if steric hindrance control phenol's biodegradability but this does not actually occur in

the Liaohe biodegraded sample suite. Although the full order of relative susceptibility of the various C_2-phenol isomers to biodegradation cannot be drawn from this data, OH-shielded isomers generally do not appear to be enriched during biodegradation as one may have expected. I tentatively establish the order of susceptibility to biodegradation for C_2 alkylphenols (from easiest to hardest): 2,5-xylenol > 2-ethylphenol, 2,6-xylenol > 4-ethylphenol, 3,4-xylenol > 2,4-xylenol.

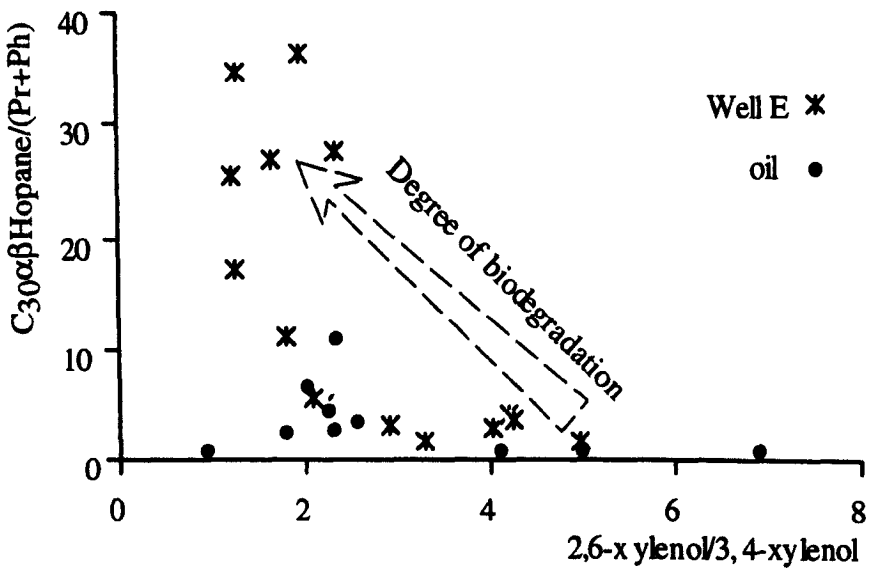

Fig. 6-18. The relationship of the ratios between 2,6-xylenol/3,4-xylenol and $C_{30}\alpha\beta$Hopane/(Pr+Ph).

6.2.6 C_3-phenol distributions

C_3-phenols are predominated by two co-eluting isomers 2,4,6- + 2,3,5-trimethylphenols in all studied samples (Fig. 6-19). Once an oil experienced biodegradation, their concentrations drop sharply. Although no clear order of susceptible to biodegradation can be draw in the C_3-phenol distributions, isopropyl- and propylphenols seem more susceptible to biodegradation than trimethylphenols and they are almost absent in the most biodegraded reservoir extracts. In more severely (> PM level 4) biodegraded reservoir extracts, the concentrations of C_3-phenols drop to less than 0.5μg/g EOM, making the quantification not very accurate with 2,4,6- + 2,3,5-trimethylphenols and 2,3,6-trimethylphenol remain as the main compounds.

6.2.7 Biodegradation pathway of alkylphenols

Phenol biodegradation can occur under both aerobic and anaerobic conditions. Under aerobic conditions phenol, cresols, and xylenols have been observed to degrade in *in situ* microcosm experiments in a sand aquifer material, in aerobic laboratory microcosm and column experiments (Hinteregger *et al.*, 1992; Semple and Cain, 1997). Under nitrate reducing conditions and iron reducing anaerobic conditions

degradation of phenol was observed in some in situ microcosms but not in all (Nielsen and Christensen, 1994; Broholm and Arvin, 2000 and reference therein).

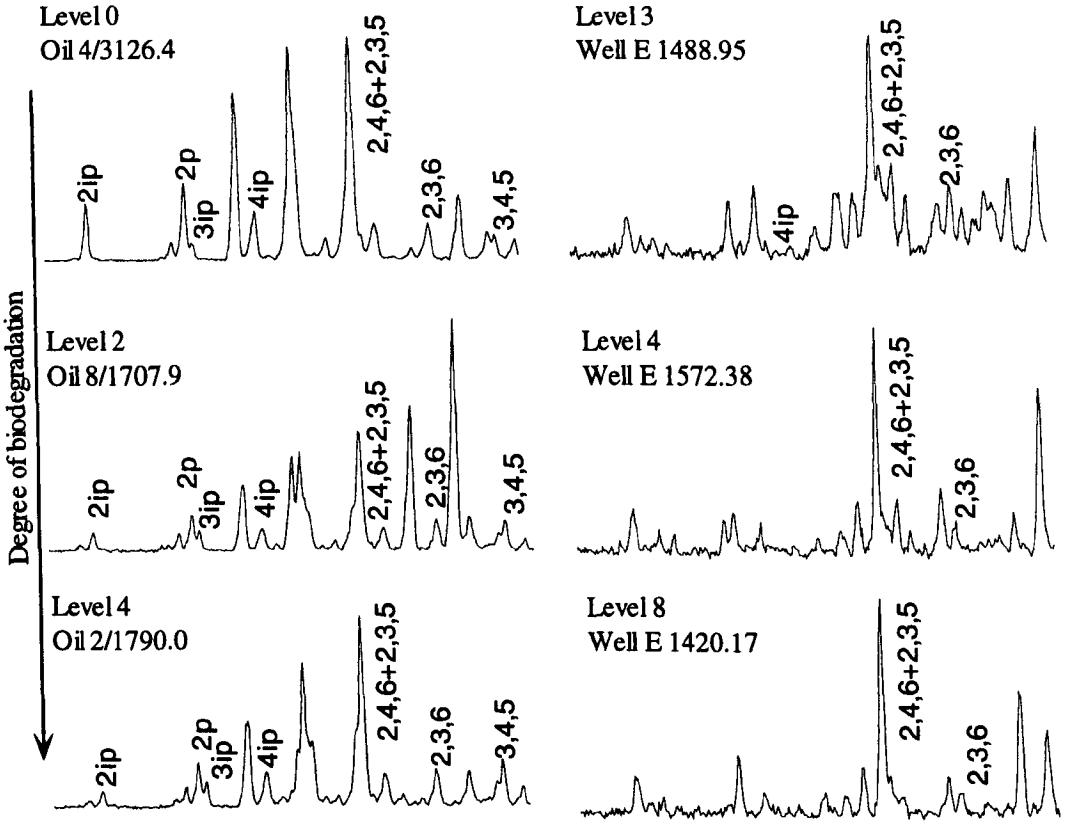

Fig. 6-19. C_3-alkylphenol distribution in different degree of biodegradation samples.

Biodegradation of phenols by oxidation to catechols or hydroxybenzoates and subsequent ring cleavage has been reported (Powlowski and Shingler, 1994; Hinteregger *et al.*, 1992). Degradation via the catechol pathway is likely to be influenced by steric hindrance of hydroxylation by the methyl substituents on the aromatic ring. Hence, the order of degradation is likely to be influenced by the position of the methyl groups. Typically, *o*-cresol is more recalcitrant than *m*-cresol, *p*-cresol or phenol (Nielsen and Christensen, 1994) and the xylenols are less degradable than phenol or cresols (Broholm and Arvin, 2000). Potential organic intermediates of phenols degradation include low molecular weight fatty acids, catechols, hydroquinones, hydroxybenzyl alcohols, hydroxybenzaldehydes, hydroxybenzoic acid and benzoic acid (Semple and Cain, 1997 and reference therein). Possible effects of biodegradation on oil composition are controlled by the substrate specificities of the bacteria involved. Under anaerobic conditions phenol, *o*- and *p*-cresol, 2,4- and 3,4-xylenol have been reported to be degraded by *para*-carboxylation or oxidation of the *para*-methylgroup to hydroxybenzoate and the respective hydroxy-methyl-benzoates. *m*-Cresol was reported to be degraded by hydroxylation of the

methylgroup. 4-Hydroxy-2-methyl-benzoate was observed to be a dead-end product of 3,4-xylenol degradation by Rudolphi *et al.* (1991).

Though effective phenol degradation under anaerobic conditions is reported (Schink *et al.*, 2000), in the multiphase environment of an oil reservoir near an oil water contact, preservation of labile reactants or biodegradation products by partition into the oil phase may prove critical to preservation of any intermediates of hydrocarbon degradation such as alkylphenols. Theoretically, the potential for degradation decreases with increasing molecular size and number of substituted alkyl groups. It seems perplexing that highly substituted isomers deplete first leading phenol and cresol to dominant in biodegraded samples. On the other hand, no specific steric hindrance of hydroxylation by the methyl substituents on the aromatic ring has been observed in cresols and xylenols. All these indicate reservoir biodegradation is more complicated than aquifer or laboratory situation.

6.3 Carboxylic acids

Carboxylic acids are known to be intermediates formed during the biodegradation of petroleum hydrocarbons (Atlas, 1984). Langbehn and Steinhart (1995) studied biodegradation of diesel fuel and lubricating oil in artificial soils. Organic acids and ketones which were not original components of the oils contaminating the soil samples were identified. Predominantly alicyclic and branched-chain aliphatic organic acids as well as diacids and aromatic ketones were formed by degradation. Laboratory experiments indicate that acids are the main intermediate products of biodegradation. Watson *et al.* (2002) noted different molecular weight branched and cyclic carboxylic acids were generated during the biodegradation of crude oil in the laboratory, while Wilkes *et al.* (2003) detected various alkylsuccinates methyl-branched and cyclopentyl-substituted fatty acids during anaerobic biodegradation of saturated hydrocarbons directly from crude oil. Relationship between acid compounds and biodegradation in reservoird oil was also clear. Jaffé and Gallardo (1993) suggested that total acidity as well as the ratio of tricyclic to pentacyclic acids were good parameters of biodegradation in these oils. Nascimento *et al.* (1999) proposed that the carboxylic acid biomarkers, more resistent to biodegradation, can provide information on past reservoir history when most important neutral biomarkers have been biodegraded. Meredith *et al.* (1999) reported a correlation between carboxylic acid content and the level of biodegradation of crude oils.

6.3.1 n-acids

Since this project has not focused specifically on the acids fraction, the acid

compounds analyzed are *n*-acids and benzoic acids occurring in the phenol fraction. Characteristic ion chromatograms of the *n*-acids from the Es3 and Es1 columns are shown in Fig. 6-20. Different from *n*-alkanes in these study columns, the *n*-acids show a complete distribution over a wide carbon range ($C_{9:0}$–$C_{30:0}$) at all biodegradation level. In the severely biodegraded Es1 column, there is a large number of unidentified peaks and an unresolved complex mixture (UCM) of medium molecular weight branched and cyclic carboxylic acids. C_{16} or C_{18} *n*-Acid is the main peak in all study samples. The abundant presence of C_{16} and C_{18} carboxylic acids could be ascribed to the input of the "fresh" biomass acting on the reservoired petroleum (Mackenzie *et al.*, 1983). Although the *n*-acids were not prominent in the ion chromatograms at the bottom of the Es1 column, which is instead dominated by a higher molecular weight UCM, *n*-acids appear in all samples and appeared much more recalcitrant to biodegradation than most of alkanes though it is possible that they are being both created and destroyed. Watson *et al.* (2002) noted significant amounts of carboxylic acids were produced during the biodegradation of crude oil in the laboratory. Medium molecular weight (C_{10}–C_{20}) carboxylic acids were rapidly produced, which coincided with the removal of the *n*-alkanes but these acids were then also rapidly biodegraded. The acid distribution in the Lengdong oilfield may reflect a biodegradation pulse where some *n*-acids were generated.

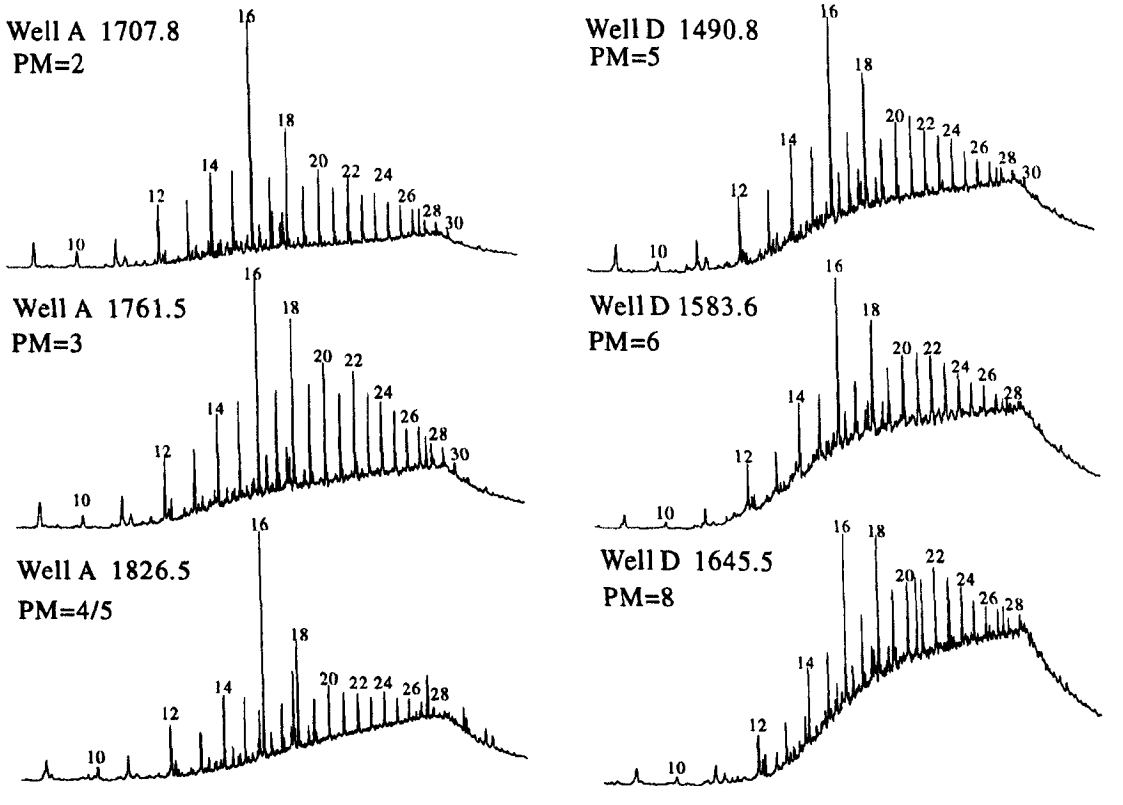

Fig. 6-20. Characteristic ion chromatograms of the *n*-acids at m/z=73 from the Es3 and Es1 columns.

The *n*-acid concentrations in reservoir extracts of the Es3 column ranging from 300 to 700 μg/g EOM. A weakly decreasing trend in the lower part of the Es3 column towards the OWC can be observed (Fig. 6-21a). More obvious decrease occurs in Well D of the Es1 column from 230 μg/g EOM to less than 100 μg/g EOM (Fig. 6-21b). It is clear that the concentrations of *n*-acids decrease at more advanced biodegradation stages. High concentrations of *n*-acids can only be found at the early stages of the biodegradation, as shown by Mackenzie *et al.* (1983) and confirmed by the observation of this case study.

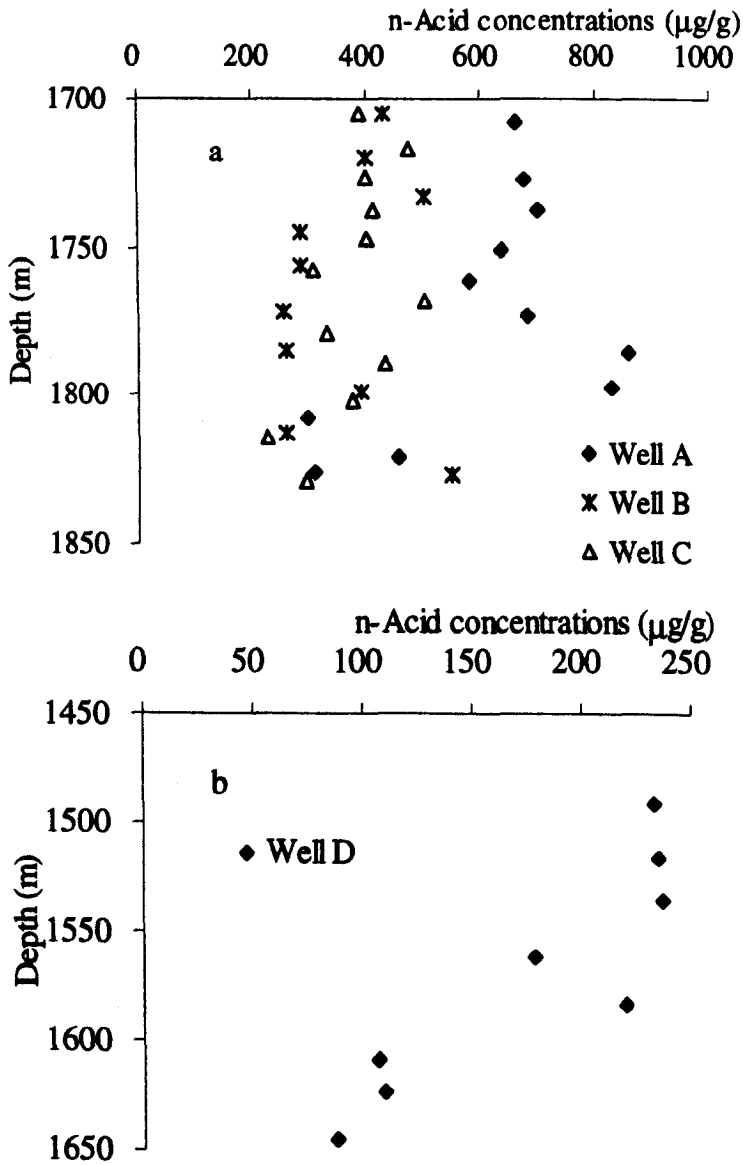

Fig. 6-21. *n*-Acid concentration variations in the Es3 (a) and Es1 (b) columns.

The concentration of the *n*-acids and the C_{30} αβhopane/(Pr+Ph) ratios from each oils and Well E extracts are shown in Fig. 6-22. The *n*-acid contents are normally low in all oils with less than 600 μg/g EOM except O7 which contains 1700 μg/g EOM *n*-acids. Slightly high amount of *n*-acids in non-biodegraded oils suggests that

biodegradation will reduce the *n*-acid contents. In the reservoir extracts the *n*-acids exhibit great variations. The upper part of more severely biodegraded samples contain low amount of *n*-acids from 400 to 950 μg/g EOM, while samples in the less biodegraded lower part of the column are extremely rich in *n*-acids with concentration ranging from 3300 to 12000 μg/g EOM. Such extreme high contents of *n*-acids in the lower part of the Well E reservoired crude oils may either be related with their low oil saturation and intensive oil water reaction or some local unknown conditions.

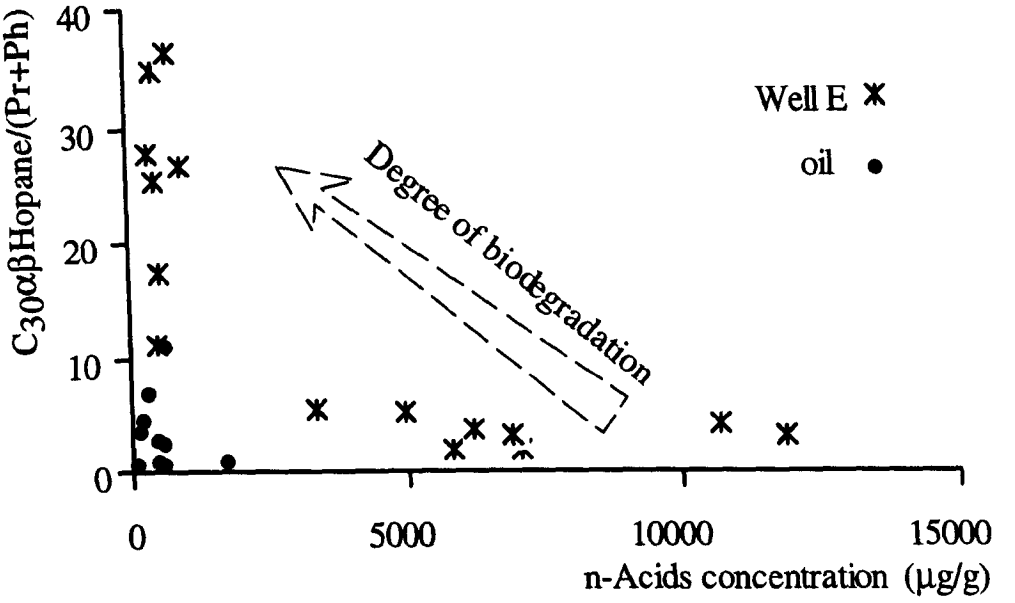

Fig. 6-22. Relationship between *n*-acid concentrations and C_{30}hopane/(Pr+Ph) ratios in the Lengdong oils and Well E reservoir extracts.

6.3.2 Benzoic acids

Laboratory experiments carried out by Wilkes *et al.* (2000) have revealed that alkylbenzenes may be removed selectively from crude oil by sulfate-reducing bacteria and alkylated benzoic acids are produced as the main metabolic by-products detected in the water phase. Benzoic acids occur in fossil fuel contaminated anoxic aquifers where they are assumed to be anaerobic oxidation products of alkylbenzenes. Several of these alkylbenzoic acids appear to be dead-end metabolites whose formation seems not to be of any benefit to the bacteria (Cozzarelli *et al.*, 1990, 1994; Schmitt *et al.*, 1996). In contrast, benzoic acids have rarely been described in reservoired oils and formation waters where a variety of acids are ubiquitous and are attributed to bacterial decomposition of sedimentary organic matter and crude oil (Meredith *et al.*, 2000).

Benzoic acid was identified by mass spectral comparisons to co-elute with 2,3-dimethylphenol in the suite of oils from the Lengdong oilfield. Total benzoic acid concentrations in non-biodegraded Liaohe oils differ greatly, ranging from 2.8 to 21.0

μg/g EOM and that of biodegraded oils from 5.2 to 11.7 μg/g EOM. No clear trend can be observed from these oils individually, suggest some local factors other than biodegradation may affect benzoic acid abundance. The Well E reservoir extracts seems richer in benzoic acids especially in the lower part of the column, ranging from 47.9 to 106.8 μg/g EOM. The total benzoic acid concentration in the upper part of the column is relatively low, ranging from 6.1 to 16.4 μg/g EOM. The relationship between the extent of hydrocarbon biodegradation and the concentration of the benzoic acid in reservoir extracts is obvious (Fig. 6-23). Total benzoic acid concentration decrease with increasing degree of biodegradation especially at more advanced stages of biodegradation (PM level 4 and after). Two samples with highest benzoic acid concentration have experienced moderate biodegradation.

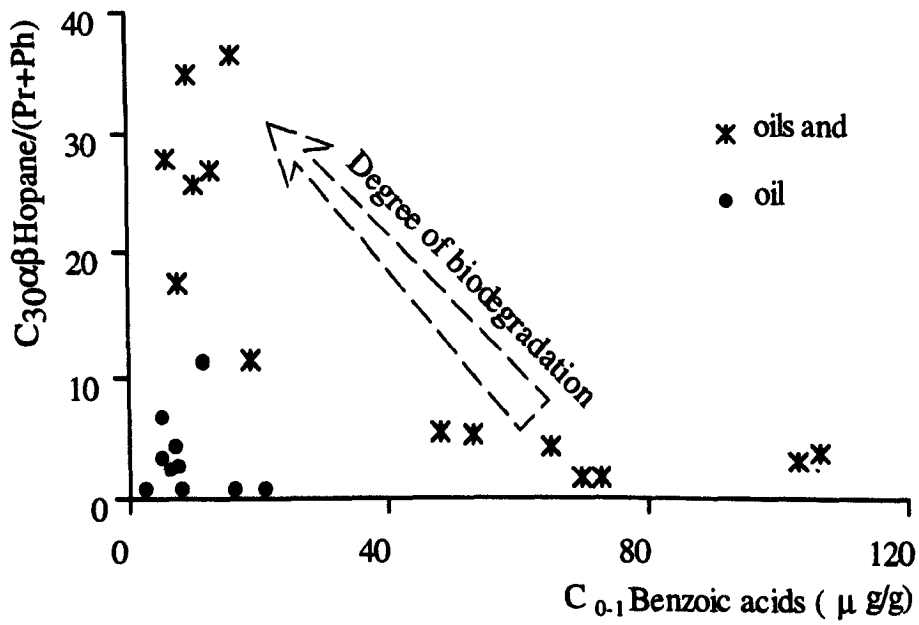

Fig. 6-23. The relationship of the total C_0-C_1 benzoic acid concentrations and C_{30} αβ hopane in the suite of Liaohe oils and reservoir extracts analysed.

Total benzoic acid concentrations in the Es3 column range from 4 to 12 μg/g EOM and also no clear trend can be observed throughout the column (Fig. 6-24a). The benzoic acids concentrations in the Well D reservoir extracts are less than 8 μg/g EOM (Fig. 6-24b). Slightly low benzoic acid concentrations in the more severely biodegraded column may reflect the effect of further biodegradation. At the moment it remains unclear if benzoic acids occur in reservoired oil as a result of anaerobic biodegradation of crude oil. However, they are clearly not dead-end metabolites as a previous study assumed (Cozzarelli *et al.*, 1994; Schmitt *et al.*, 1996) but can clearly be further mineralized at more advanced biodegradation stages (> PM level 4). Distinctly differently abundances between oils and reservoir extracts may be related to

aquifer waters and mineral phase surfaces. It makes reservoir extracts rich in benzoic acids as compared with oils.

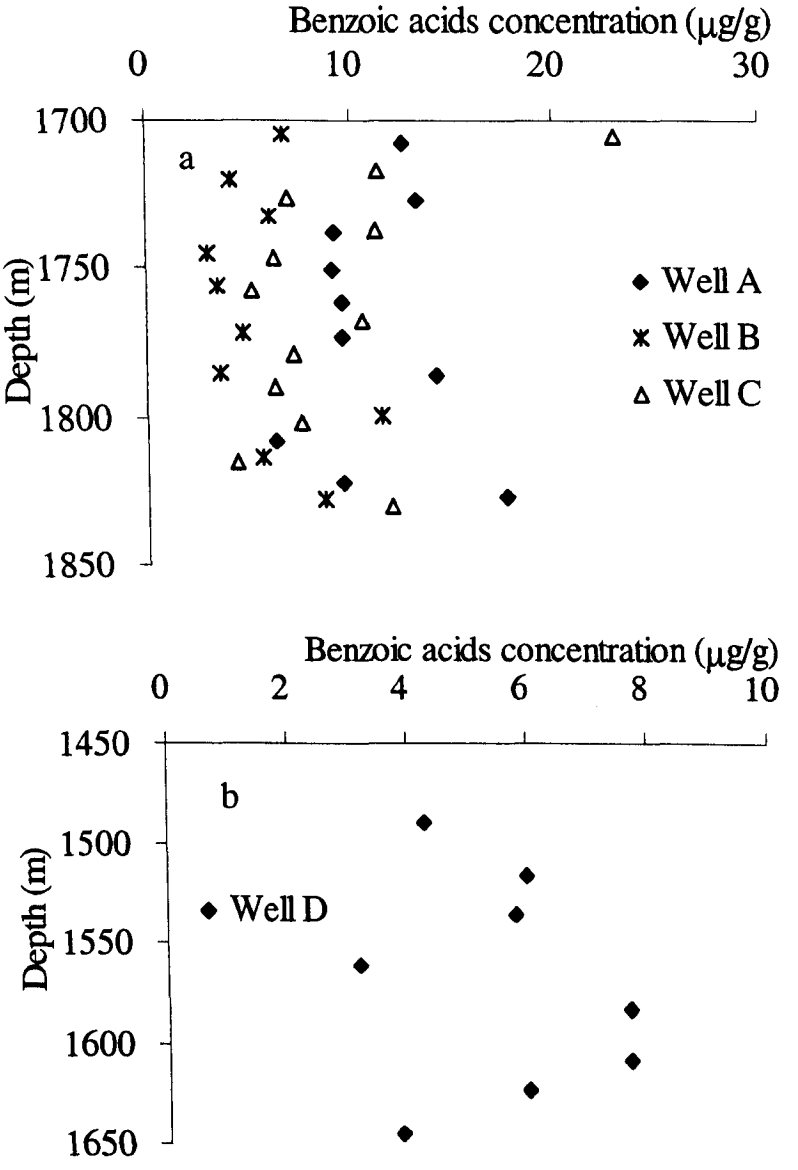

Fig. 6-24. Variations of C_0-C_1 benzoic acid concentrations in the Es3 (a) and Es1 (b) columns.

Distribution patterns of methylbenzoic acids are completely different from these cresols. Representative distributions of the methylbenzoic acids in oil and reservoir extract samples at different levels of biodegradation are shown in Fig. 6-25. In non-biodegraded oils *ortho*- and *meta*-methyl benzoic acids occur in relatively low abundance compared to *para*-methyl benzoic acid. There is an obvious increase in the relative abundance of *ortho*-methyl benzoic acid with increasing level of biodegradation, strongly suggesting that the *ortho*-substituted isomer has a higher resistance to biodegradation than the other two isomers. There is a progressive decrease in abundance of the *para*-substituted isomer. At low levels of biodegradation in reservoir extracts, *ortho*- and *para*-methyl benzoic acids have similar abundance

with lower amounts of *meta*-methyl benzoic acid (Fig. 6-25). There is an obvious decrease in the relative abundance of *para*-methyl benzoic acid with increasing level of biodegradation, leaving the *ortho*-substituted isomer predominant in the chromatogram. Hence, it appears that *para*-substituted benzoic acid is first biodegraded and *ortho*-substituted benzoic acid is the last to be biodegraded, which might suggest that *o*-substituents with steric hindrance resist biodegradation.

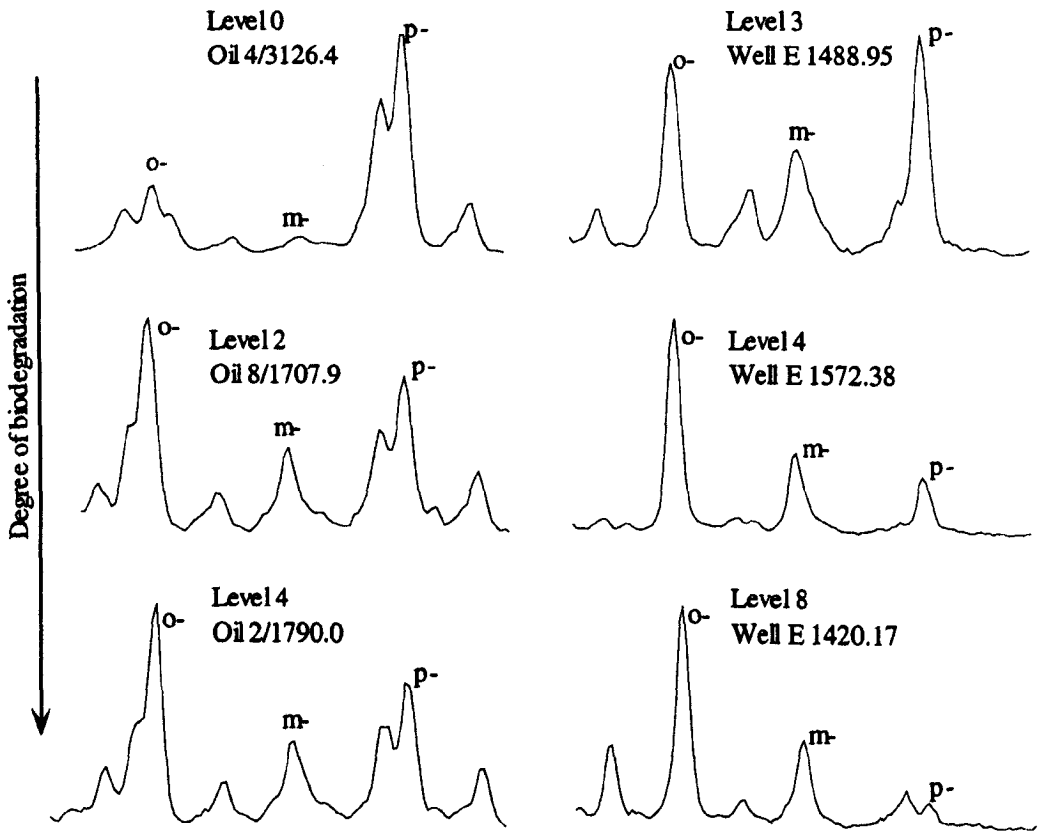

Fig. 6-25. Distribution of methyl benzoic acids in different biodegraded samples.

In the Es3 column the ratio of *o-/(m+p)*-methyl benzoic acids did not show a clear trend. In Well A and B this ratio shows a weak increase towards OWC, while in Well C this ratio show a reversed trend (Fig. 6-26a). It seems biodegradation does not take the main control on acid composition this stage. In Well D of the Es1 column the ratio of *o-/(m+p)*-methyl benzoic acids shows a consistently increasing trend, indicating *o*-methyl benzoic acid has a high ability to resist biodegradation (Fig. 6-26b).

The cross plot of the ratio $C_{30}\alpha\beta$Hop/(Pr+Ph) and the ratio of *para-* methyl benzoic acid */meta-* methyl benzoic acid for the Lengdong oils and Well E reservoir extracts shows a decreasing trend with increasing degree of biodegradation (Fig. 6-27). All these data suggest that the order of net susceptibility to biodegradation for benzoic acid is (from easiest to hardest) *para-* > *meta-* > *ortho*-methyl benzoic acid. Clearly,

these ratios may reflect both production and destruction processes. The ratio *ortho-/para*-methyl benzoic acid or *meta-/para*-methyl benzoic acid may therefore be an indicator of biodegradation.

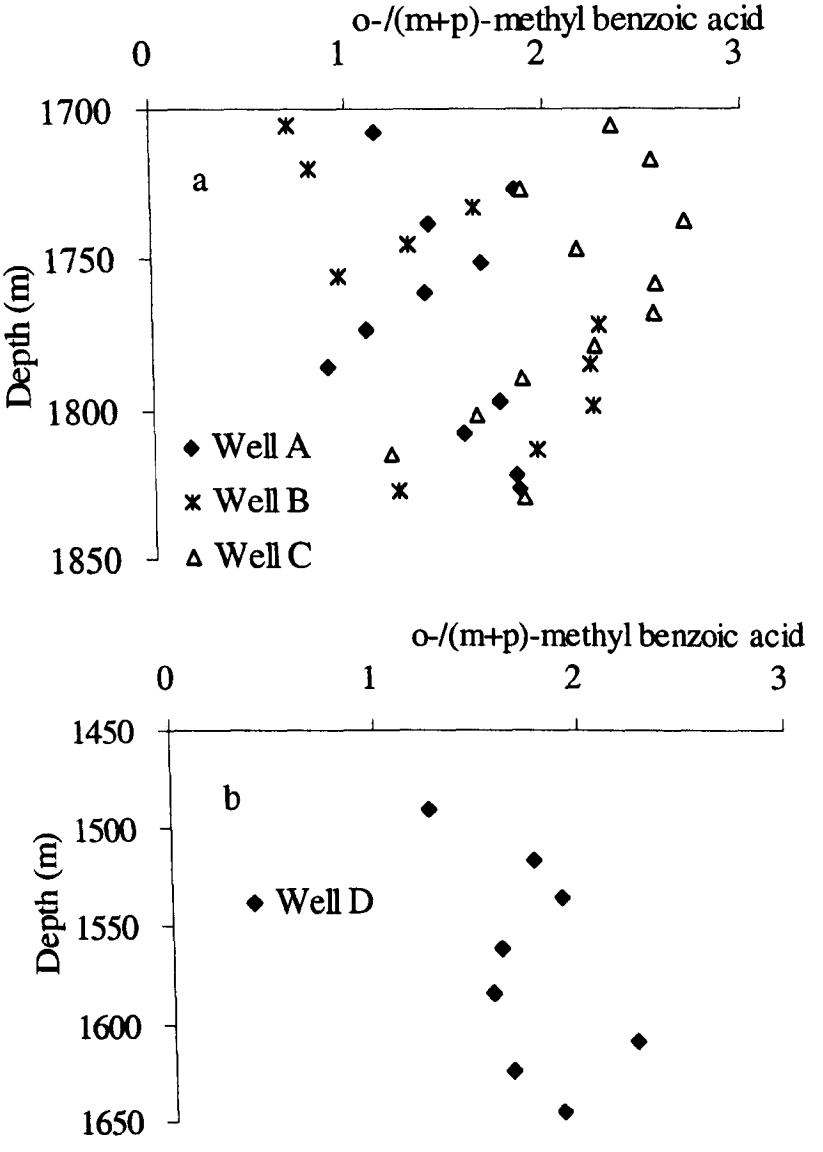

Fig. 6-26. Ratios of *o-/(m+p)*-methyl benzoic acids in the Es3 (a) and Es1 (b) columns.

Anaerobic biodegradation of crude oils carried by Wilkes *et al.* (2000) indicated that under sulphate-reducing condition alkylated benzoic acids are the main metabolic by-products detected in the water phase. The identification and systemic variations of alkylated benzoic acids in this case study confirms the intrinsic relationship between the occurrence of benzoic acids and anaerobic biodegradation, which in turn can be used as an indicator of initial biodegradation of crude oils.

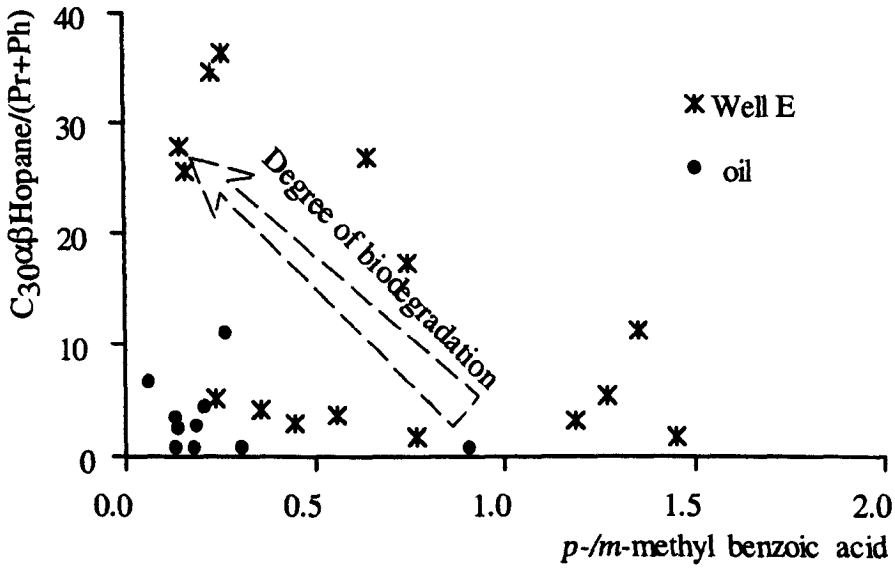

Fig. 6-27. The relationship of the ratios between *p*-/*m*-methyl benzoic acid and C_{30} αβ hopane in the suite of Liaohe oils and reservoir extracts analysed.

7 BIODEGRADATION MODEL AND MODELLING

Knowledge of biodegradation processes is especially critical to the accurate prediction of biodegradation risk in petroleum exploration. The prediction of the degree of biodegradation of oil prior to drilling an exploration well is important for the assessment of the likely value of a prospective exploration target. Clearly, these endeavors require an understanding of the factors that influence biodegradation under the dynamic conditions associated with subsurface systems. Most of the biodegradation predictions presented in the literature are empirical.

The mechanisms of oil degradation in petroleum reservoirs and the involvement of microorganisms are still poorly understood. The actual processes taking place during biodegradation of crude oil in deep reservoirs remain obscure. The site and rates of degradation, the oxidant and the nature of the reduced products are hard to quantify in most cases. It is still impossible to fully predict the biodegradation risk in a reservoir, however, I have coupled a reservoir geochemical study with geological constraints and basin modelling in order to investigate intrinsic biodegradation characteristics. The purpose of this chapter is to present a case study of the impact of mixing, diffusion and biodegradation on oil composition and to quantify these processes.

7.1 Biodegradation indicator

7.1.1 Bulk composition variation in biodegraded oil columns

As discussed in Chapter 4, the bulk C_{15+} petroleum composition data obtained by Iatroscan analysis reflect compositional gradient changes in studied oil columns. The variation in abundance of the saturated hydrocarbons in the Es3 column shows a progressive loss of saturated hydrocarbons (from 45% to ca. 25% oil w/w) over a 130 m vertical interval towards the OWC at ca. 1830m (Fig. 4-2). The bulk composition of the residual oils in the Es1 column is characterized by lower saturated hydrocarbon contents than in the Es3 column but there is still a slight decrease in abundance with depth towards the OWC (Fig. 4-3). Larter *et al.* (2003) suggested that this gradient, coupled with a diffusion reaction model, could broadly estimate the degradation rate constant for oils in the field.

7.1.2 Concentration variation in biodegraded oil columns

The gradients that have been observed in the Lengdong oilfield are the result of interactions between the processes of charging, biodegradation and mixing. Gradients

are clearly seen in individual hydrocarbon profiles. Among the saturated hydrocarbon classes, normal alkanes are usually the first compound type to be consumed by bacteria and archea. The concentration of the *n*-C_{25}-alkane decreases with depth from ca. 5000 μg/g EOM to ca. 10-20 μg/g EOM in the three wells of the Es3 column, wells A and B showing more dramatic changes than Well C (Fig. 7-1a). The concentration of isoprenoid alkanes (represented by phytane) shows similar trends to the *n*-alkane concentration but the gradient is slightly less steep, reflecting the reduced susceptibility to attack compared to the *n*-alkane (Fig. 7-1b). In the Es3 column it is quite obvious from the data that biodegradation has removed substantial amounts of normal and isoprenoid alkanes. In the shallower and more severely biodegraded Es1 column, both *n*-alkanes and isoprenoids have been completely destroyed leaving an aliphatic hydrocarbon fraction comprised largely of branched and cyclic alkanes.

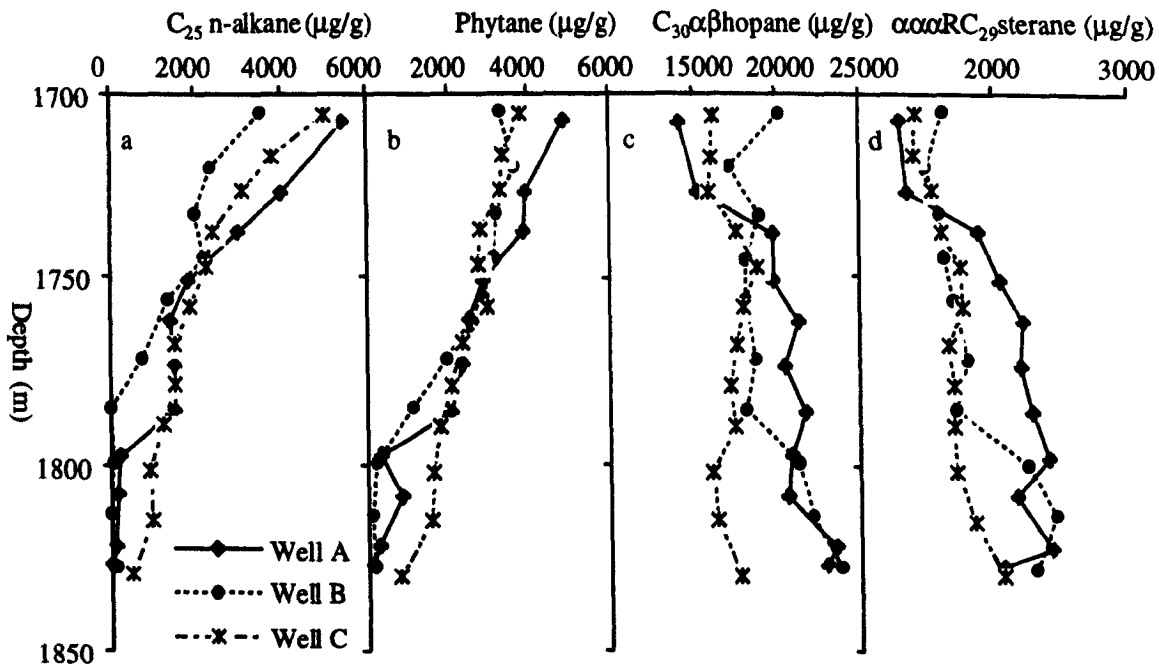

Fig. 7-1. Variation in the concentrations of C_{25} *n*-alkane, phytane, C_{30}-αβhopane and αααRC_{29}-sterane with reservoir depth in the Es3 oil column.

In contrast to the *n*-alkanes and isoprenoid alkanes, the C_{30} αβhopane concentration increases with increasing depth in the Es3 column. This reflects microbial depletion of the more easily biodegradable compounds (e.g., *n*-alkanes), the more resistant hopanes being largely unaffected at this early stage in the biodegradation sequence. The less dramatic change in hopane concentration in Well C (Fig. 7-1c) relates to the less severe degree of biodegradation, the *n*-alkanes still being present throughout the residual oil. Whereas the C_{30}αβhopane concentration increases with depth in the Es3 column, there is a sharp decrease with depth in the lower part of the Es1 column, which is at a more advanced stage of biodegradation (Fig. 7-2). Over

the same depth interval in the Es1 column, there is a concurrent increase in the concentration of $C_{29}\alpha\beta$25-norhopane (Fig. 7-2a, b). Large 'mass balance' discrepancy between the loss of hopanes and the produced 25-norhopanes indicates some other products such as hopanoid acids and demethylated hopanoid acids are also important (Aitken, 2003, personal communication).

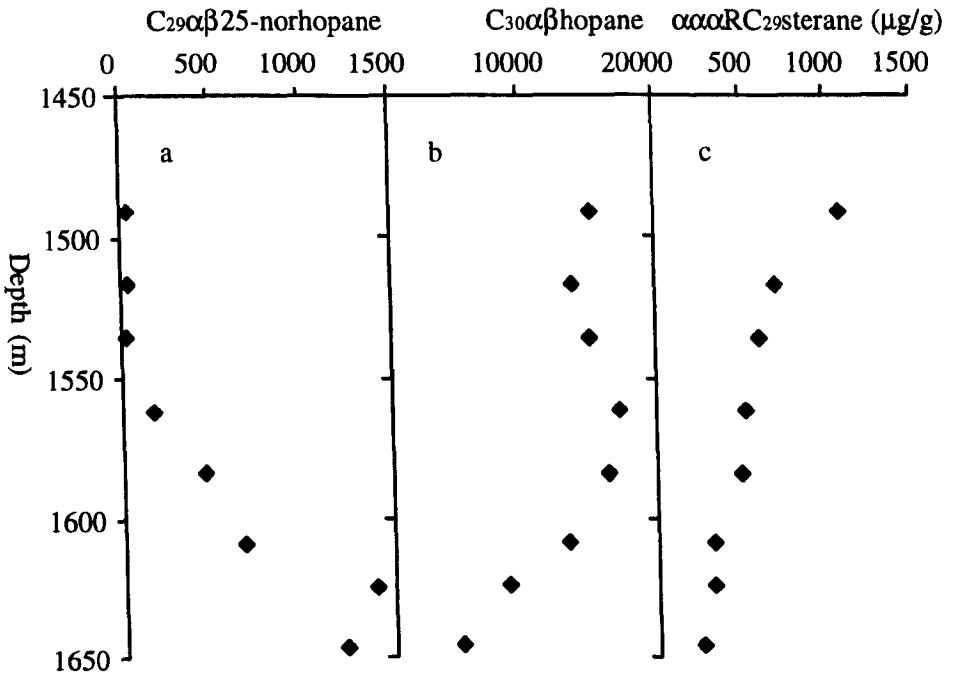

Fig. 7-2. Variation in the concentrations of $C_{29}\alpha\beta$25-norhopane, C_{30}-$\alpha\beta$hopane and $\alpha\alpha\alpha RC_{29}$-sterane with reservoir depth in the Es1 oil column.

The concentration of $\alpha\alpha\alpha RC_{29}$ sterane also shows an overall increase with increasing depth for much of the Es3 column although towards the base of Wells A and B, which are at a slightly more advanced stage of biodegradation than Well C, values begin to decrease (Fig. 7-1d). In the more highly degraded Es1 column, the concentration of sterane shows a continuous decrease with increasing depth (Fig. 7-2c). All quantitative measurements based on compositional changes at the molecular level indicate that the intrinsic level of biodegradation reaches a maximum at the bottom of the depth profile, near the OWC.

The variation in absolute concentrations of $C_{0\text{-}5}$-alkylnaphthalenes, $C_{0\text{-}3}$-alkylphenanthrenes and (C_{20} + C_{21} + C_{26}-C_{28}) triaromatic steroid hydrocarbons (TAS) with depth in the Es3 and Es1 oil columns are shown in Figures 7-3 and 7-4, respectively. The concentrations of $C_{0\text{-}5}$-alkylnaphthalenes show a clear decrease with increasing depth in the Es3 column, from ca. 1000 to 100 μg/g EOM in Wells A and B and to 350 μg/g EOM in Well C (Fig. 7-3a). In the Es1 well, the $C_{0\text{-}5}$-alkylnaphthalene concentrations are much lower than in the Es3 column but still show a decrease with increasing depth, from 267 μg/g EOM at the top of the interval to 75 μg/g EOM at the

bottom (Fig. 7-4a). The variation in concentration of C_{0-3}-alkylphenanthrenes shows the same trend as the C_{0-5}-alkylnaphthalenes in the two column sets (Fig. 7-3b, -4b). The concentration of the TAS is much more variable but appears to show the reverse trend, with values generally increasing with increasing depth in both columns (Fig. 7-3c, -4c). Although there is some scatter in the aromatic HC data, the general trend in the concentration profiles suggests the occurrence of systematic changes in oil composition. These changes again indicate that biodegradation occurs primarily at the base of the oil column and is a major factor in determining the concentration of aromatic components in the reservoired oil.

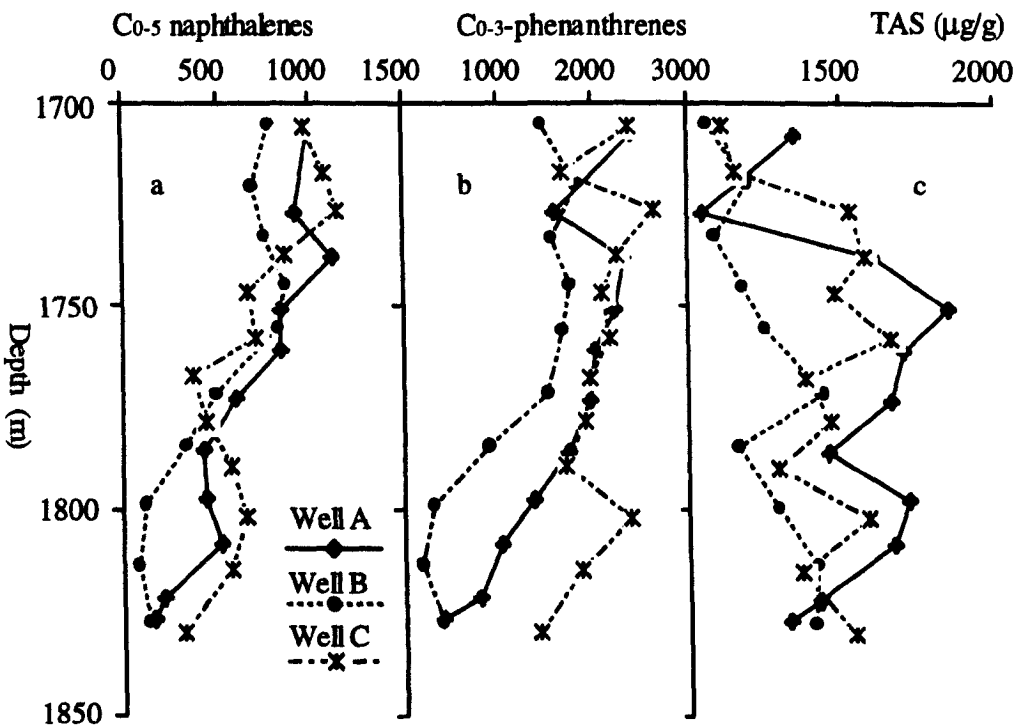

Fig. 7-3. Variation in the concentrations of C_{0-5}-alkylnaphthalenes (a), C_{0-3}-alkylphenanthrenes (b) and TAS in the Es3 column (c).

7.1.3 Biodegradation parameter profile

Several biodegradation indices based on molecular composition have been proposed. Among the most commonly used indices are the ratios pristane(Pr)/*n*-C_{17}, phytane(Ph)/*n*-C_{18}, $C_{30}\alpha\beta$hopane/(Pr+Ph) and $C_{29}\alpha\beta$-25-norhopane/$C_{30}\alpha\beta$hopane (Connan, 1984; Seifert *et al.*, 1984; Peters and Moldowan, 1993; Koopmans *et al.*, 2002). The ratio $C_{30}\alpha\beta$hopane/(Pr+Ph) in the Es3 column increases from an initial mean value of 2 at the top of the Es3 column to > 100 near the OWC in Wells A and B (Fig. 7-5a). Samples from Well C show a less dramatic increase than those from the other two wells, with a maximum value of 16.7 indicating less severe biodegradation. The highly sensitive biodegradation ratio (Pr+Ph)/(*n*-C_{17}+*n*-C_{18}) also increases with increasing depth but reaches a maximum in Wells A and B some distance (20-40 m)

above the OWC, and thereafter decreases towards the base of the column (Fig. 7-5b). This maximum does not appear to have been reached in the less-degraded samples from Well C. It is apparent that both component classes in the ratio are affected by biodegradation in this case study; the lower (Pr+Ph)/(*n*-C_{17}+*n*-C_{18}) values near the OWC in Well A and B may include a larger quantification error when both compound types occur in low abundance. Caution should be taken when using the (Pr+Ph)/(*n*-C_{17}+*n*-C_{18}) ratio to indicate degree of biodegradation, as severe biodegradation or mixing of biodegraded oil with fresh oil may give rise to abnormal and misleading values.

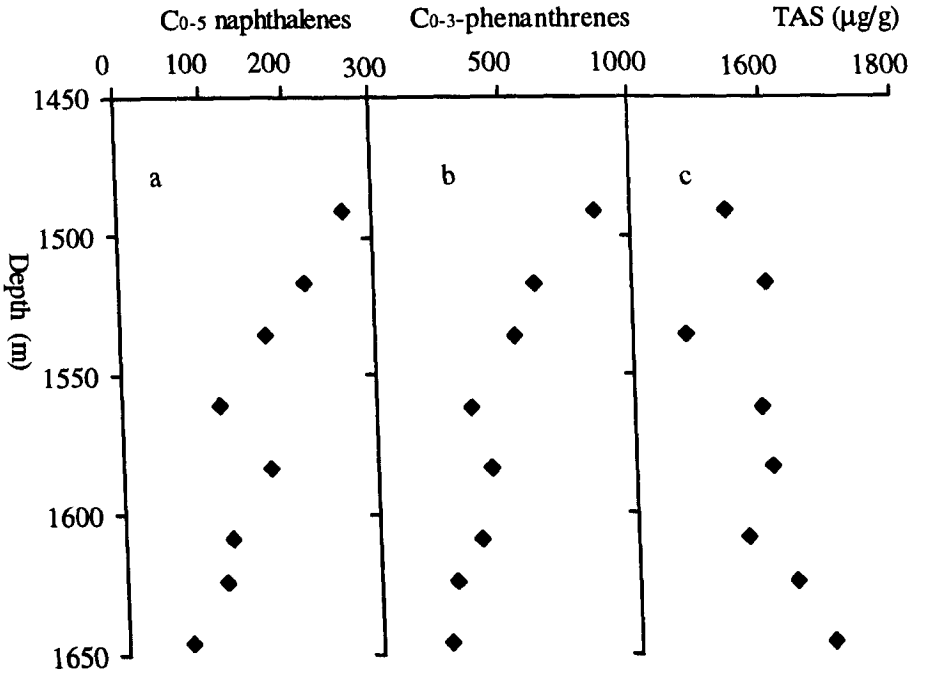

Fig. 7-4. Variation in the concentrations of C_{0-5}-alkylnaphthalenes (a), C_{0-3}-alkylphenanthrenes (b) and TAS (c) in the Es1 column.

The $C_{30}\alpha\beta$hopane/(Pr+Ph) ratio increases consistently with increasing depth over much of the Es1 column, but below 1600 m the trend appears to be reversed (Fig. 7-6a). However, hopane biodegradation is obvious in the Es1 column, seen in the marked decrease in hopane concentrations and a dramatic increase in the concentrations of the corresponding 25-norhopanes. Although the origin of 25-norhopanes is still controversial (Blanc and Connan, 1992; Moldowan and McCaffrey, 1995; Peters *et al.*, 1996), the increase in concentration of the 25-norhopanes unambiguously indicates bacterial transformation. As shown in Fig. 7-6, $C_{29}\alpha\beta$-25-norhopane/$C_{30}\alpha\beta$ hopane ratio remains low and relatively constant over much of the sampled interval but increases dramatically toward the base of the Es1 column i.e., approaching the OWC. This profile is interpreted as being attributable to biodegradation at the OWC and the consequent establishment of diffusion-controlled

concentration gradients within the oil column.

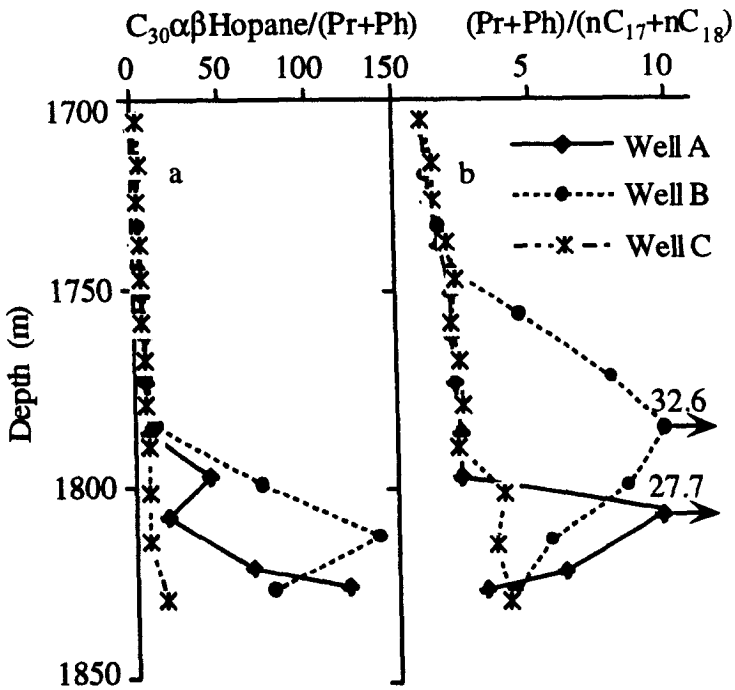

Fig. 7-5. Biodegradation indicator profile in the Es3 column. (a) $C_{30}\alpha\beta$hopane/(Pr+Ph); (b) (Pr+Ph)/(nC_{17}+nC_{18}).

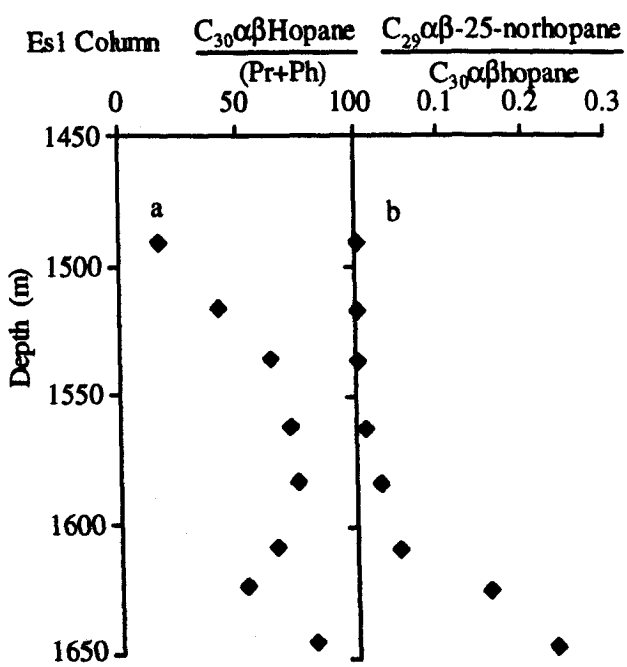

Fig. 7-6. Biodegradation indicator profile in the Es1 column. (a) $C_{30}\alpha\beta$hopane/(Pr+Ph); (b) $C_{29}\alpha\beta$-25-norhopane/$C_{30}\alpha\beta$hopane.

Similarities in the relative susceptibilities to biodegradation of certain aromatic isomers have been observed in several studies. As previous discussion in Chapter 5, 1,3,6,7-tetramethylnaphthalene (TeMN) is readily susceptible to biodegradation whereas 1,2,5,6-tetramethylnaphthalene is more resistant. van Aarssen *et al.* (1999)

proposed the tetramethylnaphthalene ratio 1,3,6,7-TeMN/(1,3,6,7- + 1,2,5,6- + 1,2,3,5-TeMN) as a measure of oil maturity. My study indicates this ratio is actually sensitive to biodegradation. The greater susceptibility of 1,3,6,7-TeMN to biodegradation compared with 1,2,5,6 + 1,2,3,5-TeMN is shown in a decrease in the TeMN ratio with increasing depth in both the Es3 and Es1 columns. The TeMN ratio decreases from 0.5 to 0.3 in Wells A and B of the Es3 column and to 0.4 in the less degraded Well C (Fig. 7-7a), while the ratio decreases from about 0.3 to less than 0.2 in the Es1 column (Fig. 7-8a). The difference in variation at the different sites most probably related to differences in the degree of biodegradation.

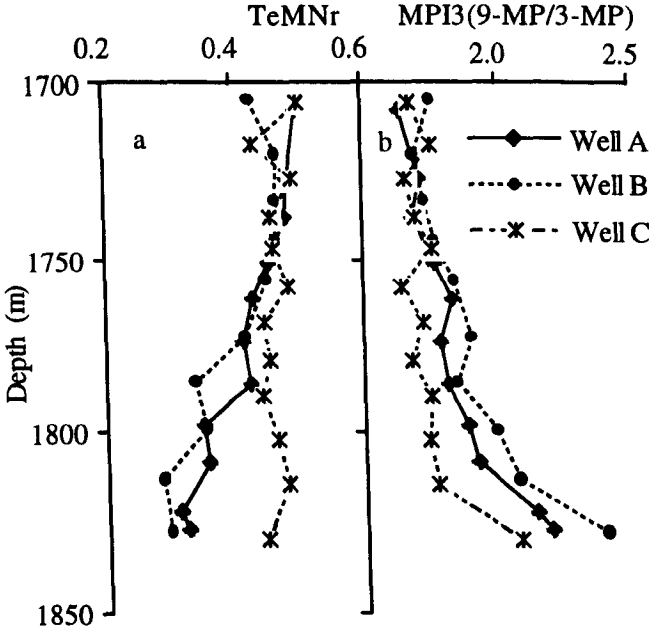

Fig. 7-7. Aromatic hydrocarbon biodegradation indicator profile in the Es3 column. (a) TeMN ratio = [1,3,6,7- /(1,3,6,7- +1,2,5,6-+1,2,3,5-TeMN)]; (b) 9-MP/3-MP.

The relative abundances of the methylphenanthrene (MP) isomers have been used as maturity parameters in several studies (Radke and Welte, 1983; Budzinski *et al.*, 1995). However, alkylphenanthrene distributions are also influenced by biodegradation. This study confirms previous observations (Rowland *et al.*, 1986; Budzinski *et al.*, 1998) that 9-methylphenanthrene is more resistant to biodegradation than other methylphenanthrenes. The ratio of 9-MP/3-MP shows a consistent increase with increasing depth in both oil columns. In the Es3 column, the 9-MP/3-MP ratio increases from 1.7 to 2.3 (Fig. 7-7b) but the most pronounced change occurs in the Es1 column where values increase from 3 to 8 (Fig. 7-8b).

The relative abundances of several other aromatic compounds have also been shown to be controlled to some extent by biodegradation e.g., the isomeric distribution of the alkylbiphenyls and alkyldiphenylmethanes (Trolio *et al.*, 1999) and

methylated 6-isopropyl-2-methyl-1-(4-methylpentyl)naphthalene and retene relative to their non-methylated counterparts (Bastow *et al.*, 1999). Since these compounds occurred at very low concentrations in present sample set, no further detailed study was carried out.

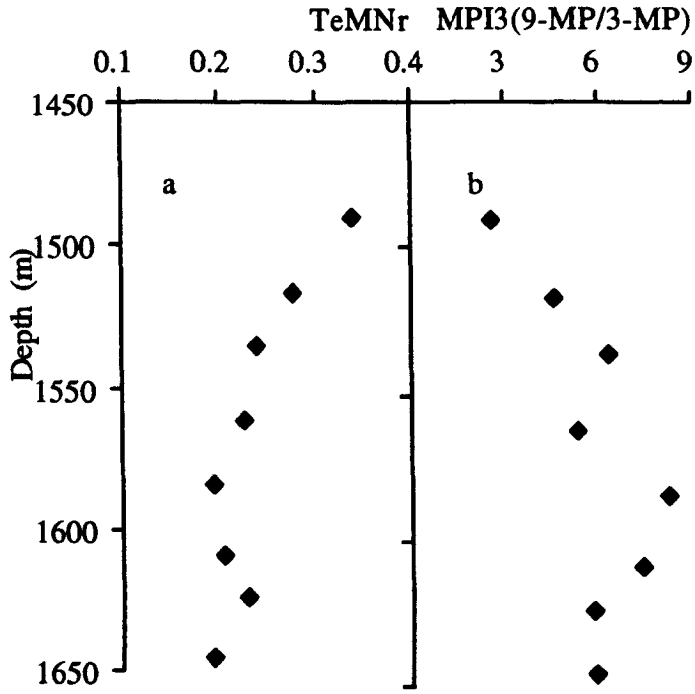

Fig. 7-8. Aromatic biodegradation indicator profile in the Es1 column. (a) TeMNr[1,3,6,7- /(1,3,6,7- +1,2,5,6-+1,2,3,5-TeMN)]; (b) 9-MP/3-MP.

7.2 Reservoir temperature and residence time

Reservoir temperature is one of the primary controls on the biodegradation degree, which can provide an empirical constraint in the prediction of biodegradation risk for a prospective target (Fig. 7-9) (Hunt, 1979; Connan, 1984; Pepper and Santiago, 2001; Larter *et al.*, 2003).

Oil API gravity versus reservoir depth from the Lengdong oilfield (Fig. 3-23) clearly indicates that biodegraded oils are found in reservoirs shallower than 2200 m (reservoir temperature less than 80 °C). While degradation level generally decreases with increasing reservoir temperature and low API heavily degraded oils are increasingly dominant in shallower reservoirs, however, at any temperature (or depth) a wide range of commercially sensitive oil properties such as viscosity or API gravity can be found in subsiding basins (see Chapter 3 for more details).

Data from the Lengdong oilfield confirms the overall control of subsurface temperature on degree of biodegradation but it is not straightforward. As discussed in previous chapters, biodegradation gradients are common in the Lengdong biodegraded

columns. The distance from the OWC takes primary control on the degree of biodegradation and the more severely biodegraded oil occurs at the bottom of the oil column where the temperature is normally higher than that at the top (Fig. 7-10). Geological controls such as fresh oil charge, mixing, water leg size etc. provide the main constraint on oil degradation rather than temperature regime. Thus biodegradation prediction can not purely rely on reservoir temperature.

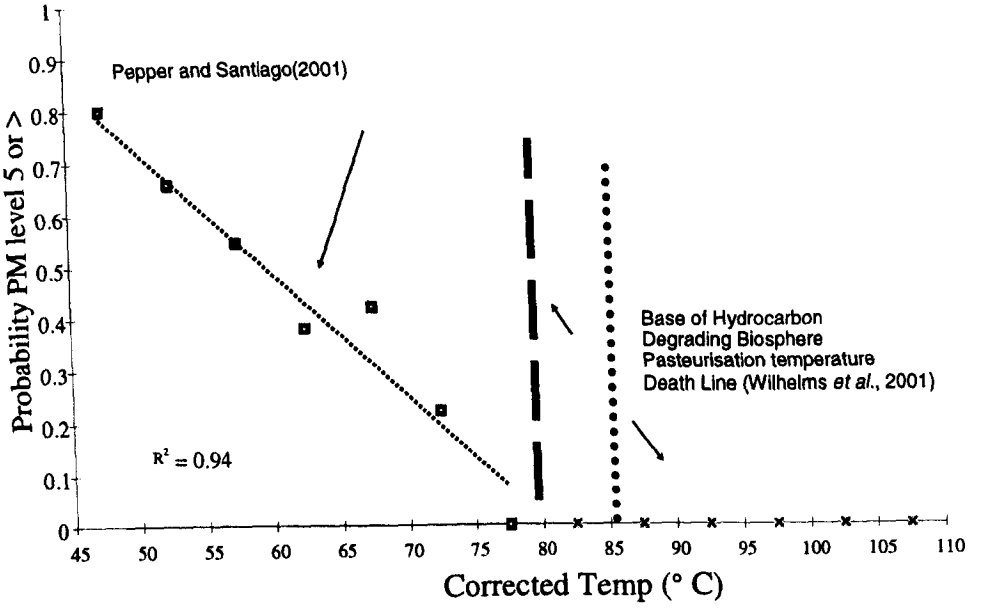

Fig. 7-9 Temperature – probability of biodegradation (PM Level 5+) (After Pepper and Santiago, 2001).

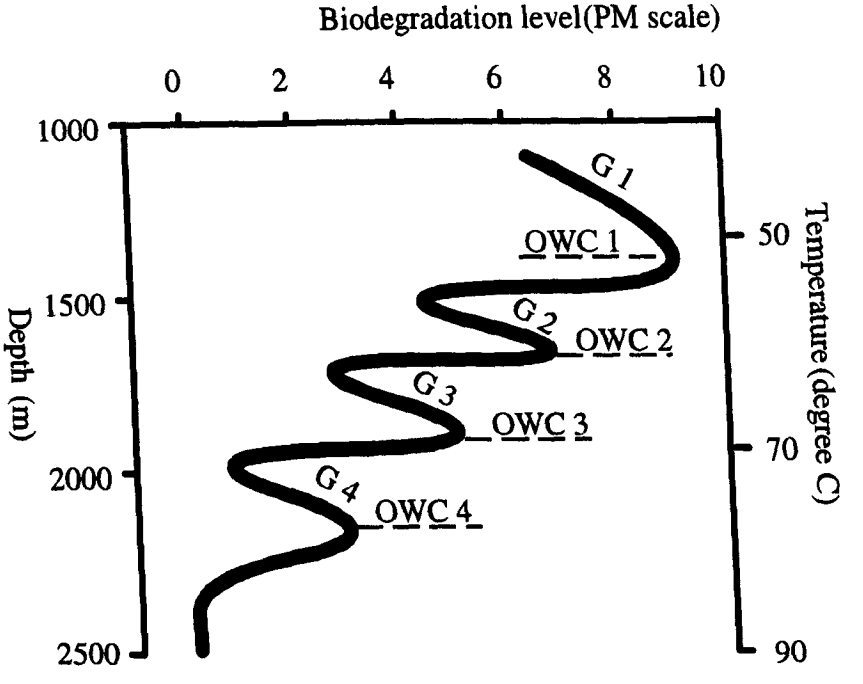

Fig. 7-10. Overall control of reservoir temperature on biodegradation levels in the Lengdong oilfield.

Under the biodegradation cut-off temperature, oil residence time is a critical

factor for how severe oil will be biodegraded due to the time available for bacterial activity. For example, an oil-charged reservoir at < 50°C, charged over a long period of time, has a greater biodegradation risk than a reservoir that was rapidly charged recently, but still under 50°C (Yu *et al.*, 2002). This implies that reservoirs undergoing recent charging with hydrocarbons may not have enough time for bacteria to degrade the oil, resulting in more mixed signatures and probably better oil quality. Residence time is important though biodegradation can occur in very short geological time.

7.3 Effect of water leg size

A wide variety of factors can affect biodegradation; these include temperature regime, formation water salinity, rock matrix grain size, bacterial consortium type and redox conditions (Connan, 1984; Barnard and Bastow, 1991; Bernard and Connan, 1992; Simoni *et al.*, 2001). However, there is no obvious difference among these factors for the three Es3 wells since they are so closely located (Huang *et al.*, 2002). So what has caused the different degree of biodegradation observed in the three Es3 wells, especially Well C compared to Well A and B?

To address this question, the reservoir topology has been investigated. In reservoir pore systems, oil coexists with water and dissolved solutes. The reservoir saturated with oil can be referred as oil leg. Below the oil leg, in the water-saturated part of the reservoir is called water leg. The water leg can vary in thickness and extent within the reservoir (water leg size) and in its degree of communication with the oil zone above. The presence and size of a water leg can also affect the degree of biodegradation in a reservoir since water is an essential requirement for biodegradation.

The stratigraphic structure of the reservoirs in Wells A, B and C comprising the Es3 oil column was studied in order to determine whether there was any relationship with the degree of biodegradation in the three wells. It was found that whereas Wells A and B have thick water legs in contact with the oil column, in Well C the water leg is separated from the oil leg by a tight layer comprised of about 15 m of shale (Fig. 7-11) i.e., the reservoir has filled almost down to the local under-seal. The geochemical data previously presented indicate that the oils in Wells A and B are more severely degraded than those in Well C. This suggests that water leg size and degree of contact with the oil leg is an important factor in controlling biodegradation within reservoirs - most likely by determining the nutrient supply to the degradation zone.

7.4 Mixing

The common co-occurrence of *n*-alkanes and demethylated hopanes in the alkane

fractions of many biodegraded oils can be explained by mixing process (Rooney *et al.*, 1998). Other geochemical parameters such as an unusually low API, high sulfur content, or a high viscosity for the oil's apparent molecular composition also suggest a complex origin for the oil (Khavari-Khorasani *et al.*, 1998). The occurrence of mixing of oils in the Es3 column is not very distinct since no obvious 25-norhopanes was co-existed with *n*-alkanes. The mixing process can be illustrated by subtle differences in the calculated thermal maturity (based on biomarker isomerization) of the residual oils since most reservoirs receive progressively more thermally mature fluids over time and slight differences can be observed within the oil column due to variation in the burial depth/average temperature of the source rock from which the petroleums were expelled.

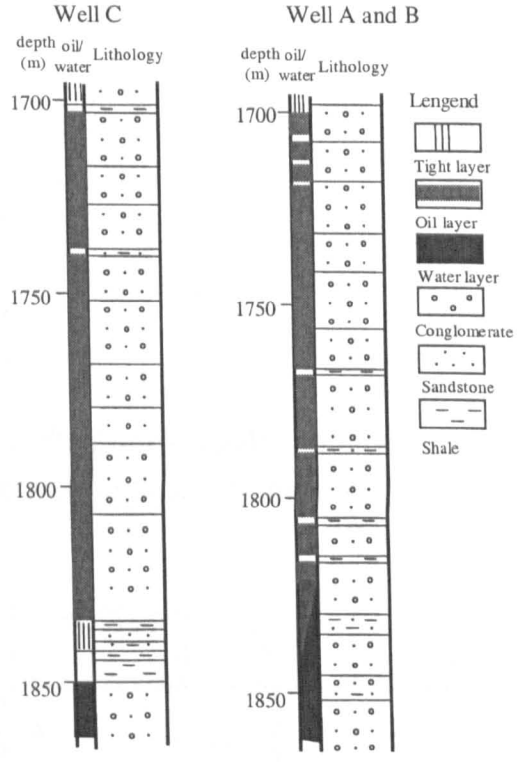

Fig. 7-11. Stratigraphic structure of the Es3 column showing differences in the OWC between Wells A/B and Well C.

The ratio C_{29}-steranes $\beta\beta/(\alpha\alpha+\beta\beta)$ is one of several commonly used maturity indicators. Higher ratio values indicate higher maturity within oil window (Mackenzie, 1984). However, the regular steranes are only moderately resistant to microbial attack and their distributions can be affected at more advanced stages of biodegradation. There has been much discussion in the literature as to the order of sterane susceptibility to degradation. There is a preference for biological epimers to be attacked by bacteria (Seifert and Moldowan, 1979; Connan, 1984; Seifert *et al.*, 1984; Peters and Moldowan, 1993), which will affect maturity ratios involving sterane abundance by this preferential degradation.

The C_{29}-steranes ββ/(αα+ββ) ratio in the Es3 column decreases slightly with increasing depth, from 0.32 at the top to 0.30 near the OWC. The slightly higher maturity signals at the top of oil column suggest that it has received a late-arriving charge of slightly more mature oil. The increase in the ratio at the base of (the more biodegraded) Wells A and B may be due to biodegradation (Fig. 7-12a). The more pronounced continuous increase in the ratio with increasing depth in the Es1 column can more confidently be attributed to biodegradation (Fig. 7-13a).

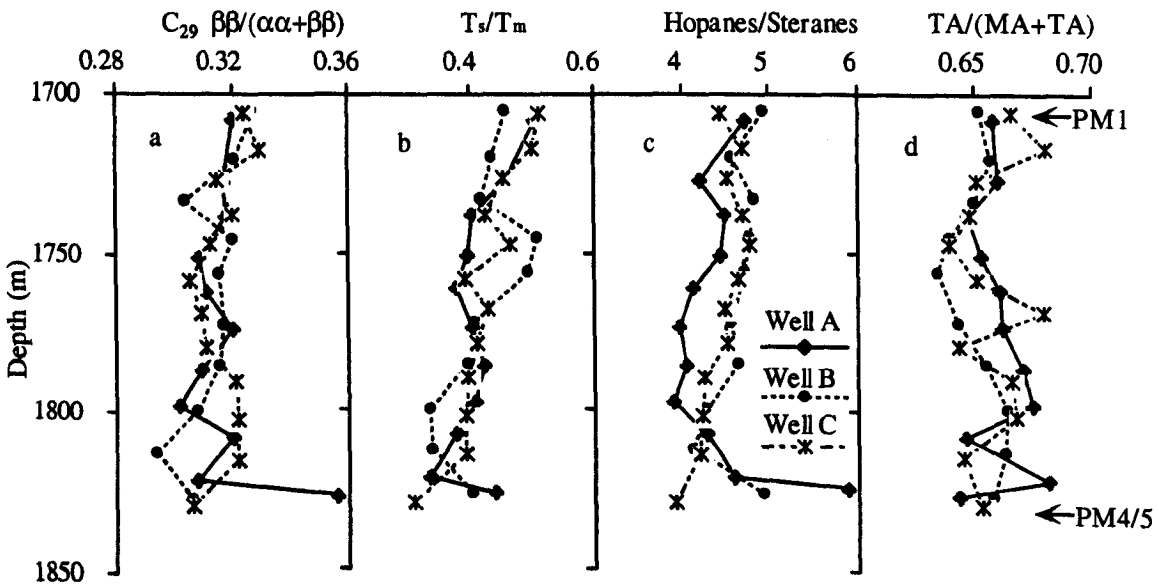

Fig. 7-12. Variation in maturity parameter values with depth in the Es3 oil column, indicating charge of more mature fluid at the top and occurrence of biodegradation near the OWC.

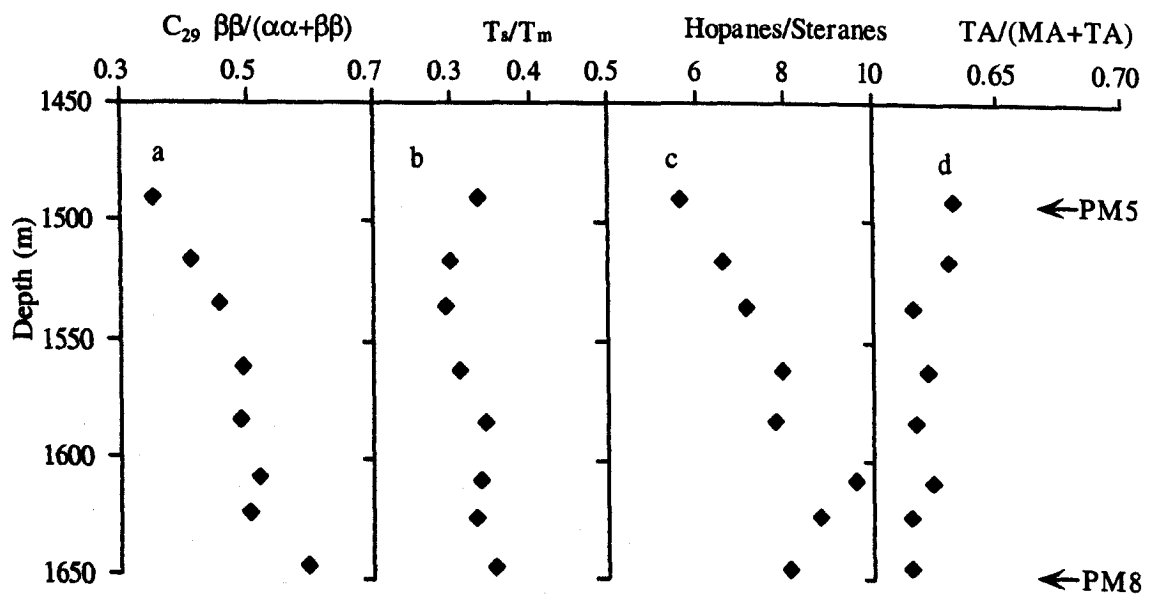

Fig. 7-13. Variation in maturity parameter values with depth in the Es1 column.

The ratio 18α(H)-22,29-30-trisnorneohopane/17α(H)-22,29-30-trisnorhopane

(Ts/Tm) shows a similar variation to the C_{29}-steranes $\beta\beta/(\alpha\alpha+\beta\beta)$ ratio. Since the oils in the Lengdong area have the same source of consistent organic facies, then the Ts/Tm ratio may be considered as more or less indicative of the maturity of the oil (Mackenzie, 1984). However, biodegradation also affects the Ts/Tm ratio, with Tm being slightly more susceptible than Ts (Peters and Moldowan, 1993). The Ts/Tm ratios in the Es3 column decrease from 0.50 to 0.38 with depth. The higher Ts/Tm ratio in the oils at the top of the reservoir suggests higher maturity due to recent charging. The increase in the Ts/Tm ratio in the Es3 column at the base of Wells A and B is attributed to biodegradation (Fig. 7-12b). In the Es1 column, the Ts/Tm ratio is relatively low but the increase in values with depth over most of the sampled interval is again attributed to biodegradation (Fig. 7-13b).

The hopane/sterane ratio is often used as a measure of the relative inputs of prokaryotic versus eukaryotic debris (Peters and Moldowan, 1993). However, the hopane/sterane values also are affected by thermal maturity and biodegradation. Hopane/sterane ratios progressively increase with increasing maturity, resulting largely from the different generation characteristics of these two biomarker compound classes (Requejo, 1994). Generally decreasing hopane/sterane ratios with depth in the Es3 column indicate a more mature oil charge at the top of the column whereas the dramatic increase in hopane/sterane ratios in Wells A and B near the OWC is more probably caused by biodegradation (Fig. 12c). Systematically increasing hopane/sterane ratios with depth in the Es1 oil column clearly indicate biodegradation effects (Fig. 13c).

Molecular evidence in support of the occurrence of mixing in the two oil columns can also be found by comparison of the internal consistency in aromatic steroid maturity parameters. An increase in the extent of aromatization of the monoaromatic steroid hydrocarbons is observed with increasing maturity and the monoaromatic steroid aromatization parameter [TA/(TA + MA)] is commonly used to determine the thermal maturity of oil (Mackenzie *et al.*, 1981). The TA/(TA + MA) ratios in the Es3 and Es1 oil columns are within a very narrow range, indicating a very narrow maturity span for the sample suite. There appears to be little consistent correlation with depth in the Es3 oil column (Fig. 7-12d) but in the Es1 column ratio values tend to show a more consistent decrease with increasing depth (Fig. 7-13d). The slightly higher values at the top of the Es3 column may suggest a subtle maturity difference whereas the decrease towards the base of the Es1 interval is more likely to be attributable to biodegradation since triaromatic steroid hydrocarbons are slightly more susceptible to biodegradation than monoaromatic steroid hydrocarbons at advanced

stages of biodegradation (Wardroper *et al.*, 1984; Lin *et al.*, 1989).

It is interesting to note that the depth-plots of the maturity parameters reveal a markedly different trend for the two columns (Figs. 7-12 and 13). In the Es3 column, these parameters more-or-less reflect maturity variation since biodegradation is at an early stage, whereas in the Es1 column the ratio values are misleading in a maturity context in that they are most likely to have been affected by severe biodegradation. The subtle but consistent differences in maturity of samples from the top of the Es3 column suggest filling of different segments of the reservoir by oil charges from the same source kitchens but at slightly different stages of thermal maturity. The top of the column has been charged with slightly more thermally mature petroleum than the lower part. This proposal is supported by Koopmans *et al.*'s (2002) diffusion model which suggested that the observed large variation in oil viscosity in the Es3 reservoir in the Lengdong oilfield was due to mixing, to various extents, of heavily biodegraded oils with less degraded oils.

Mixing of a biodegraded early oil charge and an undegraded late oil charge in the Es3 column is also supported by changes in the concentrations of both vulnerable and conservative tracers. Since the hopanes have not been significantly affected by biodegradation in the Es3 column, their concentrations can serve as an 'internal standard' when assessing the degree of biodegradation. In the less biodegraded Well C sample set, the concentration of hopanes in the residual oil increases from 4% w/w oil at the top of the interval to 5% w/w oil at the bottom, where the *n*-alkanes tend to be depleted (Fig. 7-14). In Well B the concentration of hopanes remains almost constant while that of the *n*-alkanes drops from 4% w/w oil to almost zero; there is, however, a large variation in hopane concentrations (4.8% - 6.5% w/w oil) when the *n*-alkanes have been completely removed. In Well A some samples are characterized by high concentrations of both hopanes and *n*-alkanes, whereas other samples are characterized by an absence of *n*-alkanes and a large variation in hopane concentration. No single consistent relationship between *n*-alkane and hopane concentrations is evident in the data (Huang *et al.*, 2004) (Fig. 7-14).

The most likely explanation for the variability in the data and the lack of a simple relationship between *n*-alkane depletion and hopane enrichment is multiple local charging and mixing during biodegradation. Multiple charging and continuous biodegradation lead to depletion of the most vulnerable components of the oil such as *n*-alkanes and isoprenoid alkanes, and concentration of the more refractory components such as hopanes and aromatic steroid hydrocarbons. In a single charge reservoir, hopane concentrations increase by about 25% as biodegradation removes

most of the *n*-alkanes. The occurrence of relatively high concentrations of *n*-alkanes together with high hopane concentrations may reflect an episode of reservoir recharge and subsequent mixing of the recharge oil with previously charged, biodegraded oil. This simple physical mixing between biodegraded and fresh oil will result in enrichment of the more refractory components of the oil although this will not necessarily produce a linear gradient. Thus, the charge history and the rate of mixing of fresh oil into the system are likely to be dominant controls on the apparent level of degradation within a reservoir.

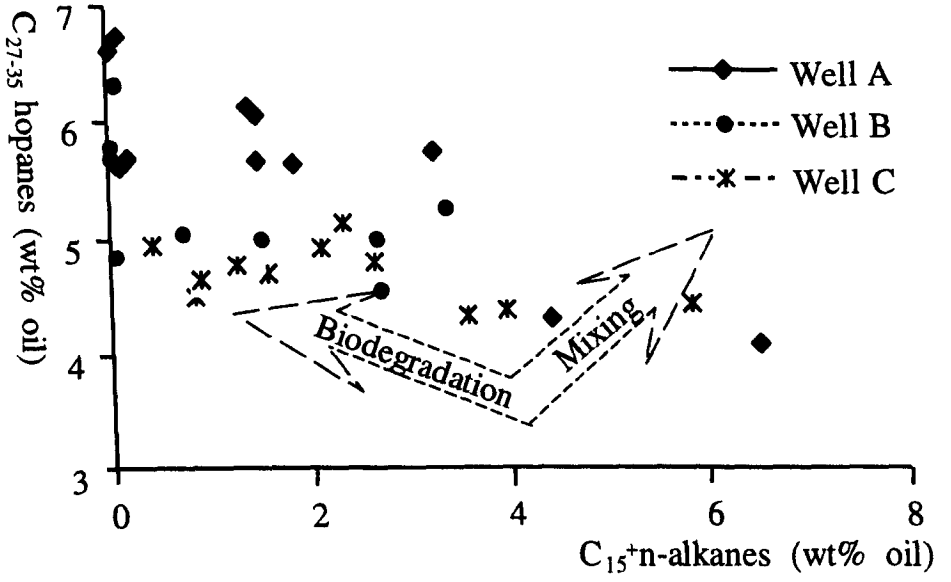

Fig. 7-14. Relationship between hopanes and *n*-alkanes concentrations, interpreted as resulting from a combination of biodegradation and mixing of undegraded oil with biodegraded oil.

7.5 Nutrients supply

Phosphorus and nitrogen are essential macronutrients necessary for the survival of virtually all living organisms. In groundwater systems, these nutrients can be quite scarce and can represent limiting elements for growth of subsurface microorganisms. In carbon-rich anoxic groundwaters where P and N are scarce, feldspars that contain inclusions of P-minerals such as apatite are preferentially colonized over similar feldspars without P (Rogers *et al.*, 1998). Studies carried out by Bennett *et al.* (2000, 2001) suggested that mineral weathering by bacteria is driven by the nutrient requirements of the microbial consortium with microorganisms destroying only beneficial minerals. Conversely, the subsurface distribution of microorganisms may, in part, be controlled by the mineralogy and by the ability of an organism to take advantage of mineral-bound nutrients.

Almost no nutrient studies under reservoir condition are available in literature.

This study investigates the possibility of crude oil itself providing nitrogen as a nutrient in the form of nitrogen compounds and total oil nitrogen content in biodegraded oils.

The change of the nitrogen content with increasing degree of biodegradation is similar to that of the carbazole concentration (see Chapter 6 for details). In the Es3 column, biodegradation level ranging from PM level 1 to 5, oil nitrogen content as well as the concentrations of carbazoles, benzocarbazoles and dibenzocarbazoles first increase until PM 3 then sharply decrease near the OWC at the bottom of the columns (PM 4-5) (Fig. 7-15). In heavily degraded Es1 column, biodegradation level ranging from PM level 5 to 8, oil nitrogen content remains relatively constant while nitrogen-containing compounds dramatically decrease in the concentrations toward the OWC (Fig. 7-16). The observation of a slight increase in total nitrogen contents and carbazole concentrations in the upper part of the Es3 column may be due to the fact that significant carbazole degradation has not yet begun in these samples and their relative enrichment is the result of depletion of other components like *n*-alkanes, isoprenoids, etc. Their sharp decrease in the lower part of the Es3 column and Es1 column where degradation is more severe may be the result of biodegradation itself, i.e. small amounts of petroleum nitrogen can be used during biodegradation above PM 3 but at lower degrees of biodegradation nitrogen as an essential nutrient has to be supplied from other sources. This study implies that only at high level of biodegradation nitrogen derived from oil may be useable as a nutrient.

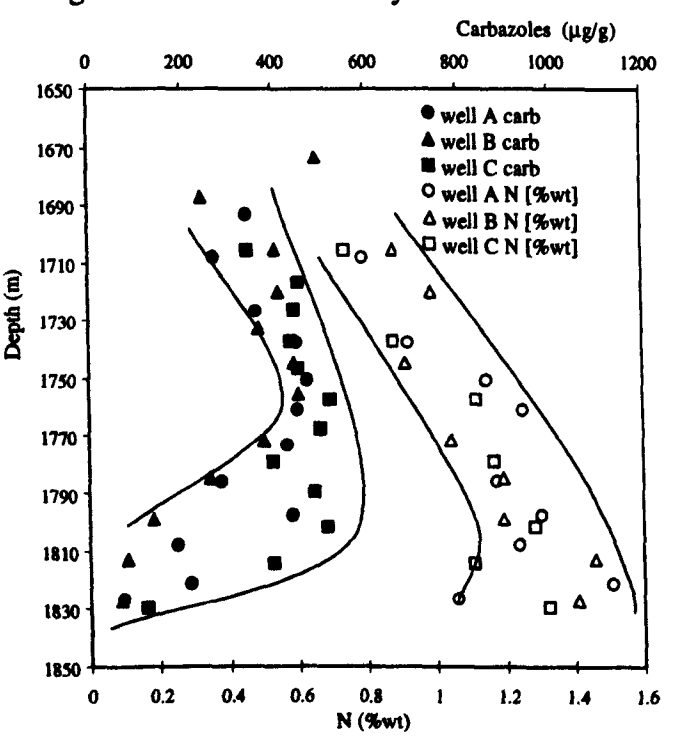

Fig. 7-15. Carbazole concentration and nitrogen content of core extracts from the Es3 column (Bacchus unpublished data).

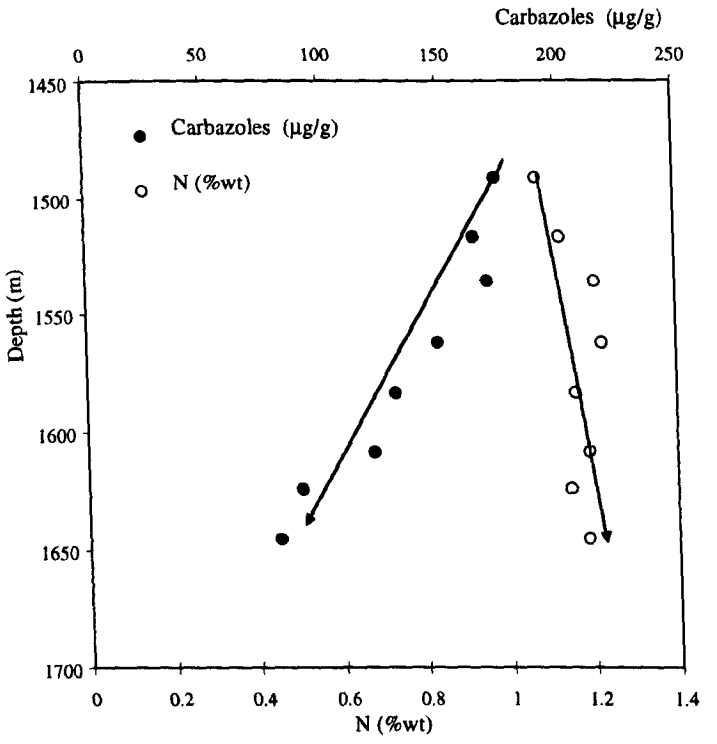

Fig. 7-16. Carbazole concentration and nitrogen content of core extracts from the Es1 column (Bacchus unpublished data).

It is obvious that oil biodegradation rate is not limited by electron donor supply (i.e. hydrocarbons) but by supply of nutrients or oxidants. Nutrients such as phosphorus are probably supplied by mineral dissolution reactions analogue to these occur in underground water (Rogers *et al.*, 1998; Bennett *et al.*, 2000; 2001). Biodegradation, like inorganic diagenesis in many petroleum reservoirs, may be isochemical involving mass transport of hydrocarbons, nutrients and oxidant largely within the reservoir. Figure 7-17 combines hydrocarbon variations in the Lengdong oilfield with nutrient consideration to summarize previous discussion. Hydrocarbons diffuse towards the oil water contact where they are degraded by microorganisms living near the oil water contact utilizing nutrients derived from the water saturated zone below the oil column. Fresh oil is charged to the reservoir contemporaneously. Compositional gradients reflect a complex charge and degradation scenario.

7.6 Biodegradation conceptual model

The complexity of the interplay of biological, chemical and physical mass transport processes in biodegradation suggests that computer modelling will be powerful tool to further our understanding of the mechanisms involved and to classify the factors which constrain biodegradability (Larter *et al.*, 2003). With this aim, a conceptual biodegradation model was proposed to provide a coherent approach to ascertain the impact of degradation on petroleums and to predict biodegradation risk for

an exploration target (Huang *et al.*, 2004) (Fig. 7-18).

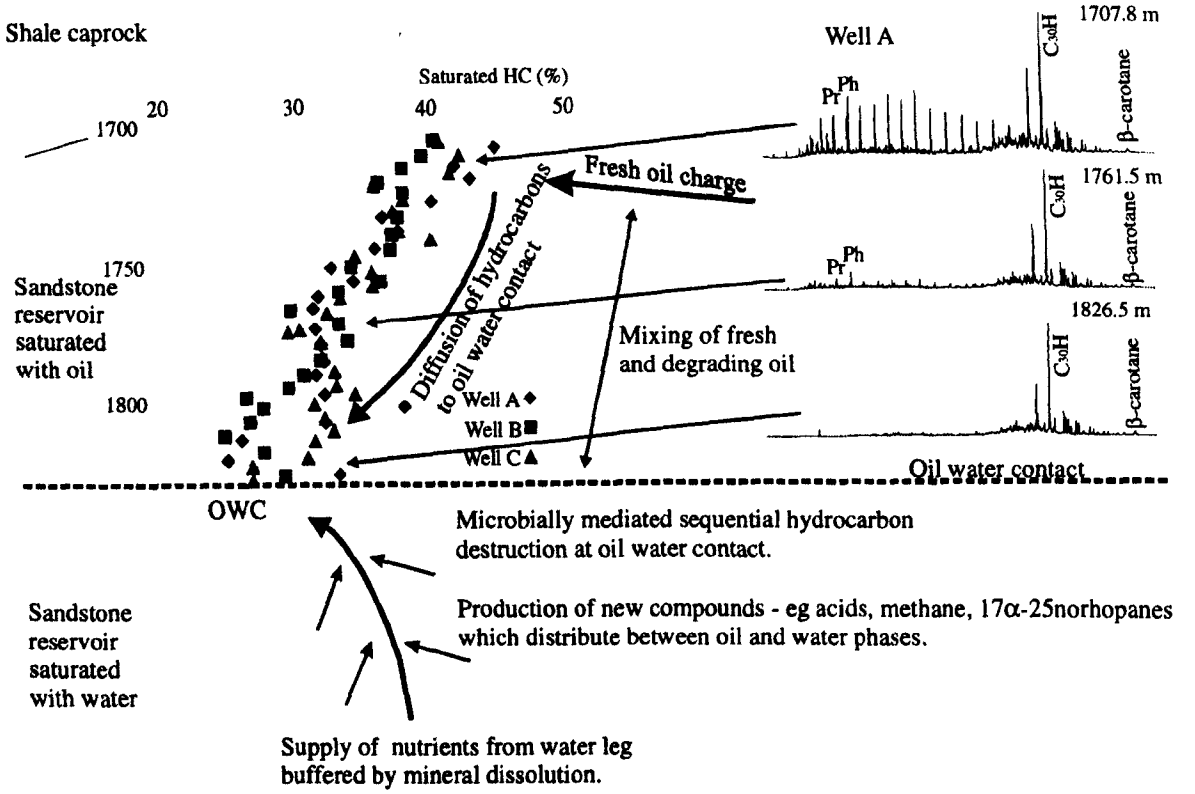

Fig. 7-17. Integrated plot shows saturated hydrocarbon contents and gas chromatograms of the Lengdong reservoir extracts coupling with nutrients consideration for oil biodegradation (Modified from Head *et al.*, 2003).

In the biodegraded oil columns described here, clear compositional gradients and a range in degree of biodegradation are observed at different sites within the same petroleum system. Biodegradation is confined mainly to a narrow region at or near the OWC. The occurrence of compositional gradients in biodegraded oil columns implies hydrocarbon diffusion towards the OWC and mass transport control on degradation rates. This in turn implies that the diffusive transport of nutrients and electron acceptors from the water leg to the site of biodegradation is the rate limiting factor. The diffusion of nutrients in the water leg may be adequate to supply the degradation zone in the Lengdong oil field. Biodegradation in some oil reservoirs may, therefore, be 'isochemical' i.e., involving only mass transport of hydrocarbons, nutrients and oxidants within the reservoir (Larter *et al.*, 2003).

Reservoir topology or structure will be important as regards the rate and site of biodegradation. The overall rate of biodegradation will depend upon the areal extent of the biodegradation zone (at the OWC), the volume of the oil and water legs (determining nutrient availability) and the degree or ease of contact between them (determining nutrient accessibility). As in many oilfields, there is no aqueous geochemical evidence for extensive water flow in the aquifer; it is therefore likely that

the volume of the aquifer will control the supply of nutrients and electron acceptors accessible by diffusion to organisms living near the oil-water contact. The size of the water leg relative to that of the oil leg may therefore be a key variable in controlling the rate and extent of biodegradation (Larter *et al.*, 2003) (Fig. 7-18a). The field case study described here indicates that where reservoirs are filled by oil down to an under-seal which prevents direct access to a water leg, if present (e.g., the shale in the Well C), the oils are frequently less biodegraded than nearby oil columns with 'accessible' water-legs (Wells A and B).

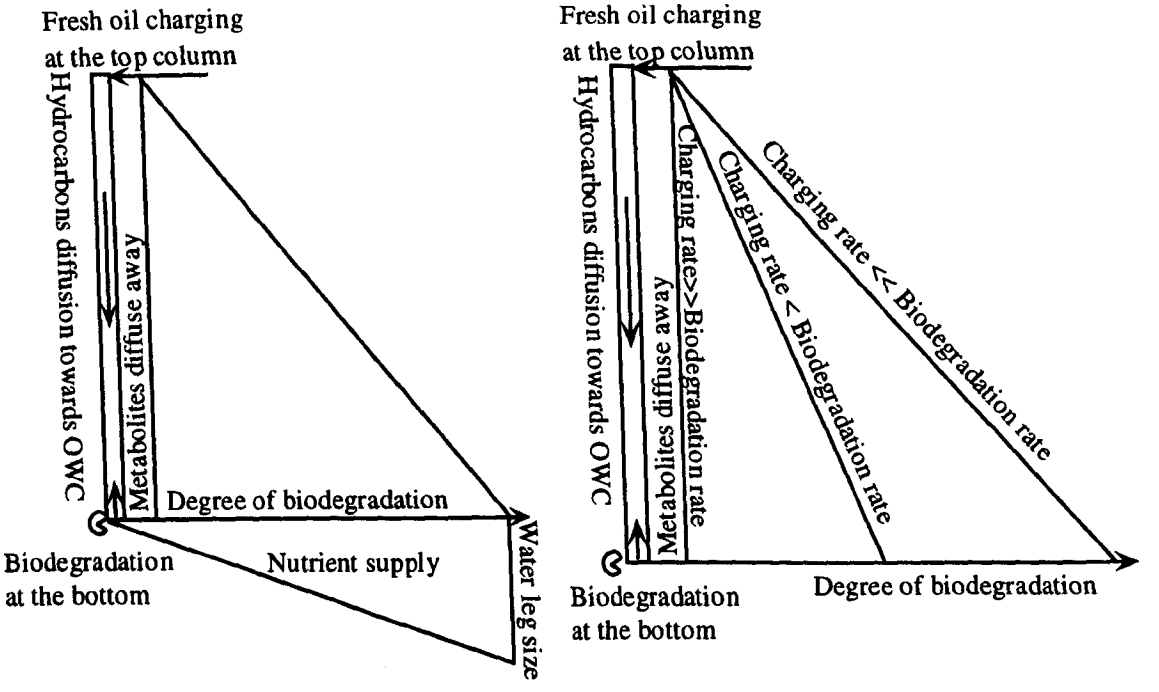

Fig. 7-18. Conceptual biodegradation model.

Compositional gradients within oil columns are controlled by the relative rate of mixing and biodegradation. In permeable reservoirs, mass transfer by diffusion and mixing processes over geological time (England *et al.*, 1987) will tend to result in the reservoired oil having a homogenous composition. However, if the initially accumulated oil is biodegraded and there is subsequently another charge (or charges) of non-biodegraded oil to the reservoir, then the occurrence of compositional gradients will be controlled by relative intensity of diffusion, mixing and biodegradation. The mixing of oils through continuous charging and diffusion of 'fresh' oil towards OWC and the diffusion of metabolites away from the reaction site may be considered as one of the most important factors controlling the biodegradation process. Compositional gradients can be conserved in biodegraded petroleum columns only if the rate of diffusive mixing is similar to or lower than the rate at which the hydrocarbons are removed. In reservoirs where diffusive mixing within the oil column is more rapid than the degradation of alkanes near the OWC, large measurable

compositional gradients throughout the oil column would not be expected to occur, and the diffusion of hydrocarbons to the OWC zone would not be the rate determining step in the biodegradation process (Larter *et al.*, 2003). The observed compositional differences in the Lengdong petroleum columns are consistent with diffusion being the primary mixing process and are useful in assessing whether the basic assumptions made for the model are adequate (Fig. 7-18b).

The ability to predict spatial variations in bulk-oil properties within a reservoir will be of significant benefit to the oil production industry. Although Smalley *et al.* (1997) successfully tracked bulk oil properties within a reservoir using geochemical parameters and analysis of densely sampled core material; they found it very difficult to map the data due to the simultaneous occurrence of biodegradation and mixing. The model proposed here can make such predictions more precise and direct, since the degree of biodegradation and the presence of a mixed charge are not random events. This conceptual model involves all of the main processes involved in the biodegradation of an oil column and opens the possibility of model-driven prediction of oil properties and production sweetspots in reservoirs.

7.7 Biodegradation Modelling

Biodegradability of organic compounds is easily demonstrated in the laboratory and the method most often used involves microcosms. In general, a quantity of the compound in question is placed in a sealed vessel with some combination of soil and water. Trials are conducted with both active and sterilized microcosms so that biotic mass loss can be differentiated from abiotic losses. However, quantification of mass reduction is difficult to demonstrate in field situations since lab approaches cannot reproduce the true subsurface conditions encountered at actual reservoir sites, even though it provides a useful means of controlling and studying the parameters. This suggests direct comparison of deep biosphere processes with those occurring in nutrient rich surface or lab microcosm environments may not be appropriate. Therefore, geochemical modelling is required to tackle this complicated reservoir biodegradation process. The model applied in present study is called Cyclops, which has been developed by Larter *et al.* (Bacchus unpublished result). This is a compositional degradation modelling approach to determine the conversion of oil during biodegradation, which takes in account the concentrations of different components of the oil that may be removed or formed by biodegradation, conserved, or supplied by charging. When combined with geological modelling (especially petroleum generation) a better understanding of the processes in the mixed oil reservoir will be obtained.

7.7.1 Mathematical model description and parameter preparation

As mentioned in previous sections, biodegradation mainly occurs in the oil/water transition zone where the bacterial population is assumed to be at equilibrium with the medium. To model in-reservoir biodegradation, reservoir topology need to be considered as one of critical geological factors since different trap styles will have different ratios of the OWC area (degradation area) to trap volume. The ratio between the areas of degradation at the OWC to reservoir volume should ultimately control overall extent of degradation. For example, parabolic traps would have double the area to volume relationship of a rectangular prismatic trap (Fig. 7-19). The Lengdong oilfield is characterized by fault bounded blocks, therefore, reservoir topology was considered as rectangular prism in this study.

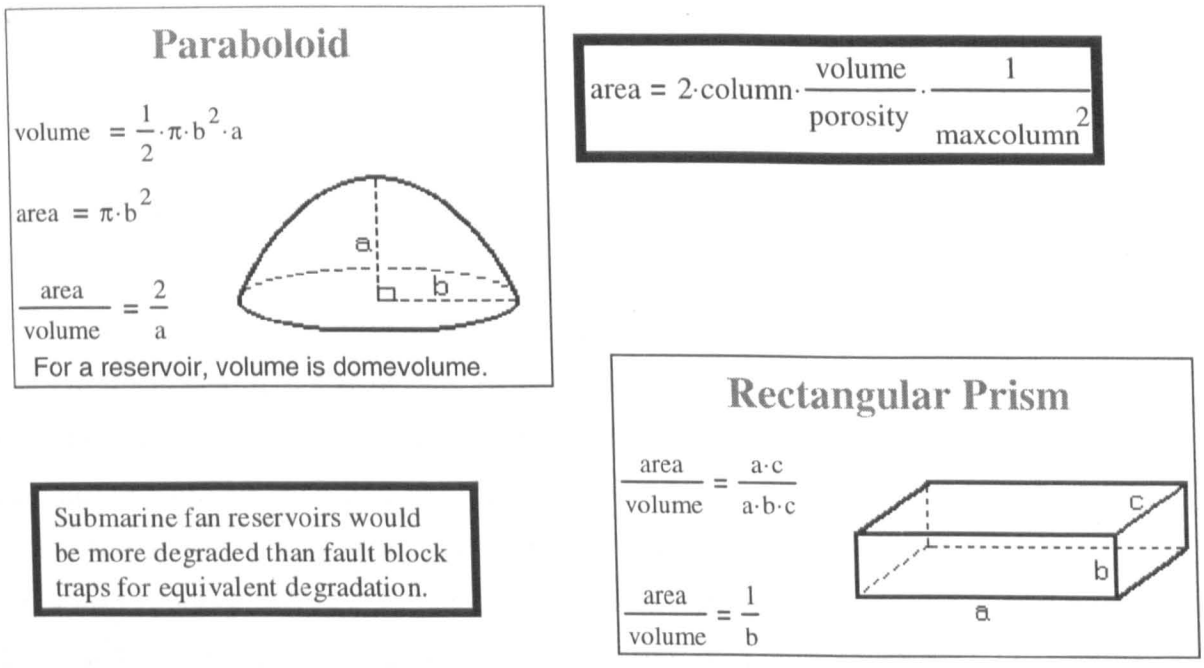

Fig. 7-19. Relationship between reservoir topology and biodegradation rate (Larter *et al.*, 2003; Bacchus unpublished data).

The Cyclops model (Bacchus unpublished result) includes oil column height, porosity, and initial oil and final oil compositions and biodegradation can be turned off and on at any time. A vertical petroleum column was simulated by dividing it equally into 50 cells, cell 1 being the top and cell 50 being the bottom of the reservoir. Biodegradation zone is located at the basal cell (2% of reservoir column height) (Fig. 7-20). The choice of a reaction zone of 2% of the oil column is a conservative value chosen to maximize biodegradation fluxes (Larter *et al.*, 2003). The petroleum components may either be mineralized to carbon dioxide and water or transformed to unknown compounds. Biodegradation flux removes material in the basal cell, diffusion redistributing material through column.

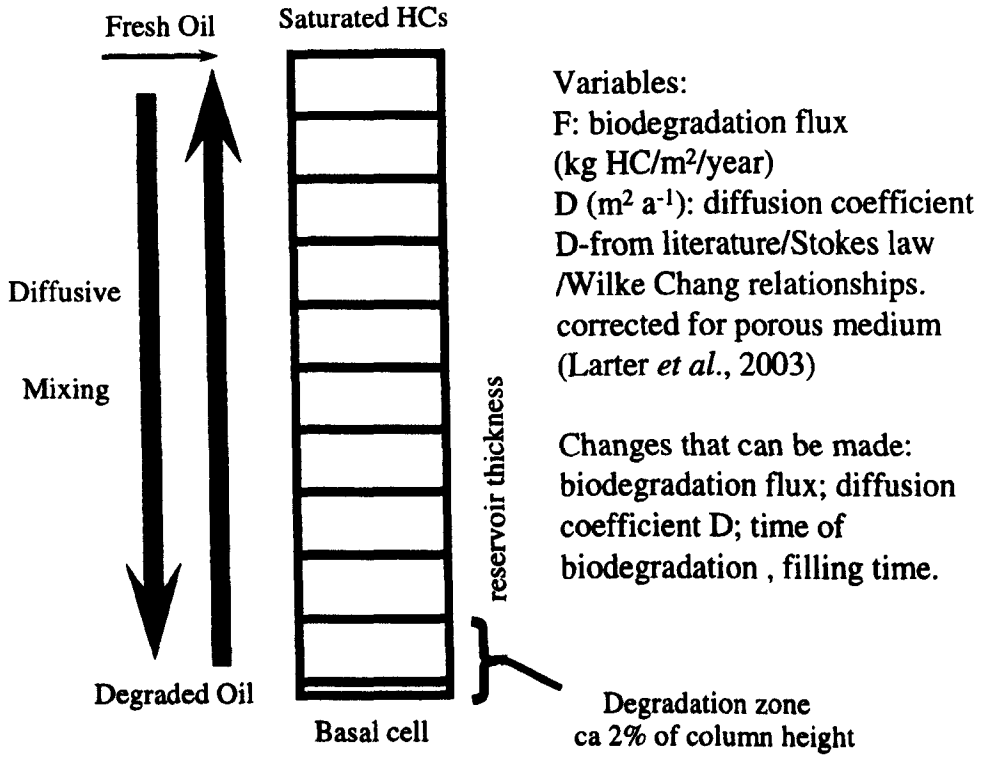

Fig. 7-20. Finite difference biodegradation/diffusion model-direct rate measurement (after Larter *et al.*, 2003; Bacchus unpublished data).

The composition of the upper cell could be controlled by adding fresh oil in the model with an initial component content equal to the current component content of the top of the petroleum reservoir column. Column length scale can be adjusted to accommodate the new oil. The charging and degradation of the petroleum column was simulated numerically using the finite difference numerical solution of the classical advection diffusion equation as described by Muller (1999). The model allows for rescaling after each calculation step thus allows simulation of simultaneous filling and biodegradation. The evolution of the component profile in the reservoir was followed both in terms of the concentration profiles of components observed and the gradient in components observed through the reservoir section. Diffusion coefficients were estimated using correlations with subsurface viscosities using the approaches described in Reid *et al.* (1987).

Degradation expressed as a rate constant requires degradation volume (oil density and porosity) and a rate constant K (/year) to be defined (Larter *et al.*, 2003). Degradation expressed as a flux (kg HCs depleted/m^2/year) requires only specification of a flux and easily fits in with geological criteria (trap volume/oil water contact area relationships) and the notion of degradation at an interface rather than a reaction volume. Fluxes have the advantage that a degradation volume does not need to be specified (Bacchus unpublished result). Varying oil water contact area with oil fill will result in varying degradation rates. Degradation flux can be related to concentration

gradients in columns via the diffusion equation:

Degradation flux = Gradient × Diffusion coefficient

Before the modelling can be carried out two assumptions have been made. The first assumption is that saturated hydrocarbons are the primary biodegraded component. Total oil destruction during biodegradation is estimated using the simple algebraic relationship. The second assumption is that C_{15-} saturated hydrocarbon composition is the same as C_{15+} composition since the saturated hydrocarbon contents are only measured on C_{15+} fractions in this case study. Obviously, both assumptions are not true, as a best approximate these assumptions are adequate.

This Cyclops modelling can deal with most possible cases occurring in geological situations. For example, one case is fresh oil charging a degraded but currently not degrading oil column and the other case can be a degrading and non filling scenario. Figure 7-21 illustrates the most realistic example in geological sense which involves three separate phases. Initially the oil column grows to 150 m while degradation is occurring during the first 12 Ma (from point A to B). Then charging ceases but degradation continues from 12 to 23 Ma and the column shrinks to 140 m (from point B to C). Finally from 23 Ma till now degradation also ceases and the column mixes up diffusively (from point C to D).

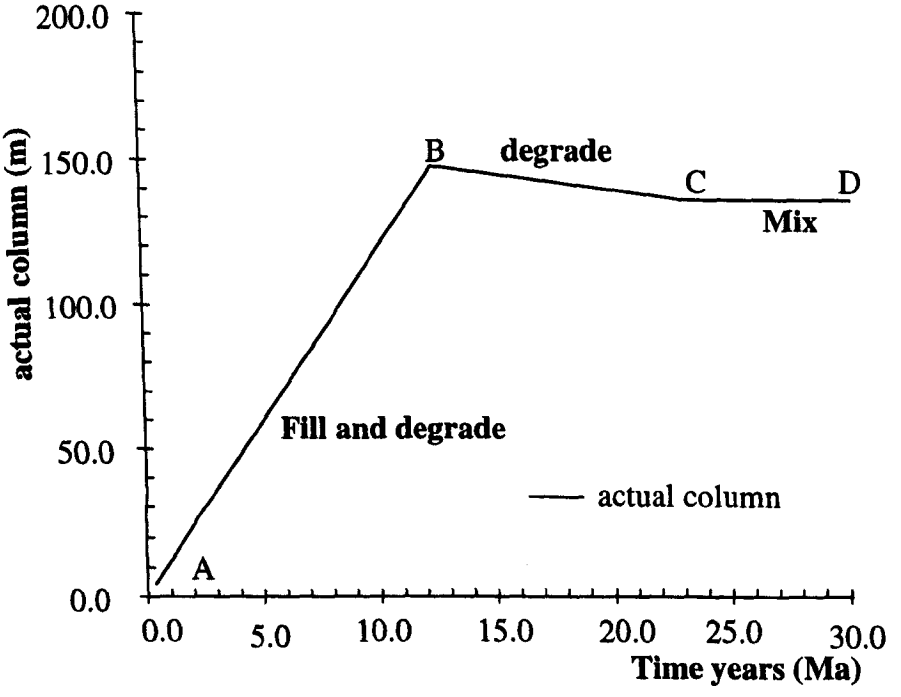

Fig. 7-21. Three separate charging/degradation phases occurring in the reservoir and their effects on actual column height.

Concentration gradients of components in the oil column can also be modelled under different scenarios. Initially the whole column has a similar saturated

hydrocarbon gradient i.e., the concentration profile is about linear with depth as observed in the Lengdong oilfield. When charging stops (point B) the top gradient reduces which probably not seen in the Lengdong case study (point C). Finally when degradation ceases the gradients reduces towards 0 as the column mixes up (Fig. 7-22).

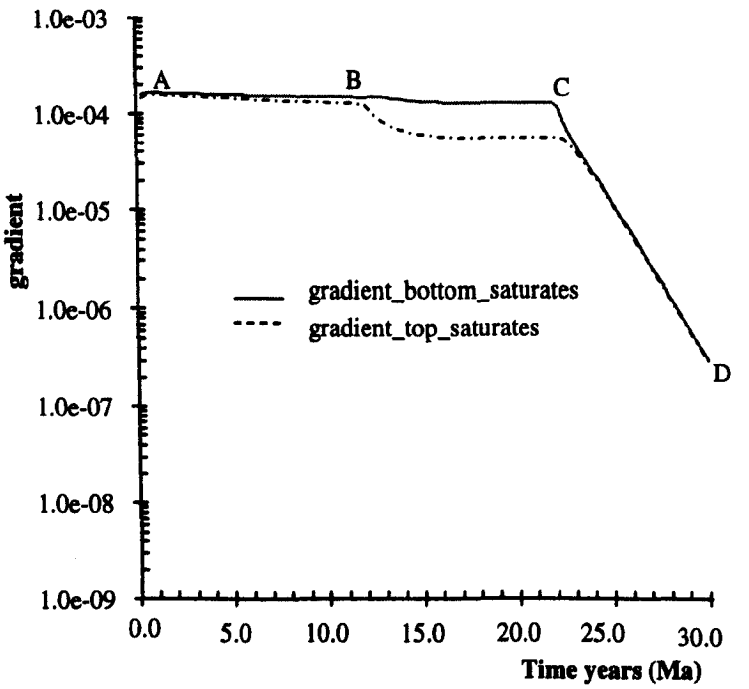

Fig. 7-22. Saturated hydrocarbon gradient (kg/kg/m) variations throughout geological time at the top and bottom of the column.

In that complicated but more realistic geological scenario the concentrations of *n*-alkane (kg alkanes/kg oil-Y axis) at the top, middle and bottom of the oil column decrease accordingly through geological time (Fig. 7-23). During filling phase the concentration of *n*-alkanes at the top of the column is fixed at the filled oil concentration, while the concentrations of *n*-alkanes at the middle and bottom decrease due to concurrence biodegradation (point A to B). During biodegradation phase the concentrations of *n*-alkanes reduce throughout the whole column with more severe degree at the bottom (point B to C). Finally, in-reservoir mixing tends to homogenize the concentration of *n*-alkanes in different cells. Degree of mixing depends on time and geological nature of the reservoir (England *et al.*, 1987). Concentrations of non degrading NSO compounds show opposite trend to *n*-alkanes which increase through removal of the saturated hydrocarbons at the top, middle and bottom of the oil column. Different cells throughout the column show varying degree of NSO compound enrichment with the most dramatic variations at the base cell (near OWC) (Fig. 7-24).

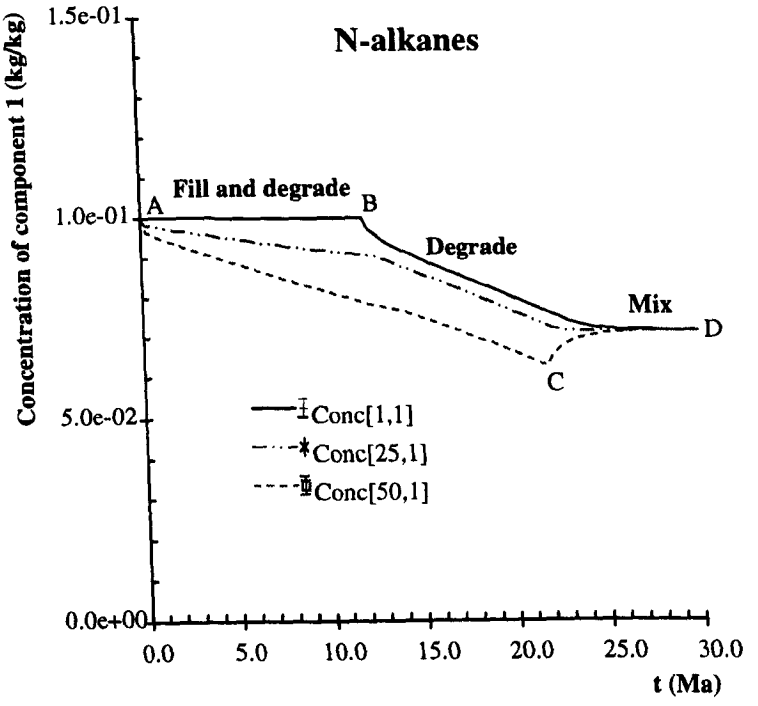

Fig. 7-23. The concentration variations of *n*-alkanes at different cells through geological time.

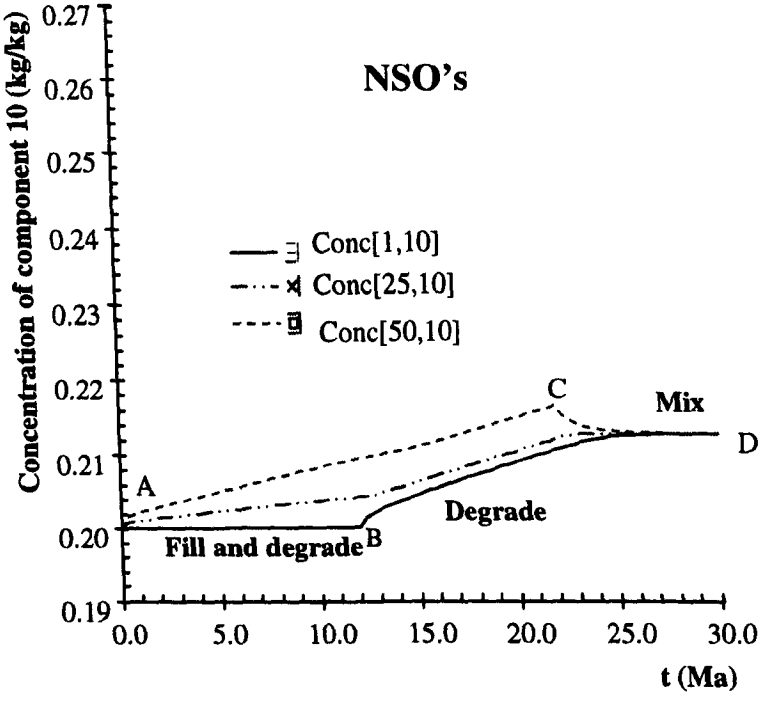

Fig. 7-24. The concentration variations of polar compounds at different cells through geological time.

Concentrations of oil components in Cyclops modelling are expressed as mass/mass oil (kg/kg). Degradation fluxes can be specified for 10 components that add up to 1 kg/kg oil. Each of the 10 components behaves independently in terms of degradation and diffusion although the same diffusion coefficient is used for all components as a simplification. When some components are removed (mineralized)

the concentrations of other components change automatically. There is then diffusive redistribution of material through column. The components can be defined as anything occurrence in the oil but in this case study 10 components are defined as follows: Component 1: *n*-alkanes; component 2: isoprenoid alkanes; component 3: steranes (regular, rearranged and 4-methy steranes); component 4: naphthalenes (C_{0-5}); component 5: phenanthrenes (C_{0-3}); component 6: aromatic steroid hydrocarbons (monoaromatic and triaromatic); component 7: other hydrocarbons (UCM and these quantified from GC-MS traces but not included in individual components, such as Sesquiterpanes, tricyclic terpanes and carotenes in the aliphatic fraction and alkylbiphenyls, fluoranthene, pyrene, alkylfluorenes and alkyldibenzothiophene in the aromatic fraction); component 8: hopanes (C_{27-35}); component 9: demethylated hopanes (C_{26-34}); component 10: non reactive NSO compounds. All hydrocarbon contents are quantified by standards while these NSO contents are quantified by Iatroscan. The discrepancy between absolute concentration quantified by standards and Iatroscan is ascribed to other hydrocarbons, ensuring 10 components add up to one unit for the whole oil. Removal of components is controlled by the degradation flux for each of the 10 components.

Flux modelling of degradation only applied for the Es3 column in present study. There are three wells in the Es3 column and each well contains 10-12 detailed analyzed points. Data applied for modelling are algebraic average values from these three wells. Concentration matrix set up in finite difference form with cell 1 being column top, 50 being column bottom etc. Compositional variations for each component in individual cells are extracted from measured data variation trend. The Es3 column in each studied well was divided into 50 cells and data at each cell for all components are the maximized fit of the variation trend at the corresponding depth in the column. Initial oil composition input for modelling for each component was equivalent the average composition from three wells at the top of the Es3 column. Interface view with initial oil composition and basic parameters input for Cyclops flux modelling was illustrated Figure 7-25. Detailed concentrations in a number of cells for each component used in the modelling from these three wells are presented in Table 7-1. 25-Norhopanes are not included in modelling since their concentrations are too low in the Es3 column.

Biodegradation time is very hard to be determined since no direct evidence available at moment. In this case study reservoir charge time was used as a reference. It is generally accepted that oil charge rates will be controlled by heating rates of the source rocks. A typically oil expelling source rock maturation over a 50 °C window at

a typical heating rate of around 3-5 °C/Ma requires charge timescale for an oilfield on the order of 10-15 Ma (Bacchus unpublished result). These filling timescales can be defined and the approach allows assessment of the timescale of degradation in terms of the timescale of filling. Larter *et al.*, (2003) suggested that field oil charging times and timescales of significant biodegradation (10% degraded) are comparable-ca 5-10 Ma. Basin modelling result in the Lengdong oilfield (see Chapter 3 for details) indicates that timing of charge is about 15 Ma. This time was used as approximate biodegradation time. Final oil column height is around 140 m.

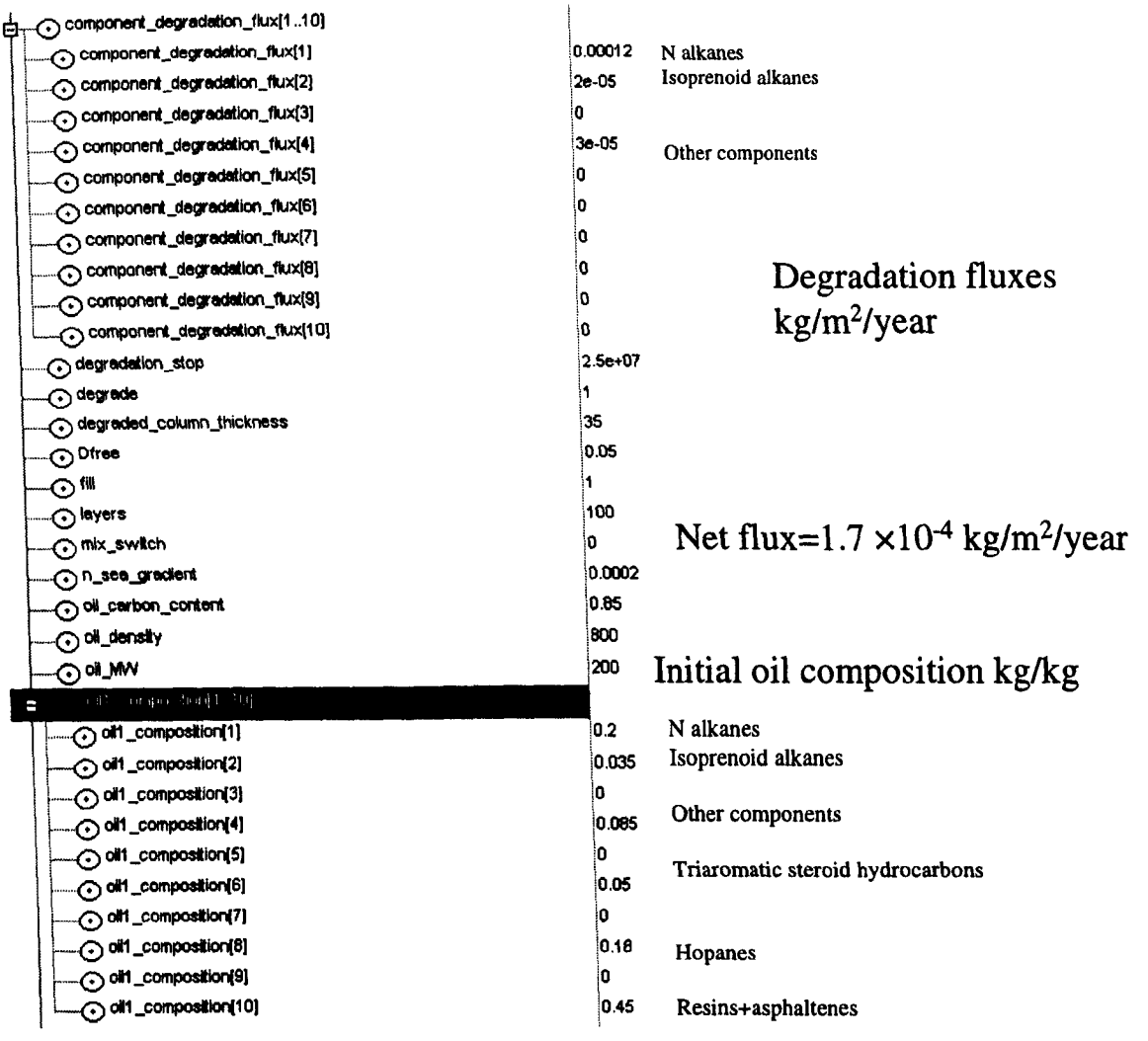

Fig. 7-25. Interface of Cyclops flux modelling with some initial input data.

Some parameters such as reservoir porosity and oil saturation are the actual values from the Es3 reservoir while others such as start column height and degradation stop time are putative. Diffusion coefficients of saturated hydrocarbons in oil were estimated using the relationships between oil viscosity and diffusion coefficient described by Reid *et al.* (1987). A diffusion coefficient of 0.5×10^{-10} m^2 s^{-1} for alkane diffusion in heavy oil was used in the model (Larter *et al.*, 2003).

Table 7-1. Component concentrations of the reservoir extracts from the Es3 column of the Lengdong oilfield.

		component1	component2	component3	component4	component5	component6	component7	component8	component9	component10
Well Name	cell No	n-Alkanes	Isoprenoids	Steranes	Naphthalene	Phenanthrene	Aro steroids	Other HCs	Hopanes	25-norhopane	Polars
Well A	C1	0.1342	0.0206	0.0178	0.0092	0.0242	0.0205	0.2202	0.0818		0.4713
Well A	C6	0.0972	0.0153	0.0208	0.0098	0.0230	0.0199	0.2154	0.0860		0.5125
Well A	C12	0.0686	0.0155	0.0262	0.0104	0.0235	0.0249	0.1800	0.1147		0.5362
Well A	C18	0.0392	0.0110	0.0259	0.0077	0.0223	0.0224	0.1921	0.1127		0.5667
Well A	C24	0.0317	0.0097	0.0299	0.0077	0.0202	0.0218	0.1719	0.1211		0.5859
Well A	C30	0.0287	0.0068	0.0309	0.0038	0.0175	0.0238	0.1755	0.1226		0.5904
Well A	C35	0.0051	0.0033	0.0299	0.0039	0.0136	0.0255	0.1751	0.1337		0.6099
Well A	C40	0.0026	0.0020	0.0308	0.0046	0.0102	0.0258	0.1643	0.1324		0.6271
Well A	C45	0.0030	0.0011	0.0270	0.0018	0.0079	0.0280	0.1435	0.1445		0.6432
Well A	C50	0.0013	0.0006	0.0210	0.0015	0.0039	0.0286	0.1703	0.1424		0.6304
Well B	C1	0.0989	0.0168	0.0220	0.0053	0.0196	0.0174	0.2330	0.0908		0.4962
Well B	C6	0.0557	0.0140	0.0205	0.0064	0.0185	0.0183	0.2726	0.1051		0.4888
Well B	C12	0.0441	0.0114	0.0209	0.0042	0.0158	0.0168	0.2882	0.0974		0.5011
Well B	C18	0.0543	0.0119	0.0212	0.0081	0.0177	0.0184	0.2538	0.0996		0.5150
Well B	C24	0.0306	0.0108	0.0215	0.0077	0.0169	0.0188	0.3240	0.0995		0.4702
Well B	C30	0.0153	0.0065	0.0225	0.0044	0.0152	0.0177	0.2960	0.1008		0.5214
Well B	C35	0.0015	0.0034	0.0212	0.0011	0.0091	0.0198	0.3117	0.0970		0.5353
Well B	C40	0.0012	0.0007	0.0270	0.0010	0.0032	0.0224	0.1710	0.1136		0.6599
Well B	C45	0.0009	0.0004	0.0286	0.0005	0.0017	0.0214	0.1680	0.1258		0.6526
Well B	C50	0.0019	0.0009	0.0260	0.0011	0.0040	0.0231	0.2111	0.1365		0.5954
Well C	C1	0.1178	0.0143	0.0204	0.0092	0.0259	0.0207	0.2220	0.0886		0.4811
Well C	C6	0.0932	0.0128	0.0195	0.0108	0.0267	0.0236	0.2143	0.0867		0.5125
Well C	C12	0.0539	0.0098	0.0208	0.0073	0.0227	0.0225	0.2133	0.0960		0.5537
Well C	C18	0.0475	0.0092	0.0219	0.0069	0.0210	0.0232	0.2380	0.0973		0.5351
Well C	C24	0.0317	0.0074	0.0212	0.0033	0.0197	0.0204	0.1949	0.0937		0.6077
Well C	C30	0.0317	0.0066	0.0211	0.0040	0.0193	0.0228	0.1933	0.0987		0.6025
Well C	C35	0.0256	0.0060	0.0228	0.0052	0.0211	0.0194	0.2392	0.0952		0.5656
Well C	C40	0.0182	0.0056	0.0203	0.0034	0.0209	0.0238	0.2237	0.1084		0.5757
Well C	C45	0.0146	0.0054	0.0231	0.0043	0.0186	0.0242	0.2381	0.1087		0.5630
Well C	C50	0.0089	0.0025	0.0256	0.0028	0.0081	0.0237	0.1730	0.1110		0.6444

7.7.2 Modelling results

The charge in concentration up to 10 components of an oil during biodegradation can now be simulated. Initial oil composition is that measured at the top of the Es3 column and the concentration variations through time are modeled. The model can simulate concentration variations through time for each cell and compare modelling result and measured data. The curves illustrated in Figures 7-26~29 represent modeled values for the top (Conc[1,component]), middle (Conc[25,component]), bottom of the oil column(Conc[50,component]). *n*-Alkane and isoprenoid alkane concentrations clearly decrease with increasing geological time at different cells of the column because of their easily degraded nature, whereas hopane and NSO compound continuously increase in their concentrations as they are resistant. Modelling result and measured data match well in all these four components at the top and bottom cells while some deviations occur at the middle cell. This is partially due to biodegradation mainly occurs near the OWC in the Es3 column (most obvious in the lower 35 meters of the reservoir) and no linear variation existed. In general the model does match reasonably considering all assumptions made.

The combined and averaged data from the three examined wells is now compared with modelling data from three charge and degrade scenarios to sort out what is the

most possible scenario. The data and modeled concentration profiles are compiled in Figures 7-30~33. Scenario 1 (diamonds) has degradation proceeding while the column fills with oil from 160-175 m over 15 Ma. The squares are the actual data. Scenario 2 (triangles) has degradation proceeding initially the column fills with fresh oil from 30-160 m over 15 Ma. The third scenario has the reservoir filled with oil of similar composition to that currently in the base of the reservoir and then without biodegradation, charges from 120-130 m in 15 Ma with fresh oil. In all these figures the X axis represents the reservoir column at 15 Ma into the model, cell 1 being the top and cell 50 being the bottom of the reservoir. Concentrations are in kg fraction/ kg oil.

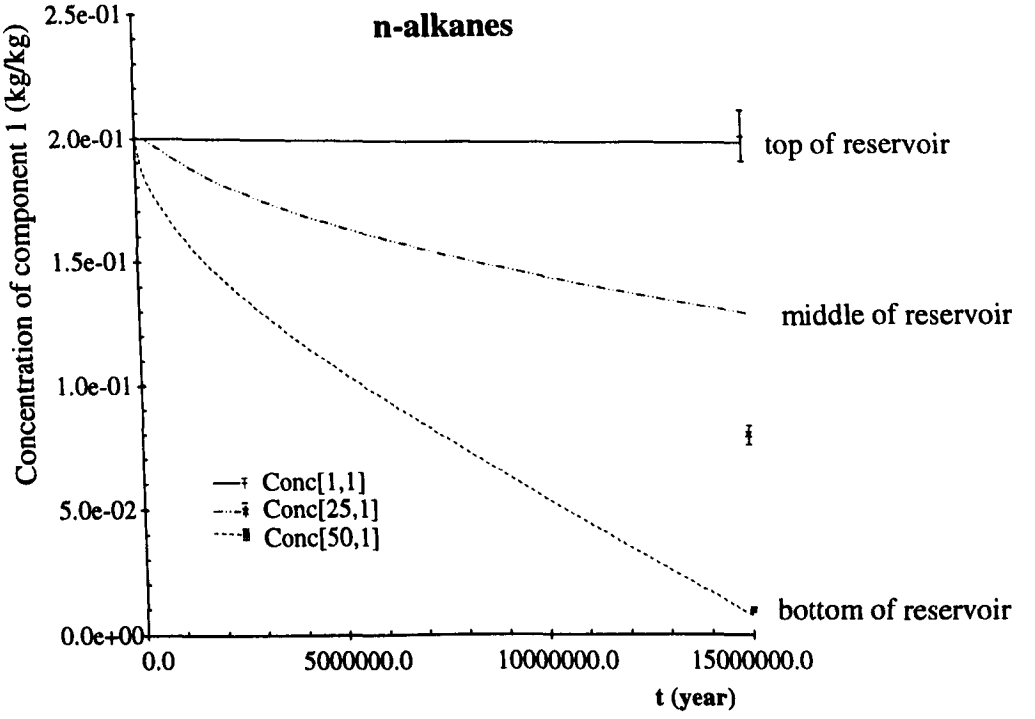

Fig. 7-26. *n*-Alkane concentration variations at different part of the Es3 column throughout geological time.

Here the concentrations of *n*-alkanes and isoprenoid alkanes at different cells of the oil column show a systematic declining trend with depth as time proceed, while the concentrations of hopanes and NSO compounds increase through removal of the alkanes. The X axis is cell number in the column and the Y axis is component concentration (kg/kg oil). These observed profiles (sub linear) for isoprenoid alkanes, hopanes and NSO compound concentrations indicate a charge and degradation process is active (Fig. 7-31~33) while the observed profile of the *n*-alkanes is much closer to a charge only scenario (Fig. 7-30).

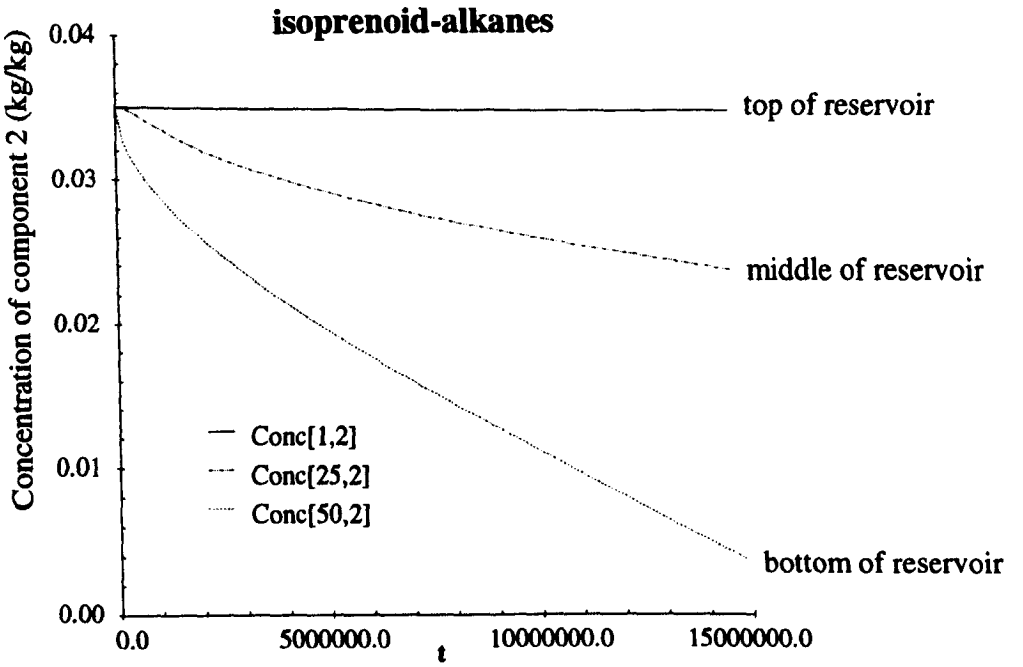

Fig. 7-27. Isoprenoid alkane concentration variations at different part of the Es3 column throughout geological time.

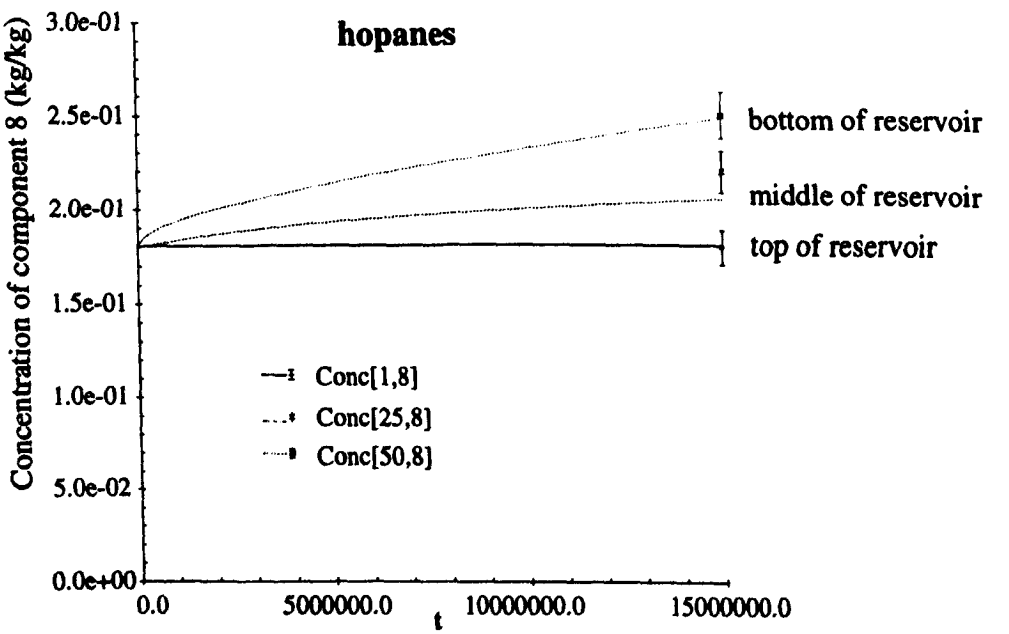

Fig. 7-28. Hopane concentration variations at different parts of the Es3 column throughout geological time.

This most likely reflects the much higher concentrations of *n*-alkanes in the currently charging oil than the other components and the fact that only small amounts of oil are degraded. This great dependence on charge in the models combined with uncertainty in the diffusion coefficients suggests caution must be taken with assessments of individual compound fluxes at this point. Much more accurate data

and diffusion coefficient data is needed. However, the dynamism of oilfields is clearly evident.

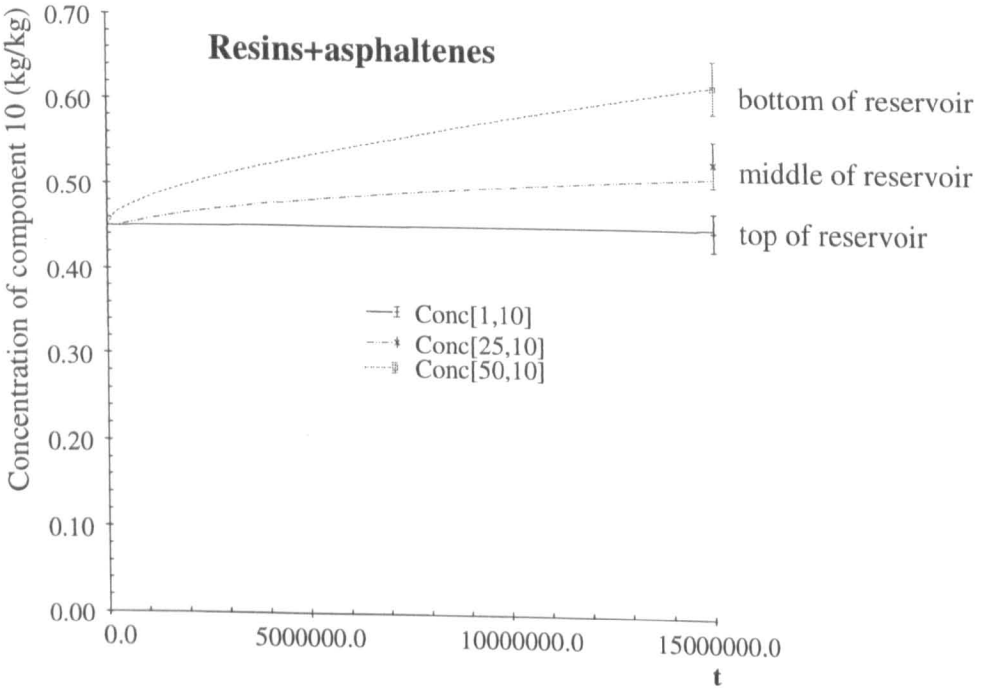

Fig. 7-29. Resin and asphaltene concentration variations at different parts of the Es3 column throughout geological time.

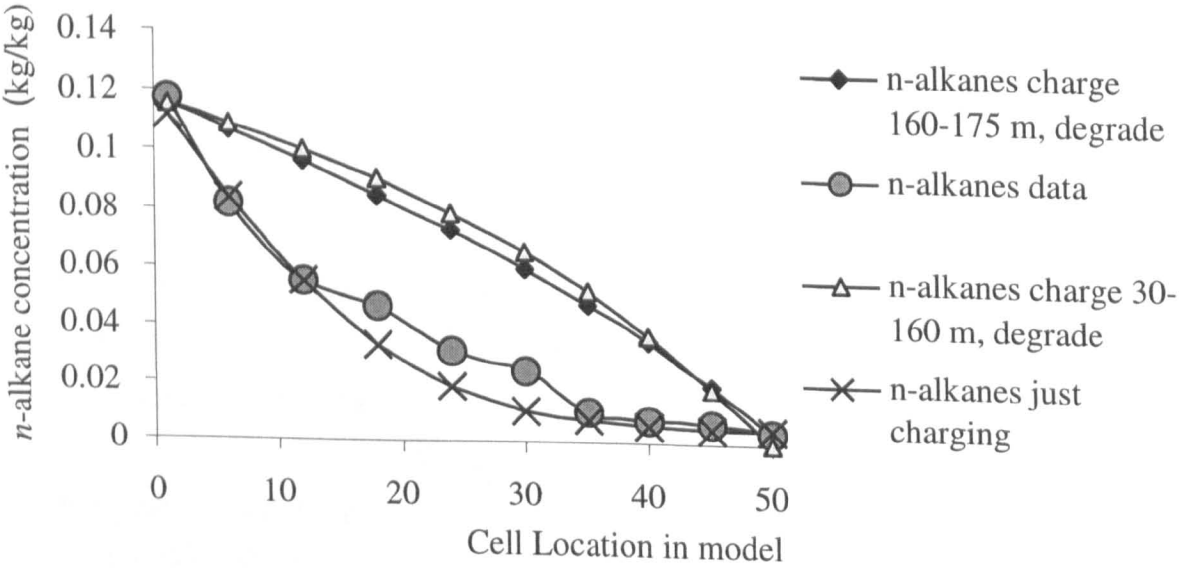

Fig. 7-30. *n*-Alkane concentration profiles under different processes.

High content of *n*-alkanes (0.12 kg/kg oil) in the top of the reservoir is quite similar to current charge composition due to slightly higher source rock maturity. If the very recent charge of more *n*-alkane rich oil is not taken into account, the modelling result may more geologically realistic. The combined and averaged data from the three examined wells is now compared with a charge and degrade scenario

where the charging oil has an *n*-alkane content of 0.08 kg/kg oil. The agreement between data and modelling result is much better. In Figures 7-34~37 the circles are the data and the diamonds are the modeled values. The modelling scenario is that the column fills from 30-160 m over 15 Ma with concurrent biodegradation. The X axis represents the reservoir column at 15 Ma into the model, cell 1 being the top and cell 50 being the bottom of the reservoir. The observed profiles also indicate that a charge and degradation process is active in the Es3 reservoir.

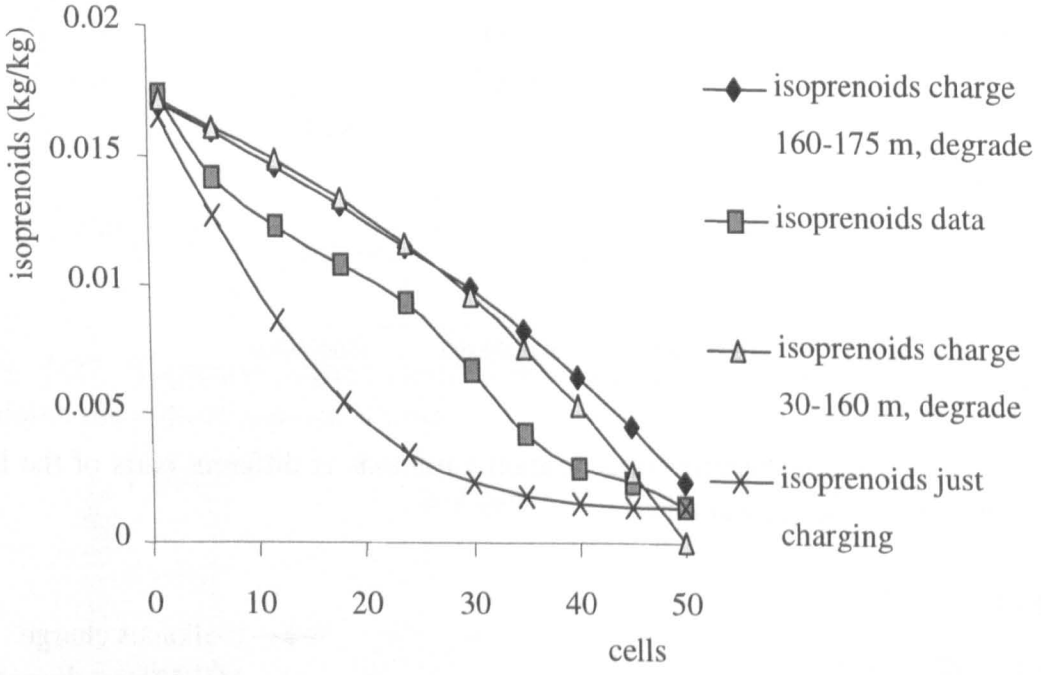

Fig. 7-31. Isoprenoid alkane concentration profiles under different processes.

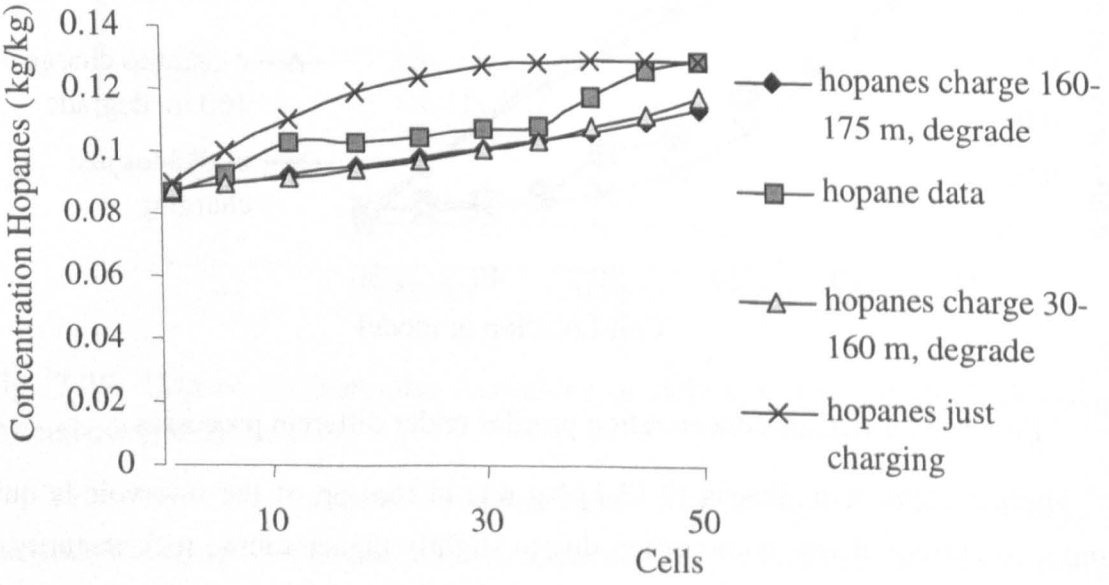

Fig. 7-32. Hopane concentration profiles under different processes.

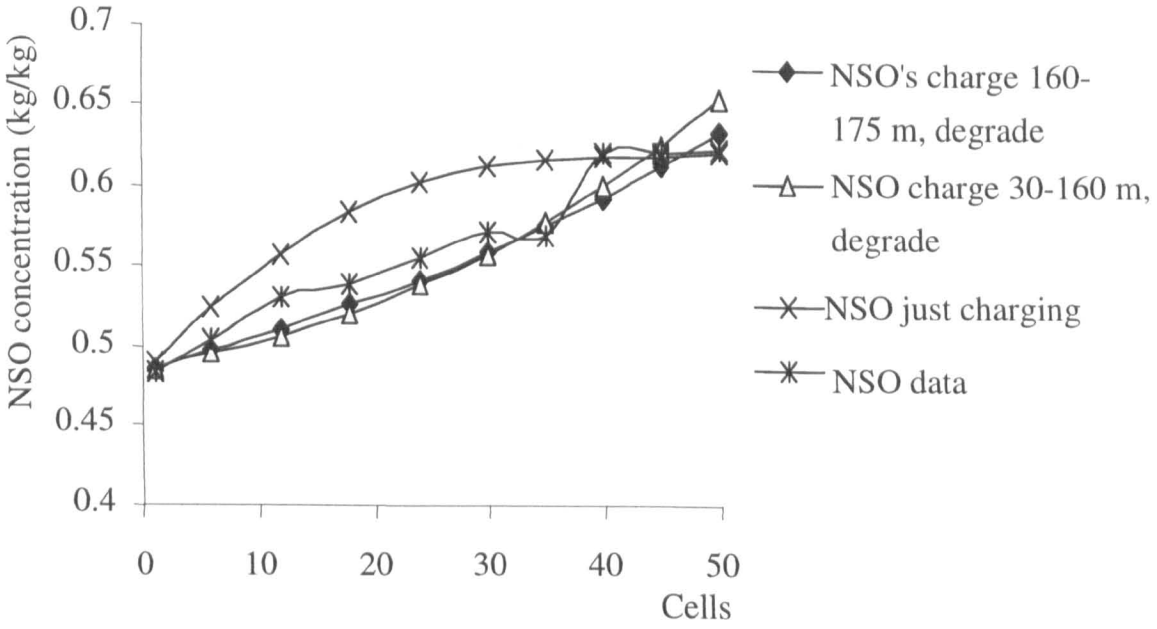

Fig. 7-33. NSO compound concentration profiles under different processes.

Major uncertainties surround these fluxes which at the moment can only be considered order of magnitude assessments. Provisional degradation fluxes for different components in the Lengdong oilfield are as followings:

n-Alkane = 1-2×10^{-4} kg/m^2/year

Isoprenoid alkanes = 1.5-4.5×10^{-5} kg/m^2/year

Other hydrocarbons = 1×10^{-5} ~1×10^{-4} kg/m^2/year

Aromatic (Naphthalenes or phenanthrenes) = 0.6-1.7×10^{-5} kg/m^2/year

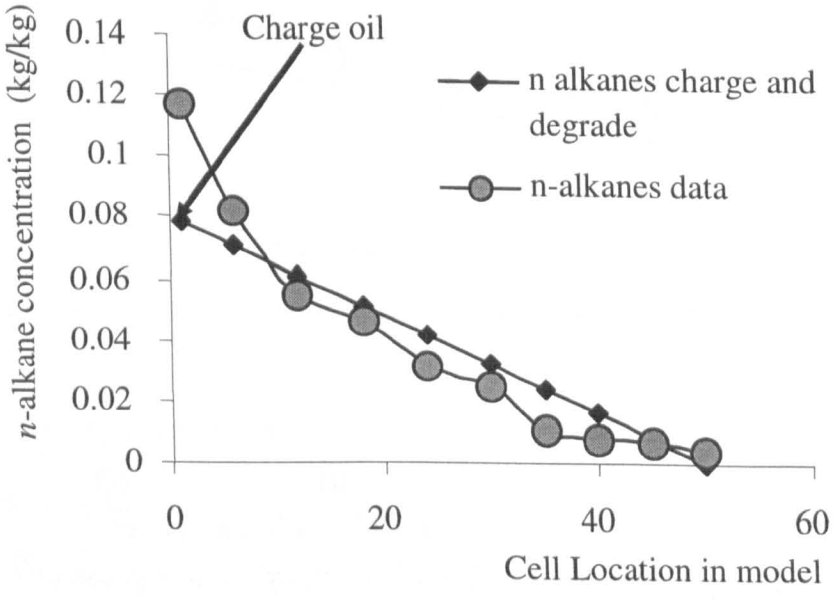

Fig. 7-34. *n*-Alkane concentration profiles under charge and degrade processes.

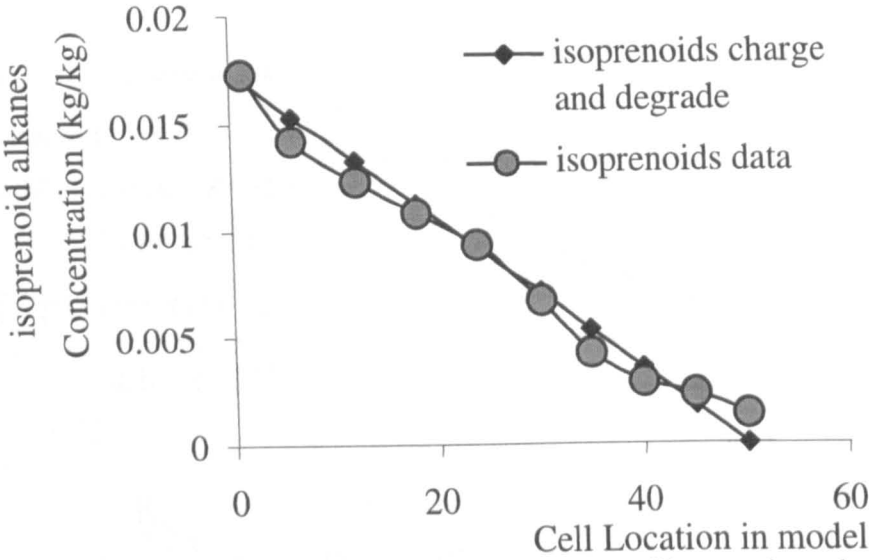

Fig. 7-35. Isoprenoid alkane concentration profiles under charge and degrade processes.

It appears that the average degradation fluxes indicated are not necessarily the maximum fluxes acting. The Queso do Minas example (Bacchus unpublished data) suggests that actual fluxes may be much higher, consistent with a pulse mode of degradation. This may well occur with periods of high instantaneous degradation rates combined with periods of quiescence giving the observed low average rates of degradation such as in the Liaohe basin. If pulses are frequently occurred the whole column gradients can easily be produced.

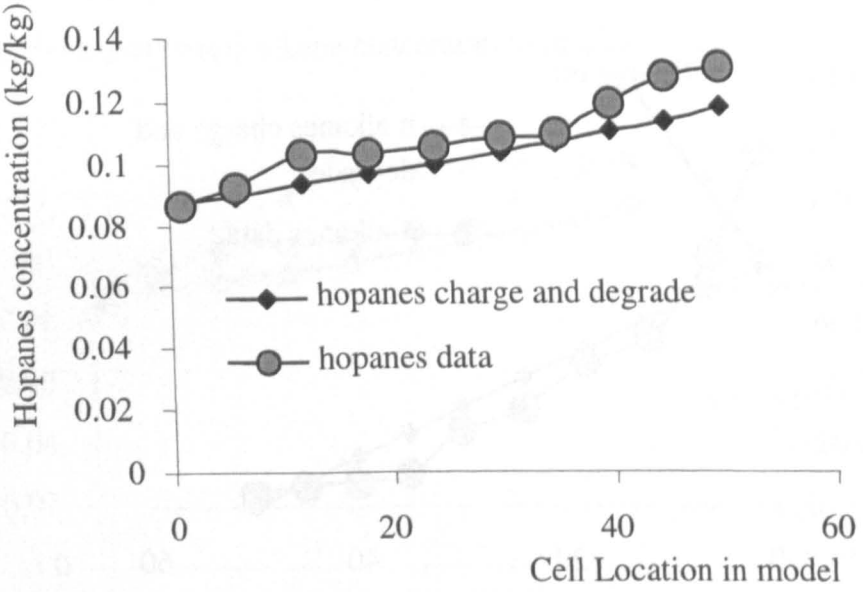

Fig. 7-36. Hopane concentration profiles under charge and degrade processes.

A net degradation flux of around 0.0001 kg/m^2/year is evident though this is not accurately defined and depends on charging too and is very sensitive to data quality. Based on this flux value the fraction of total oil destroyed during biodegradation was calculated. About up to 50% of an oil volume is degraded by PM level 5 in the

Lengdong Es3 reservoir (Fig. 7-38).

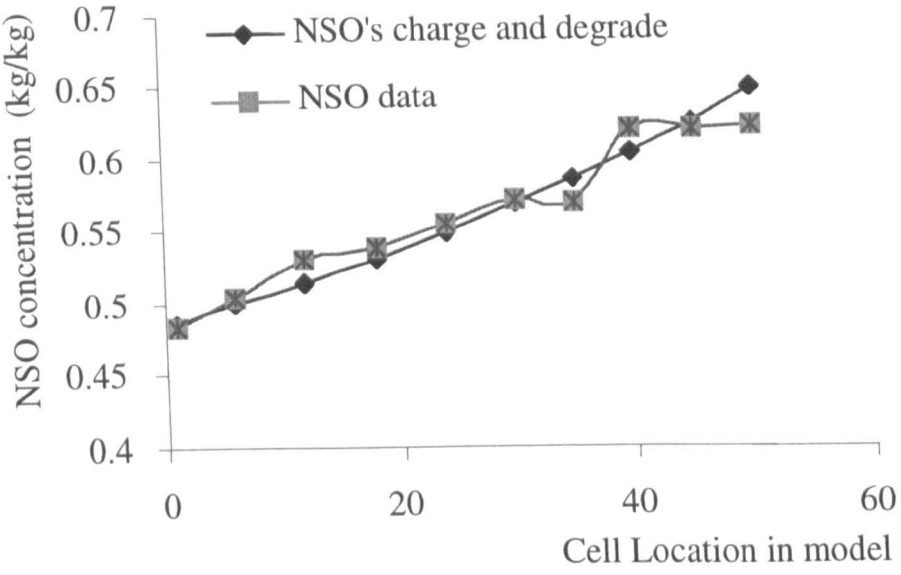

Fig. 7-37. NSO compound concentration profiles under charge and degrade processes.

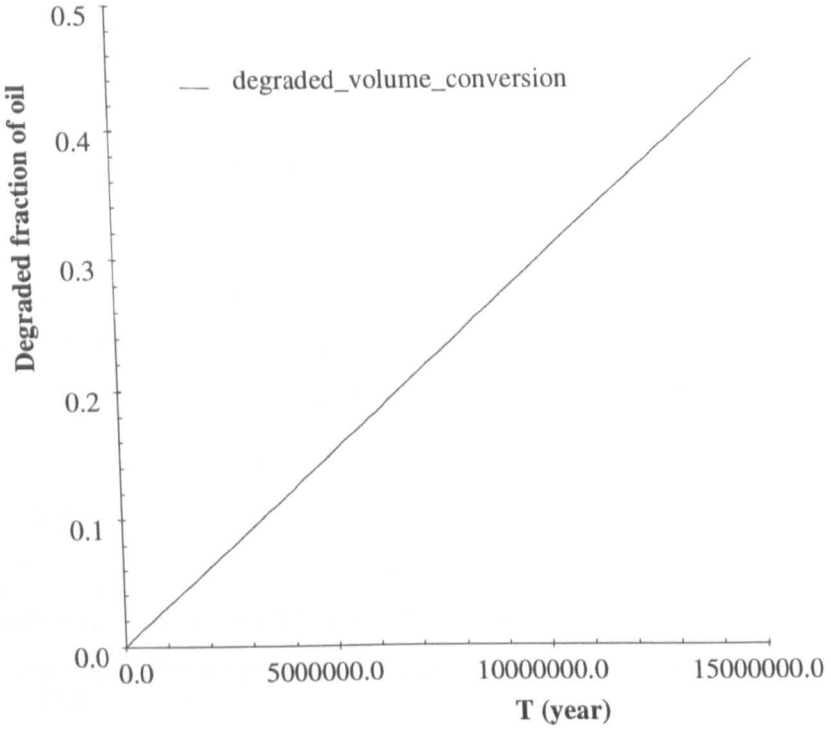

Fig. 7-38. Oil destroyed in the Es3 reservoir at biodegradation PM level 5.

Biodegradation in the subsurface consists of a series of complex biochemical and physical processes that is not yet completely understood. The modelling of geological processes relies entirely on the subsurface database. It is therefore essential that the numerical simulation is linked as closely as possible to all geological data sources. For biodegradation modelling it is very difficult since there is no clear indication of biodegradation starting time and the initial component concentrations. Similarly it is

hard to know whether the saturated hydrocarbon gradient is in a near steady state condition or not and whether the field was degrading as a static column or whether it was filling contemporaneously. In the Lengdong case study gradients are close to linear in appearance and a linear fit of observed hydrocarbon concentrations throughout a reservoir is adopted. Gradients of hydrocarbon concentrations in biodegraded reservoirs are not usually linear for a diffusion-dominated system since fresh oil charge will disturb the established gradient. Meanwhile, one important area of further study required for this project would be the techniques to obtain more accurate quantification of components in the oil.

In this model biodegradation is merely described in terms of removal of saturated hydrocarbons to gain a gross but conservative assessment of degradation fluxes. Actually, aromatic compounds and some light polar NSO compounds are also removed contemporaneously during biodegradation. So the assumption made is not true but as an approximate at this stage it is adequate. In future full compositional simulation is required for the reservoir fluid compositions.

Diffusion coefficients are poorly known and no measured data applied in this study. An average value for the saturated hydrocarbon fraction has been assumed. Better estimates of subsurface diffusion coefficients are needed.

It is desirable to be able to model biodegradation in a deterministic way to achieve some understanding of key process variables and critical factors. Cyclops flux modelling has been developed for predicting the concentrations of hydrocarbons in the reservoir. Provisional results in the Lengdong case study provide adequate estimates of degradation fluxes for a given column saturated hydrocarbon gradient. This is the first effort to simulate biodegradation in a petroleum geological context. The modelling result confirms that a charge and degradation process is active in the Lengdong reservoir. Therefore, the dynamic modelling of petroleum biodegradation could be an essential tool to improve the prediction of petroleum biodegradation risk and oil quality.

OVERALL CONCLUSIONS

Biodegradation is the primary control on the composition of reservoired oil in the Lengdong oilfield of the Liaohe basin, NE China. Consistent and systematic compositional variation with depth, seen as well-defined gradients in two oil columns, is observed in the abundance of the bulk C_{15+} saturated hydrocarbons; in the concentrations of individual component groups such as *n*-alkanes, isoprenoid alkanes, hopanes and steranes; and in a variety of molecular indicators. Whereas the Es3 column undergoes moderate biodegradation, the Es1 oil column is characterized by a relatively severe degree of biodegradation due to the shallower depth of burial.

In the aliphatic hydrocarbon fraction *n*-alkanes are the most susceptible to bacterial attack, isoprenoid distributions are distorted at moderate biodegradation levels (level 3 and above on Peters and Moldowan (1993) biodegradation scale). Hopanes are slightly more resistant to biodegradation and their concentrations increase at early stages of biodegradation (PM level 1-3). 25-norhopanes only occur in severely biodegraded situations (PM level > 5) and their concentrations increase with the degree of biodegradation. Hopane degradation proceeds via hopanoic acids and demethylated hopanoids (acids and hydrocarbons) but the acids are probably intermediates and disappear in the conversion to unrecognized material (Aitken, 2004). Concentrations of steranes also increase during early stages of biodegradation and they start to decrease at level 4.

Molecular indicators suggest biodegradation levels increase towards the oil water contact in both Es3 and Es1columns, corresponding to a range of from PM level 2 to 5 and PM level 5 to 8, respectively.

Biodegradation affects the different classes of aromatic hydrocarbons in different ways, while their isomer variation within a compound series occur slightly late (usually > PM level 4). Substantial concentration decrease for $C_{0\text{-}5}$-naphthalenes and $C_{0\text{-}3}$-phenanthrenes occurs in PM level 3 to 5. Aromatic steroid hydrocarbons are the most persistent compounds. Their concentration shows a gradual increase while their relative proportion shows a sharp increase and dominates the aromatic hydrocarbon fraction above level 4 biodegradation.

Although the degree of alkylation exerts critical control on the susceptibility to biodegradation of aromatic hydrocarbons, several exceptions were observed in my study sample suite. Slower decrease in the proportion of C_2-naphthalenes than of C_3-naphthalenes and of phenanthrene compared to methylphenanthrenes suggests

demethylation may also be an important step in aromatic hydrocarbon biodegradation in the reservoir.

The order of biodegradation of multiply alkylated naphthalenes (TMNs, TeMNs and PMNs) and phenanthrenes (methylphenanthrenes, C_2-phenanthrenes and C_3-phenanthrenes) has been established. These highly thermally stable isomers are more susceptible than thermal unstable ones during biodegradation, suggesting biodegradation have controls different from purely thermodynamically controlled processes with solubility or degradation mechanical controls being important. The validity of aromatic maturity parameters depends on biodegradation levels and the most widely used parameters are no longer valid after PM level 4 biodegradation.

Biodegradation behavior of C_{21-22}-monoaromatic steroid hydrocarbons differs from the C_{21-22}-pregnanes and C_{20-21}-triaromatic steroid hydrocarbons. Biodegradation seems to result in the preferential removal of the short side-chained triaromatic steroid hydrocarbons compared to the long-chained counterparts, whereas the short side-chained C_{21}-C_{22} pregnanes become more enriched with increasing biodegradation compared to long side-chained regular steranes. No obvious change in view distribution has been observed in the C_{27-29} monoaromatic steroid hydrocarbons up to PM level 8, indicating a very high ability to resist biodegradation for these short chain monoaromatic steroid hydrocarbons.

The concentrations and molecular distributions of carbazole, methylcarbazoles, dimethylcarbazoles and benzocarbazoles in the Lengdong oil field are largely controlled by biodegradation. Many carbazole compounds are biodegraded subsequent to the removal of the isoprenoid alkanes, and several molecular parameters based on carbazoles appear to be quite sensitive to biodegradation at PM level 4 and above.

Biodegradation results in the preferential removal of the less-alkylated compounds and there is no evidence to show that nitrogen shielded or partially shielded compounds have a systematically higher resistance to bacterial attack, as one might have expected.

Benzo[a]carbazole is the most vulnerable and benzo[b]carbazole is the most refractory component among benzocarbazoles. After level 4 biodegradation the BC ratio (benzo[a]carbazole/(benzo[a]carbazole + benzo[c]carbazole)) is no longer a valid petroleum migration distance indicator. The benzo[b]carbazole/benzo[a]carbazole ratio is sensitive to oil biodegradation at more advanced levels of biodegradation (> PM level 5).

Detailed analysis of alkylphenol and benzoic acid distributions in reservoired oils may aid assessment of biodegradation processes in petroleum reservoirs.

Many phenol compounds are biodegraded coincident with the removal of the normal alkanes. The total concentrations of phenols start to decrease at PM level 2.

Biodegradation has led to a decrease in the total concentration of alkylphenols and results in the preferential removal of the high-alkylated compounds at early stage (< PM level 4).

The biodegradation of cresols show *p*-cresol has a higher ability to resist biodegradation than *m*-cresol. *o*-Cresol does not show a clear enrichment during biodegradation.

A tentatively order of susceptibility to biodegradation for C_2-alkylphenols (from easiest to most resistant) is: 2,5-xylenol > 2-ethylphenol, 2,6-xylenol > 4-ethylphenol, 3,4-xylenol > 2,4-xylenol.

In the C_3-phenol distributions, isopropyl- and propylphenols seem more susceptible to biodegradation than trimethylphenols.

Benzoic acids are major metabolite of alkylbenzene biodegradation (Wilkes *et al.*, 2000). With increasing degree of biodegradation not only the total concentration of benzoic acids decrease but their isomer distributions also show systematic variations. *o*-Methyl benzoic acid seems very resistant to microbial attack through the biodegradation process.

Gradients in oil composition are a common feature of the Es1 and Es3 reservoirs but these relate to degradation at one point in the oil column (near the oil water contact) and subsequent vertical mixing of oil components by diffusion and other processes. Slow mixing may result in the extensive degradation of some fractions (e.g. nitrogen compounds) while classically more degradable compounds (e.g. normal alkanes) are still abundant elsewhere in the oil column.

The existence of these gradients is attributed to biodegradation at or near the oil-water contact and diffusive mixing of biodegraded oil with an undegraded oil supplied through either single/episodic recharge or continuous charging of the reservoir. Analysis of compositional gradients may allow definition of both field charge and degradation fluxes.

Reservoir and oil temperature history, charge rate and oil residence time are the primary control of degradation rate which can be measured or inferred (Wenger *et al.*, 2002; Yu *et al.*, 2002; Larter *et al.*, 2003).

Molecular evidence supporting the occurrence of mixing of biodegraded oil and undegraded oil can be found by comparing the variability in maturity parameters of the two oil columns. Mixing related to a late oil charge to the top of the Es3 column is also supported by an investigation of the changes in concentrations of both vulnerable and conservative tracers. Multiple or continuous charging of the reservoir and continuous biodegradation leads to depletion of the more biodegradable components of petroleum, such as *n*-alkanes and isoprenoid alkanes, and enrichment of the more refractory components, such as hopanes and aromatic steroid hydrocarbons. The occurrence of high *n*-alkanes concentrations together with high hopane concentrations reflects a relatively recent charging episode and subsequent mixing of the 'fresh' oil with previously biodegraded oil already in the reservoir.

Variation in the degree of biodegradation at 3 different sites in the less degraded Es3 column is controlled additionally by geological factors. Oil columns with thicker water legs (such as Well A and B) were biodegraded to a higher degree than oil columns with either a thin water leg or no water leg (Well C). The higher degree of biodegradation at the sites with the thick water leg is attributed to the greater accessibility/availability of nutrients to the reaction site which is suggested as being at or near the OWC. Therefore, the nutrient supply is a critical rate control factor in biodegradation, as it is in metabolic processes in general.

A biodegradation model based on geochemical analysis and geological observation has been established for the Lengdong petroleum system. Analyzed data suggest that biodegradation occurs within a narrow region near the base of the oil column, probably at the OWC, and that there has been a late charge of oil to the top of the column. The mixing of oils through continuous charging and the diffusion of hydrocarbons towards the OWC, and the diffusion of metabolites away from the reaction site may be considered as the most important factors controlling the biodegradation process. Biodegradation gradients within oil columns can be conserved only if the rate of charging and diffusive mixing is similar to or lower than the rate at which the hydrocarbons are destroyed. The diffusive transport of nutrients and electron acceptors from the water leg to the site of microbial activity is the limiting factor in the biodegradation of the Lengdong oils, not the hydrocarbon supply. Aquifer volume relative to oil leg volume, and the degree of contact between the two, may therefore be key variables in controlling the rate and extent of biodegradation. This conceptual model opens the possibility of model-driven prediction of oil properties and sweetspots in reservoirs.

Biodegradation, oil charging and mixing is a dynamic process hence the need for

a numerical model. The complete mass balance is still hard to reach as diffusion affects final concentrations observed. Oil supply is not limiting implying nutrient/ electron acceptors are limiting. Diffusive nutrient transport may be rapid enough to sustain the deep hydrocarbon degrading biosphere.

The timescales of oilfield degradation and filling are very similar and indicate that the degree of biodegradation will be substantially controlled by oilfield charge history.

The combined and averaged data from the three examined wells is compared with three charges and degrade scenarios. The observed profiles of the other components indicate a charge and degradation process is active. In principle column profile analysis may provide charge and degradation rates with a more sophisticated modelling and analytical calibration exercise.

Average degradation fluxes are around 10^{-4} kg/m^2/year and vary by less than 10 over the range of degraded reservoir temperatures increasing with decreasing reservoir temperature from 0 at 80 °C (Larter *et al.*, 2003). Average degradation fluxes confirm that charge time and oil mixing is the key variable for fluid property prediction.

Coupled degradation mixing models on the Lengdong case history suggest perhaps up to 50% of an oil volume is degraded by PM level 5 with little (ca 20%) mass loss after that but diffusion complicates the observed concentration increases.

FUTURE WORK

In petroleum, biomarkers are found both free in the hydrocarbons and also bound into asphaltene and resin. Bound biomarkers which are either entrapped in macromolecular networks, or become chemically bound by functional groups have a high geochemical information content. Microbes simply cannot degrade the bulk of the bound molecular components due to their crosslinked with polymeric matrix. Chemical degradation and pyrolysis studies revealed that the molecular features of biomarkers bound within resins and asphaltenes in oils are sterically protected against biodegradation (Rubinstein *et al.*, 1979; Cassani and Eglinton, 1986; Xiong and Geng, 2000). Hydropyrolysis (HyPy) of asphaltenes from crude oils yields significant amounts of crude oil-like material and it is the best way to recovery biomarker characterization in heavy biodegraded oils where most of the free biomarkers have been destroyed (Love *et al.*, 1995; 1998; Bishop *et al.*, 1998). Studies of asphaltenes and their pyrolysis released bound biomarker can be applied for correlation purposes.

Analysis of asphaltene-bound biomarkers in a biodegraded oil can provide unaltered biomarker profiles. In present project I studied the characteristics of these free biomarkers. In future more work will be done to deal with bound biomarkers since it can provide new geochemical information for biodegraded oils.

A variety kinds of metal such as V, Ni, Co, Zn, Fe, Sb, Se, U, Ti, La, As, Ba, Mn and W occur in oil. Some metal elements such as nickel and vanadium (complexed in porphyrin structures and free formed cations) generally show a constant ratio in crude oils of the same origin and valuable for oil classification (Olsen *et al.*, 1995). These metal combined porphyrins are extremely resistant to biodegradation and their absolute concentrations increase with increasing degree of biodegradation (Sundararaman and Hwang, 1993). To compare concentration variations of metal elements or porphyrin compounds between original oils with biodegraded oils may provide a supplemental means to calculate the oil lost by biodegradation.

Nitrogen contained compound analysis suggest carbazoles increase in concentration during initial stages of biodegradation – refractory up to PM level 3. Beyond PM level 3, carbazoles decrease reflecting the possible removal of these compounds as a supply of nutrient. Other nutrient supply such as phosphorus is essential for living organisms. In relation to geochemistry – there is very few data in the literature documenting the levels of phosphorus in petroleum. Many nutrients that sustain life are derived from minerals and redox reactions at mineral surfaces provide

metabolic energy. Minerals are the substrates that micro-organisms attach to, the origin of many dissolved constituents essential for metabolism, and in the case of lithotrophs, the ultimate source of their energy. Phosphorus occurs in the Earth's crust almost exclusively as the $(PO_4)^{-3}$ ion, and a large percentage of it is contained in the apatite group of minerals. In environments where phosphorus is scarce, feldspars that contain micro-inclusions of phosphorus minerals such as apatite are preferentially colonized over similar feldspars without phosphorus (Bennett *et al.*, 1993; 2000; 2001). Similar process may occur in deep reservoir, detailed study the trace element from reservoir core and its extract, coupled with mineralogy analysis, may gain through insight into nutrient supply in deep biosphere.

Biodegradation modelling remains a big challenge at moment. The provisional modelling results from the Lengdong oilfield indicate the curve for *n*-alkanes is much closer to a charge only scenario. This probably reflects the much higher concentrations of *n*-alkanes in the charging oil than the other components and only small amounts of oil are degraded. This model depends largely on charge composition. Another uncertainty arises from the diffusion coefficients. These fluxes broadly agree with fluxes from diffusion modelling but diffusion coefficients are poorly known at present. Cautions must be taken with assessments of individual compound fluxes at this point. Much more accurate data and diffusion coefficient data are needed.

REFERENCES

van Aarssen, B.G.K., Bastow, T.P., Alexander, R., Kagi, R.I., 1999. Distributions of methylated naphthalenes in crude oils: indicators of maturity, biodegradation and mixing. Organic Geochemistry 30, 1213-1227.

Ahmed, M., Smith, J.W., George, S.C., 1999. Effects of biodegradation on Australian Permian coals. Organic Geochemistry 30, 1311-1322.

Ahsan, A., Karlsen, D.A., Patience, R.L., 1997. Petroleum biodegradation in the Tertiary reservoirs of the North Sea. Marine and Petroleum Geology 14, 55-64.

Aitken, C. 2004. Identification of non-hydrocarbon metabolites of deep subsurface anaerobic petroleum hydrocarbon biodegradation. PhD thesis, University of Newcastle upon Tyne.

Alexander, R., Kagi, R. I., Rowland, S. J., Sheppard, P. N., Chirila, T. V., 1985. The effects of thermal maturity on distributions of dimethylnaphthalenes and trimethylnaphthalenes in some ancient sediments and petroleums. Geochimica et Cosmochimica Acta 49, 385-395.

Alberdi, M., Moldowan, J.M., Peters, K.E., Dahl, J.E., 2001. Stereoselective biodegradation of tricyclic terpanes in heavy oils from the Bolivar Coastal Fields, Venezuela. Organic Geochemistry 32, 181-191.

Aquino Neto, F.R., Trendel, J.M., Restle, A., Connan, J., Albrecht, P.A., 1983. Occurrence and formation of tricyclic and tetracyclic terpanes in sediments and petroleums. In: Advances in Organic Geochemistry 1981 (Ed. by M. Bjorøy, *et al.*), pp. 659-667. Wiley, Chichester.

Atlas, R.M., 1981. Microbial degradation of petroleum hydrocarbons—an environmental perspective. Microbiological Reviews 45, 180-209.

Baedecker, M.J., Cozzarelli, I.M., Eganhouse, R.P., Siegel, D.I., Bennett, P.C., 1993. Crude-oil in a shallow sand and gravel aquifer. 3. Biogeochemical reactions and mass-balance modelling in anoxic groundwater. Applied Geochemistry 8, 569-586.

Bahrami, A., Shojaosadati, S.A., Mohebali, G., 2001. Biodegradation of dibenzothiophene by thermophilic bacteria. Biotechnology Letters 23, 899-901.

Bailey, N.J.L., Krouse, H.H., Evans, C.R., Rogers, M.A., 1973. Alteration of crude oil by waters and bacteria - Evidence from geochemical and isotope studies. AAPG Bull. 57, 1276-1290.

Barnard, P.C., Bastow, M.A., 1991. Hydrocarbon generation, migration alteration, entrapment and mixing in the central and northern N. Sea. In: England, W.A. and Fleet, A.J. (Eds). Geological Society Special Publication, No. 59, Petroleum Migration, The Geological Society, London, pp. 167-190.

Baskin D.K., Jones R.W., 1993. Prediction of oil gravity prior to drill-stem testing in Monterey Formation reservoirs, offshore California. AAPG Bulletin77, 1479-1487.

Bastow, T.P., Alexander, R., Sosrowidjojo, I.B., Kagi, R.I., 1998. Pentamethylnaphthalenes and related compounds in sedimentary organic matter. Organic Geochemistry 28, 585-595.

Bastow, T.P., van Aarssen, B.G.K., Alexander, R., Kagi, R.I., 1999. Biodegradation of aromatic land-plant biomarkers in some Australian crude oils. Organic Geochemistry 30, 1229-1239.

Beller, H.R., 2000. Metabolic indicators for detecting in situ anaerobic alkylbenzene degradation. Biodegradation 11, 125-139.

Benedik, M.J., Gibbs, P.R., Riddle, R.R. and Wilson, R.C., 1998. Microbial denitrogenation of fossil fuels. Trends in Biotechnology 16, 390-395.

Bennett, B., Bowler, B.F.J., Larter, S.R., 1996. Determination of C_0-C_3 alkylphenols in crude oils and waters. Analytical Chemistry 68, 3697-3702.

Bennett, B., Larter, S.R., 2000. Quantitative separation of aliphatic and aromatic hydrocarbons using silver ion-silica solid-phase extraction. Analytical Chemistry 72, 1039-1044.

Bennett, B., Chen, M., Brincat, D., Gelin, F.J.P., Larter, S.R., 2002. Fractionation of benzocarbazoles between source rocks and petroleums. Organic Geochemistry 33, 545-559.

Bennett, P.C., Siegel, D.E. Baedecker, M.J., Hult, M.F., 1993. Crude oil in a shallow sand and gravel aquifer. I. Hydrogeology and inorganic geochemistry. Applied Geochemistry 8, 529-549.

Bennett, P.C., Hiebert, F.K., Rogers, J.R., 2000. Microbial control of mineral-groundwater equilibria: Macroscale to microscale. Hydrogeology Journal 8, 47-62.

Bennett, P.C, Rogers, J.R., Choi, W.J., 2001. Silicates, silicate weathering, and microbial ecology. Geomicrobiology Journal 18, 3-19.

Bernard, F.P., Connan, J., 1992. Indigenous microorganisms in connate waters of many oilfields: a new tool in exploration and production techniques. SPE 24811. In: 67th

Annual Technical Conference and Exhibition of the Society of Petroleum Engineers, Washington, DC, October 1992, pp 467-476.

Bharati, S., Patience, R., Mills, N., Hanesand, T., 1997. A new North Sea oil-based standard for Iatroscan analysis, Organic Geochemistry 26, 49-57.

Bigge, M.A., Farrimond, P., 1998. Biodegradation of seep oils in the Wessex Basin - a complication for correlation. In: Developement, Evolution and Petroleum of the Wessex Basin., Special Publication 133 (Ed. by J.R. Underhill), Geological Society, London, pp. 373-386.

Bishop, A.N., Love, G.D., McAulay, A.D., Snape, C.E., Farrimond, P., 1998. Release of kerogen-bound hopanoids by hydropyrolysis. Organic Geochemistry 29, 989-1001.

Blanc, P., Connan, J., 1992. Origin and occurrence of 25-norhopanes: a statistical study. Organic Geochemistry 18, 813-828.

Bogan, B.W., Lahner, L.M., Sullivan, W.R., Paterek, J.R., 2003. Degradation of straight-chain aliphatic and high-molecular-weight polycyclic aromatic hydrocarbons by a strain of Mycobacterium austroafricanum. Journal of Applied Microbiology 94, 230-239.

Bost, F.D., Frontera-Suau, R., McDonald, T.J., Peters, K.E., Morris, P.J., 2001. Aerobic biodegradation of hopanes and norhopanes in Venezuelan crude oils. Organic Geochemistry 32, 105-114.

Bowler, B.F.J., Larter, S.R., Clegg, H., Wilkes, H., Horsfield, B., Li, M., 1997. Dimethylcarbazoles in crude oils: comment on "liquid chromatographic separation schemes for pyrrole and pyridine nitrogen aromatic heterocyclic fractions from crude oils suitable for rapid characterization of geochemical samples". Analytical Chemistry 69, 3128–3129.

Bressler, D.C., Norman, J.A., Fedorak, P.M., 1997. Ring cleavage of sulfur heterocycles: how does it happen? Biodegradation 8. 297-311.

Bressler, D.C., Fedorak, P.M., 2000. Bacterial metabolism of fluorene, dibenzofuran, dibenzothiophene, and carbazole. Canadian Journal of Microbiology 46, 397-409.

Broholm, M.M., Arvin, E., 2000. Biodegradation of phenols in a sandstone aquifer under aerobic conditions and mixed nitrate and iron reducing conditions. Journal of Contaminant Hydrology 44, 239-273.

Brooks, P.W., Fowler, M.G, MacQueen, R.W., 1988. Biological marker conventional organic geochemistry of oilsands/heavy oils, Western Canada Basin. Organic

Geochemistry 12, 519-538.

Budzinski, H., Garrigues, P., Connan, J., Devillers, J., Domine, D., Radke, M., Oudin, J.L., 1995. Alkylated phenanthrene distributions as maturity and origin indicators in crude oils and rock extracts. Geochimica et Cosmochimica Acta 59, 2043-2056.

Budzinski, H., Raymond, N., Nadalig, T., Gilewicz, M., Garrigues, P., Bertrand, J.C., Caumette, P., 1998. Aerobic biodegradation of alkylated aromatic hydrocarbons by a bacterial community. Organic Geochemistry 28, 337-348.

Caldini, G., Cenci, G., Manenti, R., Morozzi, G., 1995. The ability of an environmental isolate of Pseudomonas fluorescens to utilize chrysene and other four-ring polynuclear aromatic hydrocarbons. Applied Microbiology and Biotechnology 44, 225-229.

Caldwell, M.E., Garrett, R.M., Prince, R.C., Suflita, J.M., 1998. Anaerobic biodegradation of long-chain *n*-alkanes under sulfate-reducing conditions. Environmental Science and Technology 32, 2191-2195.

Cassani, F., Gallango, O., Talukdar, S., Vallejos, C., Ehrmann, U., 1988. Methylphenanthrene maturity index of marine source rock extracts and crude oils from the Maracaibo Basin. Organic Geochemistry 13, 73-80.

Cassani, F., Eglinton, G., 1986. Organic geochemistry of Venezuelan extra heavy oils. 1. Pyrolysis of asphaltenes: a technique for the correlation and maturity evaluation of crude oils, Chemical Geology 56, 167-183.

Cassani, F., Eglinton, G., 1991. Organic geochemistry of Venezulean extra-heavy crude oils: Pt.2: Molecular assessment of biodegradation. Chemical Geology 91, 315-333.

Chakhmakhchev, A., Suzuki, M., Takayama. K., 1997. Distribution of alkylated dibenzothiophenes in petroleum as a tool for maturity assessments, Organic Geochemistry 26, 483-489.

Chang, B.V., Shiung, L.C., Yuan, S.Y., 2002. Anaerobic biodegradation of polycyclic aromatic hydrocarbon in soil. Chemosphere 48, 717-724.

Chen, M., 1995. Response of Pyrrolic and Phenolic Compounds to Petroleum Migration and In-Reservoir Processes. PhD thesis, University of Newcastle upon Tyne, England, UK.

Chosson, P., Lanau, C., Connan, J., Dessort, D., 1991. Biodegradation of refractory hydrocarbon biomarkers from petroleum under laboratory conditions. Nature 351, 640-642.

Claypool, G.E., Mancini, E.A., 1989. Geochemical relationships of petroleum in Mesozoic reservoirs to carbonate source rocks of Jurassic Smackover Formation, southwestern Alabama. AAPG Bulletin 73, 904-924.

Clegg, H., Wilkes, H., Santamaría-Orozco, D., Horsfield, B., 1998a. Influence of maturity on carbazole and benzocarbazole distributions in crude oils and source rocks from the Sonda de Campeche, Gulf of Mexico. Organic Geochemistry 29, 183-194.

Clegg, H., Horsfield, B., Wilkes, H., Sinninghe Damsté, J., Koopmans, M.P., 1998b. Effect of artificial maturation on carbazole distributions, as revealed by the hydrous pyrolysis of an organic-sulfur-rich source rock (Ghareb Formation, Jordan). Organic Geochemistry 29, 1953-1960.

Coates, J.D., Anderson, R.T., Woodward, J.C., Phillips, E.J.P., Lovley, D.R., 1996. Anaerobic hydrocarbon degradation in petroleum-contaminated harbor sediments under sulfate-reducing and artificially imposed iron-reducing conditions. Environmental Science and Technology 30, 2784-2789.

Connan, J., 1984. Biodegradation of crude oils in reservoirs. In: Brooks, J. and Welte, D., (Eds.), Advances in Petroleum Geochemistry I, Academic Press, London, pp. 299-335.

Connan, J., Lacrampe-Coulombe, G, Magot, M. 1996. Origin of gases in reservoirs. In: Proc. 1995 International Gas Research Conference, Cannes, France, 6–9 November, 1995. Government Institutes, Inc, Rockville, USA, pp 21–61.

Cozzarelli, I.M., Eganhouse, R.P., Baedecker, M.J., 1990. Transformation of monoaromatic hydrocarbons to organic-acids in anoxic groundwater environment. Environmental Geology and Water Sciences 16, 135-141.

Cozzarelli, I.M., Baedecker, M.J., Eganhouse, R.P., Goerlitz, D.F., 1994. The geochemical evolution of low-molecular-weight organic-acids derived from the degradation of petroleum contaminants in groundwater. Geochimica et Cosmochimica Acta 58, 863-877.

Curiale, J.A., Rui, L., 1991. Tertiary deltaic and lacustrine organic facies - comparison of biomarker and kerogen distributions. Organic Geochemistry 17, 785-803.

Curiale, J.A., Bromley, B.W., 1996. Migration of petroleum into Vermilion 14 field, Gulf Coast, USA - Molecular evidence. Organic Geochemistry 24, 563-579.

Dahl, J.E.P., Moldowan, J.M., Teerman, S.C., Mccaffrey, M.A., Sundararaman, P., Stelting, C.E., 1994. Source-rock quality determination from oil biomarkers. 1. A new geochemical technique. AAPG Bulletin 78, 1507-1526.

Dahl, J.E., Moldowan, J.M., Peters, K.E., Claypool, G.E., Rooney, M.A., Michael, G.E., Mello, M.R., Kohnen, M.L., 1999. Diamondoid hydrocarbons as indicators of natural oil cracking. Nature 399, 54-57.

Dale, J.D., Larter, S.R., Aplin, A.C., MacLeod, G.M., 1995. The organic geochemistry of North Sea oilfield production waters. In: J.O. Grimalt and C. Dorronsoro (Eds.), Organic Geochemistry: Developments and Applications to Energy, Climate and Human History. Selected papers from the 17th International Meeting on Organic geochemistry, 4-8 September 1995, Donostia-San Sebastian, The Basque Country, Spain, pp. 396-398.

Damsté, J.S., Kenig, F., Koopmans, M.P., Köster, J., Schouten, S., Hayes, J.M., de Leeuw, J., 1995. Evidence of gammacerane as an indicator of water column stratification. Geochimica et Cosmochimica Acta 59, 1895-1900.

Dean-Ross, D., Moody, J., Cerniglia, C.E., 2002. Utilization of mixtures of polycyclic aromatic hydrocarbons by bacteria isolated from contaminated sediment. FEMS Microbiology Ecology 41, 1-7.

Demaison, G.J., 1977. Tar sands and supergiant oil fields. AAPG Bulletin 61, 1950-1961.

Demaison, G., Huizinga, B.J., 1991. Genetic classification of petroleum systems. AAPG Bulletin 75, 1626-1643.

Diaz, M.P, Grigson, S.J.W., Peppiatt, C.J., Burgess, J.G., 2000. Isolation and characterization of novel hydrocarbon-degrading euryhaline consortia from crude oil and mangrove sediments. Marine Biotechnology 2, 522-532.

Didyk, B.M., Simoneit, B.R.T., Brassell, S.C., Eglinton, G., 1978. Organic geochemical indicators of palaeoenvironmental conditions of sedimentation. Nature 272, 216-222.

van Duin, A.C.T., Baas, J.M.A., van de Graaf, de Leeuw, J.W., Bastow, T.P., Alexander, R., 1997. Comparison of calculated equilibrium mixtures of alkylnaphthalenes and alkylphenanthrenes with experimental and sedimentary data - the importance of entropy calculations. Organic Geochemistry 26, 275-280.

van Duin, A.C.T., Larter, S.R., 1998. Application of molecular dynamics in the prediction of dynamical molecular properties. Organic Geochemistry 29, 1043-1050.

Dyreborg, S., Arvin, E., Broholm, K., 1997. Biodegradation of NSO-compounds under different redox-conditions. Journal of Contaminant Hydrology 25, 177-197.

Dzou L.I.P., Hughes W.B., 1993. Geochemistry of oils and condensates, K-field, offshore Taiwan - a case-study in migration fractionation. Organic Geochemistry 20, 437-462.

Ekweozor, C.M., Strausz, O.P., 1983. Tricyclic terpanes in the Athabasca oil sands: their geochemistry. In: Bjorøy, M. *et al.*, 1983. Advances in Organic Geochemistry 1983, Wiley, Chichester, pp. 746-766.

Ehrenberg, S.N., Jakobsen, K.G, 2001. Plagioclase dissolution related to biodegradation of oil in Brent Group sandstones (Middle Jurassic) of Gullfaks Field, northern North Sea. Sedimentology 48, 703-721.

Ehrenreich, P., Behrends, A., Harder, J., Widdel, F., 2000. Anaerobic oxidation of alkanes by newly isolated denitrifying bacteria. Archives of Microbiology 173, 58-64.

England, W.A., Mackenzie, A.S., Mann D.M, Quigley, T.M., 1987. The movement and entrapment of petroleum fluids in the subsurface. Journal of the Geological Society of London 144, 327-347.

Ernstsen, V., Gates, W.P., Stucki, J.W., 1998. Microbial reduction of structural iron in clays - A renewable source of reduction capacity. Journal of Environmental Quality 27, 761-766.

Evans, C.R., Rogers, M.A. and Bailey, N.J.L., 1971. Evolution and alteration of Petroleum in Western Canada. Chemical Geology 8, 147-170.

Farrimond, P., Fox, P.A., Innes, H.E., Miskin, I.P. Head, I.M., 1998. Bacterial sources of hopanoids in recent sediments: improving our understanding of ancient hopane biomarkers. Ancient Biomolecules 2, 147-166.

Farrimond, P., Bevan, J.C., Bishop, A.N., 1999. Tricyclic terpane maturity parameters: response to heating by an igneous intrusion. Organic Geochemistry 30, 1011-1019.

Farrimond, P., Head, I. M., Innes, H.E., 2000. Environmental influence on the biohopanoid composition of recent sediments. Geochimica et Cosmochimica Acta 64, 2985-2992.

Fedorak, P.M., Westlake, D.W.S., 1984. Microbial-degradation of alkyl carbazoles in Norman wells crude-oil. Applied and Environmental Microbiology 47, 858-862.

Fisher, S.J., Alexander, R., Kagi, R.I., 1996. Biodegradation of alkylnaphthalenes in sediment adjacent to an offshore petroleum production platform. Polycyclic Aromatic Compounds 11, 35-42.

Fisher, S.J., Alexander, R., Kagi, R.I., Oliver, G.A., 1998. Aromatic hydrocarbons as indicators of petroleum biodegradation in North Western Australian reservoirs. In: Purcell, P.G., Purcell, R.R. (Eds.), The Sedimentary Basins of Western Australia 2, Proceedings of Petroleum Exploration Society Symposium, Perth, pp. 185-194.

Galimberti, R., Ghiselli, C., Chiaramonte, M.A., 2000. Acidic polar compounds in petroleum: a new analytical methodology and applications as molecular migration indices. Organic Geochemistry 31, 1375-1386.

Ge, T., Chen, Y., 1993. Liaohe Oilfield. Petroleum Geology of China 3. Petroleum Industry Press, Beijing. (In Chinese).

Genthner, B.R.S., Townsend, G.T., Lantz, S.E., Mueller, J.G., 1997. Persistence of polycyclic aromatic hydrocarbon components of creosote under anaerobic enrichment conditions. Archives of Environmental Contamination and Toxicology 32, 99-105.

George, S.C., Llorca, S.M., Hamilton, P.J., 1994. An integrated analytical approach for determining the origin of solid bitumens in the McArthur Basin, northern Australia. Organic Geochemistry 21, 235-248.

George, S.C., Boreham, C.J., Minifie, S.A., Teerman, S.C., 2002. The effect of minor to moderate biodegradation on C_5 to C_9 hydrocarbons in crude oils. Organic Geochemistry 33, 1293-1317.

Gibson, D.T., 1991. The role of oxygenases in the microbial oxidation of aromatic compounds. ACS Abstracts 201, AGFD46.

Goldstein, T.P., Aizenshtat, Z., 1994. Thermochemical sulfate reduction a review. Journal of Thermal Analysis 42, 241-290.

Goodwin, N.S., Park, P.J.D., Rawlinson, A.P., 1983. Crude oil biodegradation under simulated and natural condition. In: Advances in Organic Geochemistry 1981 (Ed. by M. Bjorøy, *et al.*), pp. 650-658. J. Wiley & Sons, New York.

van Graas, G.W., Gilje, A.E., Isom, T.P., Tau, L.A., 2000. Effects of phase fractionation on the composition of oils, condensates and gases. Organic Geochemistry 31, 1419-1439.

De Grande, S.M.B., Aquino Neto, F.R., Mello, M.R., 1993. Extended tricyclic terpanes in sediments and petroleums. Organic Geochemistry 20, 1039-1047.

Grassia, G.S., McLean, K.M., Glenat, P., Bauld ,J., Sheehy, A.J., 1996. A systematic survey for thermophilic fermentative bacteria and archaea in high temperature petroleum reservoirs. FEMS Microbiology Ecology 21, 47-58.

Guthrie, J.M., Walters, C.C., Peters, K.E., 1998. Comparison of micro-techniques used for analyzing oils in sidewall cores to model viscosity, API gravity, and sulfur content. AAPG Bulletin 82, 1921.

Harrison, E., Telnaes, N., Wilhelms, A., Horsfield, B., Van Duin, A., Bennett, B., Larter, S.R., 1997. Maturity controls on carbazole distributions in coals and source rocks. In

Poster Sessions from the 18th International Meeting on Organic Geochemistry, Maastricht, The Netherlands, 22-26 September 1997, pp. 235-236.

Harwood, C.S., Burchhardt, G., Herrmann, H., Fuchs, G., 1998. Anaerobic metabolism of aromatic compounds via the benzoyl-CoA pathway. FEMS Microbiology Reviews 22, 439-458.

ten Haven, H.L., de Leeuw, J.W., Rullkötter, J., Sinninghe Damsté, J.S., 1987. Restricted utility of the pristane/phytane ratio as a palaeoenvironmental indicator. Nature 330, 641-643.

ten Haven, H.L., de Leeuw, J.W., Sinninghe Damsté, J.S., Schenck, P.A., Palmer, S.E., Zumberge, J.E., 1988. Application of biological markers in the recognition of palaeohypersaline environments. In: Fleet, A.J. *et al.* (Eds). Lacustrine Petroleum Source-rocksGeological Society Special Publication 40, Blackwell Scientific Publications, Oxford, pp. 123-130.

ten Haven, H.L., Rohmer, M., Rullkötter, J., Bisseret, P., 1989. Tetrahymanol, the most likely precursor of gammacerane, occurs ubiquitously in marine sediments. Geochimica et Cosmochimica Acta 53, 3073-3079.

Head, I.M., Jones, D.M., Larter, S.R., 2003. Biological activity in the deep subsurface and the origin of heavy oil. Nature 426 (6964), 344-352.

Heider, J., Spormann, A.M., Beller, H.R., Widdel, F., 1999. Anaerobic bacterial metabolism of hydrocarbons. FEMS Microbiology Reviews 22, 459-473.

de Hemptinne, J.C., Peumery, R., Ruffier-Meray, V., Moracchini, G., Naiglin, J., Carpentier, B., Oudin, J.L., Connan, J. 2001. Compositional changes resulting from the water-washing of a petroleum fluid. Journal of Petroleum Science and Engineering 29, 39-51.

Herman, D.C., Fedorak, P.M., Mackinnon, M.D., Costerton, J.W., 1994. Biodegradation of naphthenic acids by microbial-populations indigenous to oil sands tailings. Canadian Journal of Microbiology 40, 467-477.

Hinteregger, C., Leitner, R., Loidl, M., Ferschl, A., Streichsbier, F., 1992. Degradation of phenol and phenolic-compounds by pseudomonas-*putida ekii*. Applied Microbiology and Biotechnology 37, 252-259.

Ho, T.Y., Rogers, M.P., Drushel, H.V., Koons, C.B., 1974. Evolution of sulfur compounds in crude oils. AAPG Bulletin 58, 2338-2348.

Holba, A.G., Dzou, L.I.P., Hickey, J.J., Franks, S.G., May, S.J., Lenney, T., 1996.

Reservoir geochemistry of South Pass 61 Field, Gulf of Mexico: Compositional heterogeneities reflecting filling history and biodegradation. Organic Geochemistry 24, 1179-1198.

Holba, A.G., Dzou, L.I., Wood, G.D., Ellis, L., Adam, P., Schaeffer, P., Albrecht, P., Greene, T., Hughes, W.B., 2003. Application of tetracyclic polyprenoids as indicators of input from fresh-brackish water environments. Organic Geochemistry 34, 441-469.

Holliger, C., Zehnder, A.J.B., 1996. Anaerobic biodegradation of hydrocarbons. Current Opinion in Biotechnology 7, 326-330.

Horsfield, B., Schenk, H.J., Mills, N., Welte, D.H., 1992. An investigation of the in-reservoir conversion of oil to gas - compositional and kinetic findings from closed-system programmed-temperature pyrolysis. Organic Geochemistry 19, 191-204.

Horsfield, B., Clegg, H., Wilkes, H. and Santamaría-Orozco, D., 1998. Maturity control of carbazole distributions in petroleum systems. Naturwissenschaften 85, 233-237.

Horstad, I., Larter, S.R., Mills, N., 1992. A quantitative model of biological petroleum degradation within the Brent Group reservoir in the Gullfaks field, Norwegian North Sea. Organic Geochemistry 19, 107-117.

Horstad, I., Larter, S.R., 1997. Petroleum migration, alteration, and remigration within Troll Field, Norwegian North Sea. AAPG Bulletin 81, 222-248 .

Hostettler, F.D., Kvenvolden, K.A., 1994. Geochemical changes in crude-oil spilled from the Exxon-Valdez supertanker into Prince-William-Sound, Alaska. Organic Geochemistry 21, 927-936.

Howard, P.H., Boethling, R.S., Jarvis, W.F., Meylan, W.M., Michalenko, E.M., 1991. Handbook of Environmental Degradation Rates. Lewis Publishers, Chelsea, MI (725 pp.).

Hu, S., O'Sullivan P.B., Razac, A., Kohn, B.P., 2001. Thermal history and tectonic subsidence of the Bohai Basin, northern China: a Cenozoic rifted and local pull-apart basin. Physics of the Earth and Planetary Interiors 126, 221-235.

Huang, H.P., Pearson, M.J., 1999. Source rock palaeoenvironments and controls on the distribution of dibenzothiophenes in lacustrine crude oils, Bohai Bay Basin, eastern China. Organic Geochemistry 30, 1455-1470.

Huang, H.P., 2000. The nature and origin of petroleum in the Chaiwopu Sub-basin (Junggar Basin), NW China. Journal of Petroleum Geology 23, 193-220.

Huang, H.P., Ren, F.X., Larter, S.R., 2002. Influence of biodegradation on benzocarbazole

distributions in reservoired oils. Chinese Science Bulletin 47, 1734-1739.

Huang, H.P., Bowler, B.F.J., Zhang, Z.W., Oldenburg, T.B.P., Larter, S.R., 2003a. Influence of biodegradation on carbazole and benzocarbazole distributions in single oil columns from the Liaohe basin, NE China. Organic Geochemistry 34, 951-969.

Huang, H.P., Jin, G.X., Lin, C.S., Zheng, Y.B., 2003b. Origin of an unusual heavy oil from the Baiyinchagan depression, Erlian basin, northern China. Marine and Petroleum Geology 20, 1-12.

Huang, H.P., Larter, S.R., Bowler, B.F.J., Oldenburg, T.B.P., 2004. A dynamic biodegradation model suggested by petroleum compositional gradients within reservoir columns from the Liaohe basin, NE China. Organic Geochemistry (in press).

Huang, Y., Meinschein, W.G., 1979. Sterols as ecological indicators. Geochimica et Cosmochimica Acta 43, 739-745.

Hughes, W.B., Holba, A.G., Dzou, L.I.P., 1995. The ratios of dibenzothiophene to phenanthrene and pristane to phytane as indicators of depositional environment and lithology of petroleum source rocks. Geochimica et Cosmochimica Acta 59, 3581-3598.

Hunkeler, D., Jorger, D., Haberli, K., Hohener, P., Zeyer, P., 1998. Petroleum hydrocarbon mineralisation in anaerobic laboratory aquifer columns. Journal of Contaminant Hydrology 32, 41-61.

Hunt, J.H., 1996. Petroleum Geology and Geochemistry (2nd Edn.). W. H. Freeman and Co., New York.

Ioppolo-Armanios, M., Alexander, R., Kagi, R.I., 1995. Geosynthesis of organic compounds. I Ð Alkylation of sedimentary phenols. Geochimica et Cosmochimica Acta 59, 3017-3027.

Jaffé, R., Albrecht, P. and Oudin, J.L., 1988. Carboxylic acids as indicators of oil migration – I. Occurrence and geochemical significance of C-22 diastereoisomers of the (17βH,21βH) C30 hopanoic acid in geological samples. Organic Geochemistry 13, 484-488.

Jaffé, R., Gallardo, M.T., 1993. Application of carboxylic-acid biomarkers as indicators of biodegradation and migration of crude oils from the Maracaibo Basin, western Venezuela. Organic Geochemistry 20, 973-984.

Jiang, Z.S., Fowler, M.G., Lewis, C.A., Philp, R.P., 1990. Polycyclic alkanes in a biodegraded oil from the Kelamayi oil field, Northwest China. Organic Geochemistry

15, 35-46.

Johansen, S.S., Hansen, A.B., Mosbaek, H., Arvin, E., 1997. Identification of heteroaromatic and other organic compounds in ground water at creosote-contaminated sites in Denmark. Ground Water Monitoring and Remediation 17, 106-115.

Kaiko, A.R., Tingate, P.R., 1997. Suppressed vitrinite reflectance and its effect on thermal history modelling in the Barrow and Dampier sub-basins. Fuel and Energy Abstracts 38, 391.

Kaphammer, B., Kukor, J.J., Olsen, R.H., 1990. Cloning and characterization of a novel toluene degradative pathway from Pseudomonas pickettii, abstr. K-145, Abstr. 90th Annual Meeting of Am. Soc. Microbiol., p. 243.

Karlsen, D.A., Larter, S., 1991. Analysis of petroleum fractions by TLC-FID: Application to petroleum reservoir description. Organic Geochemistry 17, 603-617.

Khavari-Khorasani, G., Michelsen, J.K. and Dolson, J.C., 1998. The factors controlling the abundance and migration of heavy vs. light oils, as constrained by data from the Gulf of Suez. Part II. The significance of reservoir mass transport processes. Organic Geochemistry 29, 283-300.

Kiehlmann, E., Pinto, L., Moore, M., 1996. The biotransformation of chrysene to trans-1,2-dihydroxy-1,2-dihydrochrysene by filamentous fungi. Canadian Journal of Microbiology 42, 604-608.

Kirimura, K., Nakagawa, H., Tsuji, K., Matsuda, K., Kurane, R. and Usami, S., 1999. Selective and continuous degradation of carbazole contained in petroleum oil by resting cells of *Sphingomonas* sp. CDH-7. Bioscience Biotechnology and Biochemistry 63, 1563-1568.

Koopmans, M.P., Larter, S.R., Zhang, C., Mei, B., Wu, T., Chen, Y., 2002. Biodegradation and mixing of crude oils in Eocene Es3 reservoirs of the Liaohe basin, northeastern China. AAPG Bulletin 86,1833-1843.

Kropp, K.G., Andersson, J.T., Fedorak, P.M., 1997. Biotransformations of three dimethyldibenzothiophenes by pure and mixed bacterial cultures. Environmental Science and Technology 31, 1547-1554.

Kropp, K.G., Fedorak, P.M., 1998. A review of the occurrence, toxicity, and biodegradation of condensed thiophenes found in petroleum. Canadian Journal of Microbiology 44, 605-622.

Krouse, H.R., Viau, C.A., Eliuk, L.S., Ueda, A., Halas, S., 1989. Chemical and isotopic evidence of thermochemical sulfate reduction by light hydrocarbon gases in deep carbonate reservoirs. Nature 333, 415-419.

Kruge, M.A., Hubert, J.F., Akes, R.J., Meriney, P.E., 1990. Biological markers in Lower Jurassic synrift lacustrine black shales, Hartford basin, Connecticut, USA. Organic Geochemistry 15, 281-289.

Kruge, M.A., 2000. Determination of thermal maturity and organic matter type by principal components analysis of the distributions of polycyclic aromatic compounds. International Journal of Coal Geology 43, 27-51.

Kuo, L.C., 1994. An experimental-study of crude-oil alteration in reservoir rocks by water washing. Organic Geochemistry 21, 465-479.

Lafargue, E., Barker, C., 1988. Effect of water washing on crude-oil compositions. AAPG Bulletin 72, 263-276.

Lafargue, E., Le Thiez, P., 1996. Effect of waterwashing on light ends compositional heterogeneity. Organic Geochemistry 24, 1141-1150.

Langbehn, A., Steinhart, H., 1995. Biodegradation studies of hydrocarbons in soils by analyzing metabolites formed. Chemosphere 30, 855-868.

Larter, S., Mills N., 1991. Phase-controlled molecular fractionations in migrating petroleum charges. In: England, W.A., Fleet, A.J. (Eds.), Petroleum Migration. Geological Society Special Publications No. 59, pp. 137-147.

Larter, S.R., Aplin, A.C., 1995. Reservoir geochemistry: Methods, applications and opportunities. In: J.M. Cubitt and W.A. England (Eds.), The Geochemistry of Reservoirs. Special Publication 86, Geological Society, London, pp. 5-32.

Larter, S.R., Bowler, B.F.J., Li, M., Chen, M., Brincat, D., Bennett, B., Noke, K., Donohoe, P., Simmons, D., Kohnen, M., Allan, J., Telnaes, N., Horstad, I., 1996a. Molecular indicators of secondary oil migration distances. Nature 383, 593-597.

Larter, S.R., Taylor, P.N., Chen, M., Bowler, B., Ringrose, P., Horstad, I., 1996b. Secondary migration - visualizing the invisible - what can geochemistry potentially do? In: Glennie, K., Hurst, A. (Eds.), NW Europe's Hydrocarbon Industry. Geological Society London, pp. 137-143.

Larter, S., Hockey, A., Aplin, A., Telnaes, N., Wilhelms, A., Horstad, I., Di Primio, R., Sylta, O., 1999. When biodegradtion preserves petroleum: North Sea oil rimmed gas accumulations (ORGA'S). In: Schoell, M., and Claypool, G.E., (Eds.), Proceedings of

the AAPG Hedberg Research Conference, June 6–10, 1999.

Larter, S.R., Bowler, B.F.J., Clarke, E., Wilson, C., Moffat, B., Bennett, B., Yardley, G., Carruthers, D., 2000. An experimental investigation of geochromatography during secondary migration of petroleum performed under subsurface conditions with a real rock. Geochemical Transactions 9, .

Larter, S. R., Wilhelms, A., Head, I., Koopmans, M., Aplin, A., Di Primio, R., Zwach, C., Erdmann, M., Telnaes, N., 2003. The controls on the composition of biodegraded oils in the deep subsurface: (Part 1) Biodegradation rates in petroleum reservoirs. Organic Geochemistry 34, 601-613.

Leythaeuser, D., Rückheim, J., 1989. Heterogeneity of oil composition within a reservoir as a reflection of accumulation history. Geochimica et Cosmochimica Acta 53, 2119-2123.

Li, M.; Larter, S. R.; Stoddart, D.; Bjorøy, M., 1992. Liquid chromatographic separation schemes for pyrrole and pyridine nitrogen aromatic heterocycle fractions from crude oils suitable for rapid characterization of geochemical samples. Analtical Chemistry 64, 1337-1344.

Li, M.W., Larter, S.R., Mei, B., 1994. Early generation of 20S-5-α(H), 14-α(H), 17-α(H)-steranes and 5-α(H), 14-β(H), 17-β(H)-steranes in low-salinity lacustrine shales. Organic Geochemistry 22, 893-902.

Li, M., Larter, S. R., Stoddart, D. and Bjorøy, M., 1995. Fractionation of pyrrolic nitrogen compounds in petroleum during migration: derivation of migration-related geochemical parameters. In: Cubitt J. M., England W. A. (Eds.), The Geochemistry of Reservoirs. Geol. Soc. Spec. Publ. Vol. 86, pp. 103-123.

Li, M., Huanxin, Y., Stasiuk, L.D., Fowler, M.G. and Larter, S.R., 1997. Effect of maturity and petroleum expulsion on pyrrolic nitrogen compound yields and distributions in Duvernay Formation petroleum source rocks in Central Alberta, Canada. Organic Geochemistry 26, 731-744.

Lin, L.H., Michael, G.E., Kovachev, G., Zhu, H., Philp, R.P., Lewis, C.A., 1989. Biodegradation of tar-sands bitumens from the Ardmore and Anadarko Basins, Carter County, Oklahoma. Organic Geochemistry 14, 511-523.

Lomando A.J., 1992.The influence of solid reservoir bitumen on reservoir quality. AAPG Bulletin 76, 1137-1152.

Losh, S., Cathles, L., Meulbroek, P., 2002. Gas washing of oil along a regional transect,

offshore Louisiana. Organic Geochemistry 33, 655-663.

Love, G.D., Snape, C.E., Carr, A.D., Houghton, R.C., 1995. Release of covalently-bound alkane biomarkers in high yields from kerogen via catalytic hydropyrolysis. Organic Geochemistry 23, 981-986.

Love, G.D., Snape, C.E., Fallick, A.E., 1998. Differences in the mode of incorporation and biogenicity of the principal aliphatic constituents of a Type I oil shale. Organic Geochemistry 28, 797-811.

Lovley, D.R., Phillips, E.J.P., 1986. Organic-matter mineralization with reduction of ferric iron in anaerobic sediments. Applied and Environmental Microbiology 51, 683-689.

Lu, J., Nakajima-Kambe, T., Shigeno, T., Ohbo, A., Nomura, N., Nakahara, T., 1999. Biodegradation of dibenzothiophene and 4,6-dimethyldibenzothiophene by Sphingomonas paucimobilis strain TZS-7. Journal of Bioscience and Bioengineering 88, 293-299.

Lu, S.N., He, W., Huang, H.P., 1990. The geochemical characteristics of heavy oil and its recovery in the Liaohe basin, China. Organic Geochemistry 16, 437-449.

Lucach, S.O., Bowler, B.F.J., Frewin, N., Larter, S.R., 2002. Variation in alkylphenol distributions in a homogenous oil suite from the Dhahaban petroleum system of Oman. Organic Geochemistry 33, 581-594.

Machel, H.G, 2001. Bacterial and thermochemical sulfate reduction in diagenetic settings - old and new insights. Sedimentary Geology 140, 143-175.

Mackenzie, A.S., Hoffmann, C.F., Maxwell, J.R., 1981. Molecular parameters of maturation in the Toarcian shales, Paris Basin, France - III. Changes in aromatic steroid hydrocarbons. Geochimica et Cosmochimica Acta 45, 1345-1355.

Mackenzie, A.S., Wolff, G.A. Maxwell, J.R., 1983. Fatty acids in some biodegraded petroleums. Possible origins and significance. In: M. Bjorøy *et al.* Advances in Organic Geochemistry 1981, Wiley, Chichester, pp. 637-649.

Mackenzie, A.S., 1984. Application of biological markers in petroleum geochemistry. In: Brooks, J., Welte, D., (Eds.), Advances in Petroleum Geochemistry I, Academic Press, London, pp. 115-214.

Macleod, G, Taylor, P.N., Larter, S.R. Aplin, A.C., 1993. Dissolved organic species in formation waters; insights into rockoil-water ratios in petroleum systems. In: J. Parnell *et al.* Geofluids 93, Geol. Soc. Spec. Pub., pp18-20.

Mango, F.D., 1991. The stability of hydrocarbons under the time temperature conditions of

petroleum genesis. Nature 352, 146-148.

Magoon, L.B., Dow, W.G., 1994. The petroleum system. In: Magoon, L.B. and Dow, W.G., Editors, 1994. The petroleum system — from source to trap. AAPG Memoir 60, pp. 3-24.

Mathur, N., Raju, S.V., Kulkarni, T.G., 2001. Improved identification of pay zones through integration of geochemical and log data: A case study from Upper Assam basin, India. AAPG Bulletin 85, 309-323.

Masterson, W.D., Dzou, L.I.P., Holba, A.G., Fincannon, A.L., Ellis, L., 2001. Evidence for biodegradation and evaporative fractionation in West Sak, Kuparuk and Prudhoe Bay field areas, North Slope, Alaska. Organic Geochemistry 32, 411-441.

Mazeas, L., Budzinski, H., Raymond, N., 2002. Absence of stable carbon isotope fractionation of saturated and polycyclic aromatic hydrocarbons during aerobic bacterial biodegradation. Organic Geochemistry 33, 1259-1272.

McCaffrey, M.A., Legarre, H.A., Johnson, S.J., 1996. Using biomarkers to improve heavy oil reservoir management: An example from the Cymric field, Kern County, California. AAPG Bulletin 80, 898-913.

Mei, B.W., Zhang, C.M., Piao, M.Z., Jin, D.W., Gan, C.F., 1994. Genetic analysis and distribution characteristics of heavy oils in the Lengdong Oilfield, Western depression of the Liaohe basin. (unpublished report in Chinese).

Mello, M.R., Telnaes, N., Gaglianone, P.C., Chicarelli, M.I., Brassell, S.C. and Maxwell, J.R., 1988. Organic geochemical characterization of depositional paleoenvironments in Brazilian marginal basins. Organic Geochemistry 13, 31-46.

Meredith, W., Kelland, S.J., Jones, D.M., 2000. Influence of biodegradation on crude oil acidity and carboxylic acid composition. Organic Geochemistry 31, 1059-1073.

Merdrignac, I., Behar, F., Albrecht, P., Briot, P., Vandenbroucke, M., 1998. Quantitative extraction of nitrogen compounds in oils: Atomic balance and molecular composition. Energy and Fuels 12, 1342-1355.

Meulbroek, P., Cathles, L., Whelan, J., 1998. Phase fractionation at South Eugene Island Block 330. Organic Geochemistry 29, 223-239.

Miiller, D.E., Holba, A.G., Huges, W.B., 1987. Effects of biodegradation on crude oils. In Meyer, R.F. (Ed.), Exploration for Heavy Crude Oil and Natural Bitumen. AAPG Studies in Geology 25. Tulsa, Oklahoma, pp 233-241.

Mille, G., Almallah, M., Bianchi, M., Vanwambeke, F., Bertrand, J.C., 1991. Effect of

salinity on petroleum biodegradation. Fresenius Journal of Analytical Chemistry 339, 788-791.

Moldowan, J.M., Seifert, W.K., Gallegos, E.J., 1985. Relationship between petroleum composition and depositional environment of petroleum source-rocks. AAPG Bulletin 69, 1255-1268.

Moldowan, J.M., Fago, F.J., Carlson, R.M.K., Young, D.C., Vanduyne, G., Clardy, J., Schoell, M., Pillinger, C.T., Watt, D.S., 1991. Rearranged hopanes in sediments and petroleum. Geochimica et Cosmochimica Acta 55, 3333-3353.

Moldowan, J.M., Lee, C.Y., Sundararaman, P., Salvatori, R., Alajbeg, A., Gjukic, B., Demaison, G.J., Slougui, N.E., Watt, D.S., 1992. Source correlation and maturity assessment of select oils and rocks from the Central Adriatic basin (Italy and Yugoslavia). In Moldowan, J.M., Albrecht, P., Philp, R.P. (Eds.), Biological Markers in Sediments and Petroleum. Englewood Cliffs, New Jersey, Prentice Hall, p. 370-401.

Moldowan, J.M., McCaffrey, M.A., 1995. A novel microbial hydrocarbon degradation pathway revealed by hopane demethylation in a petroleum reservoir. Geochimica et Cosmochimica Acta 59, 1891-1894.

Mossman, D.J., Nagy, B., 1996. Solid bitumens: An assessment of their characteristics, genesis, and role in geological processes. Terra Nova 8, 114-128.

Mueller, J.G., Chapman, P.J., Pritchard, P.H., 1989. Creosote-contaminated sites—their potential for bioremediation. Environmental Science and Technology 23, 1197-1201.

Mueller, R.F., Nielsen, P.H., 1996. Characterization of thermophilic consortia from two souring oil reservoirs. Applied and Environmental Microbiology 62, 3083-3087.

Muller, C., 1999. Modelling Soil-Biosphere Interactions. CABI Publishing Wallingford, UK.

Nadalig, T., Raymond, N., Gilewicz, M., Budzinski, H., 2000. Development of a protocol to study aerobic bacterial degradation of polycyclic aromatic hydrocarbons: Application to phenanthrenes. Polycyclic Aromatic Compounds 18, 177-192.

Napitupulu, H., Ellis, L., Mitterer, R.M., 2000. Post-generative alteration effects on petroleum in the onshore Northwest Java basin, Indonesia. Organic Geochemistry 31, 295-315.

Nascimento, L.R., Rebouças, L.M.C., Koike, L., Reis, F.A.M., Soldan, A.L., Cerqueira, J.R., Marsaioli, A.J., 1999. Acidic biomarkers from Albacora oils, Campos Basin, Brazil. Organic Geochemistry 30, 1175-1191.

Nazina, T.N., Ivanova, A.E., Golubeva, O.V., Ibatullin, R.R., Belyaev, S.S., Ivanov, M.V., 1995. Occurrence of sulfate-reducing and iron-reducing bacteria in stratal waters of the Romashkinskoe oilfield. Microbiology 64, 203-208.

Nielsen, P.H. and Christensen, T.H., 1994. Variability of biological degradation of phenolic hydrocarbons in an aerobic aquifer determined by laboratory batch experiments. Journal of Contaminant Hydrology 17, 55-67.

Niu, J.Y., Hu, J.Y., 1999. Formation and distribution of heavy oil and tar sands in China. Marine and Petroleum Geology 16, 85-95.

Obermajer, M., Fowler, M.G., Snowdon, L.R., 1999. Depositional environment and oil generation in Ordovician source rocks from southwestern Ontario, Canada: Organic geochemical and petrological approach. AAPG Bulletin 83, 1426-1453.

Okpokwasili, G.C., Odokuma, L.O., 1990. Effect of salinity on biodegradation of oil spill dispersants. Waste Management 10, 141-146.

Oldenburg, T., Horsfield, B., Wilkes, H., Stoddart, D., Wilhelms, A., 1999. Benzo[b]carbazole as a continental-deltaic source indicator, offshore Norway. In: Organic Geochemistry, Poster Sessions from the 19th International Meeting on Organic Geochemistry, 6–10 September 1999, Istanbul, Turkey, pp. 541-542.

Olsen, S.D., Filby, R.H., Brekke, T., Isaksen, G.H., 1995. Determination of trace-elements in petroleum-exploration samples by inductively-coupled plasma-mass spectrometry and instrumental neutron-activation analysis. Analyst 120, 1379-1390.

Ouchiyama, N., Zhang, Y., Omori, T., Kodama, T., 1993. Biodegradation of carbazole by Pseudomonas spp. CA06 and CA10. Bioscience Biotechnology and Biochemistry 57, 455-460.

Palacas, J.G., Anders, D.E., King, J.D., 1984. South Florida Basin—a prime example of carbonate source rocks in Petroleum. In Petroleum Geochemistry and Source Rock Potential of Carbonate Rocks, eds. J. G. Palacas. AAPG Studies in Geology 18, 71-96.

Palmer S.E., 1984. Effect of water washing on C_{15+} hydrocarbon fraction of crude oils from northwest Palawan, Philippines. AAPG Bulletin 68, 137-149.

Palmer, S.E., 1993. Effect of biodegradation and water washing on crude oil composition. In: Macko, S.A., Engel, M.H. (Eds.) Organic Gechemistry, Plenum Press, New York. pp. 511-534.

Pallasser, R.J., 2000. Recognising biodegradation in gas/oil accumulations through the delta C-13 compositions of gas components. Organic Geochemistry 31, 1363-1373.

Pepper, A.S., Corvi, P.J., 1995. Simple kinetic-models of petroleum formation .1. Oil and gas generation from kerogen. Marine and Petroleum Geology 12, 291-319.

Pepper, A., Santiago, C., 2001. Impact of biodegradation on petroleum exploration and production, Observations and outstanding problems. In: Abstracts of Earth Systems Processes, Geol Soc of London, Geol. Soc of America, Edinburgh, 24-28 June 2001.

Perrodon, A., 1992. Petroleum systems: models and applications. Journal of Petroleum Geology 15, 319-326.

Perrodon, A., 1995. Petroleum systems, and global tectonics. Journal Of Petroleum Geology 18, 471-476.

Peters, K.E., Moldowan, J.M., Schoell, M., Hempkins, W.B., 1986. Petroleum isotopic and biomarker composition related to source rock organic matter and depositional environment. Organic Geochemistry 10, 17-27.

Peters, K.E., Moldowan, J.M., 1991. Effects of source, thermal maturity and biodegradation on the distribution and isomerization of homohopanes in petroleum. Organic Geochemistry 17, 47-61.

Peters, K.E. and Moldowan, J.M., 1993. The biomarker guide: interpreting molecular fossils in petroleum and ancient sediments. Prentice Hall, Englewood Cliffs, NJ, 363p.

Peters, K.E., Moldowan, J.M., McCaffrey, M.A., Fago, F.J., 1996. Selective biodegradation of extended hopanes to 25-norhopanes in petroleum reservoirs. Insights from molecular mechanics. Organic Geochemistry 24, 765-783.

Peters, K.E., 2000. Petroleum tricyclic terpanes: predicted physicochemical behavior from molecular mechanics calculations. Organic Geochemistry 31, 497-507.

Peters, K.E., Fowler, M.G., 2002. Applications of petroleum geochemistry to exploration and reservoir management. Organic Geochemistry 33, 5-36.

Phelps, C.D., Young, L.Y., 2001. Biodegradation of BTEX under anaerobic conditions: A review. Advances in Agronomy 70, 329-357.

Phelps, C.D., Battistelli, J., Young, L.Y., 2002. Metabolic biomarkers for monitoring anaerobic naphthalene biodegradation in situ. Environmental Microbiology 4, 532-537.

Philp, R.P., Gilbert, T.D., Friedrich, J., 1981. Bicyclic sesquiterpenoids and diterpenoids in australian crude oils. Geochimica et Cosmochimica Acta 45, 1173-1180.

Philp, R.P., 1983. Correlation of crude oils from the San Jorges Basin, Argentina. Geochimica et Cosmochimica Acta 47, 267-275.

Philp, R.P., Gilbert, T.D., 1986. Biomarker distribution in oils predominantly derived from terrigenous source material. Organic Geochemistry 10, 73-84.

Philp, R.P., Bakel, A., Galvez-Sinibaldi, A., Lin, L.H., 1988. A Comparison of organosulfur compounds produced by pyrolysis of asphaltenes. Organic Geochemistry 13, 915-926.

Philp, R.P., 1994. Geochemical characteristics of oils derived predominantly from terrigenous source materials. In: Scott, A.C., Fleet, A.J. (Eds), Coal and Coal-bearing Strata as Oil-prone Source Rocks? Geological Society Special Publication No. 77, London, pp. 71-91.

Powlowski, J. and Shingler, V., 1994. Genetics and biochemistry of phenol degradation by Pseudomonas sp. CF600. Biodegradation 5, 219-236.

di Primio, R., 2002. Unraveling secondary migration effects through the regional evaluation of PVT data: a case study from Quadrant 25, NOCS. Organic Geochemistry 33, 643-653.

Prince R.C., 1994. 17α(H),21β(H)-hopane as a conserved internal marker for estimating the biodegradation of crude oil. Environmental Science and Technology 28, 142-145.

Price, L.C., Schoell, M., 1995. Constraints on the origins of hydrocarbon-gas from compositions of gases at their site of origin. Nature 378(6555), 368-371.

Radke, M., Welte, D., Willsch, H., 1982. Geochemical study on a well in the Western Canada Basin: Relation of the aromatic distribution pattern to maturity of organic matter. Geochimica et Cosmochimica Acta 46, 1-10.

Radke, M., Welte D.H., 1983. The methylphenanthrene index (MPI): a maturity parameter based on aromatic hydrocarbons. In: Bjøroy, M., *et al.* (Eds.), Advances in Organic Geochemistry 1981, Wiley, Chichester, UK, pp. 504-512.

Radke, M., Willsch, H., Welte, D.H., 1986. Maturity parameters based on aromatic hydrocarbons: influence of the organic matter type. Organic Geochemistry 10, 51-63.

Radke, M., 1988. Application of aromatic compounds as maturity indicators in source rocks and crude oils. Marine and Petroleum Geology 5, 224-236

Radke, M., Garrigues, P., Willsch, H., 1990. Methylated dicyclic and tricyclic aromatic hydrocarbons in crude oils from the Handil field, Indonesia. Organic Geochemistry 15, 17-34.

Radke, M., Willsch, H., 1994. Extractable alkyldibenzothiophenes in Posidonia shale (Toarcian) source rocks: relationship of yields to petroleum formation and expulsion.

Geochimica et Cosmochimica Acta 58, 5223-5244.

Reed, W.E., 1977. Molecular compositions of weathered petroleum and comparison with its possible source. Geochimica et Cosmochimica Acta 41, 237-247.

Reid, R.C., Prausnitz, J.M. and Poling, B.E., 1987. The properties of gases and liquids. (fourth ed.), McGraw Hill, New York, 741 pp.

Requejo, A.G., Halpern, H.I., 1989. An unusual hopane biodegradation sequence in tar sands from the Pt. Arena (Monterey) Formation. Nature 342, 670-673.

Requejo, A.G., 1994. Maturation of petroleum source rocks—II. Quantitative changes in extractable hydrocarbon content and composition associated with hydrocarbon generation. Organic Geochemistry 21, 91-105.

Requejo, A.G., Sassen, R., McDonald, T., Denoux, G., Kennicutt II, M.C., Brooks, J.M., 1996. Polynuclear aromatic hydrocarbons (PAH) as indicators of the source and maturity of marine crude oils. Organic Geochemistry 24, 1017-1033.

Ribéreau-Gayon, P., 1972. Plant Phenolics. Olivier & Boyd, Great Britain.

Riolo, J., Hussler, G., Albrecht, P., Connan, J., 1986. Distribution of aromatic steroids in geological samples: their evaluation as geochemical parameters. Organic Geochemistry 10, 981-990.

Rockne, K.J., Strand, S.E., 1998. Biodegradation of bicyclic and polycyclic aromatic hydrocarbons in anaerobic enrichments. Environmental Science and Technology 32, 3962-3967.

Rockne, K.J., Strand, S.E., 2001. Anaerobic biodegradation of naphthalene phenanthrene, and biphenyl by a denitrifying enrichment culture. Water Research 35, 291-299.

Rogers, J.R., Bennett, P.C., Choi, W.J., 1998. Feldspars as a source of nutrients for microorganisms. American Mineralogist 83, 1532-1540.

Rohmer, M., Bisseret, P., Neunlist, S., 1992. The hopanoids, prokaryotic triterpenoids and precursors of ubiquitous molecular fossils. In: J.M. Moldowan, P. Albrecht and R.P. Philp (Eds.), Biological Markers in Sediments and Petroleum. Prentice Hall, Englewood Cliffs, NJ, pp. 1-17.

Röling, W. F.M., Head, I.M., Larter, S.R., 2003. The microbiology of hydrocarbon degradation in subsurface petroleum reservoirs: perspectives and prospects. Research in Microbiology 154, 321-328.

Rooney, M.A., Vuletich, A.K., Griffith, C.E., 1998. Compound-specific isotope analysis as a tool for characterizing mixed oils: an example from the West of Shetlands area. Organic Geochemistry 29, 241-254.

Rowland, S.J., Alexander, R., Kagi, R.I., Jones, D.M., Douglas, A.G., 1986. Microbial degradation of aromatic components of crude oils: A comparison of laboratory and field observations. Organic Geochemistry 9, 153-161.

Rubinstein, I., Strausz, O.P., Spyckerelle, C., Crawford, R.J., Westlake, D.W.S., 1977. The origin of oil sand bitumins of Alberta. Geochimica et Cosmochimica Acta 41, 1341-1353.

Rubinstein, I., Spyckerelle, C., Strausz, O.P., 1979. Pyrolysis of asphaltenes: a source of geochemical information. Geochimica et Cosmochimica Acta 43, 1-6.

Rudolphi, A., Tschech, A., Fuchs, G., 1991. Anaerobic degradation of cresols by denitrifying bacteria. Archives of Microbiology 155, 238-248.

Rullkötter, J., Wendisch D., 1982. Microbial alteration of 17α(H)-hopanes in Madagascar asphalts: removal of C-10 methyl group and ring opening. Geochimica et Cosmochimica Acta 46, 1545-1553.

Sabate, J., Grifoll, M., Vinas, M., Solanas, A. M., 1999. Isolation and characterization of a 2-methylphenanthrene utilizing bacterium: identification of ring cleavage metabolites. Applied Microbiology and Biotechnology 52, 704-712.

Sandvik, E.I., Young, W.A., Curry, D.J., 1992. Expulsion from hydrocarbon sources: the role of organic absorption. Organic Geochemistry 19, 77-87.

Santamaria-Orozco, D., Horsfield, B., di Primio, R., Welte, D.H., 1998. Influence of maturity on distributions of benzo- and dibenzothiophenes in Tithonian source rocks and crude oils, Sonda de Campeche, Mexico. Organic Geochemistry 28, 423-439.

Schenk, H.J., Di Primio, R., Horsfield, B., 1997. Conversion of oil into gas in petroleum reservoirs. Part 1: Comparative kinetic investigation of gas generation from crude oils of lacustrine, marine and fluviodeltaic origin by programmed-temperature closed-system pyrolysis. Organic Geochemistry 26, 467-481.

Schink, B., Philipp, B., Müller, J., 2000. Anaerobic degradation of phenolic compounds. Die Naturwissenschaften 87, 12-23.

Schmitt, R., Langguth, H. R., Püttmann, W., Rohns, H.P., Eckert, P., Schubert, J., 1996. Biodegradation of aromatic hydrocarbons under anoxic conditions in a shallow sand and gravel aquifer of the Lower Rhine Valley, Germany. Organic Geochemistry 25,

41-50.

Schneider, J., Grosser, R.J., Jayasimhulu, K., Xue, W., Kinkle, B., Warshawsky, D., 2000. Biodegradation of carbazole by Ralstonia sp. RJGII.123 isolated from a hydrocarbon contaminated soil. Canadian Journal of Microbiology 46, 269-277.

Schulz, L.K., Wilhelms, A., Rein, E., Steen, A.S., 2001. Application of diamondoids to distinguish source rock facies. Organic Geochemistry 32, 365-375.

Scott, A.R., Kaiser, W.R., Ayers, W.B. Jr., 1994. Thermogenic and secondary biogenic gases, San Juan basin, Colorado and New Mexico - implications for coalbed gas producibility. AAPG Bulletin 78, 1186-1209.

Seifert, W.K., Moldowan, J.M., 1979. The effect of biodegradation on steranes and terpanes in crude oils. Geochimica et Cosmochimica Acta 43, 111-126.

Seifert, W.K., Moldowan, J.M., 1981. Paleoreconstruction by biological markers. Geochimica Et Cosmochimica Acta 45, 783-794.

Seifert, W.K., Moldowan, J.M., Demaison, G.J., 1984. Source correlation of biodegraded oils. Organic Geochemistry 6, 633-643.

Seifert, W.K., Moldowan, J.M., 1986. Use of biological markers in petroleum exploration. In: Johns, R.B. (Ed.), Biological Markers in the Sedimentary Record 24, Methods in Geochemistry and Geophysics. Elsevier, pp. 261–290.

Semple K,T., Cain, R.B., 1997. Degradation of phenol and its methylated homologues by *Ochromonas danica*. FEMS Microbiology Letters 152,133-139.

Sepic, E., Bricelj, M., Leskovsek, H., 1998. Degradation of fluoranthene by Pasteurella sp IFA and Mycobacterium sp PYR-1: isolation and identification of metabolites. Journal of Applied Microbiology 85,746-754.

Setti, L., Farinelli, P., Di Martino, S., Frassinetti, S., Lanzarini, G., Pifferi, P.G., 1999. Developments in destructive and non-destructive pathways for selective desulfurizations in oil-biorefining processes. Applied Microbiology and Biotechnology 52, 111-117.

Shi, J.Y., Wang, B.S., Zhang, L.J., Hong, Z.Q., 1988. Study on diagenesis of organic matter in immature rocks. Organic Geochemistry 13, 869-874.

Shotbolt-Brown, J., Hunter, D.W.F., Aislabie, J., 1996. Isolation and description of carbazole-degrading bacteria. Canadian Journal of Microbiology 42, 79-82.

Simoni, S.F., Schäfer, A., Harms, H., Zehnder, A.J.B., 2001. Factors affecting mass transfer limited biodegradation in saturated porous media. Journal of Contaminant

Hydrology 50, 99-120.

Smalley, P.C., Goodwin, N.S., Dillon, J.F., Bidinger, C.R., Drozd, R.J., 1997. New tools target oil-quality sweetspots in viscous-oil accumulations. SPE Reservoir Engineering 12, 157-161.

So, M.S., Young, L.Y., 1999. Initial reactions in anaerobic alkane degradation by a sulfate reducer, *Strain AK-01*. Applied and Environmental Microbiology 65, 2969-2976.

Stasiuk, L.D., 1997. Origin of pyrobitumens in Upper Devonian Leduc Formation gas reservoirs, Alberta, Canada: An optical and EDS study of oil to gas transformation. Marine and Petroleum Geology 14, 915-929.

Stojanovic, K., Jovancicevic, B., Pevneva, G.S., Golovko, J.A., Golovko, A.K., Pfendt, P., 2001. Maturity assessment of oils from the Sakhalin oil fields in Russia: phenanthrene content as a tool. Organic Geochemistry 32, 721-731.

Sundararaman, P., Hwang, R.J., 1993. Effect of biodegradation on vanadylporphyrin distribution. Geochimica et Cosmochimica Acta 57, 2283-2290.

Sweeney, R.E., Taylor, P., 1999. Biogenic methane derived from biodegradation of petroleum under environmental conditions and in oil and gas reservoirs. In: Schoell, M., and Claypool, G.E., (Eds.), Proceedings of the AAPG Hedberg Research Conference, 6–10 June, 1999.

Taylor, P., 1994. Controls on the Occurrence of Phenols in Petroleums and Waters. PhD. thesis, University of Newcastle upon Tyne, England, UK.

Taylor, P., Larter, S., Jones, M., Dale J., Horstad, I., 1997. The effect of oil-water-rock partitioning on the occurrence of alkylphenols in petroleum systems. Geochimica et Cosmochimica Acta 61, 1899-1910.

Taylor, P., Bennett, B., Jones, M., Larter, S., 2001. The effect of biodegradation and water washing on the occurrence of alkylphenols in crude oils. Organic Geochemistry 32, 341-358.

Talukdar, S., Gallango, O., Chin-A-Lien, M., 1986. Generation and migration of hydrocarbons in the Maracaibo Basin, Venezuela: an integrated basin study. Organic Geochemistry 10, 261-279.

Telang, A.J., Ebert, S., Foght, J.M., Westlake, D.W.S., Jenneman, G.E., Gevertz, D., Voordouw, G., 1997. Effect of nitrate injection on the microbial community in an oil field as monitored by reverse sample genome probing. Applied and Environmental Microbiology 63, 1785-1793.

Terken, J.M.J., Frewin, N.L., 2000. The Dhahaban petroleum system of Oman. AAPG Bulletin 84, 523-544.

Thierry, N., Helene, B., Nathalie, R., Philippe, G., Pierre, C., 1996. Aerobic degradation of methyl-phenanthrenes by an enrichment bacterial community. Polycyclic Aromatic Compounds 11, 107-114.

Thompson K.F.M., 1987. Fractionated aromatic petroleums and the generation of gas-condensates. Organic Geochemistry 11, 573-590.

Thompson K.F.M., 1988. Gas-condensate migration and oil fractionation in deltaic systems. Marine and Petroleum Geology 5, 237-246.

Tissot, B. and Welte, D.H., 1984. Petroleum Formation and Occurrence. (2nd ed.), Springer-Verlag.

Trolio, R., Grice, K., Fisher, S.J., Alexander, R., Kagi, R.I., 1999. Alkylbiphenyls and alkyldiphenylmethanes as indicators of petroleum biodegradation. Organic Geochemistry 30, 1241-1253.

Ungerer, P., 1990. State-of-the-art of research in kinetic modelling of oil formation and expulsion. Organic Geochemistry 16, 1-25.

Vandenbroucke, M., Behar. F., Rudkiewicz, J.L., 1999. Kinetic modelling of petroleum formation and cracking: implications from the high pressure/high temperature Elgin Field (UK, North Sea). Organic Geochemistry 30, 1105-1125.

Vila, J., Lopez, Z., Sabate, J., Minguillon, C., Solanas, A.M., Grifoll, M., 2001. Identification of a novel metabolite in the degradation of pyrene by Mycobacterium sp strain AP1: Actions of the isolate on two- and three-ring polycyclic aromatic hydrocarbons. Applied and Environmental Microbiology 67, 5497-5505.

Vargas, M., Kashefi, K., BluntHarris, E.L., Lovley, D.R., 1998. Microbiological evidence for Fe(III) reduction on early Earth. Nature 395, 65-67.

Voordouw, G., Voordouw, J.K., Jack, T.R., Foght, J., Fedorak, P.M., Westlake, D.W.S., 1992. Identification of distinct communities of sulfate-reducing bacteria in oil-fields by reverse sample genome probing. Applied and Environmental Microbiology 58, 3542-3552.

Volkman, J.K., Alexander, R., Kagi, R.I., Woodhouse, G.W., 1983. Demethylated hopanes in crude oils and their applications in petroleum geochemistry. Geochimica et Cosmochimica Acta 47, 785-794.

Volkman, J.K., Alexander, R., Kagi, R.I., Rowland, S.J., Sheppard, P.N., 1984.

Biodegradation of aromatic hydrocarbons in crude oils from the Barrow Sub-basin of Western Australia. Organic Geochemistry, 6, 619-632.

Volkman, J.K., 1988. Biological marker compounds as indicators of the depositional environments of petroleum source-rocks. In: Fleet, A.J. (Ed). Lacustrine Petroleum Source-rocksGeological Society Special Publication 40, Blackwell Scientific Publications, Oxford, pp. 103-121.

Volkman, J.K., Barrett, S.M., Dunstan, G.A., Jeffrey, S.W., 1994. Sterol biomarkers for microalgae from the green algal class prasinophyceae. Organic Geochemistry 21, 1211-1218.

Volkman, J.K., Barrett, S.M., Blackburn, S.I., Mansour, M.P., Sikes, E.L., Gelin, F., 1998. Microalgal biomarkers: A review of recent research developments. Organic Geochemistry 29, 1163-1179.

Wang, P.R., Li, M.W., Larter, S.R., 1996. Extended hopanes beyond C_{40} in crude oils and source rock extracts from the Liaohe Basin, N.E. China. Organic Geochemistry 24, 547-551.

Wang, Y.X., Feng, D.S., Wang, J.Y., Wu, T.S., 2003. Present-day geothermal field and thermal history of eastern subdepression, Liaohe basin. Chinese Journal of Geophysics-Chinese Edition 46, 197-202.

Wang, Z., Fingas, M., 1995. Use of methyldibenzothiophenes as markers for differentiation and source identification of crude and weathered oils. Environmental Science and Technology 29, 2842-2849.

Waples, D.W., 2000. The kinetics of in-reservoir oil destruction and gas formation: constraints from experimental and empirical data, and from thermodynamics. Organic Geochemistry 31, 553-575.

Wardroper, A. M. K., Hoffmann, C. F., Maxwell, J. R., Barwise, A. J. G., Goodwin, N.S., Park, P.J.D., 1984. Crude oil biodegradation under simulated and natural conditions-II. Aromatic steroid hydrocarbons. Organic Geochemistry 6, 605-617.

Watson, J.S., Jones, D.M., Swannell, R.P.J., 1999. Formation of carboxylic acids during biodegradation of crude oil. In: Alleman, B.C., Leeson, A. (Eds.), In Situ Bioremediation of Petroleum Hydrocarbons and other Organic Compounds. Battelle, Columbus, Ohio, pp. 251-255.

Watson, J.S., Jones, D.M., Swannell, R.P.J., van Duin, A.C.T., 2002. Formation of carboxylic acids during aerobic biodegradation of crude oil and evidence of microbial

oxidation of hopanes. Organic Geochemistry 33, 1153-1169.

Wenger, L.M., Isaksen, G.H., 2002. Control of hydrocarbon seepage intensity on level of biodegradation in sea bottom sediments. Organic Geochemistry 33, 1277-1292.

Wenger, L.M., Davis, C.L., Isaksen, G.H., 2002. Multiple controls on petroleum biodegradation and impact on oil quality. SPE Reservoir Evaluation and Engineering 5, 375-383.

Whittaker, M., Pollard, S.J.T., 1997. A performance assessment of source correlation and weathering indices for petroleum hydrocarbons in the environment. Environmental Toxicology and Chemistry 16, 1149-1158.

Widdel, F., Rabus, R., 2001. Anaerobic biodegradation of saturated and aromatic hydrocarbons. Current Opinion in Biotechnology 12, 259-276.

Wilhelms, A., Patience, R.L., Larter, S.R., Jorgensen, S., 1992. Nitrogen functionality distributions in asphaltenes isolated from several oils from different source rock types. Geochimica et Cosmochimica Acta 56, 3745-3750.

Wilhelms, A., Larter, S.R., 1994. Origin of tar mats in petroleum reservoirs. part II: formation mechanisms for tar mats. Marine and Petroleum Geology 11, 442-456.

Wilhelms, A., Horstad, I., Karlsen, D., 1996. Sequential extraction - A useful tool for reservoir geochemistry? Organic Geochemistry 24, 1157-1172.

Wilhelms, A., Larter, S.R., Head, I., Farrimond, P., di-Primio, R., Zwach, C., 2001. Biodegradation of oil in uplifted basins prevented by deep-burial sterilisation. Nature 411, 1034-1037.

Williams, J.A., Bjoroy, M., Dolcater, D.L., Winters, J.C., 1986. Biodegradation of South Texas Eocene oils - effects on aromatics and biomarkers. Organic Geochemistry 10, 451-461.

Wilkes, H., Boreham, C., Harms, G, Zengler, K., Rabus, R., 2000. Anaerobic degradation and carbon isotopic fractionation of alkylbenzenes in crude oil by sulfate-reducing bacteria. Organic Geochemistry 31, 101-115.

Wilkes, H., Kuhner, S., Bolm, C., Fischer, T., Classen, A., Widdel, F., Rabus, R., 2003. Formation of *n*-alkane- and cycloalkane-derived organic acids during anaerobic growth of a denitrifying bacterium with crude oil. Organic Geochemistry 34, 1313-1323.

Winters, J.C., Williams, J.A., 1969. Microbiological Alteration of Crude Oil. I The Reservoir. Preprints. ACS Division of Fuel Chemistry, Paper PETR 86; E22-E31.

Worden, R.H., Smalley, P.C., 1996. H_2S-producing reactions in deep carbonate gas reservoirs: Khuff Formation, Abu Dhabi. Chemical Geology 133, 157-171.

Xiong, Y.Q., Geng, A.S., 2000. Carbon isotopic composition of individual *n*-alkanes in asphaltene pyrolysates of biodegraded crude oils from the Liaohe Basin, China. Organic Geochemistry 31, 1441-1449.

Yu, Z., Cole, G., Grubitz, G., Peel, F., 2002. How to predict biodegradation risk and reservoir fluid quality. World Oil 223, 63-74.

Zengler, K., Richnow, H.H., Rossello-Mora, R., Michaelis, W., Widdel, F., 1999. Methane formation from long-chain alkanes by anaerobic microorganisms. Nature, 401, 266-269.

Zhang, C., Zhao, H., Mei, B., Chen, M., Xiao, Q. and Wu, T., 1999. Effect of biodegradation on carbazole compounds in crude oils. Oil and Gas Geology 20, 341-343 (In Chinese with English abstract).

Zhang, D.J., Huang, D.F., Li, J.C., 1988. Biodegraded sequence of Karamay oils and semi-quantitative estimation of their biodegraded degrees in Junggar Basin, China. Organic Geochemistry 13, 295-302.

Zundel, M., Rohmer, M., 1985. Hopanoids of the methylotrophic bacteria Methylococcus capsulatus and Methylomonas sp. as possible precursors of C29 and C30 hopanoid chemical fossils, FEMS Microbiology Letters 28, 61-64.